ELECTROSPUN GELATIN BASED NANOFIBERS CROSS-LINKED BY NATURAL MOLECULES FOR BIOMEDICAL APPLICATIONS

A Thesis submitted

in partial fulfillment for the Degree of

Doctor of Philosophy

by

JALAJA K

Department of Chemistry

INDIAN INSTITUTE OF SPACE SCIENCE AND TECHNOLOGY

Thiruvananthapuram – 695 547

March 2015

To my beloved mother and grandmother: The reason for what I am today. Thanks for their great support and continuous care

To my beloved teacher Late Prof. KTK who has been a constant inspiration for me to undertake research as my career

CERTIFICATE

This is to certify that the thesis entitled **Electrospun Gelatin Based Nanofibers Cross-Linked by Natural Molecules for Biomedical Applications,** submitted by **Jalaja K,** to the Indian Institute of Space Science and Technology, Thiruvananthapuram, in partial fulfillment for the award of the degree of **Doctor of Philosophy,** is a *bona fide* record of research work carried out by her under my supervision. The contents of this thesis, in full or in parts, have not been submitted to any other Institution or University for the award of any degree or diploma.

Dr. Nirmala Rachel James
Supervisor
Associate Professor
Department of Chemistry

Thiruvananthapuram
March, 2015

Counter signature of HOD with seal

DECLARATION

I declare that this thesis entitled **Electrospun Gelatin Based Nanofibers Cross-Linked by Natural Molecules for Biomedical Applications** submitted in partial fulfillment of the degree of **Doctor of Philosophy** is a record of original work carried out by me under the supervision of Dr. Nirmala Rachel James, and has not formed the basis for the award of any other degree or diploma, in this or any other Institution or University. In keeping with the ethical practice in reporting scientific information, due acknowledgements have been made wherever the findings of others have been cited.

Jalaja K
SC10D003

Thiruvananthapuram - 695547
March, 2015

ACKNOWLEDGEMENTS

I feel indebted to many people whom, without their support and cooperation, this thesis would not have been possible. It is a pleasant aspect that I have now got an opportunity to express my gratitude to all of them.

The first person, I would like to thank is Dr. Nirmala Rachel James, my supervisor. It has been an honor to be her first Ph.D. student. I appreciate all her contributions of time and ideas to make my Ph.D. experience productive and stimulating. Her patience while correcting the manuscripts really astonished me. Besides being an excellent supervisor, she was very understanding and affectionate to me. I express my sincere gratitude and obligation for her eminent guidance, constructive criticism and incredible patience throughout the course of the investigation.

I owe my deepest gratitude to Prof. Kuruvilla Joseph (HOD, Chemistry and Dean Student's activities) who gave me inspiration, moral support and laboratory facilities all the time whenever I needed. I would like to thank all faculty members of Chemistry Department who helped and supported me along the way. I express my deepest gratitude to Dr. K N Ninan, (Visiting professor at IIST and doctoral committee member) who encouraged me to think scientifically during this research work. I would like to express my sincere thanks to all doctoral committee members who constantly monitored and encouraged me throughout this work.

I would like to thank Dr. K S Dasgupta, Director, IIST for providing me the facilities to carry out this work. Financial assistance from Department of Space by providing esteemed IIST-ISRO research fellowship is gratefully appreciated.

I would like to recognize the role played by Dr. Anil Kumar PR, SCTIMST, Trivandrum and Dr S C Kundu, IIT Kharagpur, who gave me valuable

support and instructions throughout the biological studies of my samples. I express my gratitude to Dr Tuli and Ms. Deboki Naskar from IIT Kharagpur, Vinod Kumar from SCTIMST for helping me doing the biological tests.

I am thankful to all my fellow scholars especially Sarah, Kavitha, Narasimman, Raneesh, Manjunath, Mukthar, Remya, Dhanyechi and Haripadmam for their sincere help and support. I also thank Mr. Sreekumaran Nair, Mr. Dileep, Mr. Loveson, Mrs. Rehna, Mrs. Jayasree, Mrs. Jayasree and Ms. Remya for their help and support rendered to me throughout my research work. I am thankful to staff of library, administration, accounts and stores departments for the co-operation they have extended towards me during the work of this thesis.

I am deeply indebted to members of NIIST, SCTIMST, VSSC, RGCB, HLL, Trivandrum, IIT Madras and IIT Kharagpur for offering technical, analytical and characterizations of the samples throughout my research.

I am deeply obliged to my Parents and relatives for their love and support throughout the duration of my studies. I sincerely thank all those who directly or indirectly helped me for the completion of this work.

At last but not least, my heartfelt gratitude to ‘The God Almighty’ for blessing me with a beautiful life.

ABSTRACT

Electrospinning has a unique ability to produce highly porous and interconnected nanofibers with very high surface area to volume ratio. Natural and synthetic polymers can be produced as nanofibers with diameters ranging from tens to thousands of nanometers with tunable properties. The potential of these electrospun nanofibers in human health care applications is promising in many aspects such as tissue/organ regeneration, vehicle to deliver the drugs, wound healing and dressing materials, etc. Natural polymer nanofibers catch the attention of bioengineering fields due to their biocompatibility and non-toxicity. However, fabrication of electrospun natural polymer nanofibers is challenging, due to the lack of appropriate solvents and requirement of external cross-linking agents. The solvents and cross-linking agents being employed for natural polymers are harsh and toxic materials which limit their biological applications. Electrospun gelatin based nanofibers attract attention of biomedical field because of its excellent biocompatibility and structural resemblance with native extracellular matrix. The focus of this thesis is mainly to fabricate electrospun gelatin nanofibers using benign solvent system and non-toxic and natural cross-linkers for biomedical applications and the improvement of their properties by modifying the gelatin nanofibers.

In this work, gelatin nanofibers were fabricated using an innovative cross-linking approach to minimize cytotoxic effects. The solvent system for electrospinning was optimized to keep the acetic acid concentration as minimum as possible. Gelatin was dissolved in water:acetic acid (8:2, v/v) solution and electrospun to form nanofibers with diameters in the range of 150 ± 30 nm. Electrospinning was carried out by varying the amount of gelatin until beadless and smooth fibers were formed at 30 % w/v concentration. In order to improve the water stability, the gelatin nanofibers were cross-linked with a modified polysaccharide, namely, dextran aldehyde. Cross-linking with dextran aldehyde could be achieved without compromising the nanofibrous architecture. Cross-linking was carried out in ethanol medium in presence of minimum quantity of aqueous borax solution due to the very low solubility of dextran aldehyde in ethanol. Dextran aldehyde cross-linked gelatin nanofibers maintained the fibrous morphology in aqueous medium. These mats exhibited improved tensile strength (30 ± 3.47 MPa) and Young's modulus (904 ± 68 MPa) compared to the as spun mats (8.29 ± 0.53 MPa and 394 ± 96 MPa). The cross-linked mats showed gradual degradation behaviour up to four weeks under physiological conditions. The nanofibers were evaluated for cytotoxicity, cell adhesion, viability, morphology and proliferation using L-929 mouse fibroblast cells and MG-63 osteoblast cells. The results confirmed that dextran aldehyde cross-linked gelatin mats are non-cytotoxic towards L-929 and MG-63 cells with good cell adhesion, spreading and proliferation.

The shortcoming associated with cross-linking of gelatin nanofibers using dextran aldehyde is the insolubility of dextran aldehyde in ethanol medium leading to low degree of cross-linking. Hence, a disaccharide namely, sucrose was investigated as another cross-linking agent for gelatin nanofibers. Sucrose was oxidized by periodate oxidation to introduce aldehyde functionality. Oxidized

sucrose (sucrose aldehyde) enabled better cross-linking efficiency, since it is readily soluble in ethanol. Sucrose is cost effective, commercially available in large scale and is potentially biocompatible. Cross-linking of the nanofiber mat with oxidized sucrose was achieved without compromising the nanofibrous architecture. Cross-linked gelatin nanofibers maintained the fibrous morphology even after keeping in contact with aqueous medium. Sucrose aldehyde cross-linked gelatin nanofibers also exhibited improved mechanical properties (tensile strength: 38 ± 5.47 MPa and Young's modulus: 1387 ± 90 MPa) with gradual degradation pattern under physiological conditions. The nanofibrous mats were also evaluated for cytotoxicity and cell viability using L-929 fibroblast cells and MG-63 osteoblast cells. The results confirmed that oxidized sucrose cross-linked gelatin nanofibers are non cytotoxic and promote the growth and proliferation of L-929 and MG-63 cells.

In order to further improve the physico-chemical and biological properties of gelatin based nanofibers, modifications were carried out. The modifications are based on chemical reaction, physical mixing and change in instrumental set-up. A novel nanofibrous mat using amine functionalized gelatin was fabricated. Modified gelatin known as cationized gelatin was found to be soluble in water without forming gel at room temperature unlike gelatin. Hence, electrospinning of cationized gelatin could be carried out using water as the solvent. The water stability of cationized gelatin nanofibers was improved by cross-linking with dextran aldehyde and sucrose aldehyde. The resulting cationized gelatin nanofibers were evaluated for the adhesion and proliferation of L-929 and MG-63 cells. The results demonstrated that the electrospun cationized gelatin nanofibers can be potential scaffold materials for tissue regenerations.

Coaxial electrospinning is an upcoming technology that has emerged from the conventional electrospinning process in order to realize the production of nanofibers of less spinnable materials with potential applications. In the present work, core-shell structured polymer nanofibers of purely natural origin were produced from chitosan (shell) and gelatin (core) by coaxial electrospinning. Highly spinnable gelatin is employed as core material and nanofibers were fabricated with chitosan as shell using aqueous acetic acid as solvent. This method avoided the usage of synthetic polymers as core template for the fabrication of the chitosan nanofibers. For maintaining the biocompatibility and structural integrity of the core-shell nanofibers, cross-linking was carried out using the naturally occurring cross-linking agents, dextran aldehyde and sucrose aldehyde. The biological evaluation of the cross-linked core-shell mats was carried out using L-929 and MG-63 cells. The results showed that the dextran and sucrose aldehyde cross-linked core-shell nanofibers are excellent matrices for cell adhesion and proliferation.

In order to further improve the mechanical and biological performance of gelatin based nanofibers, gelatin was blended with graphene oxide (GO). The present study examined the possibility of incorporation of GO into electrospun gelatin nanofibers *via* co-electrospinning. The interaction between GO and gelatin in the nanofiber structure was established with spectroscopic evidences. The reinforcement in mechanical strength of GO loaded gelatin nanofibers was investigated. The tensile strength was increased from 8.29 ± 0.53 MPa to 21 ± 2.03 MPa after the incorporation of GO. The composite nanofibers were cross-

linked with dextran aldehyde and showed further increase in tensile strength up to 56.4 ± 2.03 MPa. The cross-linked nanofibers were evaluated for cell adhesion and proliferation of L-929 cells. The results indicated that the presence of GO not only acted as reinforcement in mechanical properties, but also encouraged the adhesion and proliferation of L-929 fibroblast cells. GO incorporated gelatin nanofibers were evaluated also for antibacterial activity against gram positive (*S.aureus*) and gram negative (*E.coli*) bacteria. However, the interaction between gelatin and the basal planes of GO rendered the composite nanofibers inactive against bacteria. Hence, antibacterial activity was induced into the composite nanofibers by incorporating a broad spectrum antibiotic, gentamicin. The drug loaded mat exhibited an initial burst release during the first 6 h followed by a gradual release of gentamicin. The mats showed antibacterial property against *S. aureus* and *E. coli.*

TABLE OF CONTENTS

LIST OF TABLES

LIST OF FIGURES

ABBREVIATIONS

AFM	Atomic Force Microscopy
CG	Cationized Gelatin
DA	Dextran Aldehyde
DMSO	Dimethyl sulfoxide
DSC	Differential Scanning Calorimeter
DTG	Differential Thermogram
ECM	Extracellular Matrix
EDA	Ethylene diamine
EDC	1-Ethyl-3-(3-dimethylaminopropyl)carbodiimide
EG	Expanded Graphite
FDA	Fluorescein Diacetate
FTIR	Fourier Transform Infrared Spectroscopy
GO	Graphene Oxide
GPC	Gel Permeation Chromatography
GT	Glutaraldehyde
HDPE	High density polyethylene
HFIP	Hexafluoro-2-propanol
MTT	3-(4,5-dimethylthiazol-2-yl)-2,5-diphenyltetrazolium bromide
PBS	Phosphate Buffered Saline
PCL	Polycaprolactone
PD	Polydispersity

PI	Propidium iodide
PLGA	Poly(lactic-co-glycolic acid)
PLLA	Poly-L-lactic acid
PVC	Polyvinyl chloride
RPM	Rotation Per Minute
SA	Sucrose Aldehyde
SEM	Scanning Electron Microscopy
TEM	Transmission Electron Microscopy
TFE	2,2,2-Trifluoroethanol
TGA	Thermogravimetric Analyzer
TNBS	2,4,6-Trinitrobenzenesulfonic acid
UV	Ultra-Violet
XPS	X-Ray Photoelectron Spectroscopy
XRD	X-Ray Diffractometer

NOTATIONS

θ	Angle of diffraction
Å	Angstrom
cm	Centimeter
^{o}C	Degree centigrade
eV	Electron volt
g	Gram
h	Hour
MG-63	Human osteoblast-like cell
IU/ml	International units per millilitre
kV	Kilovolt
MPa	Megapascal
μm	Micrometer
ml	Millilitre
mm	Millimeter
min	Minute
mol	Mole
L-929	Mouse fibroblast cell
nm	Nanometer
M_w	Weight-average molecular weight

CHAPTER 1

INTRODUCTION

The aim of this chapter is to provide a foundation for understanding the versatility of nanofibrous materials and the fabrication methods for the development of nanofibers, by reviewing and discussing the relevant literature. Attempt is made to establish the importance of the nanofibrous materials compared to the bulk materials in different aspects of applications. Basic terminologies associated with this work are introduced for a better understanding of the process and evaluation of the properties of different nanofibrous materials developed in this work. This chapter provides an insight into the objective and scope of the research work and the organization of the entire thesis.

1.1 Nanofibers

Nanofibers are generally defined as the fibers with diameter ranging from ten to thousands of nanometers (10^{-9} m). The nanofibers come under the category of one-dimensional nanomaterials similar to nanotubes and nanorods, but with flexible nature (Huang et al., 2003; Ramakrishna et al., 2005). Nanofibers possess an extremely high surface area to volume ratio and interconnected porous structure. These unique characteristics of the nanofibers in conjunction with enhanced surface functionality and superior mechanical performance make them an exciting new class of materials for a variety of applications. Because of the multifaceted properties of the nanofibers, they find applications as components of electronic and optical devices, energy conversion and storage devices, chemical and biological sensors and air and water filtration membranes. Applications of nanofibers in biomedical field are being investigated extensively (Lu et al., 2009b; Sahay et al., 2012). Conductive nanofibers are used in the fabrication of several electronic devices such as Schottky junctions, sensors and actuators (Kundu et al.,

2011). Nanofibrous membranes with ionic, electric and photoelectric conductivity can be used for electrostatic dissipation, corrosion protection, and electromagnetic interference shielding (Huang et al., 2003). Conducting nanofibrous mats with high porosity can be used as battery separators and electrode materials. Nanofibers are also reported as high performance filtration membranes. Due to the very high surface area to volume ratio and resulting high surface cohesion, tiny particles of the order of < 0.5 mm can be easily trapped in the nanofibrous membranes (Graham et al., 2002; Huang et al., 2003). Several nanofibrous membranes are reported as gaseous and liquid filters. Nanofibers can also be used as effective reinforcement filler for composites in order to improve their structural and functional properties (Bergshoef and Vancso, 1999; Kim and Reneker, 1999). During the past few years, nanofibers are attracting enormous research interests in medical and pharmaceutical fields. As far as the biomedical application is concerned, the nanofibrous network plays a significant role as tissue engineering scaffold, drug delivery matrices, wound dressing materials and others (Greiner and Wendorff, 2007). The following section provides the significance of nanofibers to be used in various biomedical applications.

1.1.1 Nanofibers in bioengineering

The nanofibers attract wide attention as a potential solution for existing challenges in bioengineering field such as tissue and organ repair, burn and wound care, and drug delivery. Nanofibers are attractive in these fields due to many reasons and the most important is the one-dimensional nanostructure with very large surface area to volume ratio (Leung and Ko, 2011). This property enables a better cellular growth, cell-material interaction, adhesion of cells, proteins and drug molecules, etc. From the biological point of view, almost all of the human tissues and organs are deposited in nanofibrous structures. All of them are characterized by well-organized hierarchical fibrous structures in nanometer scale (Ramakrishna et al., 2005). For tissue engineering and wound dressing, nanofibers are treated as scaffold materials for cell growth and proliferation. In drug delivery applications, nanofibers are considered as a potential drug carrier.

1.1.1.1 Tissue engineering

Tissue engineering is an emerging multidisciplinary approach to repair or replace damaged tissues and organs by comprehending bioengineering, chemistry, physics, life sciences and clinical sciences. Tissue engineering is an alternative solution for the problems of donor site morbidity and life-long medication and potential rejection encountered in traditional clinical therapies (Hutmacher et al., 2001). Tissue engineering has attracted many scientists and surgeons with anticipation to treat patients in a minimally invasive and less painful way (Salehahmadi and Hajiliasgari, 2013). There are three basic elements of tissue engineering paradigm, they are: scaffold, cells, and growth factors. General strategy for tissue engineering involves harvesting of a donor tissue from patient's body and dissociation into cells using enzymes, the culture of living cells outside the body, seeding of the populated cells *in vitro* on a porous construct known as scaffold and implantation of the cell-scaffold construct into patient's body. Eventually, the scaffold degrades and resorbs into the body and the cells produce their own natural scaffold known as extracellular matrix (ECM) (Freyman et al., 2001; Ratner, 2004). Thus, tissue engineering is to a large extent dependent on the scaffolds technology (Dhandayuthapani et al., 2011). Since the major goal of developing the scaffold is to mimic the structural and functional properties of the native ECM, a profound knowledge of the ECM may be advantageous for the design of scaffolds for desired tissue types (Yanzhong, 2006). The ECM is a collection of macromolecules which serves as the major structural component of the body. It is known to be a complex three-dimensional nanofibrous network which is mainly made up of structural proteins (e.g., collagen, elastin, etc.) and carbohydrates. The ECM provides structural and mechanical support for cell attachment, migration, proliferation and differentiation (Sell et al., 2010). Figure 1.1 shows the schematic of the general strategy of tissue engineering.

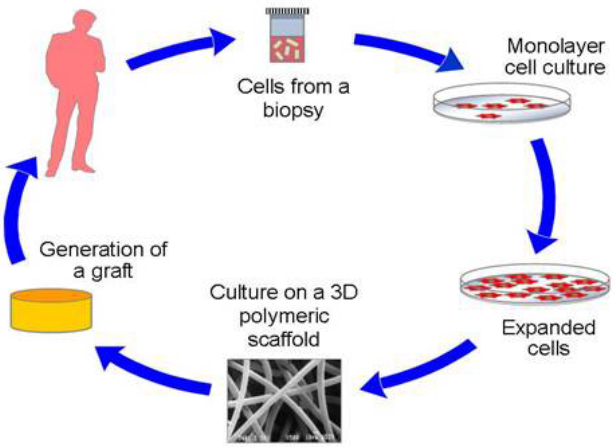

Figure 1.1: Schematic of tissue engineering approach (Image source: http://textile.iitd.ac.in/highlights/fol8/01.htm)

A scaffold acts an important constituent for tissue engineering (Chan and Leong, 2008b). Scaffolds, typically made of polymeric biomaterials, provide the structural support for cell attachment and subsequent tissue development. However, researchers often come across huge variety of choices when selecting scaffolds for tissue engineering (Chan and Leong, 2008a). An ideal scaffold for an engineered tissue should simulate the ECM of the target tissue with biological and physical properties matching with the physiological conditions of ECM (Lu et al., 2009a; Puppi et al., 2010). The major function of the scaffold is to provide a temporary support to body structures, to allow the stress transfer over-time to injured sites, and to facilitate tissue regeneration on the scaffold. Materials used for scaffold construction define the surface properties of the scaffold and determine the interaction with proteins and cells. They also determine the mechanical properties of the three-dimensional structure and subsequently that of the cell-scaffold construct (Cheung et al., 2007). Biodegradable polymers are the broadest and the most diverse class of biomaterials for scaffold development.

1.1.1.2 Wound dressing

Wound dressing is a treatment to repair the damaged skin by injury from surgical and accidental lacerations, burns, pressure ulcers, etc (Chen et al., 2009).

Wound repair is a key application of tissue engineered products and it provides significant advance in wound repair (Metcalfe and Ferguson, 2007). The first tissue engineered product is artificial skin which is still in use today. The first commercially available engineered skin substitute is known by the name Integra® (Bello et al., 2001; Chen et al., 2009). It consists of a matrix of cross-linked collagen and chondroitin sulfate copolymer to form the dermal matrix. One side of the matrix is attached with a silicon sheet that functions as a temporary epidermal layer. Integra® is predominantly used for the treatment of deep-burn wounds, which are prone to form undesirable scars. The matrix undergoes biodegradation while the cells invade and proliferate within the matrix, thus promoting skin regeneration while inhibiting wound contraction, leading to a better function and appearance of the healed wound (Stiefel et al., 2010). The goal of wound dressing is the development of an ideal structure which provides higher porosity with good barrier property towards microbes, appropriate porosity in order to help the fluid drainage and good oxygen permeability (Ramakrishna et al., 2005). The matrices for wound dressing must be selected cautiously to have these properties.

1.1.1.3. Drug delivery

Drug delivery is the method of administering a pharmaceutical ingredient to achieve the therapeutic effect in humans or animals towards certain diseases. Wide varieties of drug delivery systems are investigated to improve the therapeutic effect and to reduce the toxicity of conventional dosage forms (Ramakrishna et al., 2005). In conventional method, the patients suffering from diseases take drugs orally. Even though the drug is delivered to the affected site, the amount of delivered drug against the initial drug dose is less as the drugs also spread to other healthy parts of the body. As a result, the patient needs to take excess amount of drugs and occasionally that leads to undesirable side effects. These factors stimulate the interest in the development of novel drug loading devices, concepts, and techniques which can reduce these difficulties. An ideal drug delivery matrix must deliver the required amount of drug specifically at the

disease site. Several drug delivery systems based on polymeric materials in nanoscale formulations such as liposomes, polymeric micelles, complexes, and nanofibers attract special attention in recent times (Hu et al., 2014a).

1.1.1.4 Advantages of nanofibrous morphology in bioengineering

The architecture of scaffolds used for tissue regeneration and drug delivery is of critical importance. An ideal scaffold should have several chemical and structural features: (1) a three-dimensional architecture with desired shape, volume and appropriate mechanical strength, (2) an interconnected pore structure and high porosity to ensure cellular penetration and adequate diffusion of nutrients to cells within the construct and (3) the scaffold degradation products should be able to exit the body without any toxic effect for other organs and surrounding tissues (Papenburg, 2009). Figure 1.2 exhibits different scaffold architectures that are being employed for tissue regeneration. Among these, nanofibers play a critical role in forming neo-tissues, healing of wounds and delivering of active pharmaceutical ingredients.

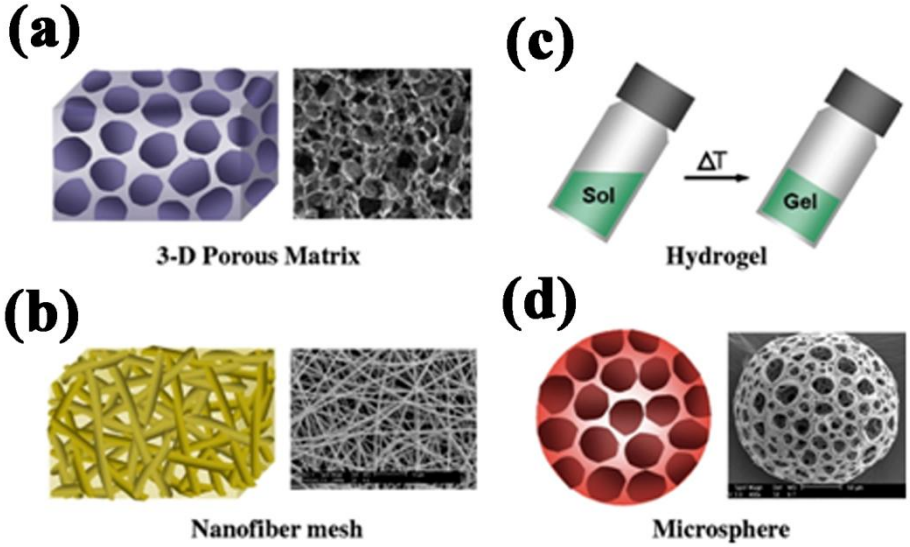

Figure 1.2: Different forms of polymeric scaffolds for tissue engineering and drug delivery: (a) a typical 3-D porous matrix in the form of a solid foam, (b) a nanofibrous matrix, (c) a thermosensitive sol–gel transition hydrogel, and (d) porous microsphere (Chung and Park, 2007)

The ECM of human tissue consists of large number of fibrous components that are made up of protein fibers such as collagens, elastin, keratin, laminins, fibronectin, and vitronectin. These ECM fibers provide structural support and mechanical integrity to tissues as well as locations for cell adhesion and regulation of cell functions such as proliferation, shape, migration, and differentiation (Beachley, 2011). Due to these reasons, human cells can attach and organize around fibers with nano/micro sized diameters (Zhang et al., 2006). Human tissues such as blood vessel, cartilage, bone, nerve, and skin consist of nanofibrous forms (Ramakrishna et al., 2005). The scaffold in the form of three-dimensional nanofibrous structure can impart mechanical strength, support for cell attachment, and act as reservoirs for delivery of bioactive molecules in similar way as the natural fibrous components of the ECM (Beachley and Wen, 2010). Hence, for the biomedical related applications, polymer nanofibers have been utilized for engineering tissues such as cartilages, bones, arterial blood vessels, heart, nerves, skin, etc. In addition, they have also been intended as dressings for protection of wounds to advance the healing process. Wound dressing with nanofibrous structures can meet the requirements like oxygen permeation, protection of wound from infection, and dehydration (Chen et al., 2009). The rate of epithelialization is increased and dermis is well-organized in nanofibrous membranes which lead to effective healing of the wounds. Nanofibers with large number of pores facilitate fluid drainage ability and exhibit controlled evaporative water loss (Ramakrishna et al., 2005). Another potential use is for controlled drug release, which can be coupled to work together while developing tissue engineering scaffolds or nanofibrous dressings. Extremely high surface area to volume ratio of the nanofibers provides higher drug loading per unit mass than any other drug loading device. The instantaneous release of drugs from the nanofiber surface enables facile dosage control suitable for some specific applications such as prevention of bacterial infection occurring within few hours after surgery (Yoo et al., 2009). The rate of drug release can be tailored easily by tuning the porosity, fiber diameter and the drug binding mechanism of the nanofibers.

1.2 Nanofiber Fabrication Techniques

Techniques for fabrication of nanofibers are important aspects in tuning the properties and applicability of the resulting fibrous structures. Nanofibers have been fabricated by a wide variety of techniques, namely, template synthesis, phase separation, self-assembly, electrospinning, etc. Conventional synthetic fibers produced *via* template synthesis and phase separation are characterized by diameters in the range of a few micrometers and above. Also, fibers are discontinuous and few micrometers in length. Self-assembly produces non-woven nanofibrous mats whereas the length and continuity of the nanofibers is not under control (Laurencin et al., 2008). Of these, electrospinning is the most versatile technique that can be used to produce continuous and fine fibers of diameter less than 100 nm. Electrospinning can be applied to diverse materials including polymers, ceramics and polymer-metal composites (Wang et al., 2009a; Zong et al., 2002). Following sections discuss the recent nanofiber production techniques which involve template synthesis, phase separation, self assembly and electrospinning.

1.2.1 Template synthesis

Template synthesis is a method in which a porous membrane is taken as template for the production of polymeric nanofibers or nanowires. Polymer nanofibers can be fabricated using metal oxide membranes with pores of nanoscale diameter (Long et al., 2011). Alumina network templates with varying pore diameters from 50 to 500 nm, and pore depths from around 100 nm to several hundred micrometers have been fabricated (Feng et al., 2002). On applying water pressure on one side of the membrane, extrusion of the polymer takes place, which upon contact with solidifying solution, gives rise to nanofibers whose diameter depends on the size of the pores. Polymer nanofibers can be obtained from these templates by destruction or mechanical removal of the templates. Nanofibers and nanowires based on conducting polymers such as polyaniline (Martin, 1994), polypyrrole, etc., are fabricated by template method

(Martín et al., 2012). Development of single and continuous nanofibers by this approach has become difficult and researchers are searching for alternative strategies for fabrication of polymer nanofibers (Vasita and Katti, 2006).

1.2.2 Self-assembly

Self-assembly is a process in which a disordered system or components organize themselves into an ordered structure or pattern as a result of specific interactions in the absence of any external agent. It is a spontaneous and reversible organization of molecular units into ordered structures by non-covalent interactions. By virtue of the modifications possible in the structure of the polymer, a variety of self-assembled structures can be obtained. The shape of the molecular unit determines the overall shape of the macromolecular nanofiber. Berndt et al. synthesized a peptide amphiphile-based self-assembling system with the goal of designing a simple self-assembly system that allows for the formation of thermally stable protein-like molecular architecture. The authors developed peptide amphiphiles that consisted of a dialkyl chain moiety (hydrophobic component/tail group) attached to an N-alpha amino group of a peptide chain (hydrophilic component/head group) (Berndt et al., 1995). In another study, Hartgerink et al. investigated the effect of variations in the molecular structure of the peptide amphiphiles on the self-assembled nanofibers. It is observed that modifications in the alkyl chain length of the peptide amphiphile alter the pH sensitivity of nanofibers, which affects self-assembly (Hartgerink et al., 2002). Obtaining nanofibers of appreciable length using self-assembly technique is a time consuming process.

1.2.3 Phase separation

Thermally induced liquid – liquid phase separation is being used for the formation of nanofibrous foam materials (Zhang and Ma, 2001). The motivation for this process has been obtained from the three-dimensional structure of collagen and several successful attempts have been made to mimic the collagen

structure. This technique involves five basic steps: dissolution of polymer, liquid–liquid phase separation process, polymer gelation (controls the porosity of nanoscale scaffolds at low temperature) and extraction of the solvent from the gel with water and freezing followed by freeze-drying under vacuum (Vasita and Katti, 2006). The advantage of the phase separation process is that it is a relatively simple procedure and the requirements are very minimal in terms of equipment compared with the previously discussed techniques. However, continuous nanofibers with tunable physical properties cannot be achieved by this technique.

1.3 Electrospinning

Electrospinning or electrostatic spinning is a process of producing nanofibers, from a variety of materials, with diameters in the range of nanometers to sub micron levels using an electrostatic potential (Bhardwaj and Kundu, 2010). Compared to other nanofiber fabrication techniques, electrospinning is the widely accepted one because of its ability to produce continuous nanofibers using a wide variety of materials (Garg and Bowlin, 2011). The cost effective nature of the set-up and the simplicity in the process makes electrospinning an attractive technique for nanofiber production (Valizadeh and Farkhani, 2014). The fibers can be collected in different forms such as tubes, yarns, mats, aligned and non-aligned fibers, etc., according to the applications of interest (Zhan and Lan, 2013). It is less complex and can be used for a wide range of materials compared to self-assembly and phase separation. Electrospinning has attracted immense research attention in the past few years for different biomedical and industrial applications due to the ease of obtaining fibers with wide range of properties. Electrospinning offers some unique advantages such as high surface area to volume ratio, adjustable porosity of electrospun structures, the flexibility to spin into a variety of shapes and sizes, and tunability of mechanical, electrical, biological and other properties (Garg and Bowlin, 2011).

1.3.1 History and background of electrospinning

The process of electrospinning is first observed by Rayleigh in 1897 and studied in detail by Zeleny in 1914 on electrospraying (Rayleigh, 1882; Zeleny, 1917). The history of electrospinning as a fiber fabrication technology is known from 80 years back. In 1934, Anton and Formahls secured a series of patents on fabrication of polymer filaments by applying electrostatic potential (Anton, 1934). Later in 1966, Simons patented an apparatus for the production of lightweight and ultrathin non-woven fabrics. He studied the polymer properties and fabricated different patterns of continuous and ultra thin fibers from polymers by tuning the viscosity of polymer solutions (Simons, 1966). The mechanism of electrospinning and the formation of fluid jet are revealed by Taylor in 1969. He explained the deformation of polymer droplets when the electrostatic potential counter acts the surface tension of the polymer droplets. The elongated and conical shaped polymer droplet is named as Taylor cone after he invented the phenomena (Taylor, 1969). After this era, the process of electrospinning has achieved large interest amongst researchers owing to the vast application fields of nanofiber based materials. Now, electrospinning is accepted as a powerful method for the fabrication of nanofibrous structures (Atchison and Schauer, 2012). Electrospinning has been an area of enormous interest in the medical community because of its ability to produce nano sized fibers with high surface area that mimic the ECM which can be used in a variety of biomedical applications (Greiner and Wendorff, 2007).

1.3.2 Principle, mechanism and instrumental set-up

Electrospinning is a process that creates nanofibers through an electrically charged jet of polymer solution or melt. This technique is applicable to almost all polymer solutions or melts and is capable of spinning fibers in a variety of shapes and sizes with a wide range of properties to be used in a broad range of biomedical and industrial applications. Electrospinning requires a very simple and

inexpensive set-up but is a complex process that depends on several molecular, processing, and technical parameters (Chronakis, 2010; Garg and Bowlin, 2011).

The basic electrospinning set-up consists of three major components: a syringe pump, a high voltage power supply, and a collector separated at a specific distance. Figure 1.3 represents the schematic diagram of the basic components of an electrospinning apparatus.

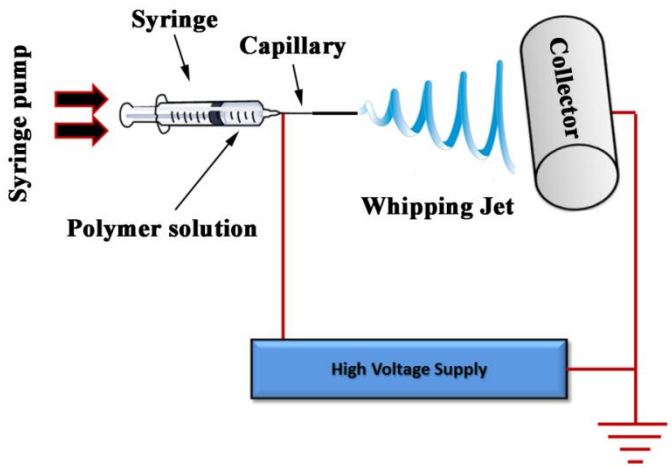

Figure 1.3: Basic components of electrospinning set-up

In a typical electrospinning process, a high voltage (5-50 kV) is applied depending on the electrospinnability of the polymeric solutions or melts. As a result, an electrical field is induced between the needle and the collector. A programmable syringe pump allows the polymer solution to be fed at a controlled rate (Lu et al., 2009c). From the high voltage power supply, one electrode is connected to the syringe needle holding the spinning solution in order to charge the polymer fluid. The other electrode from the power supply is attached to the opposite polarity collector, which is usually grounded (Abdel-Hady et al., 2011).

At first, the polymer solution is held at the tip of the needle as a droplet due to the surface tension effect. On applying the high voltage in the range of 5-50 kV, the droplet surface gets charged at the tip of the needle. The charged jet experiences two types of electrostatic forces, namely mutual electrostatic

repulsion between the surface charges of the droplet and the columbic force by the external electric field (Zhang, 2014). These electrostatic interactions cause the liquid droplets to elongate to a conical shape which is referred to as Taylor cone. At the threshold voltage, as the electrostatic forces overcome the surface tension effect of the fluid droplet, a charged fluid jet is ejected from the tip of the Taylor cone (He et al., 2005). This jet is then stretched thousands or millions of times, during which the complete evaporation of the solvent occurs on moving towards the collector. The jet initially travels in a linear path and after a certain distance; it undergoes chaotic movements which is due to the instability of the charged jet. From the point where the instability starts, the jet follows a diverging helical path. As the jet spirals towards the collector, higher order bending and whipping instabilities happen, resulting in a completely chaotic trajectory. The interaction of the charges of the jet with the external electrical field and solvent evaporation causes bending and spraying (Riboux et al., 2011). This results in the deposition of long and continuous nanofibres as a non-woven structure. This process typically gives rise to randomly oriented nanofibers due to the electric field induced stretching of the jet towards the collector. The morphology and alignment of the nanofibers can be tuned by judicious selection of the collector geometry and architecture. A rotating drum collector can be used to make aligned nanofibers, which are reported to exhibit improved mechanical properties compared to randomly oriented nanofibers (Neves et al., 2007).

1.3.3 Coaxial electrospinning

Several modifications are made into the basic electrospinning set-up in order to improve the quality and functionality of the nanofibers. Coaxial electrospinning is an important modification among them and it facilitates the production of core-shell structured and hollow structured nanofibers (Elahi et al., 2013). In the process of coaxial electrospinning, two polymer solutions can be co-electrospun without direct mixing, using two concentrically arranged nozzles. On applying a high voltage in the coaxial spinneret, the droplet deforms to form a compound Taylor cone. A jet is ejected from the tip of the compound Taylor cone,

which produces the core-shell nanofibers (Garg and Bowlin, 2011). Since the solvent evaporation predominates, the mixing between the two components is very limited. For fabrication of core-shell nanofibers, it is necessary that both core and shell solutions are sufficiently viscous and the solvents are immiscible. In principle, the rheological behaviours of the two solutions must be matched significantly (McKinley and Sridhar, 2002; Reddy et al., 2009). A typical coaxial electrospinning set-up is schematically sketched in Figure 1.4.

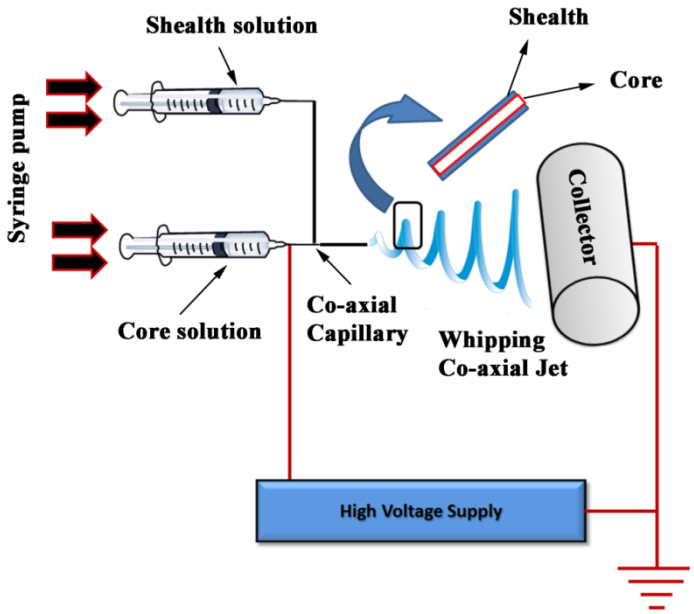

Figure 1.4: Set-up of coaxial electrospinning along with the compound Taylor cone formation

It is found that the core-shell nanofibers exhibit the properties of both core and shell materials similar to the composite nanofibers. Overall, this technique is useful in producing different types of dual composition nanofibers, surface-modified nanofibers, functional graded nanofibers and continuous hollow and core-sheath nanofibers (Garg and Bowlin, 2011). Core-shell structures can be of use for loading drugs and bioactive molecules as well as nanoparticles so that it will be suitable for controlled drug release, bioactive tissue scaffolds (Zhang et al., 2007), highly sensitive biochemical sensors (Sun et al., 2003), etc.

In order to form a fiber, a solution must have sufficient concentration such that the polymer chains are entangled, which is referred to as critical entanglement concentration (C_e) of polymers. Coaxial electrospinning is a powerful approach in cases where a particular polymer solution is not capable of producing nanofibers because of its fluid characteristics. It is especially important in the case of polymers which possess poor solubility and the viscosity window that does not meet a critical entanglement concentration for the formation of fibers (Rutledge et al., 2005). For instance, the critical entanglement density for the important biomaterials chitosan and alginate cannot be easily reached without gel formation (Du and Hsieh, 2007). For coaxial electrospinning to occur, a biopolymer solution does not have to meet the critical entanglement for fiber formation, however, merely match the zero shear flow viscosity of the template polymer solution, where the template polymer solution is above its critical entanglement concentration (Hu and Yu, 2013; Palangetic et al., 2014). Coaxial electrospinning improves the spinnability of an unspinnable material with the help of a highly spinnable material as either core or shell template. Several synthetic polymers are being used as template materials, and immense researches are being undertaken for exploring new and easily available materials as templates (Ji et al., 2013; Pakravan et al., 2012). Hence, coaxial electrospinning technique will be a powerful tool in expanding the feasibility window for electrospinning towards non-spinnable materials.

1.3.4 Electrospinning parameters

Understanding of the parameters affecting the elctrospinning process is crucial for obtaining fibers with desired size, shape and orientations. The size and morphology of the fibers are highly dependent on the solution and spinning parameters (Beachley and Wen, 2009). These are the key determinants for fiber characteristics such as diameter, morphology, tensile strength, conductivity and others (Tan et al., 2005). Parameters are broadly categorized into three: solution variables (solution concentration, viscosity, charge density, surface tension, etc.), controlled variables (applied voltage, flow rate, tip to collector distance, etc.) and

ambient variables (temperature, humidity and air flow) (Doshi and Reneker, 1993). In order to produce nanofibers with fine structure and morphology, the above mentioned parameters have to be optimized. The formation of beads along with fibers is a major concern and has to be rectified. Similarly, shapes of the fibers can be varied to ribbon-like and branched structures depending on several parameters. Extensive researches are being undertaken to figure out nanofibers in the best form. In 1971, Baumgarten investigated the effect of various processing parameters on the fiber size and morphology. In his studies, Baumgarten used solution of poly(acrylonitrile) in DMF for electrospinning (Baumgarten, 1971). In this system, he establishes that, fiber diameter has a direct dependence with solution viscosity. By varying the solution and processing parameters, he was able to prepare nanofibers with diameters ranging from 500 to 1100 nm. Polymer concentration determines the spinnability of particular polymers. The solution must have a high enough polymer concentration for chain entanglements to occur. Solutions, too dilute or too concentrated, lead to fibers with beads and bundles. The polymer concentration influences both the viscosity and the surface tension of the solution (Desai et al., 2008). In recent studies, greater understanding of processing parameters has led to the formation of fibers with diameters ranging from 100 to 500 nm. There is an optimal range of electric field strength for a certain polymer/solvent system, as either too weak or too strong electric field leads to the formation of beaded fibers. As the electric field increases further, the Taylor cone disappears and rough and discontinuous fibers appear instead (Xu et al., 2011). By varying the electrospinning parameters, it is possible to get nanofibers with different morphologies. Other than beaded and non-beaded fibers, electrospinning is capable of producing nanofibers with diverse and interesting morphologies such as highly porous, ribbon-like, flattened, branched, etc. (Ramakrishna et al., 2005).

1.4 Electrospun Polymer Nanofibers

There are numerous materials available for electrospinning process. Choice of precursor materials for electrospun nanofibers depends on the projected

properties and applications. Materials such as polymers and polymer composites can be directly used for electrospinning to form nanofibers. In the case of precursors such as metals and ceramics, post processing of electrospun fibers is required (Li and Xia, 2004a). Metals (Barakat et al., 2008) and ceramic materials (Li et al., 2006a) are mixed with suitable polymers to produce nanofibers. Subsequently, during post-treatment polymer matrix is removed to obtain metal and ceramic nanofibers. Recently, carbon nanofibers are obtained from polymer nanofibers after carbonization of the electrospun nanofibers (Hou and Reneker, 2004). Most of the polymers are inexpensive, have easily tunable chemistry and can be synthesized from appropriate monomers in tailor-made structures. As already mentioned, the polymer solution must have a critical entanglement concentration for the formation of continuous fibers without breaking. Insufficient chain entanglement causes the formation of droplets which leads to 'bead on string' morphology (Nie et al., 2009). The high molecular weights of the polymers make possible sufficient entanglements in the solution to form continuous fibers during the electrospinning process. The viscosity window of the polymer solution should be sufficient to create the entanglements. Hence, the molecular weight, viscosity of the polymer solution in a solvent and its concentration are interrelated and greatly affect the electrospinning process (Bhardwaj and Kundu, 2010). Most of the polymers and few oligomers are capable of forming fibers by this method (Picciani et al., 2011).

Large numbers of synthetic and natural polymer nanofibers are available in literature (Pham et al., 2006). The most commonly used synthetic polymers are biodegradable aliphatic polyesters which are derived from three monomers, namely lactide, glycolide and caprolactum (Gupta et al., 2014b). The hydrolytic susceptibility of the ester bond is responsible for the degradation of these polymers (Nair and Laurencin, 2007). Electrospun nanofibers of polylactic acid (Wang et al., 2009a), polyglycolic acid (Yu et al., 2014) and polycaprolactum (Alves da Silva et al., 2010) and their composite nanofibers (Kumbar et al., 2008) are widely explored for different biomedical applications especially as tissue engineering scaffolds. Polyurethane is another well-established synthetic polymer

whose electrospun nanofibers are known for artificial blood vessels, wound dressing and healing applications (Kanani and Bahrami, 2010). Natural polymers have several value added properties other than biodegradability. They are biocompatible, non-cytotoxic and their degradation products are bioresorbable. Natural polymers have distinct advantages over synthetic polymers as far as biomedical applications are concerned (Sell et al., 2010). The following section gives an insight into the fabrication of natural polymer nanofibers by electrospinning.

1.4.1 Natural polymer nanofibers

Natural biopolymers are of enormous interest in tissue regeneration as they simulate the biomimetic environment and are identical to the macromolecular substances present in the human body. Natural polymer nanofibers attract wide attention in biomedicine due to the proven biocompatibility, biodegradability and non-cytotoxicity (Ratner, 2004). When compared with synthetic polymers for the construction of three-dimensional scaffolds, natural polymers, such as proteins or polysaccharides, play a significant role in determining cell behaviour, and several other cellular functions (Helan and Yiqi, 2014). However, the efficiency of natural polymer nanofibers is limited due to their poor mechanical properties and fast biodegradability. The rate of degradation of natural polymers can be tuned either by cross-linking treatments or by other chemical modifications (Ramakrishna et al., 2005). Natural polysaccharide and protein nanofibrous materials not only serve as ideal carriers for drug delivery but also as matrices for skin, bone, cartilage, vascular, neural, and cardiac tissue engineering (Sridhar et al., 2015). Proteins and polysaccharides are the well-known natural biopolymers used for wide range of applications. Some of the polysaccharides used for electrospinning are chitosan, alginate, hyaluronic acid, cellulose, etc. (Schiffman and Schauer, 2008). Proteins that form nanofibers by electrospinning are collagen, gelatin, fibrinogen, silk proteins, and elastin (Sell et al., 2010). All these materials are well-studied for various tissue engineering and drug delivery applications.

Several recent studies on polysaccharide based electrospun nanofibers are available that find potential applications in regenerative medicine (Lee et al., 2009). However, drawbacks regarding the processibility of the polysaccharides, such as lack of solubility and high viscosity have limited their applications (Maeda et al., 2014). Electrospinning of polysaccharides such as alginate, dextran, hyaluronic acid, chitin and chitosan has been studied extensively and demonstrated as scaffold materials for various tissue regenerations and drug delivery applications (Bhardwaj and Kundu, 2010). Among these polysaccharides, chitosan is an interesting bioactive polymer because of their desirable properties such as biocompatibility, biodegradability, antibacterial properties, non-immunogenicity, etc. (Lee et al., 2009; Zhao et al., 2015). The significance of this cost-effective biopolymer also includes the structural similarity to the glycosaminoglycans (GAG) found in vertebrate bone and the capability for induction of osteoconductivity. Chitosan is derived from chitin, which is an omnipresent natural polysaccharide after cellulose on earth. Chitin consists of (1, 4)-linked N-acetyl D-glucosamine units. However, the use of chitin in many applications is limited due to the poor solubility in organic solvents (Dutta et al., 2004). The N-acetylated chitin is known as chitosan, obtained by the deacetylation of chitin. Chitosan is soluble in aqueous acidic solution when the deacetylation of chitin exceeds about 50 %. Chitosan is a cationic polysaccharide composed of (1-4)-linked 2-acetamide-2-deoxy-β-D-glucopyranose and 2-amino-2-deoxy-β-D-glucopyranose residues. The properties of chitosan solution depend on the degree of deacetylation and the molecular weight. Electrospinning of chitosan is difficult due to the polyelectrolyte nature. The free amino groups in its molecular backbone make it polycationic in acidic solution. The polycationic character increases the surface tension of the solution (Zhao et al., 2015). Electrospinning of chitosan nanofibers are achieved using harsh and toxic solvents such as trifluoroacetic acid and concentrated acetic acid (Ohkawa et al., 2004; Sangsanoh and Supaphol, 2006; Schiffman and Schauer, 2007). These solvents facilitate the electrospinning of chitosan because the amino groups of chitosan form salt that prevent the strong interactions among the molecules. Geng et al. have reported fabrication of chitosan nanofibers using concentrated acetic acid

(Geng et al., 2005). This method is found to be applicable to chitosan of a particular molecular weight only. Problems associated with electrospinning of chitosan are avoided by employing blending of chitosan with other synthetic polymers such as polyethylene oxide (PEO) (Bhattarai et al., 2005), polyvinyl alcohol (Charernsriwilaiwat et al., 2014), polylactic acid (Ignatova et al., 2009) and polycaprolactone (Shalumon et al., 2010). For improving the biological performance of the chitosan derived nanofibers, researchers have attempted electrospinning of chitosan along with natural polymers such as gelatin (Chen et al.; Dhandayuthapani et al., 2010; Qian et al., 2011), collagen (Chen and Su, 2011), and silk fibroin (Chen et al., 2012). A recent advancement in fabricating the chitosan nanofiber is based on the technique of coaxial electrospinning. The core-shell nanofibers are fabricated with highly spinnable synthetic polymers as core or shell templates (Ji et al., 2013; Ojha et al., 2008; Pakravan et al., 2012). Ojha et al. have reported the fabrication of chitosan nanofibers *via* coaxial electrospinning with PEO as shell template. The biological properties of pure chitosan and blends of chitosan and other polymers based nanofibers are evaluated extensively. Bhattarai et al. reported that the chitosan/PEO nanofibrous scaffolds promoted the attachment of human osteoblasts and chondrocytes and maintained characteristic cell morphology and viability (Bhattarai et al., 2005). The human foetal osteoblast proliferation and bone formation are studied by Zhang et al using hydroxyapatite/chitosan composite nanofibers containing 10 % ultra-high-molecular-weight polyethylene as fiber forming additive (Zhang et al., 2008). Wang et al studied the efficiency of electrospun chitosan nanofibers on Schwann cell alignment and positive effect of this nanofiber on peripheral nerve regeneration (Wang et al., 2009b). Chitosan-polycaprolactone (PCL) nanofibrous scaffold with unidirectional fiber orientation by electrospinning is reported by Cooper et al. They investigated the effect of the fiber alignment on cell organization and differentiation in comparison with randomly oriented nanofibers for skeletal muscle tissue reconstruction (Cooper et al., 2010). A ternary composite nanofiber of chitosan with tannic acid and pullulan has been developed and evaluated for the anti bacterial activity and wound healing property (Xu et al., 2015).

Electrospun protein based nanofibers are of great interest recently. A protein is a linear polymer of amino acids that take up a complex three-dimensional structure. Proteins exhibit wide range of properties that is important in tissue regeneration, cell and drug delivery, wound dressing materials and others (Khadka and Haynie, 2012). Proteins form fibrous structure that primarily functions as a structural or mechanical support for cells in the ECM of mammalian cells. Protein fibers in nano/micro regime can be considered as good candidates that enable scaffolding, stabilization, and protection of cells. Protein fibers are the major constituent of ECM. Structural and functional features of protein nanofibers are increasingly being explored as artificial ECM and as additives for other synthetic polymers in order to enhance their biological performance (Dror et al., 2008). Most of the structural proteins such as collagen, elastin, fibronectin, laminin, etc., are found in ECM structures. Among these, collagen is the most abundant protein in the ECM. It is found in ECM as fibrillar protein and provides the structural support to the cells (Sell et al., 2010). Collagen nanofibers are fabricated by electrospinning to provide a biomimetic environment for the regeneration of various types of tissues (Kelleher and Vacanti, 2010). One limitation of collagen and other protein based nanofibers is poor mechanical properties and lack of suitable solvent system for electrospinning. Several researches are being carried out to overcome these hurdles by using alternative solvent systems and appropriate cross-linking agents. Pure collagen nanofibers and collagen with other polymer blended nanofibers are extensively studied for a variety of biomedical applications (Chen et al., 2010; Dong et al.; Matthews et al., 2002; Taravel and Domard, 1996). Apart from collagen, gelatin is another protein derived from collagen by acid or alkaline hydrolysis. Gelatin is an attractive material for bioengineering field due to the biological origin and structural similarity to collagen. Gelatin has been used for many years in drug delivery, cell culture and tissue engineering on account of its excellent biocompatibility, easy processability and cost effectiveness (Malafaya et al., 2007). Gelatin has been shown to have advantages over collagen, in many aspects such as its non-immunogenicity (Chang and Gupta, 2010), better solubility in aqueous systems and a sol-gel transition at 35 °C (Bohidar and Jena, 1994). Furthermore, gelatin is

relatively inexpensive compared to collagen (Ratanavaraporn et al., 2006). Based on these perspectives, gelatin based electrospun nanofibers are extensively explored for different applications. The following section discusses, in detail, the processing and applications of electrospun gelatin nanofibers.

1.5 Gelatin-Based Electrospun Nanofibers

Electrospun gelatin nanofibers attract the attention of bioengineering research community, because of their excellent biocompatibility, biodegradability, non-immunogenicity and structural and functional resemblance with natural ECM. Electrospun gelatin nanofibers have been reported in literature for various tissue engineering and drug delivery applications. The gelatin nanofibers are fabricated in different forms such as thick mat, tubular structure and coating over some surfaces for various applications (Zhan and Lan, 2013). Besides pure gelatin nanofibers, gelatin-synthetic polymer and gelatin-natural polymer blends nanofibers are fabricated by electrospinning technique (Dhandayuthapani et al., 2010; Zhang et al., 2005b).

1.5.1 Solvents used for electrospinning of gelatin

The first important step in electrospinning of a polymer is the preparation of electrospinning solution in a suitable solvent. Gelatin is a biopolymer of high polarity. There are a very few high polarity organic solvents available to dissolve gelatin. They are fluorinated alcohols such as trifluoroethanol (TFE) and hexafluoroisopropanol (HFIP) (El-Hady, 2013). Spinning is usually done in the presence of these solvents and are highly toxic and corrosive to the living tissues, if present in the nanofibrous structure even in trace quantity (Huang, 2012). Various protein nanofibers based on collagen, gelatin, solubilized alphaelastin, and human tropoelastin as tissue engineered scaffolds have been developed by electrospinning using HFIP as the solvent (Li et al., 2005). Later on, electrospinning of gelatin is carried out in organic acids such as formic acid (Ki et al., 2005), acetic acid and mixture of solvents such as ethyl acetate/water and

acetic acid/water systems. Effects of different solvent systems on the morphology and size of the electrospun gelatin nanofibers are evaluated by Choktaweesap et al. They studied pure acetic acid, acetic acid/TFE, acetic acid/dimethyl sulfoxide (DMSO), acetic acid/ethylene glycol and acetic acid/formamide mixtures for electrospinning. Among these solvents, acetic acid and TFE are selected as the best solvents for gelatin nanofiber fabrication. These studies show that the solvent polarity and volatility have significant effects on the morphology and the size of the nanofibers (Choktaweesap et al., 2007). S P Volta et al developed gelatin nanofibers using 60 % acetic acid as solvent and a naturally occurring material, genipin as a cross-linking agent (Panzavolta et al., 2011). When gelatin nanofibers are fabricated from organic acids, high acid concentration causes the degradation of gelatin (Ki et al., 2005). Gelatin nanofibers are also reported to be made using benign solvents such as water at high temperature (50 °C) (Pandya et al., 2010) and ethanol/phosphate buffer saline mixture (Zha et al., 2012).

1.5.2 Cross-linking of electrospun gelatin nanofibers

Electrospinning of gelatin in suitable solvent produces gelatin nanofibers that are unstable in aqueous environments or high degree of moisture content. A post treatment, namely cross-linking is essential in order to improve the water resistant ability of gelatin and other protein based nanofibers. Furthermore, the cross-linking treatment remarkably improves the mechanical properties and degradation behaviour of the nanofibers. The degradability and mechanical strength of the scaffold should match with the desired tissue type which varies from tissue to tissue. Cross-linking process can tailor the rate of biodegradation and mechanical strength. That is, gelatin nanofibers with the specific rate degrade into bioresorbable components as cells produce their own ECM. Cross-linking is accomplished by the reaction of functional groups on the cross-linking agents that can form bonds between the surfaces of gelatin nanofibers to form a water-resistant network. A number of cross-linking methods are available, that have successfully improved the stability and mechanical properties of gelatin based nanofibers (Nguyen and Lee, 2010; Sisson et al., 2009; Su and Mo, 2011). The

cross-linking can be realized either by chemical reaction between the functional groups or merely through physical interactions among the groups. Even though, the physical interaction can avoid the involvement of potential toxic materials, the extent of degree of cross-linking attainable is very limited. Therefore, chemical cross-linking treatment is the preferred method for gelatin based nanofibers (Ratanavaraporn et al., 2010).

The chemical cross-linking agents commonly employed for gelatin nanofibers are glutaraldehyde (GT) (Zhang et al., 2006), 1-ethyl-3-(3-dimethylaminopropyl) carbodiimide (EDC) (Li et al., 2006b), hexamethylene diisocyanate (HMDI) (Li et al., 2005), glyceraldehydes, genipin (Sisson et al., 2009), etc. Glutaraldehyde (GT) is an organic compound commonly used as a chemical preservative and cell fixative. It is a bifunctional molecule which contains two terminal aldehyde groups. These aldehyde groups can react with the primary amino groups of gelatin to form an aldimine. This reaction is termed as Schiff's base formation reaction and the aldimine thus formed is known as the Schiff's base (Figure 1.5).

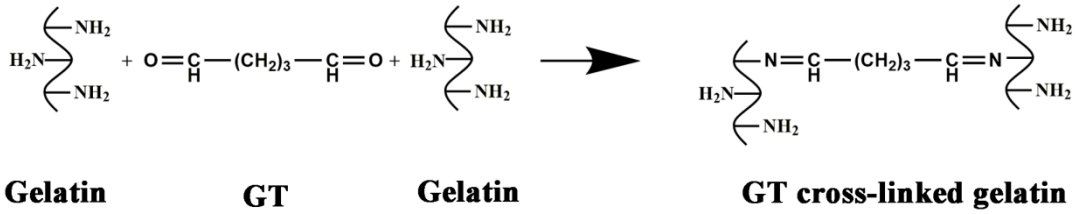

Figure 1.5: Schematic of the cross-linking of gelatin by glutaraldehyde

The advantage of GT cross-linking with nanofibers is that, the nanofibrous mats can be exposed to GT vapours for a stipulated time period. An effective cross-linking occurs during this period, without affecting the structure and morphology of the nanofibers. Several reports on utilizing GT as cross-linking agents for gelatin nanofibers are found in literature. Zhang et al prepared gelatin nanofibers and cross-linked using GT vapour (Zhang et al., 2006). The effective cross-linking occurred after exposing the mats for 3 days to GT vapours. The

resulting GT cross-linked gelatin nanofibers are evaluated for human dermal fibroblast cells, which show that the presence of residual GT causes an initial toxic response towards the cells. Another report by Wu et al studied the fabrication of gelatin nanofibers cross-linked with GT for lesser time period say 15 min to 360 min. The adhesion and growth of MG-63 osteoblast cells on these nanofibrous mats were studied and it is observed that mats cross-linked for 45 min showed better cellular activity. With an increase in the duration of cross-linking of gelatin in GT vapours, the cellular activity decreases, because of the toxic effect of residual GT. This is a direct evidence of the presence of toxic response of the residual GT on gelatin nanofibers (Wu et al.). Even though, GT is an effective protein cross-linker, the presence of unreacted GT or GT released into the body as a result of the degradation of the material, leads to redundant toxic response. GT is a highly toxic material and it is commonly used to fix cells, and during which GT kill the cells by reacting with the protein present in it (Kiernan, 2000). A comparative performance of different cross-linking agents for gelatin nanofibers is carried out by Sisson et al. In this study, gelatin nanofiber is fabricated using a ternary mixture of acetic acid/ethyl acetate/water in a volume ratio of 50:30:20. The cross-linking agents employed in this study are, vapour-phase GT, aqueous phase genipin, and glyceraldehyde, and reactive oxygen species from plasma cleaner (Sisson et al., 2009). Since GT at high concentrations has been shown to be toxic, they explored other cross-linking methods. Using reactive oxygen species from plasma cleaner is an easy alternative; however, the degradation reaction dominated the cross-linking reaction and the gelatin nanofibers degraded immediately, in aqueous medium at 37 °C. Among these cross-linkers, GT and genipin are established as good options for cross-linking agents because of the comparatively low toxicity of these cross-linkers towards MG-63 osteoblast cells.

Another effective cross-linking agent for gelatin nanofibers is carbodiimide. Carbodiimide treatment is used to form cross-links between amino groups and carboxyl groups within the gelatin molecules, without itself being incorporated (Tomihata and Ikada, 1996; Zeeman, 1998). The cross-linking reaction establishes an amide bond between the amino and carboxyl groups from

the amino acid residues of gelatin. They form inter or intra-molecular cross-linking reactions among gelatin chains. Among different carbodiimides, 1, ethyl 3-methyl aminopropyl carbodiimide (EDC) is commonly used for cross-linking of gelatin nanofibers. EDC reacts with carboxylic acid groups of gelatin to form an active o-acylisourea intermediate that is easily displaced by nucleophilic attack from primary amino groups from lysine residue of gelatin. The primary amino group forms an amide bond with the carboxyl group, and an EDC by-product is released as a soluble urea derivative which can be easily removed from the reaction mixture. Since EDC does not participate directly in the cross-linking reaction, it does not leave any residue in the cross-linked products. Hence, these types of cross-linkers are termed as "zero length" cross-linkers. EDC has been used to enhance the biostability of gelatin fibers in the presence of N-hydroxysuccinimide (NHS), which helps to prevent the formation of side products and to increase the reaction rate (Li, 2013). For electrospun gelatin nanofibers, solvents which can preserve fiber morphologies are required. The solvents being employed for EDC cross-linking are pure ethanol and ethanol/water mixture. The chemical reactions of EDC cross-linking on gelatin are outlined in Figure 1.6.

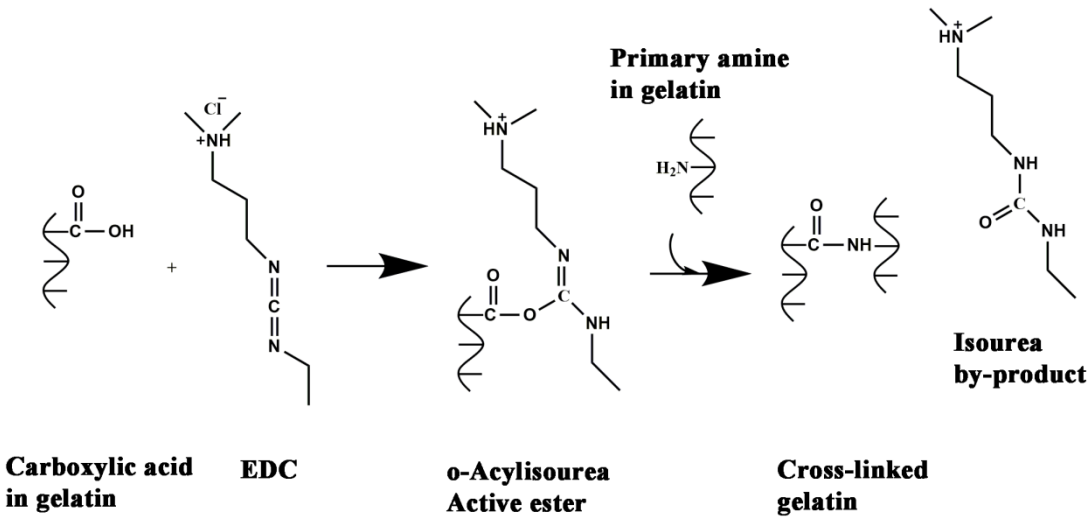

Figure 1.6: Schematic of cross-linking process of gelatin in presence of EDC

Nanofibers cross-linked by EDC are being investigated for biomedical applications. Li et al fabricated gelatin/polyaniline hybrid nanofibers for tissue engineering applications. Cross-linking of the resulting nanofibers is carried out by dipping the mats in 9:1 ethanol/water mixture containing EDC and NHS (Li et al., 2006b). Nie et al fabricated electrospun gelatin nanofibers cross-linked by EDC and NHS in 8:2 (v/v) ethanol/water mixture (Nie et al., 2010). Electrospun gelatin nanofibers cross-linked with various cross-linking agents, namely carbodimide, genipin and UV cross-linking using trans-cinnamic acid are reported by Chung and co-workers. They suggest that a better cross-linking performance and cyto-compatibility is shown by genipin cross-linked nanofibrous mats. The result obliquely proves that EDC also has an adverse effect on cell culture studies (Ko et al., 2010). Even though, EDC is considered as zero-length cross-linkers, the minute quantity of unreacted EDC left in the nanostructures found to induce the toxicity (Hao et al., 2011).

Among all the cross-linking agents mentioned, genipin is found to score the best in several aspects (Ko et al., 2010; Sisson et al., 2009). Genipin is a natural cross-linking agent which is derived from geniposide found in the fruits of gardenia jasminoides ellis. It has been used in herbal medicine as an agent against inflammation and fever. The anti-inflammatory properties of genipin could be useful for tissue engineering and wound dressing. When genipin reacts with primary amino groups, it produces a dark blue pigment and the colour gets intensified on increasing the rate of the reaction. The colour developed is due to the formation of cross-linked product from genipin and amino groups of gelatin (Chiono et al., 2008; Touyama et al., 1994). Many studies have demonstrated the remarkably low cytotoxicity and genotoxicity of genipin compared to GT and other commonly used cross-linking agents. Sung et al. showed that genipin might be about 5000–10000 times less cytotoxic than GT (Sung et al., 1999; Tsai et al., 2000). Panzavolta et al cross-linked electrospun gelatin fibers with genipin under a range of experimental conditions and the fibers maintained fibrous morphologies upon exposure to aqueous environment. The resulting nanofibers are non-cytotoxic and it enhances the proliferation of vascular wall mesenchymal

stem cells (Panzavolta et al., 2011). Gelatin nanofibers prepared by electrospinning with and without genipin cross-linking are systemically investigated. With increase of cross-linking time, thermal stability and mechanical properties are enhanced. Moreover, bovine serum albumin (BSA) as a model drug is successfully incorporated into the nanofibers. The release rate of BSA from fibrous mats decreases with increase of cross-linking time (Su and Mo, 2011). Genipin is an excellent alternative for GT and carbodiimide. However, genipin is a highly expensive material and the usefulness of genipin is not favourable in real life applications.

Several researches are being undertaken to investigate alternate cross-linking approaches based on natural, biocompatible and cost-effective materials. In the case of protein based hydrogel systems, such materials are developed based on oxidized polysaccharides. Polysaccharides are well-established biomaterials and they possess many special properties to be used as scaffolds for tissue engineering, matrices for drug delivery and wound dressings. Cross-linking of gelatin using partially oxidized polysaccharides such as dextran, alginic acid, chondrotin sulphate and carboxymethyl cellulose have been reported in literature for development of hydrogel systems (Balakrishnan and Jayakrishnan, 2005; Balakrishnan et al., 2013; Boanini et al., 2010; Dawlee et al., 2005; Schacht et al., 1997). These gels are designed to be used as wound dressings, tissue adhesives and scaffolds for tissue engineering. Biocompatibility of the polysaccharide aldehyde cross-linked gelatin hydrogels is evaluated *in vitro* and *in vivo* and is ranked as acceptable. This is regarded as an excellent alternative cross-linking approach for protein moieties to replace the toxic cross-linking agents and being used for the development of biocompatible protein based hydrogels. Successful reports of injectable hydrogel based on gelatin and oxidized alginate are available (Balakrishnan and Jayakrishnan, 2005). Rapid cross-linking occurred between amino groups of gelatin and aldehyde groups of oxidized alginate leading to hydrogel formation at appropriate pH in aqueous medium. Similar methodologies have been adopted for the cross-linking of matrices based on other proteins and

polysaccharides also (Dash et al., 2013; Hu et al., 2014b; Nair et al., 2011; Xu et al., 2012).

1.5.3 Biomedical applications of electrospun gelatin nanofibers

The gelatin mat provides space for cell and tissue to grow and so the electrospun gelatin nanofibrous scaffolds have been engineered for a variety of biomedical applications such as bone regeneration, skin tissue engineering, nerve tissue engineering, cardiac tissue engineering, tubular scaffold, drug delivery and so on. Electrospun gelatin nanofibers attract great attention in these fields because of their proven biocompatibility, tunable biodegradability, non-antigenicity and structural and functional resemblance with native ECM. Some pioneer and significant works on using gelatin nanofibers for biomedical applications are discussed briefly in the following section.

Gelatin nanofibers based biomaterials for cardiac and neural tissue engineering are developed by adding a conducting polymer, polyaniline into gelatin during electrospinning process. The study showed that the gelatin – polyaniline composite nanofibers supported attachment, migration, and proliferation of H9c2 rat cardiac myoblasts (Li et al., 2006b). Zhang et al fabricated the gelatin/poly-caprolactone composite fibrous membranes and is investigated as a promising scaffold for bone-marrow stromal cell (BMSC) culture (Zhang et al., 2005a). Wu et al fabricated electrospun gelatin nanofibers and reported the potential of gelatin mats for bone tissue engineering applications. The mats are found to support the growth and proliferation of MG-63 osteoblast cells (Wu et al.). The adhesion, viability and proliferation properties of osteoblast cells on the gelatin/nylon-6 composite nanofibers are analyzed by an *in vitro* cell compatibility test. The results suggest that the incorporation of gelatin into nylone-6 increases the cell compatibility of nylon-6 and therefore the composite mat obtained has great potential in hard tissue engineering (Pant and Kim, 2013). Another study illustrated the possibilities of fabricating γ-glycidoxypropyl trimethoxysilane cross-linked gelatin nanofibres by electrospinning technique.

The *in vitro* study reveals that these nanofibrous mats support the proliferation of neonatal olfactory bulb ensheating cells and thus promote peripheral nerve regeneration (Tonda-Turo et al., 2013b). Hydrophilic and compliant polyurethane namely, Tecophilic (TP) blended with gelatin is electrospun to fabricate a tubular composite nanofibrous scaffold with biomechanical properties closely simulating those of the native blood vessels. The hydrophilic properties of the composite scaffold induced non-thrombogenicity while the incorporation of gelatin molecules within the scaffold greatly improves the capacity of the scaffold to serve as an adhesive substrate for vascular smooth muscle cells (SMCs), in comparison to pure polyurethane. The study establishes the potential of these tubular nanofibrous structure as vascular graft (Vatankhah et al., 2014b). A potential bone tissue engineering scaffold based on electrospun gelatin/PCL with calcium phosphate nanoparticle is investigated by Rajzer et al. In this study, normal human primary osteoblast cell lines are used and the cell culture studies showed higher alkaline phosphatase activity and better mineralization in composite scaffold than in pure PCL scaffolds (Rajzer et al., 2014). Another interesting study on gelatin nanofibers demonstrated the potential of electrospun gelatin mats, incorporating rat decellularized brain extracellular matrix, to act as effective scaffold, providing a suitable microenvironment for mesenchymal stromal cell adhesion, proliferation and survival. It acts as an excellent matrix for neural tissue engineering (Baiguera et al., 2014).

The potential for use of silver containing electrospun gelatin nanofiber mats as functional wound dressings is assessed by observing their antibacterial activity against some common bacteria found on burn wounds such as *E. coli*, *P. aeroginosa*, *S. aureus* and *MRSA* (Rujitanaroj et al., 2008). In another study, electrospun silk fibroin/gelatin nanofibrous mats loaded with astragaloside IV (primary active ingredient in Astragalus extract, a herbal extract which has been used for many medical conditions) are fabricated and studied the potential healing ability for deep partial-thickness burn wound. This nanofibrous dressing is found to be an excellent therapeutic that can be used to promote healing and bring out anti-scar effects on partial-thickness burn wound (Shan et al., 2015).

Vatankhah et al studied the potential of electrospun cellulose acetate/gelatin composite nanofibers as effective wound healing matrix promoting skin tissue regeneration (Vatankhah et al., 2014a). In another study, a series of cost-effective nanofibrous scaffolds aimed at full-thickness wound healing are fabricated by blending gelatin with poly(L-lactic acid)-b-poly(ε -caprolactone) (PLLCL) and electrospun to obtain composite nanofibers. *In vitro* and *in vivo* evaluation of these materials shows the potential as scaffold for wound healing and skin regeneration (Jin et al., 2014).

The drug delivery properties of electrospun gelatin membranes are studied by loading an antibiotic, namely cefradine. Although nearly 50 % of the initial burst is observed within 4 h and the release ended after almost 80 h, the release rate of cefradine absorbed in the gelatin mats is slower than that in the casting film. Such a rapid drug release profile is highly desirable for preventing infections in the early stage as wound dressings (Nie et al., 2010). Electrospun gelatin nanofibers containing methanolic crude extract of *Centella asiatica* (a medicinal plant widely known for its traditional medical applications including its wound healing ability) are fabricated by Sikareepaisan et al (Sikareepaisan et al., 2008).

1.6 Scope and Objectives

Electrospinning has emerged as a new scaffold fabrication technology for tissue regeneration applications. This is because, electrospun fibers are potentially able to mimic the physical structure of the major components of fibers in the native ECM. There is a rapidly growing interest in natural polymer nanofibers due to their proven biocompatibility, biodegradability under physiological conditions and non-cytotoxicity. Main challenges involved in electrospinning of natural polymers intended to be used in biomedical applications are associated with toxicity due to solvents and cross-linking agents. Making use of benign solvent systems and cost-effective natural cross-linking materials will be helpful to overcome these issues. Yet, such an approach has rarely been attempted at the nanofibers level. The major aim of the present work is to develop electrospun

gelatin nanofibers by minimizing the toxicity effects from solvents and cross-linking agents. Another aim is to improve the physico-chemical and biological performance of gelatin based nanofibers by chemical or physical modifications. Attempt is also made to employ the highly spinnable gelatin as a core template for enabling electrospinning of unspinnbale natural polymers. In order to achieve these goals following objectives have been set.

- Fabrication of gelatin nanofibers by electrospinning using benign aqueous based solvent system.

- Stabilization of gelatin nanofibers by cross-linking with natural molecules such as dextran and sucrose and evaluation of their properties.

- Modification of gelatin nanofibers by cationization of gelatin to improve cell adhesion properties.

- Fabrication of core-shell nanofibers using gelatin as core template and chitosan as shell and evaluation of properties.

- Fabrication of composite nanofibers by incorporating graphene oxide (GO) into gelatin and to study the structural and biological performance.

1.7 Organization of Thesis

The thesis is composed of eight chapters and organized as follows.

Chapter 1 begins with an introduction which provides a brief outline of the research background and the state-of-the-art of electrospun nanofibers as scaffolds for tissue engineering, drug delivery and wound dressing materials. It provides the basics of nanofibers production, scaffold technology and physiological properties of the scaffolds to be used in bioengineering field. The properties and applications of natural polymer nanofibers based on chitosan and

gelatin are explained in detail. The chapter also presents the objectives and scope of this research work and the organization of the entire thesis.

Chapter 2 provides the experimental methodologies adopted in this work. Preparation of the cross-linking agents, fabrication of nanofibers, modification of gelatin, spectroscopic, microscopic characterizations and other physico-chemical characterizations and biological studies are explained in detail.

Chapter 3 describes the fabrication of gelatin nanofibers by electrospinning technique. Benign solvent system based on 8:2 (v/v), water/acetic acid mixture is used for the electrospinning process. A novel cross-linking agent, namely dextran aldehyde is used as the cross-linker for the resulting gelatin nanofibers. The physico-chemical and biological properties of the dextran aldehyde cross-linked electrospun gelatin nanofibers are studied.

Chapter 4 discusses the preparation of a disaccharide, namely sucrose based cross-linking agent for gelatin nanofibers, by periodate oxidation of the sucrose. The cross-linking conditions of gelatin nanofibers with sucrose aldehyde are optimized. The properties of sucrose aldehyde cross-linked electrospun gelatin nanofibers are evaluated.

The chemical modification of gelatin by amination/cationization and subsequent fabrication of cationized gelatin nanofibers using pure water as solvents are described in **Chapter 5**. The resulting cationized gelatin nanofibers are cross-linked using dextran aldehyde and sucrose aldehyde. The bio-physical characterizations of cross-linked cationized gelatin nanofibers are performed.

Chapter 6 demonstrates the development of core-shell structured composite nanofibers by coaxial electrospinning using gelatin as core and chitosan as shell. The core-shell nanofibers also are cross-linked with dextran aldehyde and sucrose aldehyde. The cross-linked core-shell nanofibers are evaluated for biological performance to be used as tissue engineering scaffold.

In **Chapter 7**, the effect of graphene oxide on mechanical and biological properties of gelatin nanofibers is reported. The cytotoxicity of graphene oxide – gelatin nanofibers on normal cells and bacterial cells are examined and the antibacterial property is induced by incorporating a broad spectrum antibiotic, gentamicin.

The results of the current research work are summarized and future recommendations are provided in **Chapter 8**.

CHAPTER 2

EXPERIMENTAL METHODS

2.1 Materials

Type A gelatin (porcine skin, 225 bloom) was procured from MP Biomedicals, India. Dextran from leuconostoc mesenteroides with average molecular weights of 40,000 and 500,000, sodium tetraborate decahydrate (borax), trinitro benzene sulfonic acid (TNBS), minimum essential medium (MEM), propidium iodide (PI), fluorescein diacetate (FDA), 3-(4,5-dimethylthiazol-2yl)-2,5,diphenyltetrazolium bromide (MTT), Hoechst 33258, glutaraldehyde and paraformaldehyde were obtained from Sigma Aldrich, Saint Louis, USA. Commercial chitosan of 90 % deacetylation was obtained from India Sea foods, Cochin, India. Foetal bovine serum (FBS), trypsin, rhodamine-phalloidin, alamar blue dye and Alexa Fluor 594 were procured from Gibco, Invitrogen, India. Sucrose, sodium metaperiodate, sodium chloride, disodium hydrogen phosphate, sodium dihydrogen phosphate, hydroxyl amine hydrochloride, ethylenediamine, potassium permanganate, sulphuric acid, hydrogen peroxide, acetic acid, ethanol and acetone were procured from Merck, Mumbai, India. Gentamicin (GEN) and o-pthalaldehyde were purchased from Himedia Mumbai, India and 1-ethyl,3-[3 dimethyl aminopropyl] carbodiimide (EDC) was obtained from Spectrochem Pvt. Ltd, Mumbai, India. Expanded graphite (EG) (grade-3805) was obtained from Asbury Carbons, USA. All the reagents and solvents were of analytical grade and were used as received. Cellulose dialysis tubings with molecular weight cut-offs of 3,500 and 6,500 were procured from Spectrum Laboratories Inc.CA, USA. Double distilled water was employed in all the experiments and Milli Q water (Millipore) was used for cell culture.

2.2 Preparation Methods

2.2.1 Preparation of dextran aldehyde

Dextran aldehyde (DA) was prepared by periodate oxidation of dextran with sodium metaperiodate ($NaIO_4$) according to the procedure reported by Sokolsky-Papkov et al., (2006). In brief, 2.66 g (0.012 mol) of $NaIO_4$ was dissolved in 10 ml of water containing 1 g of dextran (0.0062 mol) and the reaction mixture was stirred under dark for 6 h at 25 °C. Resulting solution was dialyzed against double distilled water for 3 days by changing water until it was free from the periodate. Each time, the dialysate was treated with silver nitrate solution and the absence of turbidity indicated the complete removal of sodium periodate. Samples were then stored at -30 °C in deep freezer and thereafter dried by lyophilization.

2.2.2 Preparation of sucrose aldehyde

Sucrose aldehyde (SA) was obtained by periodate oxidation of sucrose (Schoevaart et al., 2005). In brief, 3.42 g (0.01mol) of sucrose was dissolved in 50 ml of water and to this 4.26 g (0.02 mol) of $NaIO_4$ was added. After stirring the reaction mixture under dark for 6 h, excess amount of acetone was added and cooled on ice to precipitate the unreacted sodium periodate. Filtration of the precipitate and evaporation of the acetone yielded a 50 ml solution of oxidized sucrose. The resulting solution was kept in deep freezer at -30 °C and thereafter dried by lyophilization to get oxidized sucrose in powder form.

2.2.3 Preparation of cationized gelatin

Cationized gelatin was prepared by chemically converting carboxyl groups of gelatin into amino groups (Shen et al., 2007). Briefly, 15.1 ml of ethylenediamine (EDA) was added into 200 ml of 0.1 M phosphate-buffered saline (PBS, pH = 5.0) containing 5 g of gelatin. The pH of the solution was

maintained at 5.0 by adding 5 M HCl immediately. EDC (5.35 g) was added to this solution, which was made up to 250 ml with PBS. The reaction mixture was agitated at room temperature for 18-20 h and then dialyzed against double distilled water for 3 days. The dialyzed solution was dried by lyophilization to obtain cationized gelatin.

2.2.4 Preparation of graphene oxide

Graphene oxide (GO) was prepared from expandable graphite flakes, which is a form of intercalated graphite. Expanded graphite (EG) is obtained by inserting/intercalating a material between the graphene layers of a graphite crystal. Intercalation, results in graphite material with several new properties depending on the intercalating material and the way it associates with graphite layers. Intercalation process helps to impart graphite flakes the ability to expand and exfoliate when applying thermal shock.

GO was prepared by oxidation of EG in modified Hummer's method (Aboutalebi et al., 2011). EG was obtained by subjecting expandable graphite to thermal shock at 1050 °C. Expandable graphite (1 g) and 200 ml of sulfuric acid were mixed and stirred in a three-necked flask. Potassium permanganate (10 g) was added dropwise to the mixture. The mixture was transferred into an ice bath, and 200 ml of deionized water and 50 ml of hydrogen peroxide were poured slowly into the mixture, by observing the colour change of the suspension to light brown. The solution was stirred for another 30 min and the graphite oxide was then washed and centrifuged with HCl solution (9:1 water : HCl by volume), then centrifuged again and washed with deionized water until the pH of the solution became about 5 to 6. The graphite oxide was then diluted using deionized water and exfoliated by gentle shaking to obtain GO. For obtaining GO in powder form, aqueous GO dispersion was frozen at -30 °C and subsequently lyophilized to obtain smooth and velvet-like GO sponge.

2.3 Fabrication of Nanofibers by Electrospinning

2.3.1 Electrospinning of gelatin nanofibers

The set-up and process of electrospinning technique is explained in detail in Chapter 1. An in-house designed electrospinning apparatus was used for the fabrication of nanofibers in the current study (Figure 2.1). Solution for electrospinning was prepared by dissolving various concentrations of gelatin (24-30 %, w/v) in water/acetic acid mixture ((8:2, v/v), minimum concentration of acetic acid helped to prevent the gelation of gelatin in water) at 40 ^{o}C. Electrospinning was performed by ESPIN-NANO electrospinning machine fabricated by Physics Instruments Co. Ltd; Chennai, India. It composed of a high voltage power supply (Gamma high voltage, voltage range from 5-50 kV), programmable syringe pumps (BD Scientific) and a rotating drum target. The syringe pump was aligned horizontally to the drum collector. Solution for electrospinning was taken in a 5 ml plastic syringe (Dispovan) capped with a needle of 0.60 × 25 mm and placed on the syringe pump. Electrospinning was performed with an applied voltage of 25 kV, tip to collector distance of 15 cm, and a flow rate of 0.3 ml/h at room temperature and collector speed of 1500 RPM. Electrospun mats were collected over 0.5 mm thick aluminium foil wound over the rotating collector. These fibrous mats were kept for drying in a vacuum oven prior to further processing.

2.3.2 Electrospinning of cationized gelatin nanofibers

Aqueous solutions of cationized gelatin were prepared in different concentrations (30, 35, 40, 45 and 50 % (w/v)) and were poured into 5 ml plastic syringes mounted on the syringe pump. Fiber mats were collected on an aluminum foil attached to a drum collector kept 15 cm away from the needle. Flow rates of 0.2−0.3 ml/h, voltage range of 25−30 kV and collector speed of 1500 RPM were used as process parameters. The electrospinning parameters used were chosen based on trial and error optimization procedure.

Figure 2.1: Horizontal electrospinning set-up used for fabrication of nanofibers

2.3.3 Electrospinning of core-shell structured gelatin-chitosan nanofibers

Core-shell structured nanofibers were produced by modifying the basic electrospinning set-up with a coaxial spinneret. The core and shell solutions come out from different syringes and meet at the tip of the spinnerets. The compound Taylor cone thus developed, leads to the formation of core-shell nanofibers. Chitosan and gelatin solutions of different concentrations were prepared in 50 % and 20 % acetic acid respectively. The solutions were transferred to 10 ml syringes connected to the coaxial set-up (ESPIN NANO, Physics Instrument Company, Chennai, India). In this set-up, the coaxial spinneret and drum collector were aligned in a horizontal manner. The coaxial electrospinning set-up used in the present study is shown in Figure 2.2. Electrospinning was attempted with various concentrations of gelatin and chitosan, with a flow rate of 0.2 ml/h and potential in the range of 25 - 30 kV. The tip to collector distance was 15 cm and drum collector speed was 1000 RPM. The resulting nanofibers were collected on a 0.5 mm thick aluminium foil wound over the drum collector. The optimization of concentration and potential was based on the formation of beadless and smooth fibers (Table 2.1).

Figure 2.2: Coaxial electrospinning set-up used to fabricate core-shell nanofibers

Table 2.1: Optimization of concentration and voltage for gelatin/chitosan core-shell nanofibers

Solution concentration Gelatin/chitosan (% wt ratio)	**Applied voltage (kV)**	**Observations**
30/Nil	25	Smooth and fine fibers
30/Nil	30	Smooth and fine fibers
30/3	25	Spraying of chitosan
30/3	30	Spraying of chitosan
30/5	25	Beaded fibers
30/5	30	Smooth and fine fibers
30/7	25	Clogging of chitosan at the tip
30/7	30	Clogging of chitosan at the tip

2.3.4 Electrospinning of GO-gelatin composite nanofibers

The dried spongy GO was mixed with aqueous gelatin solution (30 % w/v) in 8:2 (v/v) water/ acetic acid mixture) and ultrasonicated for 1 h to obtain the homogeneous solution for electrospinning. Solutions with GO loadings of 0.25 to 1 % (w/w) were prepared. Pure gelatin (30 % w/v) in water/acetic acid (8:2 v/v) was used as the reference sample for comparison. In both the reference and the GO loaded sample, the amount of gelatin was maintained same. The solution was

loaded into 5 ml plastic syringe fitted with blunt needles. A syringe pump was used to control the flow rate of the solution. The applied voltage was adjusted between 25 and 30 kV, flow rate was kept as 0.3 ml/h and collector speed was 1500 RPM. Fibers were collected on a grounded metal collector (wrapped with an aluminum foil) which was kept at a distance of 20 cm away from the needle.

2.3.5. Electrospinning of gentamicin loaded GO-gelatin nanofibers

To the 0.5 % GO dispersed gelatin solution, gentamicin, a broad spectrum antibiotic (2.5 % weight of gelatin) was added and again ultrasonicated for 5 min for the complete dissolution of gentamicin. The resulting gentamicin loaded GO-gelatin solution was electrospun using the same conditions as mentioned in section 2.3.4.

2.4 Cross-linking Methods of Nanofibers

2.4.1 Cross-linking of gelatin nanofibers using dextran aldehyde

Dextran aldehyde (DA) (0.05 g) was taken in 10 ml of pure ethanol and was stirred for 24 h. A minimum amount of aqueous borax (300 µl, 0.02 M) was added and again stirred for 3 h for complete dissolution. Even though the presence of borax would enhance the cross-linking efficiency, the amount was restricted to avoid precipitation in ethanol. Cross-linking was carried out by immersing 0.5 g of nanofiber mats in 10 ml of DA solution at 37 °C for 1, 3 and 5 days. The cross-linked nanofibers are represented as DA-GNF (dextran aldehyde cross-linked gelatin nanofibers). Effect of cross-linking was examined by immersing the cross-linked mats in aqueous medium.

2.4.2 Cross-linking of gelatin nanofibers using sucrose aldehyde

Cross-linking of gelatin nanofibrous mats using sucrose aldehyde (SA) was carried out in two different methods for the purpose of optimization.

Method I:

Ethanolic solutions of SA were prepared in various concentrations (0.1, 0.5, 1 and 2 % (w/v)). Cross-linking was carried out by immersing 0.5 g of nanofiber mats in 10 ml of the above solutions for 1, 3 and 5 days at 37 ºC. Subsequently the mats were rinsed in ethanol and dried under reduced pressure. These nanofibrous mats are represented as SA-GNF-PE (sucrose aldehyde cross-linked gelatin nanofibers from pure ethanol medium)

Method II:

In this method, a minimum amount of aqueous borax (300 µl, 0.02 M) was also added to the ethanolic solution of oxidized sucrose. Cross-linking was carried out as mentioned above and the cross-linked nanofibrous mats are represented as SA-GNF-BE (sucrose aldehyde cross-linked gelatin nanofibers from borax/ethanol medium)

2.4.3 Cross-linking of cationized gelatin nanofibers using dextran aldehyde and sucrose aldehyde

Dextran aldehyde (0.05 g) was dissolved in 10 ml of ethanol containing a minimum quantity of aqueous borax (300 µl, 0.02 M). About 0.5 g of the electrospun cationized gelatin mats were cut into rectangular pieces and placed in this cross-linking medium for 7 days at 37 ℃ to obtain dextran aldehyde cross-linked cationized gelatin nanofibers (DA-CG).

Sucrose aldehyde (0.1 g) was dissolved in 10 ml of pure ethanol. About 0.5 g of cationized gelatin nanofibrous mats were kept dipped in the ethanol solution of sucrose aldehyde for 7 days at 37 °C to obtain sucrose aldehyde cross-linked cationized gelatin nanofibers (SA-CG).

2.4.4 Cross-linking of core-shell gelatin/chitosan nanofibers using dextran aldehyde and sucrose aldehyde

Dextran aldehyde (0.05 g) was dissolved in 10 ml of ethanol containing a minimum quantity of aqueous borax (300 µl, 0.02 M). About 0.5 g of the electrospun gelatin/chitosan core-shell mats were cut into rectangular pieces and placed into this cross-linking medium for 5 days at 37 ^{o}C to obtain dextran aldehyde cross-linked core-shell nanofibrous mats (DA-CS).

Sucrose aldehyde (0.1 g) was dissolved in 10 ml ethanol containing 300 µl, 0.02 M, aqueous borax. About 0.5 g of gelatin/chitosan core-shell mats were kept dipped in the ethanol solution of SA for 5 days at 37 °C to obtain sucrose aldehyde cross-linked core-shell mats (SA-CS). Minimum of 5 days were required for the effective cross-linking of core-shell nanofibers in order to maintain the fibrous morphology.

2.4.5 Cross-linking of GO-gelatin (GO-GEL) and gentamicin loaded GO-GEL nanofibers using dextran aldehyde

Dextran aldehyde (0.05 g) was dissolved in 10 ml of pure ethanol containing a minimum quantity of aqueous borax (300 µl, 0.02 M). About 0.5 g of the electrospun GO-gelatin mats and gentamicin loaded GO-gelatin mats were cut into rectangular pieces and placed into this cross-linking medium for 5 days at 37 ^{o}C to obtain dextran aldehyde cross-linked GO-gelatin (DA-GO-GEL) mats and gentamicin loaded GO-gelatin (DA-GO-GEL-GEN) mats.

2.4.6 Cross-linking of nanofibers using glutaraldehyde (GT) vapour

For comparison of the results, the nanofibrous mats were cross-linked using glutaraldehyde vapour. Cross-linking was carried out by placing 0.5 g of

nanofibrous mats over a petridish containing 10 ml of 25 % glutaraldehyde solution (aqueous). The mats along with petridish was kept inside a sealed desiccator and allowed to cross-link with glutaraldehyde vapour for 72 h at room temperature. The cross-linked mats were then washed in double distilled water and dried under reduced pressure.

2.5 Physico-chemical Characterization

2.5.1 Degree of oxidation and aldehyde content

Aldehyde content and degree of oxidation of the cross-linkers, namely DA and SA, were estimated by chemical analysis (Zhao and Heindel, 1991;Manju et al., 2011). Estimation was based on the principle that the aldehyde groups in the cross-linkers would react with hydroxyl amine hydrochloride resulting in the release of HCl. One mole of HCl would be released per mole of the aldehyde group reacted. Amount of HCl released was estimated by titrating against standardized NaOH solution. For estimating the aldehyde content in the cross-linkers, 0.10 g of the cross-linker was dissolved in 25 ml of 0.25 N hydroxyl amine hydrochloride prepared in distilled water. Two drops of methyl orange indicator (0.05 % solution) were added and allowed to stand for 2 h. The mixture was then titrated against 0.1 N NaOH taken in the burette. At the end point, the colour of the solution changed from red to yellow and the number of moles of NaOH reacted was calculated. This is equivalent to the number of moles of aldehyde groups present in the sample. From the number of moles of aldehyde groups obtained, percentage degree of oxidation was calculated. The estimation was performed in triplicate and the average values for degree of oxidation and aldehyde content are reported.

2.5.2 Trinitrobenzenesulfonic acid (TNBS) Assay

The amino groups present in as spun and cross-linked samples were estimated by the conventional TNBS assay based on the calibration curve prepared by β-alanine (Sheu et al., 2001). Briefly, 2 mg of the nanofiber sample to

be analyzed was added to 1 ml of 4 % sodium bicarbonate and 0.1 % freshly prepared TNBS solution. After thorough mixing, the solutions were placed in water bath at 40 °C for 2 h. For complete dissolution of the samples, 3 ml of 6 N HCl was added and temperature was raised to 60 °C and heated for 1 h. Blank solutions were prepared using the same procedure without the test samples. Absorbance values of the solutions were then determined spectrophotometrically (at 346 nm; UV-Visible Spectrophotometer, Cary win UV). From the β-alanine calibration curve prepared using the same method, amino groups of the samples were quantified and the cross-linking degree of the samples were determined using the equation 2.1.

$$Degree\ of\ crosslinking = 1 - \{\left(\frac{absorbance_{cl}}{mass_{cl}}\right) X \left(\frac{absorbance_{ucl}}{mass_{ucl}}\right)^{-1}\} \quad (2.1)$$

The subscripts cl and ucl stand for the cross-linked and uncross-linked gelatin nanofibers.

2.5.3 Release of gentamicin from DA-GO-GEL mats

Gentamicin is loaded into GO-gelatin nanofibers during the electrospinning process itself. A drug payload of 2.5 % weight of gelatin was added in the electrospinning solution. Gentamicin loaded GO-gelatin mats (10 mg) with a drug payload of 0.25 mg of the mat was taken for the study. The mats were dipped in 10 ml of PBS solution and incubated at 37 °C. At regular interval, 1.5 ml aliquots were withdrawn and replenished with 1.5 ml of fresh PBS. The withdrawn aliquot was then treated with 1.5 ml of o-pthalaldehyde reagent and concentration of gentamicin released was spectrophotometrically determined (UV-Visible Spectrophotometer, Cary win UV).

The o-pthalaldehyde reagent was prepared by the procedure report by Biji et al (Balakrishnan et al., 2012). It was prepared by adding 2.5 g of o-phthalaldehyde, 62.5 ml methanol and 3 ml of 2-mercaptoethanol to 560 ml of

0.04 M aqueous borax. The reagent was stored in a brown bottle in dark and kept to settle for 24 h prior to use.

2.5.4 Spectroscopic characterizations

2.5.4.1 Fourier Transform Infrared Spectroscopy (FTIR)

In the present study FTIR spectroscopy was carried out to analyze the structural changes happening during electrospinning, cross-linking, blending and so on. FTIR spectra were obtained using Spectrum 100, Perkin Elmer, USA, with universal attenuated total reflectance accessory (UATR). The crystal used for UATR accessory is standard ZnSe and light path angle of incidence of 45^{o}. For each spectrum, 32 scans were accumulated at 4 cm^{-1} resolution, in the scanning range of 4000-650 cm^{-1}.

2.5.4.2 Ultraviolet-Visible spectroscopy (UV-Vis)

UV-Vis spectra of the samples were obtained using Varian Cary 50 UV-Visible Spectrophotometer; Agilent technologies USA with inbuilt Cary win UV software.

2.5.4.3 X-Ray Diffraction (XRD)

The X-Ray Diffraction (XRD) techniques have been used from long time for the crystallographic study of different materials. This technique is used to investigate various aspects of the structures of semi crystalline polymers. XRD analysis of the samples was carried out using Bruker D 8 discover small angle X-ray diffractometer with 2θ ranging from 5 to 90°.

2.5.4.4 X-Ray Photoelectron Spectroscopy (XPS)

X-ray photoelectron spectroscopy (XPS), also known as Electron Spectroscopy for Chemical Analysis (ESCA), is the widely used surface analysis

technique due to the simplicity in processing and data interpretation. The sample is irradiated with monochromatic X-rays causing photoelectrons to be emitted from the sample surface. An electron energy analyzer determines the binding energy of the photoelectrons. From the binding energy and intensity of the photoelectron peak, the elemental identity, chemical state, and quantity of an element are determined. The XPS also provides insights about the surface layers or thin film structures which gives information about the polymer surface modifications. In this study, the measurements were conducted with X-ray photoelectron spectrophotometer (Ultra axis, Kratos analytical, Shimadzu, Japan) using monochromatic aluminium Kα X-rays (1486 eV).

2.5.5 Thermal analysis

It is important to investigate the thermal characteristics of the electrospun protein based nanofibers before and after cross-linking treatment and the composite nanofibers in order to compare them with neat protein nanofibers. The glass transition temperature, melting temperature, denaturation temperature and thermal degradation are the indications of structural changes which might have occurred after cross-linking treatment or after making composites. Therefore, differential scanning calorimetry (DSC) and thermo gravimetric analysis (TGA) were performed to get information regarding the thermal behaviour of the nanofibers.

The denaturation temperature, glass transition and melting temperatures of gelatin based electrospun nanofibers were evaluated using DSC (Q-20, TA instruments, USA). The temperature calibration was performed using an Indium standard provided by TA Instruments. The samples were heated from -20 °C to 280 °C at a heating rate of 10 °C/min in a T zero aluminium pan under nitrogen environment.

The effect of cross-linking on thermal degradation pattern of the nanofibers was studied by TGA. The analysis was carried out in nitrogen

atmosphere (Q-50, TA instruments, USA). Indium was used to calibrate the temperature reading and the instrument was weight calibrated according to the instruction from TA instruments. The heating rate used was 10 °C/min from room temperature to 600 °C. The results obtained from DSC and TGA were analyzed using TA Universal analysis software. From the TGA data, the derivative thermograms (DTG) were also recorded for the samples.

2.5.6 Viscosity studies

A thorough characterization of the rheological behaviour of polymer solution is essential to optimize the solution parameters in the electrospinning process. It helps to select the appropriate solvent composition and solute concentration for electrospinning process. Rheological behaviour of samples was analyzed by means of Rheometer (Anto paar, MCR 102, USA) using cone and plate accessory (CP 50) with zero gap of 0.106 mm and the cone angle of 0.4°. The experiment was carried out by varying the shear rate and temperature to predict the flow behaviour of polymers under stress and temperature.

2.5.7 Zeta potential

Surface zeta potential is an important feature of material surface and its interaction in biological environments. The zeta potential of the samples was determined to find out the surface positive charges. An increase or reduction in zeta potential is a measure of the presence of charges on the dissociated surface functional groups. In case of gelatin, negatively charged groups such as carboxylic acid cause decrease of zeta, whereas the positively charged groups such as amino groups enhance the zeta potential value. It is highly dependent on environmental pH value and if plotted versus pH, will be positive at low pH and negative at higher pH. Zeta potential of the samples in the present study was determined at 1 % (w/v) concentration in PBS using Zetasizer, Malvern Instrument Ltd (UK). Measurement was carried out using a disposable folded

capillary cell. The folded capillary cell provides the benefits of the accuracy of measurement and eliminates the potential contamination issues.

2.5.8 Gel Permeation Chromatography (GPC)

In this study, the molecular weight and polydispersity of the polymers were determined using GPC instrument (Waters, Singapore). Samples at a concentration of 0.01 mg/ml were eluted with 0.02 M sodium nitrate solution through an ultrahydrogel column (Waters ultrahydrogel columns 2000/1000/500 in series) at a flow rate of 1 ml/min. Dextran standards of molecular weights 3,44,000, 21,100 and 9,600 were used for relative calibration.

2.5.9 Microscopic techniques

2.5.9.1 Scanning Electron Microscopy (SEM)

A scanning electron microscope operating at 20 kV and 10 μA was used to analyze the morphology and size of the nanofibers (FEI- Quanta, FE-SEM). All the samples were mounted using carbon tape on aluminum SEM stubs after gold sputtering.

2.5.9.2 Transmission Electron Microscopy (TEM)

The morphology of the gelatin nanofibers, core-shell nanofibers and composite nanofibers were observed using High-Resolution Transmission Electron Microscope (HRTEM, FEI Tecnai G230). The samples for TEM analysis were prepared by exposing carbon coated copper grid onto the collector for a few seconds. The image was observed using HRTEM at an accelerating voltage of 100 kV.

2.5.9.3 Atomic Force Microscopy (AFM)

Atomic Force Microscope (AFM) is a high-resolution microscopy technique which produces precise topographic images of a sample by scanning the surface with a nanometer-scale probe known as cantilever. Samples for the analysis were prepared by drop casting the dispersion on a mica sheet and characterized after drying, using scanning probe microscope (Agilent 5500, USA) in non contact mode.

2.5.10 Mechanical testing

Mechanical properties of the nanofibrous mats were determined by Universal Testing Machine (Instron 5050, Instron USA) with a load cell of 100 N capacity. Specimens were cut in the form of rectangular strips (6 × 0.4 cm^2) with an average thickness of 0.2 mm, and tested at a crosshead speed of 10 mm/min. Stress at break and Young's modulus were measured based on stress-strain curve.

2.5.11 Swelling characteristics

Swelling behaviour of electrospun mats was examined in phosphate buffered saline (PBS) at 37 °C for different time intervals (Draye et al., 1998). The swelling behaviour of as spun and the cross-linked mats were measured by swelling the mats in 10 ml of PBS (0.1 M, pH 7.4) at 37 °C. Pre-weighed dry mats (approximately 0.05 g) were immersed in PBS for a stipulated time. The mats were withdrawn from the solutions at different time intervals and their swollen weight was determined after blotting with a filter paper. The swelling ratio was calculated using the equation 2.2

$$Swelling\ ratio\ (\%) = \left(\frac{W_s - W_d}{W_d}\right) X\ 100 \qquad (2.2)$$

(Where W_d and W_s are the weights of the samples in the dry and swollen states,

respectively).

2.5.12 *In vitro* degradation

In vitro degradation of as spun and cross-linked mats was evaluated in PBS. Previously weighed and dried samples were immersed in 5 ml of PBS at 37 °C for time periods ranging from one week to five weeks. Experiment was performed in aseptic conditions. Different sets of samples were used for each week. After the predetermined time period, medium was removed and weights of the samples were measured after lyophilization.

$$Weight\ ratio\ = \left(\frac{W_2}{W_1}\right) \tag{2.3}$$

Where, W_1 and W_2 are the initial and final weights of the sample

2.6 Biological Characterization

2.6.1 *In vitro* biocompatibility evaluation of nanofibers using mouse fibroblast cells (L-929)

2.6.1.1 Cleaning and sterilization of nanofiber samples

The cross-linked nanofibrous samples with adequate dimensions were rinsed for 5 min with double distilled water for around 10 times. The cleaned samples were dried in vacuum desiccators for 2-3 days. The dried samples were dipped in 70 % ethanol and exposed to UV ray for 15 min. After 15 min, the ethanol was removed and the samples were washed with PBS for three times prior to the cell culture experiments.

2.6.1.2 *In vitro* cytotoxicity evaluation – Direct Contact Test

An *in vitro* cytotoxicity test by direct contact method was performed on cross-linked nanofiber mats with high density polyethylene (HDPE) and stabilized

poly vinyl chloride (PVC) as negative and positive controls respectively as per ISO 10993-5. Mouse subcutaneous fibroblast cells (L-929 cell line, American Type Cell Culture Collection) were maintained in MEM supplemented with 10 % FBS, 100 IU/ml Penicillin and 100 µg/ml Streptomycin in a CO_2 incubator (Sanyo, Japan) set at 37 °C, 5 % CO_2 and > 90 % relative humidity. The cells were detached using trypsin and seeded in a 24 well plate at a density of 1×10^5 cells per well. When the cells reached subconfluency, sterilized nanofibrous samples, negative control and positive control having approximate size of 10 % of cell area were placed on the cells. The cells were incubated inside CO_2 incubator for 24 - 26 h. Cytotoxicity was assessed by observing the cells around the test and control samples under phase contrast microscope (Motic AE31, Hong Kong).

2.6.1.3 MTT assay

Cell proliferation was analyzed by 3-(4,5-dimethylthiazol-2-yl)-2,5-diphenyltetrazolium bromide (MTT) assay (Ciapetti et al., 1993). MTT assay is performed to measure the metabolic activity of the cells to reduce yellow coloured tetrazolium salt to purple coloured formazan. Sterilized samples were washed with 1xPBS for three times. Trypsinized mouse fibroblast cells (L929) were seeded on the samples (2000 cells/ sample) and incubated for specific time period under standardized conditions (humidified incubator with 37 °C and 5 % CO_2). After every 72 h, the cell culture medium was replenished with fresh one. After 3^{rd} and 5^{th} day, the samples were washed with PBS solution and incubated with MTT solution (0.5 mg/ml) for 4 h at 37 °C. After 4 h, the MTT solution was replaced with DMSO solution to dissolve the formazan crystals. Spectrophotometric analysis of the DMSO solution was done using ELISA reader (BioradiMark) at 595 nm.

Quantitative assessment of cytotoxicity of cross-linked nanofiber mats was carried out using the extract of the materials with L-929 cells using MTT assay. Extracts of cross-linked nanofiber mats were prepared by incubating 3 cm^2 of each of the sample with culture medium with serum at 37±1 °C for 24 ± 2 h.

Cells cultured in normal medium were considered as control. Extract of the test samples (100 %) in triplicate were placed on subconfluent monolayer of L-929 cells. After incubation of the cells with the test samples and controls at 37 ± 1 °C for 24 ± 2 h and 72 ± 2 h, extracts and the control medium were replaced with 50 µl of MTT solution (1mg/ml in medium without supplement), wrapped with aluminium foil and were incubated at 37 ± 2 °C for 2 h. After discarding the MTT solution, 100 µl of isopropanol was added to all the wells and swayed the plate. The colour developed was quantified by measuring absorbance at 595 nm using a spectrophotometer. The data obtained for the test samples were compared with the cell control.

2.6.1.4 Cell adhesion and viability

Cells were allowed to adhere and grow on the cross-linked nanofiber mats for 48 h and then processed for analyzing cell adhesion and morphology. The mats were seeded with L-929 cells at a density of 2000 cells/cm^2 and cultured for 48 h. Cells cultured on cover glass were considered as control. The viability of the cells adhered on the mats was examined by incubating with FDA (10 µg/ml in serum free medium) for 5 min followed by treatment with PI (1 µg/ml) for 5 min. Stained samples were observed under fluorescence microscope (Leica DMIL, 6000B, Germany) using the filter cubes designated for FDA (I3) and PI (N 2.1).

The cell adhesion was analyzed by visualizing the morphology of the adhered cells by staining the actin cytoskeleton structures. L-929 cells were seeded on cross-linked nanofiber mats and control glass cover slips as described above and cultured for 48 h. Cells were fixed using 4 % paraformaldehyde for 2 h and rinsed with PBS. The cell membrane was permeabilized by treating with 0.1 % Triton-X 100 for 1 min and actin filaments were stained by incubating the samples with rhodamine-phalloidin (1:1000 dilution in PBS) for 15 min. The cell nucleus was counter stained using Hoechst 33258 dye (0.1 µg/ml in PBS). The cell adhesion was observed under fluorescence microscope using Leica filter cubes specified for Hoechst (A) and Rhodamine (N2.1).

2.6.2 *In vitro* biocompatibility evaluation of nanofibers using human osteoblast-like cells (MG-63)

2.6.2.1 Cleaning and sterilization of nanofiber samples

The nanofiber samples were sterilized by 70 % ethanol followed by exposure to UV ray in a similar manner as explained in section 2.6.1.1.

2.6.2.2 MTT assay

Cell proliferation was analyzed by MTT assay. The sterilized samples (0.5 cm x 1 cm) were washed with 1xPBS for three times. MG-63 cells were seeded on the samples (2000 cells/sample) and incubated for specific time period under standardized conditions (humidified incubator with 37 ºC and 5 % CO_2). After every 72 h, the cell culture medium was replenished with fresh one. After 3^{rd} and 5^{th} day, the samples were washed with PBS solution and incubated with MTT solution (0.5 mg/ml) for 4 h at 37 ºC. After 4 h, the MTT solution was replaced with DMSO solution to dissolve the formazan crystals. Spectrophotometric analysis of the DMSO solution was done using ELISA reader (BioradiMark) at 595 nm.

2.6.2.3 Alamar blue assay

The proliferation of MG-63 cells at different day points on the mats was investigated using Alamar blue assay. The cell seeded mats were transferred to a new 24 well tissue culture plate aseptically. On the desired day point (day1, day 3, day 5 and day 7), the spent supernatant medium was removed and Alamar blue solution (diluted 1:10 in incomplete DMEM medium) was added to the mats following manufacturers' protocol. The plates were incubated in CO_2 incubator for 4 h under dark. After incubation, the supernatant medium was collected in a new 96 well flat bottom tissue culture plate and fresh medium was added in each mat allowing the cells to grow. Reduction of the dye was measured

photometrically using 570 nm and 600 nm filters of a microplate reader (Thermo Scientific Multiskan Spectrum, Japan).

2.6.2.4 Cell adhesion and viability

The cell adhesion was analyzed by visualizing the morphology of the adhered cells by staining the actin cytoskeleton structures. After the stipulated time period, MG-63 cells were fixed (48 h and 5^{th} day respectively) using 4 % paraformaldehyde for 1 h at room temperature and rinsed with PBS. The cell membrane was permeabilized by treating with 0.1 % Triton-X 100 for 5 min and actin filaments were stained by incubating the samples with rhodamine - phalloidin (1:500 dilutions in PBS) for 1 h. The cell nucleus was counter stained using Hoechst 33258 dye (1:600 dilutions in PBS) by incubating the samples with the dye for 5 min. The cell adhesion was observed under confocal laser scanning microscope (Olympus Fluo View FV 1000) using 405 nm laser for Hoechst and 543 nm laser for rhodamine - phalloidin.

2.6.3 Antibacterial activity analysis

2.6.3.1 Agar diffusion method

Antibacterial activity of GO-Gelatin and gentamicin loaded GO-Gelatin nanofibrous mats was evaluated on two bacterial strains, namely, *E. coli* ATCC 25922 and *S. aureus* ATCC 25923 (Kim et al., 2000). The test microorganisms were inoculated into the Mueller Hinton agar plate at a density of 1 x 10^5 cfu/ml by pour plate method. The mats (6 mm diameter discs) were placed on the agar plate and incubated at 37 °C for 48 h. After 2 days, the mats were removed and then the agar beneath the mats was cut out and homogenized in 5 ml of sterile PBS. The PBS was then subjected to serial dilution. The dilutions were subcultured on nutrient agar plates and incubated for 2 days at 37 °C. The number of colonies grown in all the plates was counted and total count was thus calculated. All the experiments were done in triplicate.

2.6.3.2 Bacterial adhesion method

The adhesion behaviour of *E. coli* ATCC 25922 and *S.* aureus ATCC 25923 bacterial strains on DA-GO-GEL and gentamicin loaded DA-GO-GEL mats were tested by incubating the materials along with bacterial strains at 37 °C for 18 h. The number of bacteria adhered on the samples were determined by observing the test bottles after overnight incubation. The turbidity shows the presence of bacterial cells and clear solution indicates the absence of bacterial adhesion.

2.6.4 Statistical analysis

Statistical analysis for the determination of difference in mean among the groups was accomplished by one way ANOVA (using Origin Pro 8.5 software). At least 8 replications were analyzed from each sample of each day point. The symbol '***' denotes statistically significant difference among the groups at alpha value 0.001. Statistical analysis of two sets of data was performed by Student's t-test with $p < 0.05$ (shown by the symbol '*') considered as being statistically significant. All the data are presented as mean value with standard error (mean ± SE).

CHAPTER 3

FABRICATION OF GELATIN NANOFIBERS BY ELECTROSPINNING AND CROSS-LINKING WITH OXIDIZED DEXTRAN

3.1 Introduction

Gelatin is a biopolymer obtained from partial denaturation of collagen, a major structural protein present in the human body. Gelatin does not show antigenicity and has high haemostatic properties compared to its precursor collagen. Moreover, gelatin is biodegradable, biocompatible and displays many integrin binding sites for cell adhesion and differentiation (Kuijpers et al., 2000; Lu et al., 2011). Electrospun gelatin nanofibers are a promising class of biomaterials possessing excellent biocompatibility, non-cytotoxicity, structural and functional resemblance with native extracellular matrix (ECM) (Huang et al., 2004; Tonda-Turo et al., 2013a; Wu et al., 2011). These are found to be potential candidates for tissue engineering scaffolds, drug delivery matrices, wound dressing materials, etc. Fabrication of gelatin nanofibers by electrospinning is challenging in the field of bioengineering, due to the lack of suitable solvent system for electrospinning. Huang et al fabricated gelatin nanofibers using trifluoroethanol (TFE) as the solvent (Huang et al., 2004). Other solvents which are conventionally being employed for electrospinning of gelatin are formic acid (Ki et al., 2005), hexafluoroisopropanol (HFIP) (Kim et al., 2005), etc. However, most of the organic solvents cause severe toxicity to the cells and hence there is an attempt in recent times to replace these solvents by benign solvents such as water at elevated temperature and acetic acid/water mixture (50 ^{o}C) (Pandya et al., 2010; Panzavolta et al., 2011).

Gelatin nanofibers when in contact with water, lose the fibrous morphology due to high hydrophilicity and solubility. Hence, a cross-linking treatment is necessary to improve the water resistant ability as well as mechanical performance to make them suitable for biomedical applications. Gelatin nanofibers are subjected to cross-linking treatment with various cross-linking agents, the most effective one being glutaraldehyde (GT) (Zhang et al., 2006). Cross-linking is achieved either by dipping the nanofibers in GT solution or by exposure to the vapours. In many instances, carbodiimide chemistry is being exploited in realizing the cross-linking of gelatin nanofibers. In this case, nanofibers are dipped in ethanolic solution of 1-ethyl-3-(3-dimethyl aminopropyl) carbodiimide (EDC) in presence of N-hydroxysuccinimide (Li et al., 2006b). These materials either released into the body due to degradation or remaining unreacted in the nanostructures may lead to toxicity (Hao et al., 2011; Panzavolta et al., 2011; Zhang et al., 2006). Recently, Panzavolta et al. have shown that genipin, a naturally occurring material, could be an alternative cross-linking agent for gelatin nanofibers. Cross-linking of the nanofibers is achieved by dipping the nanofibrous mat in ethanolic solution of genipin (Panzavolta et al., 2011). In many aspects, genipin is found to be a better cross-linking agent compared to those mentioned earlier, but the high cost of genipin can limit its applicability. Cross-linking of gelatin nanofibers with polysaccharide is another attractive possibility as demonstrated in the case of gelatin hydrogels. This approach has not been attempted for the cross-linking of nanofibers. However, polysaccharides are soluble only in aqueous medium where the gelatin nanofibers would dissolve, resulting in the complete destruction of the fibrous morphology. Thus, it is necessary to use a suitable cross-linking medium in which solubility of polysaccharide is realized without compromising the fiber morphology.

In this chapter, the fabrication of gelatin nanofibers using a benign solvent system and an innovative cross-linking approach to minimize the toxicity effects from solvents and cross-linking agents are illustrated. Gelatin is dissolved in water/acetic acid (8:2, v/v, i e, 20 % acetic acid) mixture and eventually electrospun to form nanofibers with diameter in the range of 150 ± 30 nm. Here,

the feasibility of utilizing modified polysaccharide, namely, dextran aldehyde (DA) for the cross-linking of gelatin nanofibers is demonstrated. DA from dextran of molecular weight, M_r ~ 40,000 can be dissolved in ethanol in the presence of minimum quantity of aqueous borax. Nanofibers are cross-linked by dipping in this medium and the cross-linked nanofibers are found to maintain the fibrous morphology even after keeping in contact with water. The feasibility of these cross-linked nanofibers to be used in biomedical applications is demonstrated in terms of cytotoxicity, cell adhesion and proliferation using mouse fibroblast cells (L-929) and human osteoblast like cells (MG-63). These results demonstrate that dextran aldehyde cross-linked gelatin nanofibers (DA-GNF) are non-cytotoxic, biocompatible and can promote cell adhesion and proliferation.

3.2 Results and Discussion

3.2.1 Fabrication of gelatin nanofibers

Electrospinning of gelatin in water cannot be realized at room temperature due to its gel forming property below 35 ^{o}C. This is due to the aggregation of gelatin molecules owing to inter and intra molecular interactions (Zandi, 2008). Hence in this work, acetic acid is employed to prevent the gelation. However, it has been reported that high concentration of acetic acid in water (6:4 (v/v) acetic acid/water) can cause degradation of gelatin (Panzavolta et al., 2011). So, an attempt has been made to use lower concentration of acetic acid without prompting the degradation. Smooth and fine nanofibers are obtained using 8:2 (v/v) water/acetic acid mixture. Presence of 20 % acetic acid in the solvent system is essential to prevent the gelation (Figure 3.1).

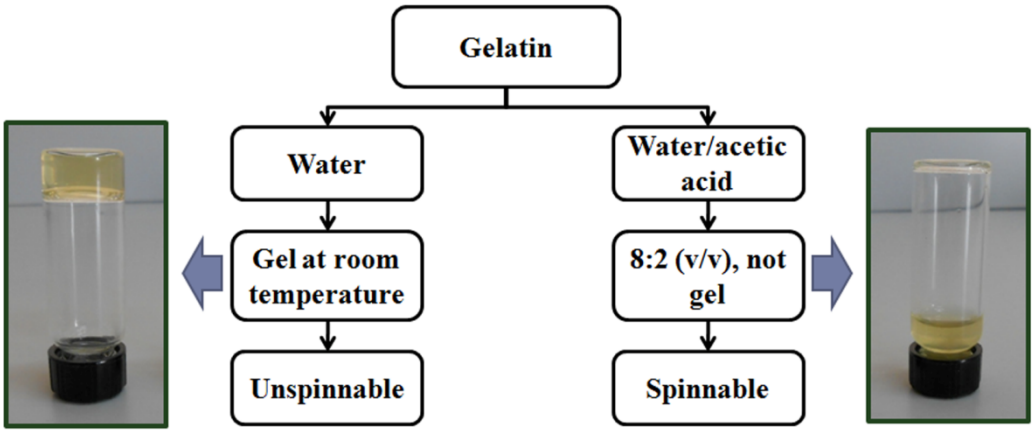

Figure 3.1: Effect of acetic acid on gelling behaviour of gelatin in aqueous medium

Solutions for electrospinning are prepared by dissolving different concentrations of gelatin (24 % w/v to 30 % w/v) in 8:2 (v/v) water/acetic acid solvent system. It is found that, as the concentration increases, the fibers become smoother with lesser beads. A gelatin concentration of 30 % w/v is found to produce smooth fibers with minimum number of beads. This is illustrated by the SEM images shown in Figure 3.2. It is found that gelatin type A (bloom 225) is giving better fibers in the concentration range of 28 - 30 % (w/v) in 8:2 water/acetic acid solvent. For further studies, nanofibers produced from 30 % w/v gelatin are used. Figure 3.3 shows the fiber diameter distribution of the nanofibers fabricated from 30 % w/v gelatin, obtained by measuring the diameters of randomly selected 150 individual fibers from SEM images using ImageJ software. The smooth fibers with 150 ± 30 nm are obtained by adjusting the solution and spinning parameters by trial and error optimization procedures. The optimized solution and electrospinning parameters are listed in Table 3.1.

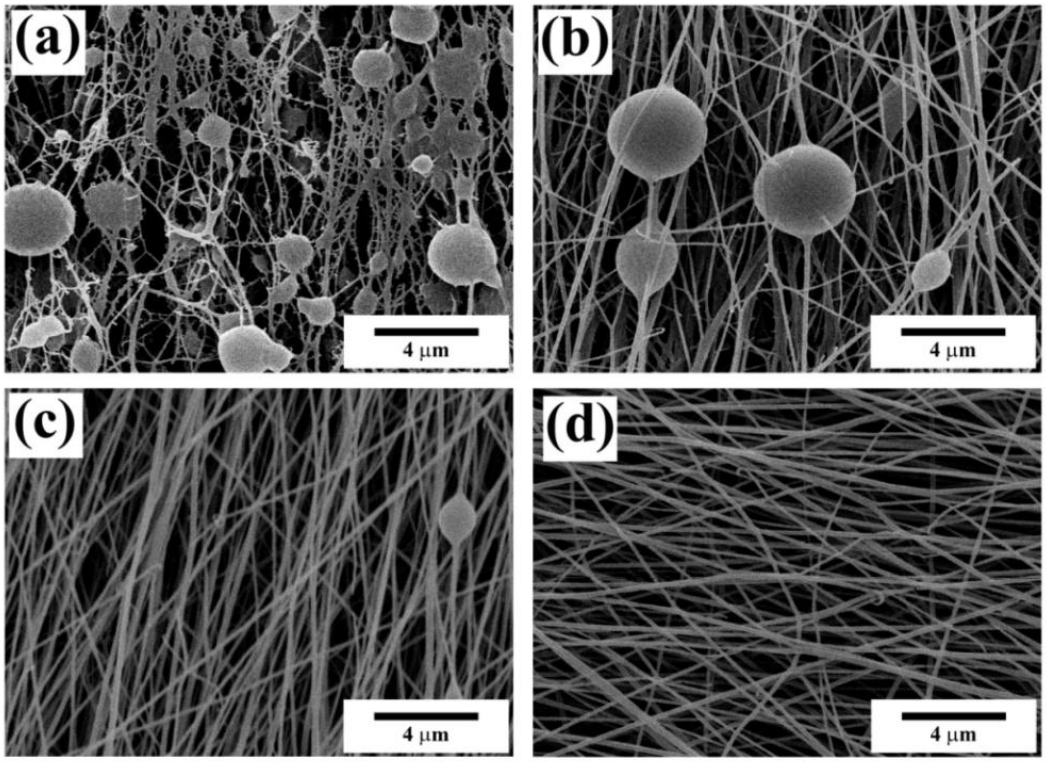

Figure 3.2: SEM images of electrospun gelatin nanofibers fabricated from (a) 24 %, (b) 26 %, (c) 28 % and (d) 30 % (w/v) gelatin solutions

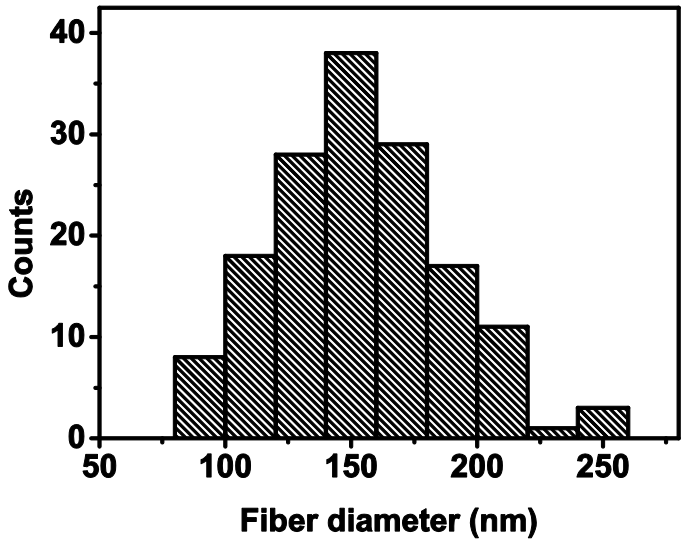

Figure 3.3: Fiber diameter distribution of the nanofibers fabricated from 30 % w/v gelatin

Table 3.1: Optimized conditions for electrospinning of gelatin

Parameters	Optimized Conditions
Solvent system	8:2 (v/v) water/acetic acid
Concentration of the polymer solution	30 % (w/v)
Flow rate	0.3 ml/h
Voltage applied	25 kV
Working distance	15 cm
Drum collector speed	1500 RPM

3.2.2 Water stability of gelatin nanofibers: Requirement of cross-linking treatment

When in contact with water, gelatin nanofibers lose the fibrous morphology completely, due to the high solubility of gelatin in water. It has been found that electrospun fibers gradually form point bonds at the fiber junctions if placed in a high humidity (80 – 90 %) for a certain period of time (Zhang et al., 2006). Researchers have adopted different cross-linking approaches to overcome these issues. In the present work, a polysaccharide, namely, dextran into which aldehyde functional groups are introduced by periodate oxidation is employed as the cross-linking agent. Dextran aldehyde (DA) is prepared by controlled oxidation of dextran by sodium metaperiodate. Schematic representation of the formation of DA is shown below in Figure 3.4.

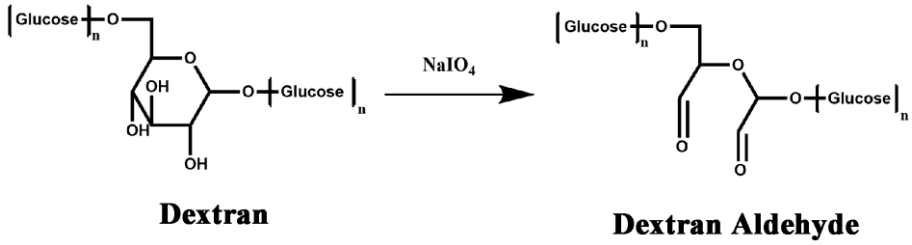

Figure 3.4: Schematic of the formation of DA using $NaIO_4$

FTIR spectra of dextran and DA are shown in Figure 3.5. The spectrum of dextran contains a broad band at 3290 cm^{-1} due to the –OH stretching. The bands within 1500 – 900 cm^{-1} belong to the fingerprint region of CH deformation, CO stretching and OH bending modes of dextran. The bands at 1150 and 1000 cm^{-1} have been assigned to the glycosidic linkage of dextran. The spectrum of DA shows two additional peaks at 1738 and 2851 cm^{-1} besides the absorption bands from dextran. These peaks are associated with stretching of –C=O and –C–H bonds respectively, due to the aldehyde groups of DA.

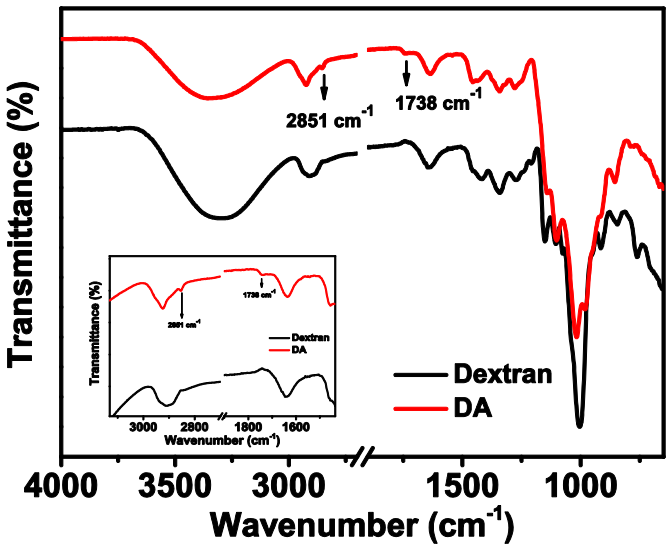

Figure 3.5: FTIR spectra of dextran and DA

The aldehyde content and degree of oxidation in DA are measured by hydroxylamine hydrochloride reaction followed by titration with NaOH. DA is found to be 87 % oxidized with aldehyde content of 10.7 ± 0.25 x 10^{-3} mol/g (Table 3.2). Weight average molecular weight (M_w) and polydispersity indices (PDI) of dextran and DA are obtained by GPC analysis (Table 3.2). It can be seen that there is little variation in the M_w of dextran and DA. The polydispersity of DA is higher (PDI = 3.5) than dextran (PDI = 1.86) due to the excess amount of periodate used for the oxidation (Sokolsky-Papkov et al., 2006). Apart from the oxidation of cis-diol groups, $NaIO_4$ might have caused the formation of low molecular weight products.

Table 3.2: Properties of dextran and DA

Properties	Dextran	DA
Degree of oxidation (%)	0	87 ± 2 %
Aldehyde content (mol/g)	0	$10.7 \pm 0.25 \times 10^{-3}$
Weight average molecular weight (M_w)	37352	36489
Polydispersity index	1.86	3.5

3.2.3 Cross-linking and characterization of gelatin nanofibers

The cross-linking agents need to be dissolved in an appropriate medium in which the nanofibers would be placed for cross-linking reaction to occur. The selected medium should be able to dissolve the cross-linking agent without affecting the nanofibrous morphology. Polysaccharide aldehydes are soluble only in aqueous solutions (either in PBS or in borax solution). High molecular weight dextran (M_r ~ 500,000) and low molecular weight dextran (M_r ~ 40,000) are oxidized and attempted to be used as cross-linking agents. DA obtained from high molecular weight dextran is found to be soluble only in aqueous borax or PBS. However, it can be dissolved in 7:3 (v/v) ethanol/water mixture in presence of minimum amount of borax. Cross-linking is carried out by dipping the gelatin mat in this medium for different time periods. However, cross-linked mats completely lose the fibrous morphology due to the presence of 30 % water in the medium. Hence, the possibility of using DA obtained from low molecular weight dextran is considered. This DA can be dissolved in ethanol containing minimum quantity of aqueous borax solution (300 μl of 0.015 M borax in 10 ml ethanol). The concentration of DA in ethanol is optimized to be 0.5 % w/v based on the maximum amount of DA that can be dissolved in the ethanol-borax medium. Addition of more borax would cause DA to be precipitated from ethanol. Thus, the dissolution of DA (0.5 % w/v) in ethanol is ensured by keeping the amount of water to be as minimum as possible. Nanofibrous mats are kept immersed in this cross-linking medium for 1, 3 and 5 days for cross-linking. Figure 3.6 shows the SEM images of as spun mat (a), mat after immersing in water (b), mat after

immersing in ethanol containing minute amount of borax for 5 days (c), mat cross-linked with high molecular weight dextran-derived DA in 7:3 ethanol/water (d) and mat cross-linked with low molecular weight dextran-derived DA in ethanol containing minute amount of borax (e). It is clear that, slight swelling and hence an increase in diameter is occurred when the mats are dipped for 5 days in the cross-linking medium without DA. The mat cross-linked with low molecular weight dextran-derived DA in ethanol containing minimum amount of aqueous borax maintains the structural integrity of the nanofibers. Hence, for further studies, cross-linking with low molecular weight dextran-derived DA is employed.

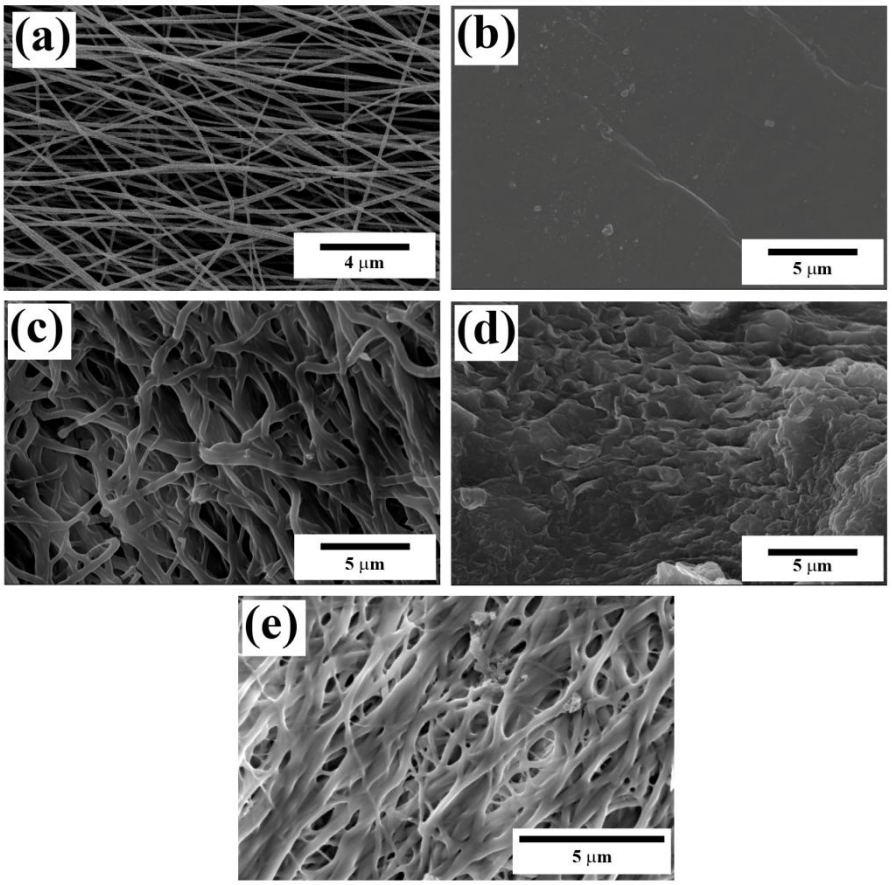

Figure 3.6: SEM images of (a) as spun mat, (b) as spun mat after dipped in water, (c) mat after dipped in ethanol/borax medium for 5 days, (d) mat cross-linked in high molecular weight dextran-derived DA in 7:3 ethanol/water and (e) mat cross-linked with low molecular weight dextran-derived DA in ethanol/borax medium

The effect of cross-linking is examined by keeping the mats in aqueous medium for 1 h. It is observed that the sample cross-linked for 1 day becomes transparent and sticky, while the samples cross-linked for 3 and 5 days remain intact. Figure 3.7 (a) shows the photograph of gelatin mat cross-linked for 5 days and as spun mat immersed in water. Schematic representation of cross-linking reaction between aldehyde groups of DA and amino groups of gelatin side chains in the nanofibrous structure is shown in Figure 3.7 (b). Cross-linking is occurred by the Schiff's base formation between primary amino groups of gelatin side chain and carbonyl groups of DA. The cross-linking site mentioned in the cartoon represents the aldimine linkage formed as the result of cross-linking.

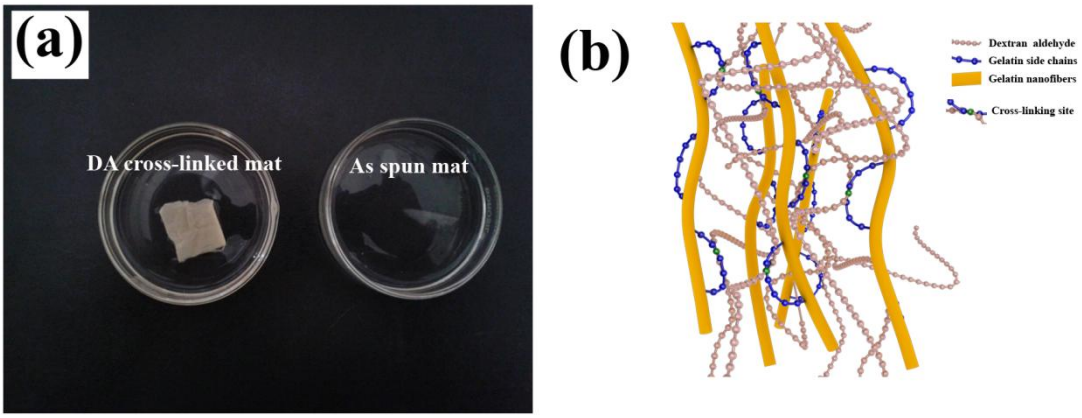

Figure 3.7: (a) DA cross-linked and as spun gelatin mats immersed in water medium, (b) schematic representation of cross-linking between aldehyde groups of DA and amino groups of gelatin in the nanofibrous structure

Morphological analysis of the cross-linked fibers is carried out by SEM. The morphologies of cross-linked and swelled mats are shown in Figure 3.8. The images reveal that the samples have undergone cross-linking and can maintain the fibrous structure after cross-linking treatment. The mat cross-linked for 5 days exhibits better morphology after swelling in water (Figure 3.8 (e)) compared to the mats cross-linked for 1 and 3 days (Figure 3.8 (b) and 3.8 (d)). It can be seen that, swelling the mats in water causes the fibers to fuse together in the case of mats cross-linked for 1 and 3 days. Whereas, the mat cross-linked for 5 days shows discrete fibrous morphology. However, fiber diameter is found to increase as a result of the cross-linking treatment and increases further after swelling in

water (Table 3.3). Diameter of the fibrous component is an important parameter when considering the material as scaffold for tissue regeneration. The diameter of the nanofibers before cross-linking is 150 ± 30 nm while the diameter after 5 days of cross-linking are found to be 220 ± 65 nm and 280 ± 90 nm before and after swelling, respectively. Such small size fibers can physically mimic the structural dimension of the extracellular matrix of various native tissues and organs, which are deposited and proliferated on fibrous structures ranging from nanometers to micrometers (Ramakrishna et al., 2005). Human cells can attach and proliferate in good health around fibers with diameters smaller than those of the cells. Hence, the fibrous scaffolds prepared from electrospinning can be considered as ideal candidates as matrices for tissue regeneration (Xu et al., 2004; Zhang et al., 2006).

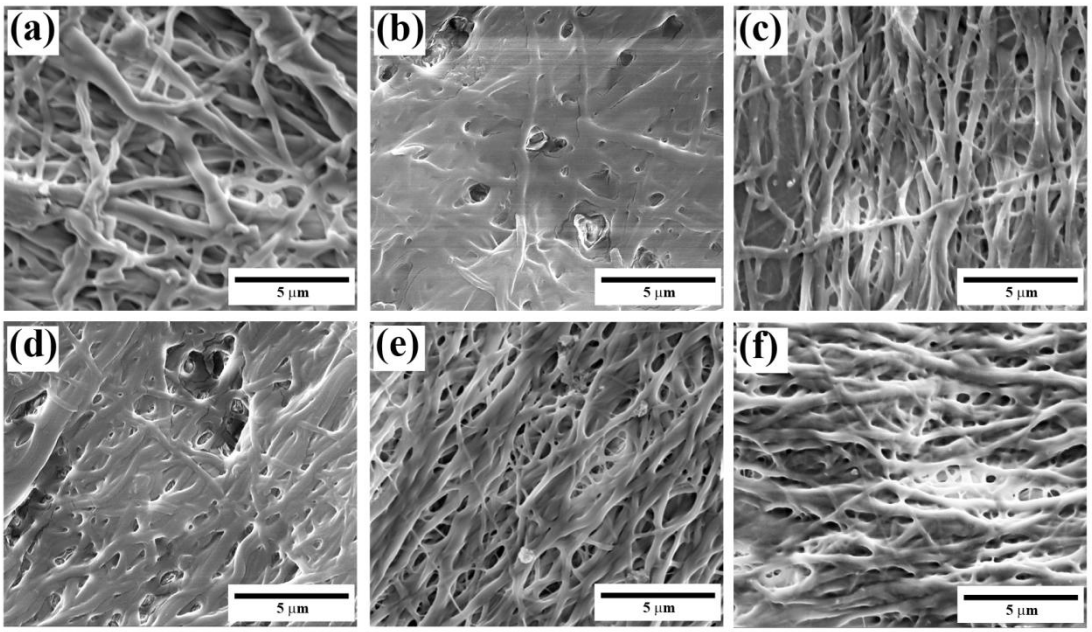

Figure 3.8: SEM images of (a) 1 day cross-linked mat, (b) 1 day cross-linked mat after swelled in water, (c) 3 days cross-linked mat, (d) 3 days cross-linked mat swelled in water, (e) 5 days cross-linked mat and (f) 5 days cross-linked mat swelled in water (swelling is performed for 24 h)

Table 3.3: Fiber diameters of as spun and DA-GNF mats cross-linked for different time periods before and after swelling in water. Mean ± standard deviations are reported.

Cross-linking time (days)	Diameter (nm)	
	Before swelling in water	After swelling in water
0	150 ± 30	No fibrous structure
1	258 ± 90	390 ± 100
3	225 ± 70	360 ± 100
5	220 ± 60	280 ± 90

The cross-linking of gelatin nanofibers occurs by Schiff's base reaction of amino groups of gelatin with aldehyde groups of DA. The cross-linking reaction is found to progress slowly as evident from the required time of at least 5 days for maintaining the fibrous morphology in aqueous medium. The cross-linking reaction between amino groups of gelatin and aldehyde groups of polysaccharide in presence of aqueous borax is reported to be very fast, where both the reacting species are dissolved in aqueous medium (Balakrishnan and Jayakrishnan, 2005). However, in the present work, gelatin is in solid phase and the cross-linking agent, DA is in ethanolic medium resulting in the prolonged time required for cross-linking.

Cross-linking of gelatin nanofibers with genipin has been carried out by dipping the nanofibrous mat in ethanolic solution of genipin (Panzavolta et al., 2011). Even though, genipin is a small molecule which can penetrate into the fibrous mats easily, effective cross-linking is achieved after dipping the nanofibrous mats in the medium for 5 to 7 days. DA is a large molecule and cross-linking would have happened on the surface of the nanofibers. Here, effective cross-linking can be achieved by dipping the fibrous mats for 5 days in the cross-linking medium. Hence, the mats cross-linked with DA for 5 days (DA-GNF) are selected for further characterizations.

The extent of cross-linking is estimated by comparing the unreacted ε-amino groups in DA-GNF and as spun mats using TNBS assay. The degree of cross-linking is found to be 42 ± 2 %. Cross-linking of gelatin nanofibers with glutaraldehyde and genipin have resulted in higher cross-linking degrees (~ 90 %) (Panzavolta et al., 2011; Wu et al., 2011). The lower cross-linking degree obtained in the present work can be justified on the basis of the macromolecular nature of the cross-linking agent employed. The swelling ability of a scaffold in water is an important aspect for its suitability for various tissue engineering applications. The swelling behaviour of DA-GNF and as spun nanofibers is studied and the results indicate the effect of cross-linking on the swelling properties. These results demonstrate that swelling ratio of the DA-GNF mat is significantly lower than that of as spun mat (Figure 3.9). Swelling of the nanofiber mat is reduced due to the cross-linking treatment. The higher swelling ratio of as spun mat is due to the large amount of water absorption of the highly porous structure of the fibrous mats. The experiment cannot be performed for as spun mat beyond 40 min because of the dissolution. The DA-GNF mat attains equilibrium swelling within 20 min.

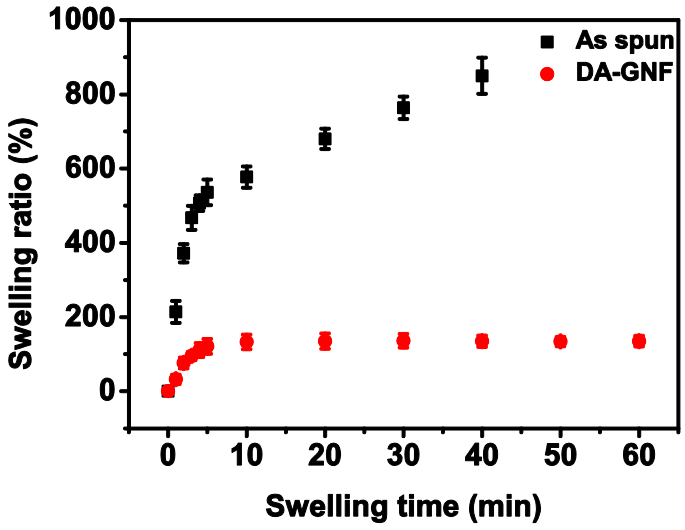

Figure 3.9: Swelling characteristic of as spun and DA-GNF (5-days cross-linked) mat

The degradation behaviour of the nanofibers is evaluated by examining the weight loss of the nanofibers with time in PBS at 37 °C. Figure 3.10 shows the

degradation behaviour of as spun and DA-GNF mats. It can be seen that the as spun mats dissolve completely in the first week itself. The DA-GNF mat is found to be stable for one week and thereafter shows a linear decrease in weight up to four weeks. The complete dissolution of the mat occurs at the end of five weeks demonstrating the degradability of the nanofiber mats in the physiological pH. A comparison of the degradation behaviour of DA-GNF mat with glutaraldehyde (GT) cross-linked gelatin mat (GT-GNF) is also carried out. It is found that the latter exhibits similar degradation behaviour as that of DA-GNF mat. Gradual degradation of DA-GNF mat with time would make them suitable matrices as tissue engineering scaffolds. The hydrolytic susceptibility of Schiff's base and the biodegradability of gelatin and DA cause the degradation and dissolution of the cross-linked nanofibers. Degradation profile of the nanofibers is mainly determined by the polymer itself as hydrolysis of the polymer backbone is believed to be the usual mechanism. Gelatin contains random coil structure (amorphous) with occasional triple helical region (crystalline). In the absence of an enzyme, water penetrates the surface of the nanofiber mat and preferentially attacks the amorphous region, converting the long polymer chains into shorter and eventually water-soluble species. Since the crystalline regions are still intact, the nanofibers do not fall apart. When hydrolysis continues, the nanofibers eventually start to disintegrate and disappear (Liu et al., 2012).

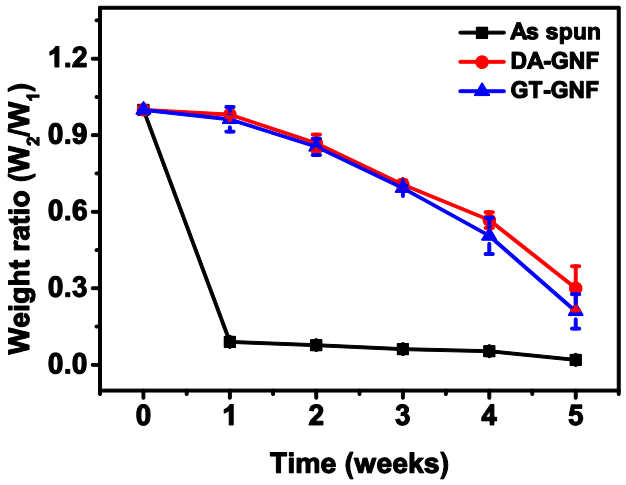

Figure 3.10: Degradation behaviour of as spun, DA-GNF (5 days cross-linked) and GT-GNF mats

The effect of DA cross-linking on the chemical composition of the surface of the gelatin mat is determined by XPS measurements. Survey scan spectrum of gelatin nanofiber mat, DA and DA-GNF mat (Figure 3.11) also shows the incorporation of DA into gelatin mat after the cross-linking reaction. The decrease in the intensity of N1s peak shows the relative increase in the C and O atomic compositions on the surface of the cross-linked mat. Table 3.4 gives the atomic composition of gelatin and DA-GNF surfaces obtained from high resolution XPS spectra. The results show that DA-GNF mat exhibits higher values compared to gelatin mat for C/N ratio (7.3 versus 3.59) and O/N ratio (2.7 versus 1.29). This is due to the fact that during cross-linking, polysaccharide moieties are introduced on gelatin *via* imine bond formation by the reaction between aldehyde groups of DA and primary amino groups of gelatin. Consequently, percentage atomic composition of carbon and oxygen increases, enhancing the C/N and O/N ratio. This indicates the incorporation of DA into the gelatin network and shows the presence of DA moieties on the surface of the mats.

Table 3.4: Elemental composition of as spun gelatin mat, DA and DA-GNF mat from high resolution XPS spectra

Element	**As spun**	**DA-GNF**	**DA**
C (%)	61	66	57
N (%)	17	9	0
O (%)	22	25	43

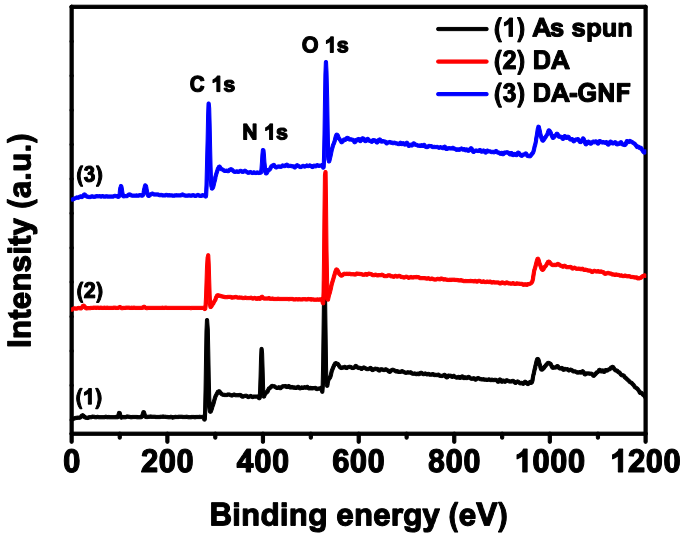

Figure 3.11: XPS survey scan spectra of as spun gelatin mat, DA and DA-GNF mat

FTIR spectra of DA, as spun and DA-GNF mats are given in Figure 3.12. The cross-linked mat (DA-GNF) shows the characteristic peaks of gelatin and dextran. The presence of dextran moieties in the DA-GNF mat can be inferred from the characteristic C-O-C stretching band of DA observed at 1012 cm^{-1}.

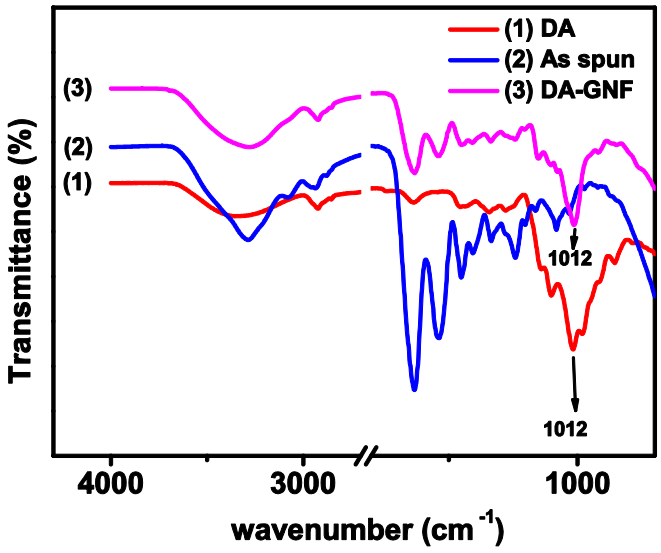

Figure 3.12: FTIR spectra of dextran, DA, as spun mat and DA-GNF mat

TGA and DSC analysis are performed on as spun and DA-GNF mats in order to investigate the effect of cross-linking on the thermal stability of the

nanofibers. TGA thermograms and its first order derivative curves (DTG) of as spun and DA-GNF mats from 25 to 500 °C are presented in Figure 3.13 (a). The TGA plot of pure gelatin in this range normally displays two stages of weight loss. That is, loss of water, between 25 and 100 °C and gelatin decomposition, between 250 and 450 °C. DTG thermograms show that as spun mat exhibits maximum decomposition at 291 °C while it has been shifted to 304 °C in the case of DA-GNF mat demonstrating an improved thermal stability upon cross-linking. DSC thermograms of as spun and DA-GNF in the range of -20 to 250 °C are carried out in order to identify the effect of cross-linking on the thermal transitions of gelatin nanofibers. The DSC thermogram of gelatin exhibits two endothermic peaks corresponding to helix to coil transition in the range of 90 to 110 ^{o}C and decomposition of gelatin in the range of 200 to 230 ^{o}C. On comparing the DSC curves of as spun and the cross-linked mats, it is found that the denaturation temperature of as spun mat is 88 ^{o}C which is shifted to 101 ^{o}C after cross-linking (Figure 3.13 (b)). This observation confirms that the DA-GNF has higher thermal stability than the as spun fibers. Zhang et al (2006) have reported similar thermal behaviour for glutaraldehyde cross-linked gelatin nanofibers (Zhang et al., 2006).

The mechanical properties of as spun and DA-GNF mats are examined. The stress-strain behaviour of as spun and DA-GNF mats is shown in Figure 3.14. Based on the stress-strain measurements of these membranes, tensile strength and Young's modulus are summarized in Table 3.5. The results indicate that the cross-linking treatment significantly improves the mechanical performance of gelatin nanofibers. After cross-linking, both the tensile strength and modulus are enhanced about three times than those of the as spun gelatin nanofibers. The results suggest that remarkable improvement in the mechanical behaviour is achieved by treatment with DA. Covalent bonds formed along the gelatin nanofibers by the Schiff's base reaction with DA are responsible for this tremendous improvement.

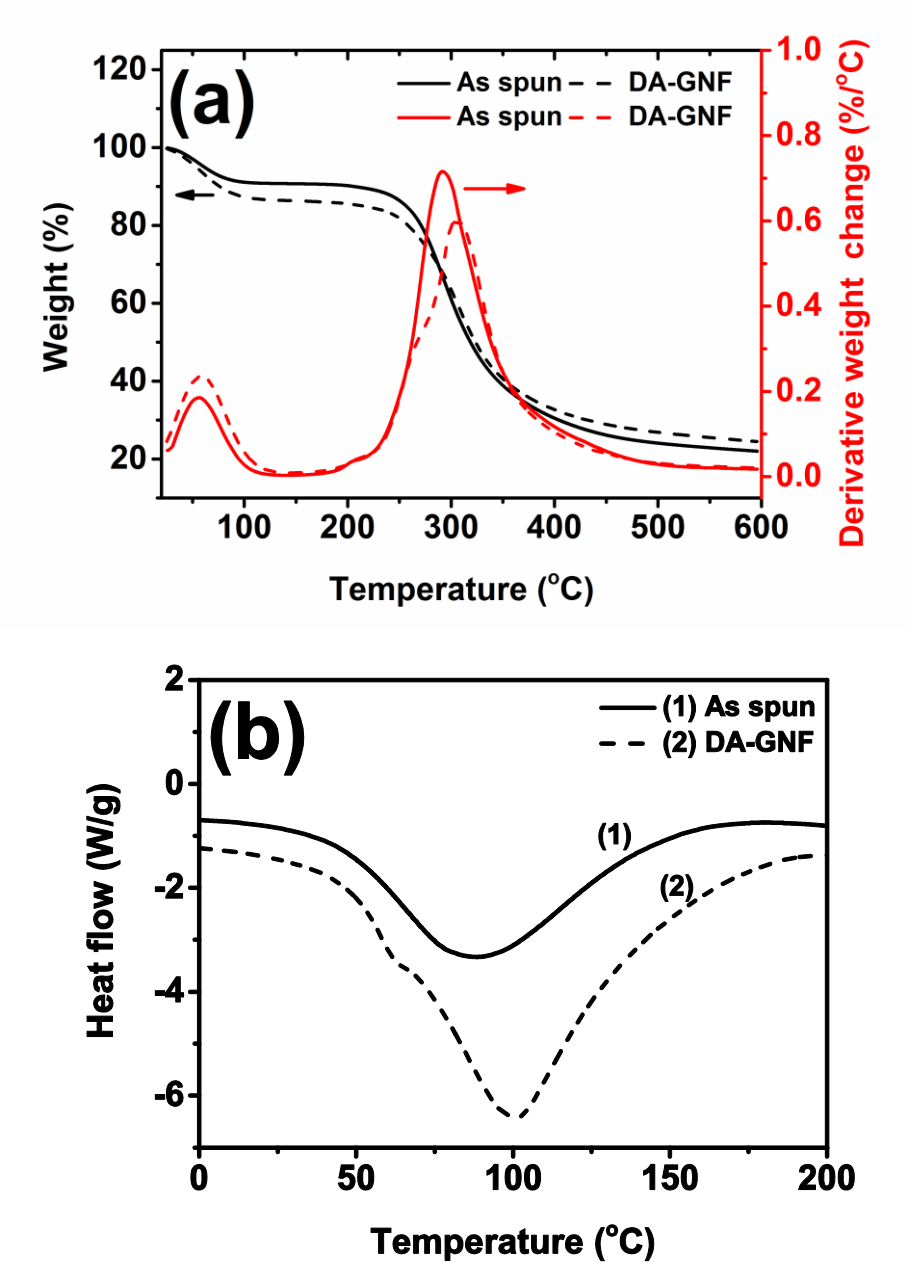

Figure 3.13: (a) TGA and DTG thermograms and (b) DSC thermograms of as spun and DA-GNF (5 days cross-linked) mats

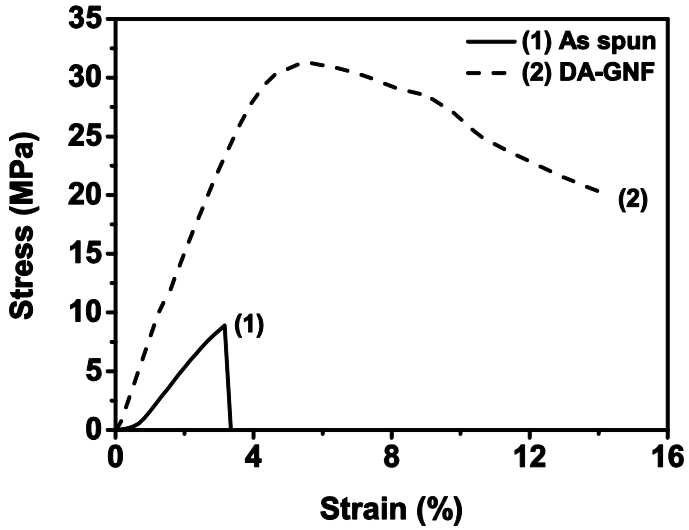

Figure 3.14: Stress-strain behaviour of as spun and DA-GNF mats

Table 3.5: Mechanical properties of as spun and DA-GNF (5-days cross-linked) mats

Mechanical Properties	As spun	DA-GNF
Stress at break (MPa)	8.29 ± 0.53	30 ± 3.47
Young's Modulus (MPa)	394 ± 96	904 ± 68

Nanofibrous gelatin mats of tensile moduli 20-100 MPa have been investigated for hard and soft tissue engineering applications (Panzavolta et al., 2011; Zhang et al., 2006). Mechanical properties as well as degradation behaviour of the nanofibrous mats can be tuned by the type of the cross-linking agent and cross-linking time. The properties can also be tailored by incorporating various synthetic polymers such as poly(L-Lactide) (An et al., 2010), poly(caprolactum) (Zhang et al., 2004), polyaniline (Li et al., 2006b), etc. Controlling the mechanical properties and degradation behaviour of the nanofibers will help to optimize the scaffolds for regeneration of a specific tissue type.

3.2.4 Biological studies

3.2.4.1 *In vitro* cytotoxicity and proliferation assay using L-929 cells

Cytotoxicity test methods help in screening the materials that are intended to be used in medical devices. *In vitro* cytotoxicity tests with mammalian

cells serve as the first step in evaluating biocompatibility of a biomaterial. *In vitro* direct contact cytotoxicity test using L-929 fibroblast cells with DA cross-linked gelatin mats show non cytotoxic reactivity to fibroblast cells after 24 h contact. The cells around DA-GNF mat maintain the characteristic spindle morphology without causing any toxic responses like cell detachment, lysis, etc. (Figure 3.15). The negative control (HDPE) shows non-cytotoxicity and positive control (PVC) shows severe cytotoxicity to L-929 cells. Comparison with negative and positive controls confirms the non-cytotoxicity of DA-GNF mat.

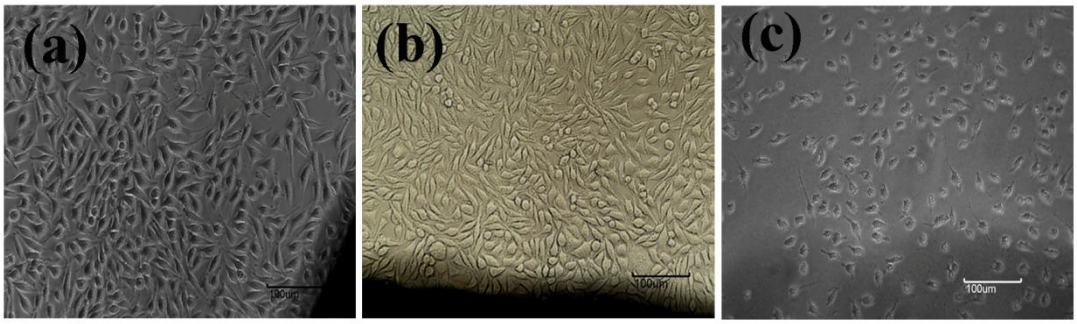

Figure 3.15: Light microscopic images of L929 cells on (a) HDPE control, (b) DA-GNF mat and (c) PVC disc after 24 h contact

Cytotoxicity of DA-GNF and GT-GNF mats is quantitatively assessed by MTT assay in terms of cell metabolic activity using the extract of the material for 3 and 5 days. DA-GNF mat shows metabolic activity of 82 % on the first day and 114 % on the third day with respect to the cell control. This clearly demonstrates that DA cross-linked gelatin nanofiber mat is non cytotoxic and the viability increases during 3 to 5 days of contact with the extract. Extract of GT-GNF mat shows severe toxicity on the third day itself and it prevents further cell proliferation during 3 to 5 days of contact with the extract (Figure 3.16).

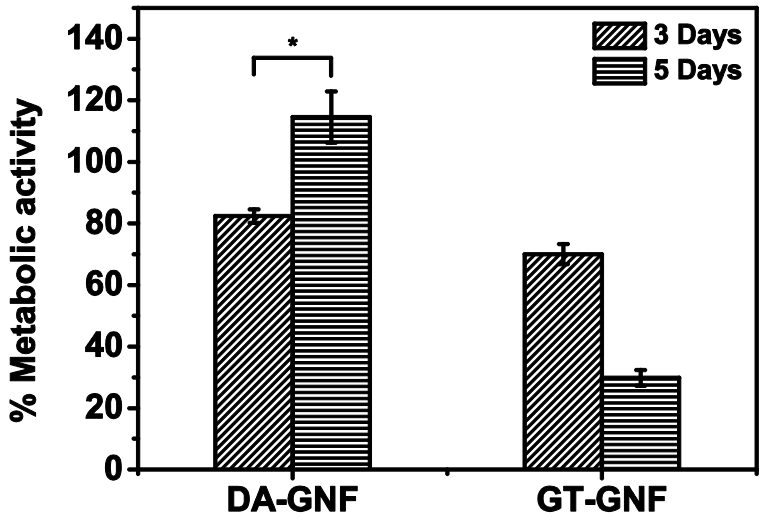

Figure 3.16: MTT assay of L-929 cells in contact with the extracts of DA-GNF and GT-GNF mats (* $p < 0.05$)

Proliferation of L-929 cells on DA-GNF mat is studied *in vitro* by MTT assay. For a comparison, cell proliferation assay on GT-GNF mat also is performed. Figure 3.17 indicates the activity of L-929 fibroblast cells on DA-GNF and GT-GNF mats for 3 and 5 days in terms of the absorbance. The absorbance values increase during 3 to 5 days confirming better cellular viability and proliferation on DA-GNF mat compared to GT-GNF mat. In the case of latter, the absorbance value has come down on the 5^{th} day indicating toxic response of GT on the cells. Statistical analysis of the absorbance values for 3 and 5 days for the DA-GNF mat shows that there is statistically significant difference between the two time points ($p < 0.05$).

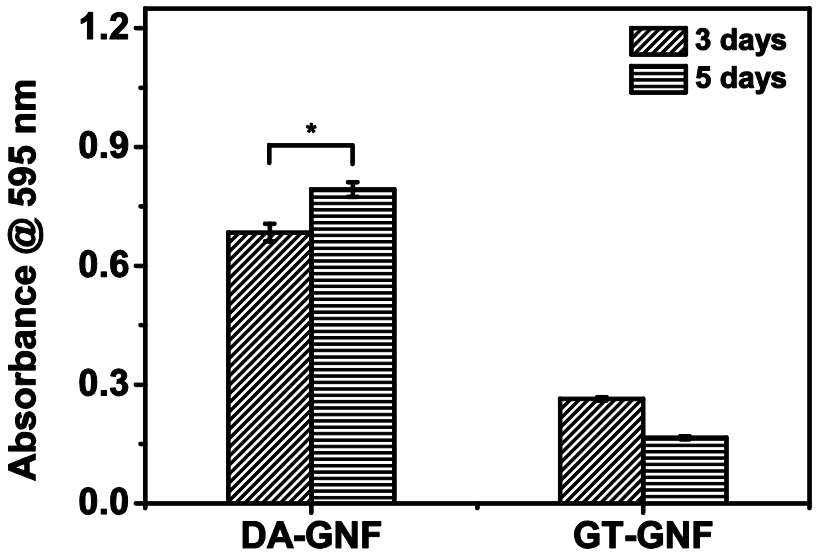

Figure 3.17: MTT assay of L-929 cultured on the surface of DA-GNF and GT-GNF mats (* $p < 0.05$)

3.2.4.2 Adhesion of L-929 cells

Most of the tissue-derived cells are anchorage dependent that require a surface to adhere and grow. Hence, cell adhesion on biomaterial is of much interest as it is the initial event that is followed by many critical processes such as attaining morphology, spreading, migration and cell function. Cells are allowed to adhere and grow on DA-GNF mat for 48 h and viability of the cells on the fibrous mat is ascertained by live-dead staining. Viable cells are observed as green and nucleus of dead cells are stained red. The fluorescence microscopic image (Figure 3.18) shows that, the cells are viable on DA-GNF mat.

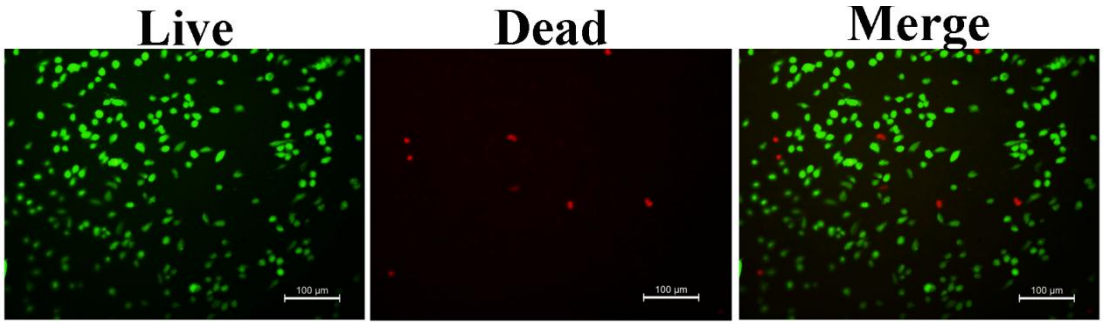

Figure 3.18: Fluorescence microscopic images of live and dead cells on DA-GNF mat obtained by FDA-PI staining

One of the key requirements in tissue engineering is ensuring robust adhesion between cell and biomaterial (Metcalfe and Ferguson, 2007). Spreading of cells on the nanofiber mat is analyzed by observing the morphology of the adhered cells by fluorescence microscopy. The actin cytoskeleton structure of the fixed cells is stained by phalloidin (red) and the nuclei are stained by Hoechst 33258 (blue) stains. Cells cultured on the nanofiber mat show spread fibroblast morphology with well defined actin and nuclei. The results indicate good cell adhesion and spreading on DA-GNF mat similar to the cells on the control cover glass (Figure. 3.19).

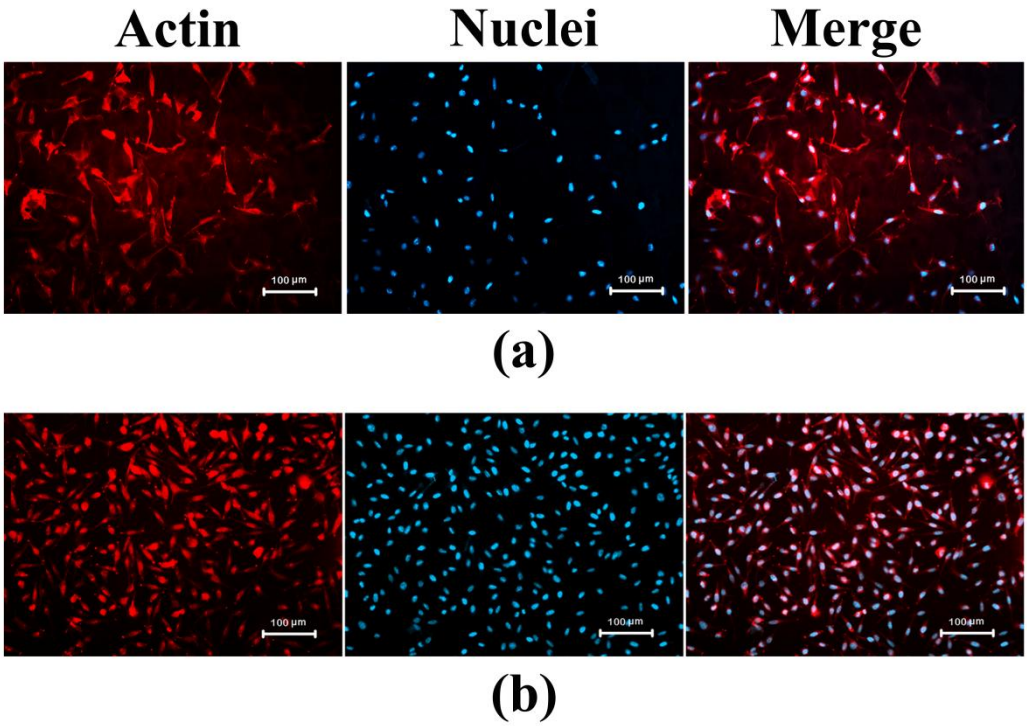

Figure 3.19: Actin cytoskeleton and nucleus staining of L-929 cells using phalloidin (red) and Hoechst 33258 (blue) on (a) DA-GNF mat and (b) cover glass

3.2.4.3 Proliferation of osteoblast (MG-63) cells

Proliferation and growth of MG-63 osteoblast-like cells when cultured on DA-GNF and GT-GNF mats are evaluated for 3 and 5 days (Figure 3.20). There is a statistically significant difference between the absorbance values of 3 and 5 days for DA-GNF. This indicates proliferation of osteoblast cells on DA-GNF mat.

Whereas GT-GNF retards the cell proliferation during 3 to 5 days of culture due to the toxic response of GT towards the cells. This again substantiates the cytocompatibility of DA-GNF mats.

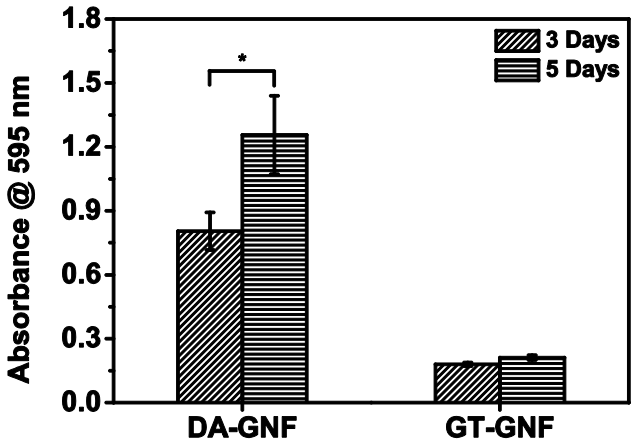

Figure 3.20: MTT assay of MG-63 osteoblast cells cultured on the surface DA-GNF and GT-GNF mats (* $p < 0.05$)

3.3 Conclusion

Gelatin nanofibers are fabricated using a solvent mixture of water and acetic acid keeping the acetic acid concentration as minimum as possible (20 % v/v). The presence of acetic acid prevents the gelation of gelatin by disrupting the hydrogen bonding interactions. The electrospun nanofibers can be effectively cross-linked with DA. The cross-linked nanofibers maintain the fibrous morphology after keeping in contact with water and exhibit a significant improvement in the mechanical behaviour. Preliminary *in vitro* cytotoxicity study of the nanofibers reveals that DA cross-linked gelatin mat is non-cytotoxic towards L-929 cells with good cell adhesion, viability and proliferation. The biocompatibility of the cross-linked mat is evaluated also using MG-63 cells. Nanofibers cross-linked with DA possess gradual degradation behaviour under physiological conditions and have great potential as scaffolds for tissue engineering. Fabrication of gelatin nanofibers by minimizing or avoiding the toxicity issues from solvent and cross-linking agents will greatly enhance the

scope of these materials in a variety of applications such as tissue engineering, drug delivery and wound dressing. The novel cross-linking method explored in this study provides directions about other easily available and biocompatible cross-linking agents based on natural materials.

CHAPTER 4

CROSS-LINKING OF ELECTROSPUN GELATIN NANOFIBERS WITH OXIDIZED SUCROSE

4.1 Introduction

In order to make use of electrospun gelatin nanofibers for biomedical applications, it is desirable to use a cross-linking agent that is not only suitable for cross-linking of gelatin nanofibers, but also of low toxicity to achieve a stable and biocompatible product. However, most of these reagents are reported to induce cytotoxicity when released into the body due to degradation or left unreacted in the nanostructures (Hao et al., 2011; Sisson et al., 2009; Sokolsky-Papkov et al., 2006; Wu et al., 2011). For eliminating the problems associated with toxicity, recent researches attempt to use non-toxic cross-linking agents. Gelatin and other collagenous materials are cross-linked by periodate oxidized products of dextran (Draye et al., 1998), alginic acid (Hu et al., 2014b), hyaluronic acid (Nair et al., 2011), pectin (Gupta et al., 2014a), sucrose (Cortesi et al., 1998), etc.

The previous chapter dealt with cross-linking of gelatin nanofibers with periodate oxidized dextran in ethanolic medium. Dextran aldehyde is only sparingly soluble in ethanol and hence high degree of cross-linking cannot be achieved. Hence, attempt is made to use a disaccharide as the cross-linking agent for gelatin nanofibers. The disaccharide, namely sucrose is oxidized by sodium metaperiodate ($NaIO_4$) to sucrose aldehyde (SA) and is used as the cross-linking agent. Since SA is readily soluble in ethanol, it is hypothesized that cross-linking with SA would result in higher extent of cross-linking. Sucrose is cost-effective, commercially available in large scale and is potentially biocompatible. SA is reported to be effective in cross-linking of gelatin and chitosan microspheres (Cortesi et al., 1998) and hydrogels (Pourjavadi et al., 2008). However, this

method has not been utilized for the cross-linking of gelatin and other protein based nanofibers.

The present chapter outlines cross-linking of gelatin nanofibers using sucrose aldehyde (SA) and evaluation of the effect of sucrose cross-linking on the physico-chemical and biological properties of the cross-linked mats. Cross-linking is performed by dipping the gelatin nanofibrous mats in ethanolic medium of SA. The cross-linked nanofibers maintain the fibrous morphology even after immersed in water. The present chapter also discusses the likelihood of applying these cross-linked nanofibers in biomedical applications in terms of cytotoxicity, cell adhesion and proliferation using mouse fibroblast cells (L-929) and human osteoblast-like cells (MG-63). The results demonstrate that SA is a useful cross-linking agent for gelatin nanofibers for various biomedical applications.

4.2. Results and Discussion

4.2.1. Periodate oxidation of sucrose

It is preferable and advantageous to use natural and non-toxic materials as cross-linking agents to prevent the toxic side effects due to bifunctional protein cross-linkers mentioned above. In the present work, sucrose is oxidized using sodium metaperiodate in a mole ratio (sucrose: sodium metaperiodate) of 1:2. The cis-diol groups of the disaccharide moiety are cleaved by periodate oxidation resulting in di and tetra aldehydes. It is reported that, three equivalence of $NaIO_4$ are required for the complete oxidation, resulting in the formation of tetra aldehydes (Schoevaart et al., 2005). The formation of sucrose aldehyde (SA) is schematically shown in Figure 4.1.

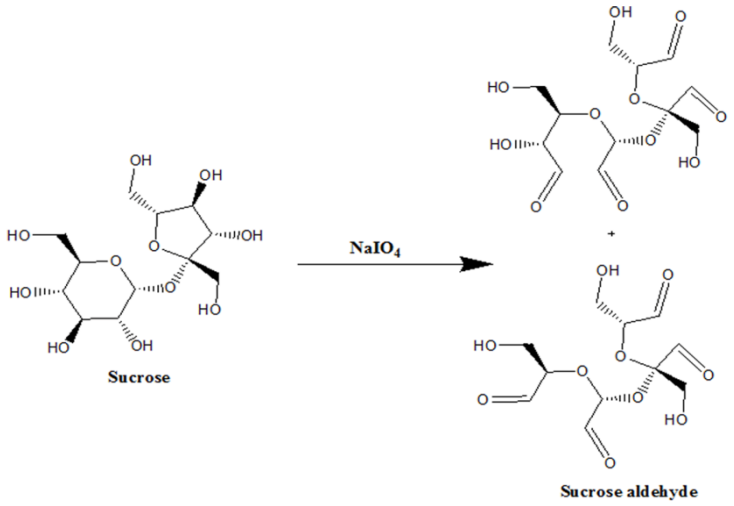

Figure 4.1: Schematic of oxidation of sucrose by sodium metaperiodate

FTIR spectra of sucrose and SA are shown in Figure 4.2. The typical aldehyde peak observed in the IR spectrum of SA at 1718 cm^{-1} shows the presence aldehyde group formed as the result of oxidation.

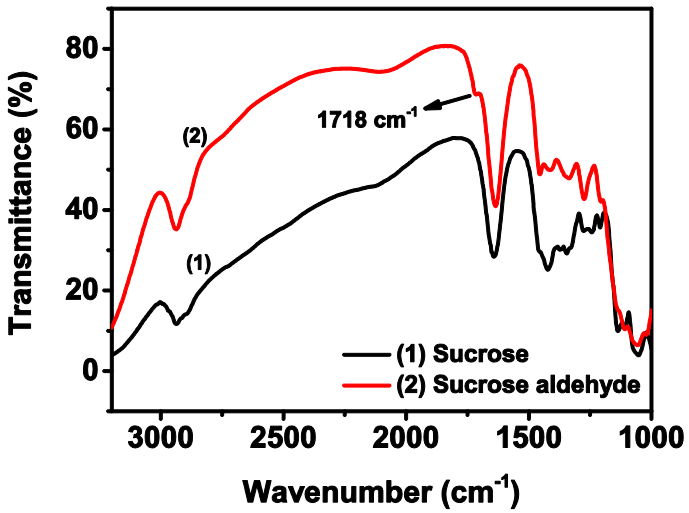

Figure 4.2: FTIR spectra of sucrose and SA

Degree of oxidation and aldehyde content are measured using hydroxylamine hydrochloride test. From the amount of HCl released, the aldehyde content and there by the degree of oxidation is estimated. It is found that almost 45 % of the cis-diol groups have undergone oxidation. The degree of oxidation and aldehyde content are summarized in Table 4.1.

Table 4.1: Properties of SA (Mean ± standard deviations are reported)

Properties	SA
Degree of oxidation (%)	44.5 ± 2.5
Aldehyde content (mol/g)	$5.5 \pm 0.32 \times 10^{-3}$

4.2.2. Cross-linking and characterization of gelatin nanofibers

Sucrose aldehyde (SA) is soluble in pure ethanol as well as in aqueous medium. In the case of gelatin nanofibers, aqueous medium for cross-linking needs to be avoided in order to preserve the fibrous morphology. Cross-linking of gelatin nanofibers with genipin, carbodiimide, etc., is achieved in ethanol by immersing the mats in the medium for 5-7 days. Hence in this study, ethanol is selected as the medium for cross-linking. Cross-linking is performed in two methods, by dipping the nanofibrous mats in a medium of SA dissolved (i) in pure ethanol and (ii) in ethanol containing minute amount of aqueous borax (300 μl, 0.02 M borax in 10 ml of ethanol). The resulting SA cross-linked gelatin nanofibers are indicated by the notations SA-GNF-PE and SA-GNF-BE for mats cross-linked from pure ethanol and borax/ethanol medium, respectively. Concentration of SA in the cross-linking medium is optimized based on the degree of cross-linking of SA-GNF-BE mats by TNBS assay (Table 4.2). Degree of cross-linking increases with increase in concentration of the cross-linking agent in the medium. Cross-linking with SA solution of 0.1 % (w/v), results in lower degree of cross-linking compared to that obtained by 0.5 % (w/v) solution which in turn is lower than that for 1 % (w/v) solution. However, the degree of cross-linking achieved with 1 % and 2 % (w/v) solutions did not show significant difference. The mats become intense brown in colour due to the formation of more aldimine linkages (Figure 4.3) as the concentration of SA increases. FTIR spectrum of the mat cross-linked in 2 % (w/v) solution shows characteristic stretching bands of aldehyde groups due to the presence of residual aldehyde which is absent in the mat cross-linked in 1 % (w/v) solution (Figure 4.4). Hence, 1 % (w/v) solution of SA is selected as the cross-linking medium for further

studies. Cross-linking is carried out by dipping the mats in the cross-linking medium for time periods of 1, 3 and 5 days.

Table 4.2: Degree of cross-linking of SA-GNF-BE mats cross-linked in solutions of different concentrations of SA

SA-GNF-BE mats cross-linked in	Degree of cross-linking (%)
0.1 % (w/v) of SA	41 ± 8
0.5 % (w/v) of SA	67 ± 3
1 % (w/v) of SA	76 ± 4
2 % (w/v) of SA	77 ± 3

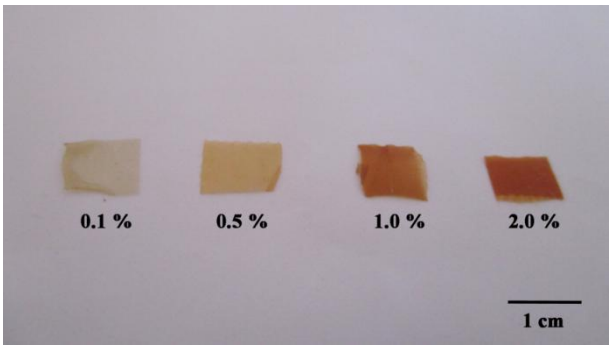

Figure 4.3: Photograph of the mats cross-linked with various concentrations of SA

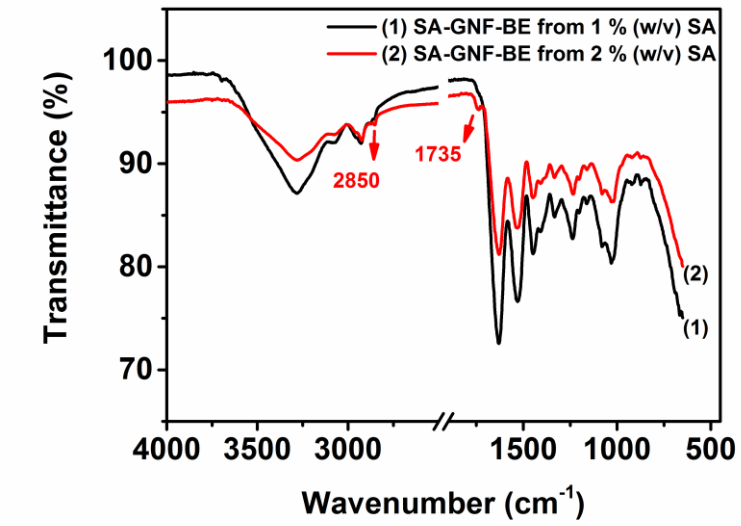

Figure 4.4: FTIR spectra of the cross-linked mats with various concentrations of SA

Figure 4.5 (a) shows the stability of as spun and cross-linked mats in water, revealing the effect of cross-linking. It can be seen that the as spun mat gets completely dissolved in water medium within 1 h, while the cross-linked mat remains intact. Figure 4.5 (b) represents the schematic of cross-linking of gelatin nanofibers with SA. The primary amino groups of lysine and hydroxylysine from gelatin undergo cross-linking reaction with aldehyde groups of SA through the formation of Schiff's base. Thus, SA is an effective cross-linker for protein based nanofibers.

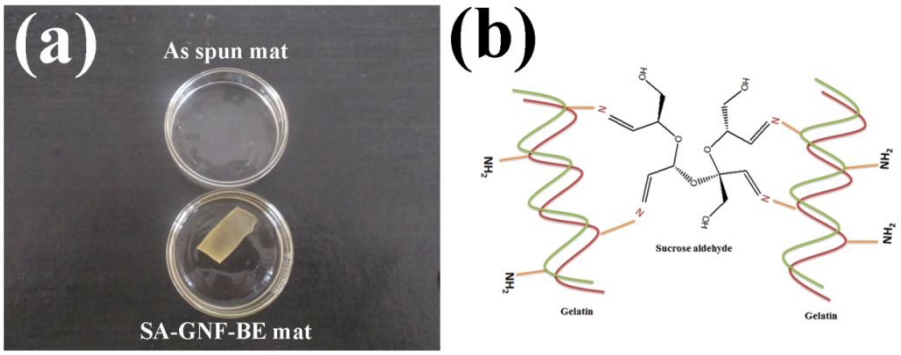

Figure 4.5: (a) Photograph of as spun and SA-GNF-BE (5-days cross-linked) mats in water medium, (b) Schematic representation of cross-linking process of SA with gelatin

Table 4.3 shows the variation of degree of cross-linking of SA-GNF-PE and SA-GNF-BE mats with duration of cross-linking obtained by TNBS assay. The degree of cross-linking is found to be higher for mats cross-linked in presence of aqueous borax (SA-GNF-BE) as compared to the mats cross-linked in pure ethanol (SA-GNF-PE). Degree of cross-linking increases as the cross-linking time varies from 1 to 5 days. This result shows that SA-GNF-BE mat cross-linked for 5 days exhibits the highest degree of cross-linking among the samples. The higher degree of cross-linking exhibited by SA-GNF-BE demonstrates the effect of aqueous borax on the Schiff's base formation between aldehyde groups of SA and amino groups of gelatin. This can be explained on the basis of the alkaline pH of the cross-linking medium (pH 10) due to the presence of borax and the complexing ability with hydroxyl groups of SA. The effect of borax on the cross-linking efficiency has already been reported by Balakrishnan et al for the cross-linking of gelatin and alginate dialdehyde (Balakrishnan and Jayakrishnan, 2005).

Alkaline pH has an important role in determining the degree of cross-linking between amino groups of gelatin and aldehyde groups of the cross-linking agent. pH higher than the isoelectric point of gelatin is found to favour the Schiff's base formation (Balakrishnan and Jayakrishnan, 2005; Balakrishnan et al., 2013; Farris et al., 2009; Migneault et al., 2004). The small amount of water also makes possible, a better interaction between the aldehyde and amino groups. The effect of aqueous borax on cross-linking can be further validated and explained in terms of the swelling behaviour of SA-GNF-PE and SA-GNF-BE mats.

Table 4.3: Degree of cross-linking of SA-GNF-PE and SA-GNF-BE mats with change in duration of cross-linking

Duration of cross-linking	**Cross-linking degree (%)**	
	SA-GNF-PE	**SA-GNF-BE**
1 day	37 ± 5	53 ± 4
3 days	47 ± 5	71 ± 3
5 days	56 ± 6	76 ± 4

The swelling behaviour of as spun and cross-linked electrospun mats is studied in PBS and the results demonstrate the effect of cross-linking on the swelling properties. From Figure 4.6 (a), it is clear that the cross-linked mats exhibit significantly lower swelling ratio as compared to as spun gelatin mat. Swelling ratio of the cross-linked mats decreases as duration of cross-linking increases from 1 to 5 days. Figure 4.6 (b) indicates the variation of swelling ratios of SA-GNF-PE and SA-GNF-BE for different periods of cross-linking. In accordance with cross-linking degree, the swelling ratio of SA-GNF-BE is found to be lower than that of SA-GNF-PE. Since, 5 days cross-linked SA-GNF-BE mats are showing better cross-linking degree and lower swelling ratio, further characterizations and biological studies are performed with 5 days cross-linked SA-GNF-BE mats.

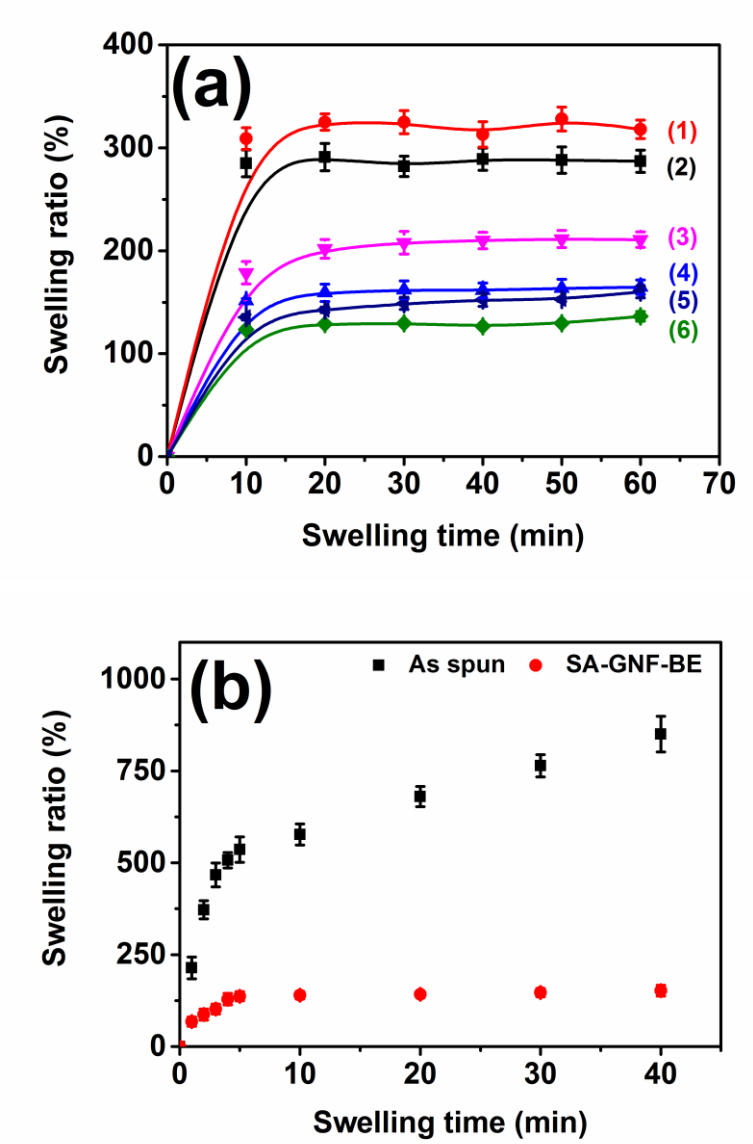

Figure 4.6: (a) Swelling ratios of SA-GNF-PE (1, 3 and 5) and SA-GNF-BE (2, 4 and 6) cross-linked for 1, 3 and 5 days, respectively (b) Swelling ratio of as spun and SA-GNF-BE (5 days cross-linked) mats

The degradation profile of SA-GNF-BE mat in physiological pH is shown in Figure 4.7. The cross-linked mats as expected, exhibit a gradual degradation pattern up to six weeks. This clearly reveals that, SA is an effective cross-linker for gelatin nanofibers. The hydrolytic susceptibility of the Schiff's base formed as a result of cross-linking causes the degradation of the cross-linked mat in the absence of enzymes. Also, since gelatin is partially amorphous in nature, degradation preferentially happens in the amorphous region by hydrolytic process. Enzymatic degradation contributes in the later stage of the degradation process

(Ma and Elisseeff, 2010). In this case, at the end of the sixth week, 45-50 % weight of the sample remains in the medium as the degradation is performed in the absence of enzymes.

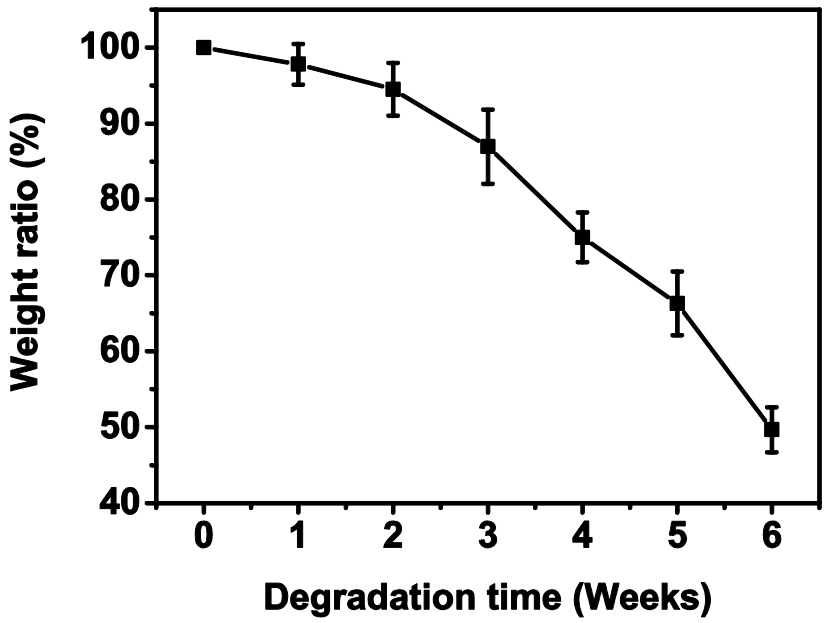

Figure 4.7: Degradation behaviour of SA-GNF-BE (5 days cross-linked) mat in PBS at 37 °C

It is well known that gelatin nanofibers lose its fibrous morphology when exposed to high degree of moisture. Hence, cross-linking treatment is essential to enhance their water resistant ability. Figure 4.8 shows the SEM images of SA-GNF-PE and SA-GNF-BE mats before and after swelling in water. SEM images reveal that cross-linking has occurred and cross-linked fibers maintain the fibrous morphology even after keeping in contact with water. Cross-linked mats obtained by method II (SA-GNF-BE) maintain a better fibrous morphology (Figure 4.8 (d)) compared to that obtained by method I (SA-GNF-PE) (Figure 4.8 (b)) after keeping in contact with water. This can be attributed to the more effective cross-linking achieved in the presence of small amount of aqueous borax.

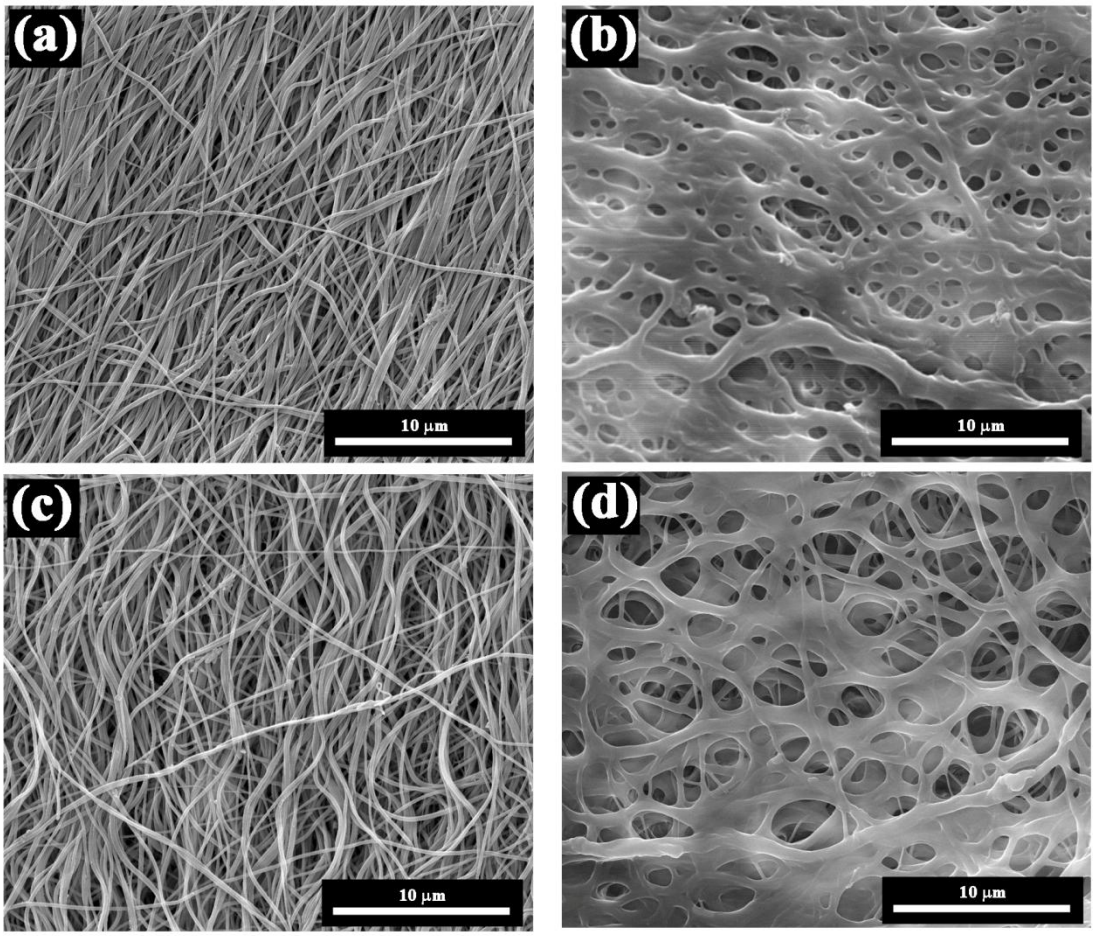

Figure 4.8: SEM images of SA-GNF-PE and SA-GNF-BE mats before swelling in water (a and c) and after swelling in water (b and d)

FTIR spectra of as spun and SA-GNF-BE mats are given in Figure 4.9. The spectrum of SA-GNF-BE shows a strong peak at 1030 cm^{-1} corresponding to C-O-C stretching frequency of sucrose moiety. This indicates that the incorporation of SA into the gelatin nanofiber network. The mechanical properties of as spun and cross-linked gelatin nanofibrous mats are also examined. The stress-strain behaviour of as spun and SA-GNF-BE mats is shown in Figure 4.10. The tensile strength and Young's modulus based on the stress-strain measurements are summarized in Table 4.4. The results indicate that the cross-linking treatment significantly improves the mechanical performance of gelatin nanofibers. After cross-linking, both the tensile strength and modulus are enhanced remarkably. Controlling the mechanical properties of the nanofibers will enable better utility of the biomaterial as scaffold for engineering a specific tissue type. The mechanical properties of gelatin based nanofibrous mats can be tuned

further by varying the type of cross-linkers and the extent of cross-linking.

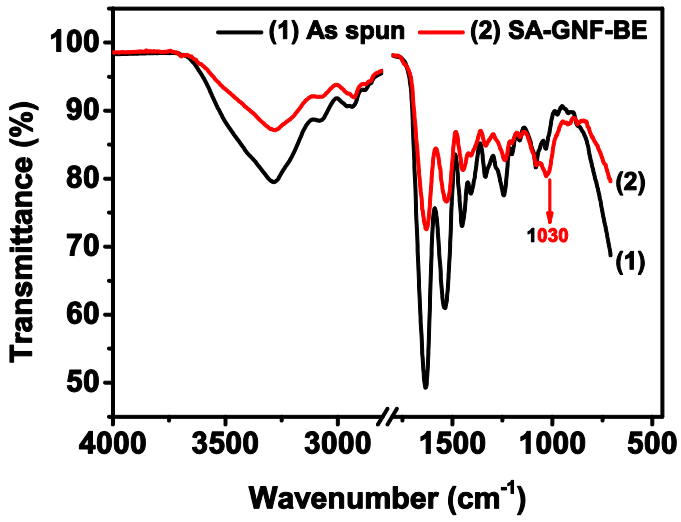

Figure 4.9: FTIR spectra of as spun and SA-GNF-BE (5 days cross-linked) mats

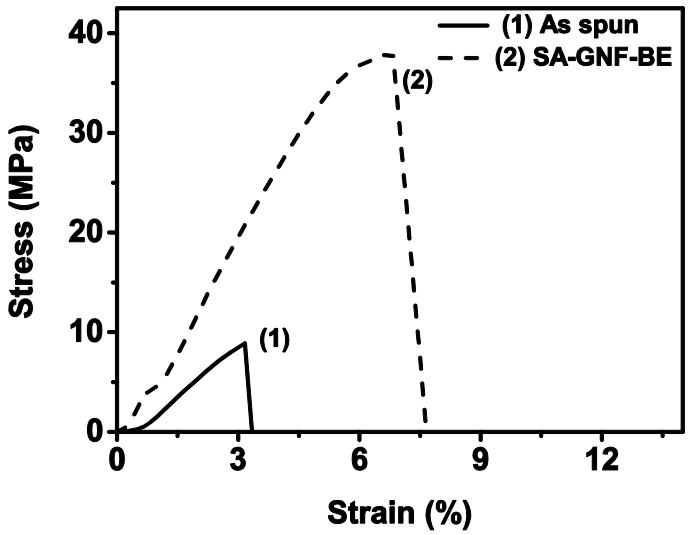

4.10: Stress-strain behaviour of as spun and SA-GNF-BE (5-days cross-linked) mats

Table 4.4: Mechanical behaviour of as spun and SA-GNF-BE (5-days cross-linked) mats (Mean ± standard deviations are reported)

Mechanical Properties	As spun mat	SA-GNF-BE mat
Stress at break (MPa)	8.29 ± 0.53	38 ± 5.47
Young's Modulus (MPa)	394 ± 96	1387 ± 90

DSC analysis is performed on as spun and SA-GNF-BE mats in order to investigate the effect of cross-linking on the thermal behaviour of the nanofibers. The DSC thermogram (Figure 4.11 (a)) of gelatin exhibits an endothermic peak corresponding to helix to coil transition in the range of 90 to 110 ^{o}C which is known as denaturation temperature. At this temperature, the triple helical structure of gelatin melts and dissociates to form randomly coiled structures. On comparing the DSC curves of as spun and SA-GNF-BE mats, it is clear that the denaturation temperature of the cross-linked mat has got shifted to higher temperature (from 88 to 106 ^{o}C). This observation confirms that the SA-GNF-BE mats have higher thermal stability than that of the as spun fibers. Similar observations of enhanced thermal stability for cross-linked gelatin nanofibers are available in literature (Zhang et al., 2006). Derivative thermograms of the as spun and SA-GNF-BE mats are shown in Figure 4.11 (b). It can be seen that, for SA-GNF-BE mats, the temperature at which the maximum decomposition occurs has got shifted to a higher temperature (from 292 to 314 ^{o}C).

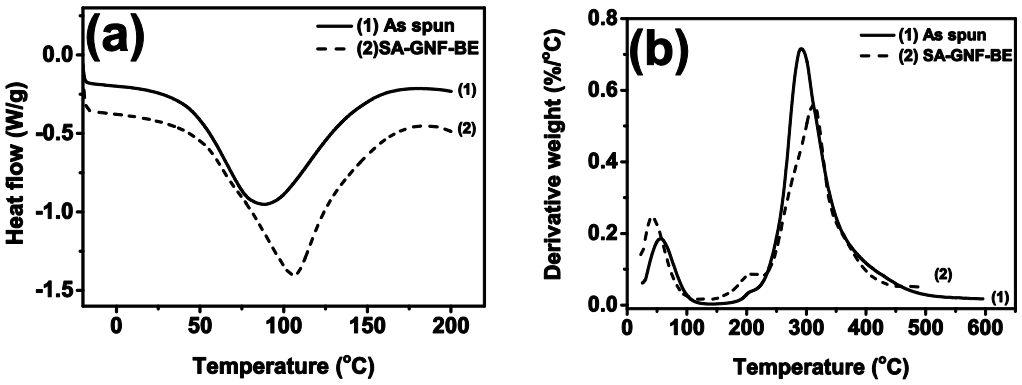

Figure 4.11: (a) DSC thermograms and (b) DTG thermograms of as spun and SA-GNF-BE mats

4.2.3 Biological studies

4.2.3.1 *In vitro* cytotoxicity and proliferation assay using L-929 cells

In vitro cytotoxicity test methods are employed primarily to screen the materials that are intended to be used in biomedical devices. As far as the experimental evaluation of biocompatibility is concerned, cytotoxicity tests are

widely cited as the first step in evaluating biocompatibility of a biomaterial (Sell et al., 2010). *In vitro* direct contact test using L-929 fibroblast cells with SA-GNF-BE mat exhibits non-cytotoxic response to fibroblast cells after 24 h of contact (Figure 4.12). The cells around the cross-linked mats maintain the characteristic spindle morphology without causing cell detachment and lysis. The negative control (HDPE) shows non-cytotoxicity and positive control (PVC) shows severe cytotoxicity to L-929 cells. Comparison with negative and positive controls confirms the non-cytotoxicity of SA cross-linked gelatin nanofibrous mats.

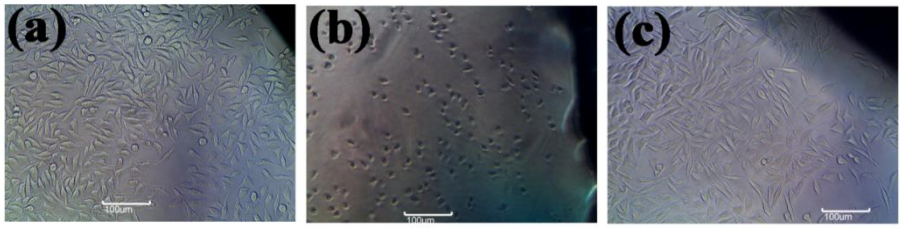

Figure 4.12: Light microscopic images of L-929 cells on (a) high density polyethylene (negative control), (b) stabilized poly vinyl chloride (positive control) and (c) SA-GNF-BE (5-days cross-linked) mat after 24 h contact

Further, the cell viability of L-929 fibroblast cells in contact with the extract of the cross-linked mat is assessed quantitatively in terms of the metabolic activity by colorimetric MTT assay. For a comparison, experiment is performed with glutaraldehyde cross-linked gelatin nanofibers (GT-GNF) also. Figure 4.13 represents the metabolic activity of L-929 fibroblast cells in contact with extract of SA-GNF-BE and GT-GNF mats for 1 and 3 days. The SA-GNF-BE mat shows 80 and 111 % metabolic activity for 1 and 3 days, respectively. Analysis of this result clearly reveals a statistically significant difference in the cellular activity between 1 and 3 days ($p < 0.05$). The relative increase in the metabolic activity is a measure of the increased viability due to proliferation of the cells during the period. The GT-GNF mat shows 77 and 69 % of metabolic activity for 1 and 3 days, respectively. This observation indicates that GT-GNF mat is not promoting cell proliferation, may be due to the toxic response of residual GT. Thus, in comparison to GT-GNF mat, cell proliferation is significantly higher for SA-GNF-BE mat.

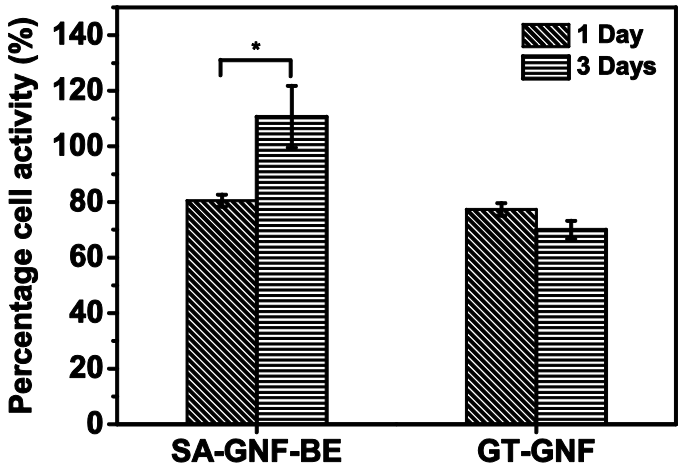

Figure 4.13: MTT assay of L-929 cells in contact with extracts of SA-GNF-BE (5-days cross-linked) and GT-GNF mats (* $p < 0.05$)

Figure 4.14 further shows the proliferation effects of L-929 cells on the surface of the cross-linked mats. Similar trend of proliferation is observed in this case also. Adverse effect of GT on proliferation of the cells can also be found in literature (Chang et al., 2003; Sisson et al., 2009; Wu et al., 2011; Zhang et al., 2006).

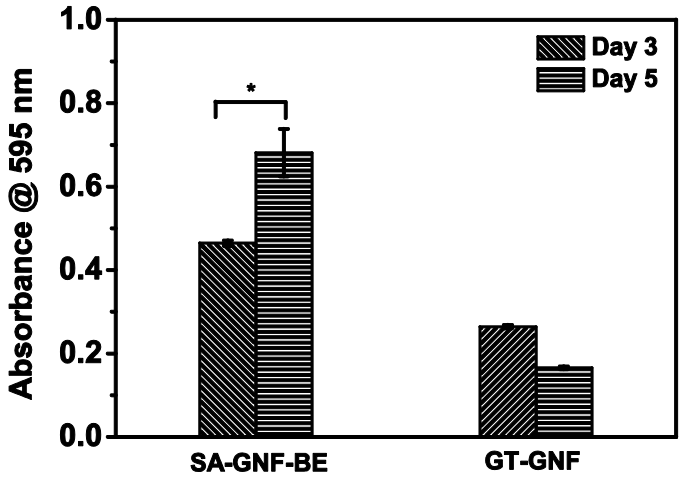

Figure 4.14: MTT assay of L-929 cells on the surface of SA-GNF-BE (5-days cross-linked) and GT-GNF mats (* $p < 0.05$)

4.2.3.2 Adhesion of L-929 cells

The adhesion and morphology of the adhered L-929 cells on the surface of SA-GNF-BE mats are evaluated by actin cytoskeleton staining followed by fluorescent microscopy. Figure 4.15 shows the actin cytoskeleton and nuclei structure of L-929 cells cultured on SA-GNF-BE mats and cover glass. The result reveals that L-929 cells are adhered on the cross-linked mat and show well distributed actin and nuclei.

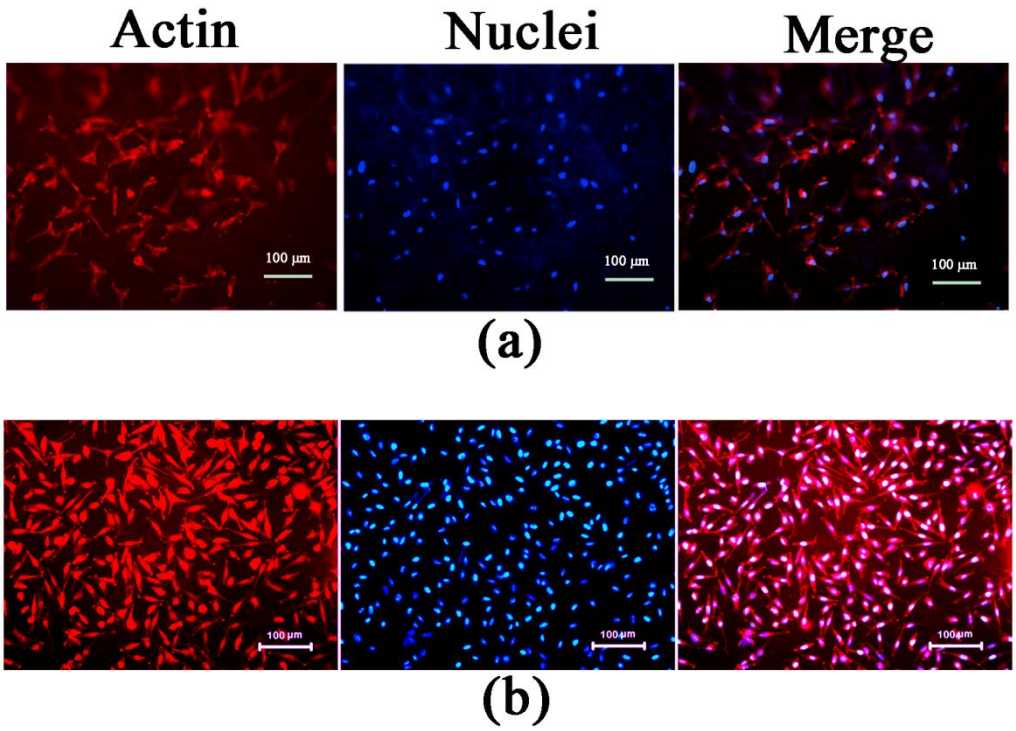

Figure 4.15: Actin cytoskeleton staining of L-929 cells adhered on (a) SA-GNF-BE (5-days cross-linked) mat and (b) cover glass

4.2.3.3 Proliferation of osteoblast (MG-63) cells

Proliferation of MG-63 osteoblast cells on SA-GNF-BE and GT-GNF mats are studied by MTT assay (Figure 4.16). The absorbance values for SA-GNF-BE mats during 3^{rd} and 5^{th} days show a statistically significant difference, indicating appreciable growth rate. Cells are well-proliferating on SA-GNF-BE

mats indicating that SA cross-linked surface is compatible to MG-63 cells. GT-GNF mat is observed to retard the growth of the cells due to the cytotoxic effects of the residual GT on the mat.

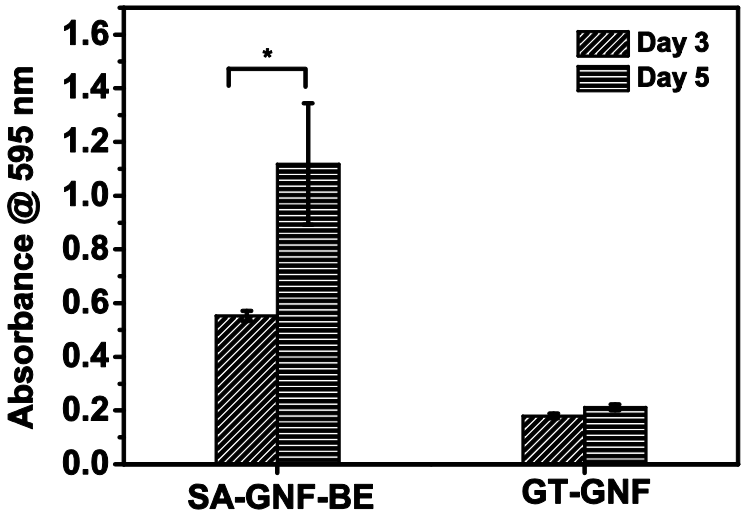

Figure 4.16: MTT assay of MG-63 cells cultured on the surface of SA-GNF-BE (5-days cross-linked) and GT-GNF mats (* $p < 0.05$)

4.4. Conclusion

In this chapter, SA is demonstrated as an effective, naturally derived cross-linker for gelatin nanofibers. The cross-linked nanofibrous mats maintain the fibrous morphology after keeping in contact with water and exhibit a significant improvement in the mechanical behaviour. Preliminary *in vitro* cytotoxicity study of the nanofibers reveals that SA cross-linked gelatin mat is non-cytotoxic and promote the proliferation of L-929 and MG-63 cells. The results presented here illustrate that SA can act as an effective GT analog for cross-linking gelatin nanofibers.

CHAPTER 5

FABRICATION AND CHARACTERIZATION OF CATIONICALLY MODIFIED GELATIN NANOFIBERS

5.1 Introduction

Apart from the initial objective to develop novel cross-linkers for electrospun gelatin nanofibers, the present study also deals with the chemical modification of gelatin followed by electrospinning process to obtain modified gelatin nanofibers. The main aim of the modification is to improve the biocompatibility and physico-chemical properties of gelatin based nanofibers by minimizing the toxicity effects from the solvents and the cross-linking agents. As mentioned in the previous sections, the fabrication of gelatin nanofibers by electrospinning requires toxic organic solvents such as TFE (Huang et al., 2004), HFIP (Matthews et al., 2002), formic acid (Ki et al., 2005), acetic acid (Panzavolta et al., 2011) and others. These solvents if left in the nanostructures can be toxic to the living tissues (Angarano et al., 2013).

Gelatin is composed of 18 different amino acids with both positive and negative charges, which are distributed non-uniformly. Gelatin has an inherent cationic property due to the basic amino acid residues such as lysine and arginine (Gómez-Guillén et al., 2011). Gelatin is derived from collagen, which is obtained by acidic or basic treatment, resulting in gelatin type A with an isoelectric point of 7–9.5 and gelatin type B with an isoelectric point of 4.5–5.3 (Samal et al., 2012; Zhou et al., 2012) respectively. The alkaline process hydrolyses the amide groups of asparagine and glutamine into carboxyl groups, resulting in gelatin with a higher density of carboxyl groups, making it negatively charged at neutral pH and lowering its isoelectric point. In contrast, an acidic pre-treatment does not

significantly affect the amide groups (Gorgieva and Kokol, 2011). Gelatin shows cationic behaviour at pH values below its isoelectric point *via* protonation of amino groups. The cationic density is higher for gelatin type A and lower for gelatin type B. Gelatin can be cationized by introducing amino groups onto the gelatin backbone, usually realized by carbodiimide chemistry. Cationic gelatin is obtained by coupling ethylenediamine or spermine through a carbodiimide mediated reaction (Morimoto et al., 2008). Gelatin is usually cationically modified to facilitate the interactions with biomolecules of anionic nature (Morimoto et al., 2008; Wang et al., 2001). Anchorage of excess amino groups on gelatin surface provides a suitable way to enhance the cell affinity of biomaterials. Several reports on cationized gelatin (CG) matrices for drug and gene delivery are available (Fujii et al., 2011; Santoro et al., 2014). A few reports are also found on the tissue regeneration using cationic gelatin as a coating over synthetic polymers (Chen and Su, 2011; Shen et al., 2007). Core-shell nanofibers are fabricated using polycaprolactum (PCL) as core and CG as shell material using trifluoroethanol (TFE) as solvent. Cationized gelatin as shell material can provide a biocompatible surface. This allows the immobilization of negatively charged bioactive molecules, which facilitates the cell adhesion and proliferation (Lu et al., 2009d). It is envisioned that pure CG nanofibers can act as a better biocompatible material for tissue regeneration. CG is found to be highly soluble in water without forming gel at room temperature. Hence, in the present work, water is selected as the solvent for CG nanofiber production. It replaces all other toxic solvents such as TFE, HFIP, formic acid and acetic acid, which are being conventionally employed.

The present chapter explores the electrospinnig of CG nanofibers using water as the solvent. This method will greatly assist the efforts of the researchers to reduce the toxicity due to the presence of solvents in the case of protein nanofibers. Also, the cationic surface of the nanofibers would enable better interaction with the anionic cell surface, which in turn promotes greater cell attachment and proliferation (Chen and Su, 2011). Since CG is highly hydrophilic in nature, cross-linking treatment is necessary to improve the water resistance of

nanofibers for tissue regeneration applicability. The external cross-linkers are reported to be a common source of toxicity in a biodegradable material. The biocompatibility and non-toxicity of dextran aldehyde (DA) and sucrose aldehyde (SA) cross-linked gelatin nanofibers are already established as discussed in the previous chapters. Hence, the fabricated CG nanofibers are cross-linked using DA and SA to avoid toxicity issues. The results indicate that, this greener way of nanofiber fabrication is a promising approach for tissue regeneration applications.

5.2 Results and Discussion

5.2.1 Characterization of CG

Gelatin can be cationically modified to augment interactions with biomolecules and cell membranes, which are anionic in nature. It is reported that the surface of poly-L-glycolic acid (PLGA) and poly-L-lactic acid (PLLA) films and sponges when modified with CG show enhanced cell attachment and growth of mouse NIH 3T3 fibroblasts cells and articular chondrocytes cells, respectively, in comparison with gelatin (Chen and Su, 2011; Shen et al., 2007). The large number of positive charges on the surface of CG would enable a better interaction with the negatively charged cell surface. This can provide an excellent cellular adhesion and proliferation. In the present work, novel gelatin based nanofibers are fabricated from cationically modified gelatin. The purpose of the study is not only to minimize the toxicity effects from solvents and cross-linking agents, but also to improve the cell attachment and growth on the nanofibrous substrate. Cationic modification of gelatin is accomplished by introducing amino groups onto the gelatin backbone through carbodiimide mediated reaction. This reaction establishes amide bonds between carboxylic groups of gelatin and amino groups of ethylenediamine as shown in Figure 5.1.

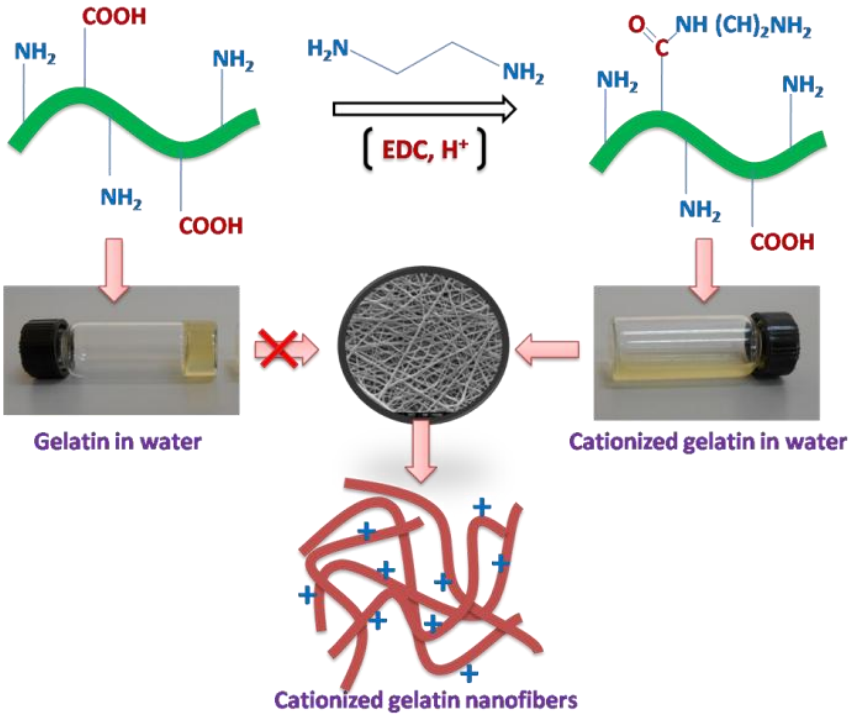

Figure 5.1: Schematic for CG formation and nanofiber fabrication from aqueous solution

FT-IR spectra of gelatin and CG are shown in Figure 5.2. The spectrum of gelatin contains a broad band at 3280 cm^{-1} due to–OH and –NH stretching. Bands at 1627 and 1534 are assigned to amide I and amide II bonds, respectively. Other than the peaks from gelatin, the IR spectrum of CG shows an additional peak at 2925 cm^{-1} associated with the C-H stretching from ethylenediamine groups.

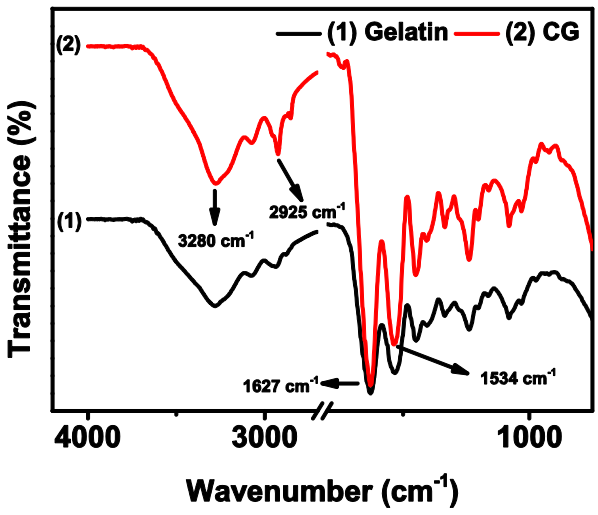

Figure 5.2: FTIR spectra of gelatin and CG

Thermal analysis of gelatin and CG is carried out in order to know the effect of cationization on thermal behaviour of gelatin. TGA thermograms of gelatin and CG are shown in Figure 5.3 (a). CG shows similar thermal degradation pattern as that of gelatin, but with higher char residue. In the TGA thermogram, it can be seen that as a result of incorporation of large number of ethylenediamine groups, there is an increase in the carbon yield for CG (29 %) compared to gelatin (23 %) at 500 ^{o}C. The DSC thermogram (Figure 5.3 (b)) shows endotherm corresponding to the denaturation temperature of gelatin. The DSC thermogram exhibits lower denaturation temperature for CG than gelatin. During the preparation process of CG, the rupture of triple helix of gelatin takes place, which lowers the thermal stability of CG and hence the endotherm is shifted to a lower temperature compared to gelatin (from 97 to 84 °C).

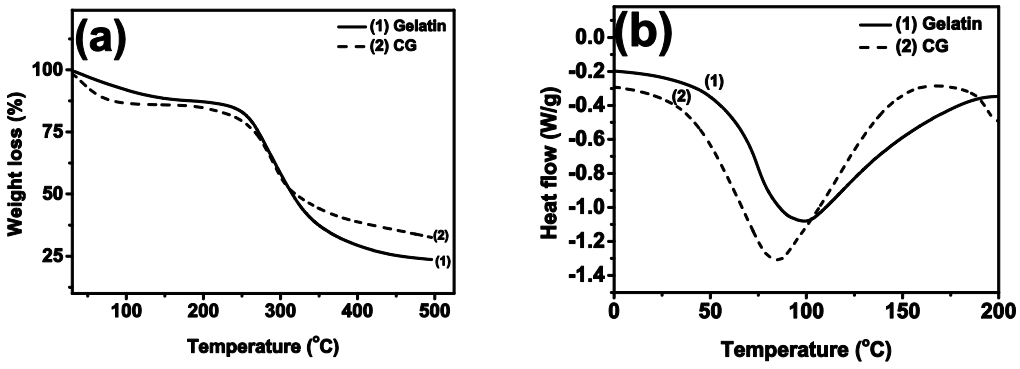

Figure 5.3: (a) TGA and (b) DSC thermograms of gelatin and CG

The excess amino groups introduced on gelatin as a result of cationization are determined by TNBS assay. The number of amino groups in gelatin and CG are 2.2×10^{-4} and 4.75×10^{-4} mol/g, respectively. The molar ratio of amino groups on CG to that on gelatin is found to be 2.16, close to the value reported in literature (Chen and Su, 2011). The zeta potential of CG is determined to find out the surface positive charge. An increase or reduction in zeta potential value is a measure of the presence of charges on the dissociated surface functional groups. In case of gelatin, the negatively charged groups such as carboxylic acid cause decrease of zeta, whereas the positively charged groups such as amino groups

enhance the zeta potential value. In comparison with gelatin (-2.1 mV), CG exhibits a more positive zeta potential value of +2.9 mV and confirms the formation of CG.

In order to understand the structural property and surface composition of CG, XRD and XPS analyses are carried out. Gelatin shows a wide crystalline XRD peak at 2θ = 20.9° due to the triple-helical crystalline structure of collagen renatured in gelatin. This peak is absent in the pattern of CG (Figure 5.4 (a)) indicating the amorphous nature of CG. It is seen from the XRD pattern that, the wide crystalline peak at 2θ = 20.9° observed in the pattern of gelatin is absent in the case of CG, indicating the destruction of the triple helical structure as a result of cationization. This may be due to the reduced extent of hydrogen bonding in the CG as a result of protonation of primary amino groups. XPS survey scan spectra of gelatin and CG are shown in Figure 5.4 (b). The results clearly reveal that, the N1s peak intensity increases as a result of cationization, which also supports the other observations. From the high resolution C1s, N1s and O1s spectra, the relative atomic percentages are calculated and are summarized in Table 5.1. From the elemental composition of gelatin and CG obtained from XPS spectra, it is clear that the N1s peak intensity increases as a consequence of cationization. These data also well-support the presence of large number of amino groups on the surface of CG.

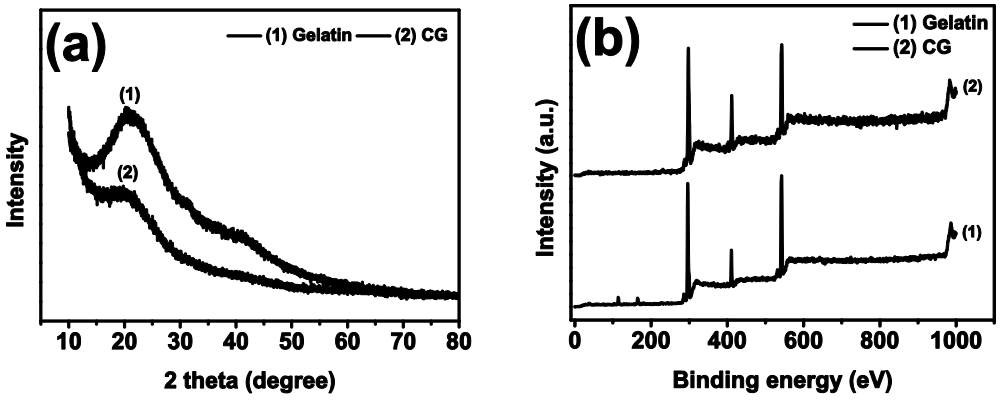

Figure 5.4: (a) XRD patterns and (b) XPS survey scan spectra of gelatin and CG

Table 5.1**:** Elemental composition of gelatin and CG from high resolution XPS spectra

Element	CG	Gelatin
C (%)	60.5	67
N (%)	18.5	11.5
O (%)	21	21.5

The rheological behaviour of gelatin and CG in aqueous solution is examined. Figure 5.5 (b) shows the viscosity values of gelatin and CG solutions (20 % w/v) at 25 and 37 °C. The values are recorded at a shear rate of 100 s^{-1}. The rheological behaviour of aqueous solution of gelatin and CG shows that, after cationization, the viscosity is reduced drastically (Figure 5.5 (a) and Figure 5.5 (b)). This is mainly due to the rupture of the triple helical structure of gelatin leading to the reduction in the extent of hydrogen bonding interactions. The higher viscosity value of aqueous gelatin at 25 °C is due to the gelation, as a result of the formation of inter and intramolecular hydrogen bonding among gelatin molecules. When temperature increases to 37 °C, hydrogen bonding breaks and viscosity is drastically reduced. On the other hand, CG shows very low viscosity at 25 °C, compared to gelatin. This is due to the destruction of triple helical structure and loss of hydrogen bonding as a result of cationization. The amino groups are protonated and hence they are not available for hydrogen bonding. Even at 37 °C, there is not much variation in the viscosity of CG solution compared to that at 25 °C. These data obviously provide the evidence for the formation of CG and its solubility in water without undergoing gelation.

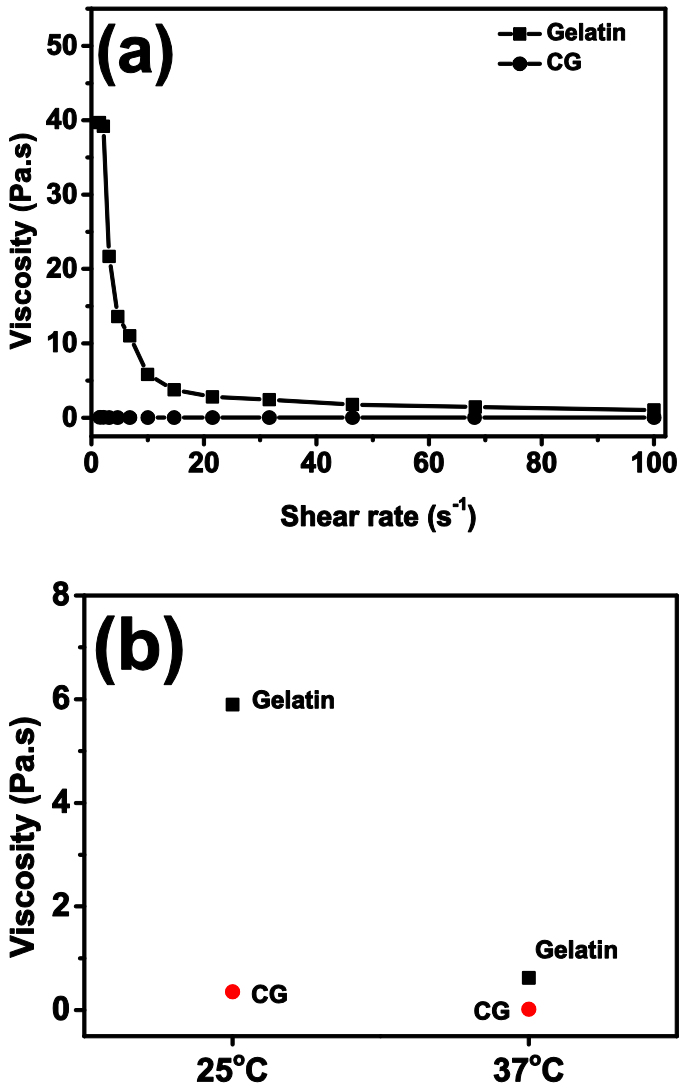

Figure 5.5: Variation of viscosity with (a) shear rate and (b) temperature for aqueous solutions of 20 % w/v gelatin and CG

5.2.2 Electrospinning of CG

For circumventing the limitations associated with solvents for electrospinning, gelatin is modified by cationization. CG prepared in the present work shows excellent water solubility without forming gel as is the case with gelatin. This characteristic is clear from Figure 5.6, which shows the photographs of 20 % aqueous solutions of gelatin and CG taken in sample vials at room temperature. This can aid processing of the material for different applications.

This observation throws light towards a green fabrication strategy for CG nanofibers by electrospinning using water as the solvent.

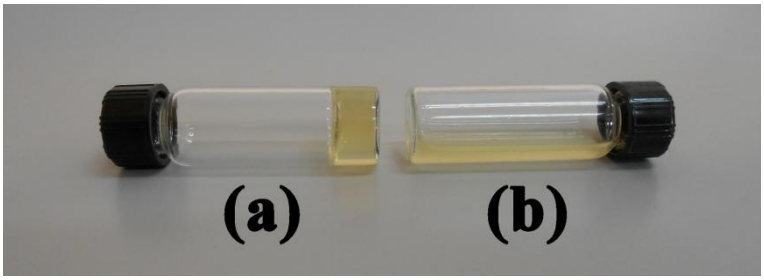

Figure 5.6: (a) Gelatin (20 % w/v) in water and (b) CG (20 % w/v) in water at room temperature

Electrospinning of CG is performed by varying the solution and spinning parameters in a trial and error method. The concentrations of CG are varied from 30 to 50 % (w/v). Fibers start forming when CG concentration is 45 % (w/v) and beadless smooth fibers are collected when CG concentration is 50 % (w/v) in water with flow rate of 0.2 ml/h, potential of 25-30 kV and working distance of 15 cm. The nanofibers collected are dried under vacuum and analysed for morphology. SEM image of the CG nanofibers fabricated from pure water at room temperature is shown in Figure 5.7 (a). The fiber diameter distribution is obtained by measuring the width of 200 individual nanofibers from the SEM image (Figure 5.7 (b)). The fiber diameter is found to be 130 ± 40 nm.

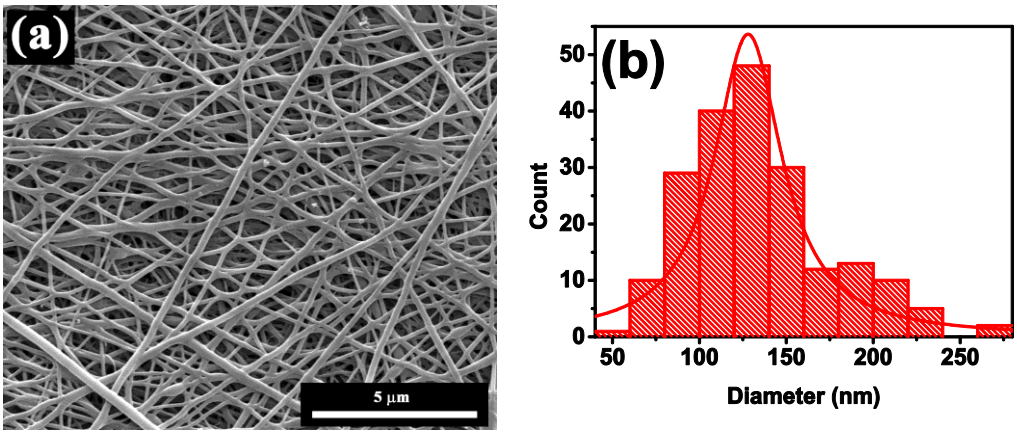

Figure 5.7: (a) SEM image and (b) diameter histogram of CG nanofibers prepared from 50 % (w/v) solution of CG in water

5.2.3 Cross-linking and characterizations of CG nanofibers

CG nanofibers are cross-linked using dextran aldehyde (DA) and sucrose aldehyde (SA). Cross-linking is carried out by dipping the CG nanofibrous mats in ethanol solution of DA and SA for 7 days. The resulting nanofibers are represented as DA-CG and SA-CG respectively, for cross-linking with DA and SA. The large number of amino groups introduced on gelatin as a result of cationization enable effective cross-linking between amino groups on CG and aldehyde groups on the cross-linking agent by Schiff's base formation. Cross-linking is confirmed by observing the SEM images of cross-linked and swelled mats (Figure 5.8 (a-d)). SEM images reveal that, cross-linking and subsequent swelling process cause the fibers to lose its discreteness with increase in fiber diameter. However, compared to as spun CG mats, cross-linked mats maintain the fibrous morphology even after dipped in water. The mats are found to be stable in water up to one week without affecting its structural integrity. Thus DA and SA are effective cross-linking agents for CG nanofibers. Cross-linking ability of DA and SA for gelatin nanofibers is already established and discussed in the previous chapters.

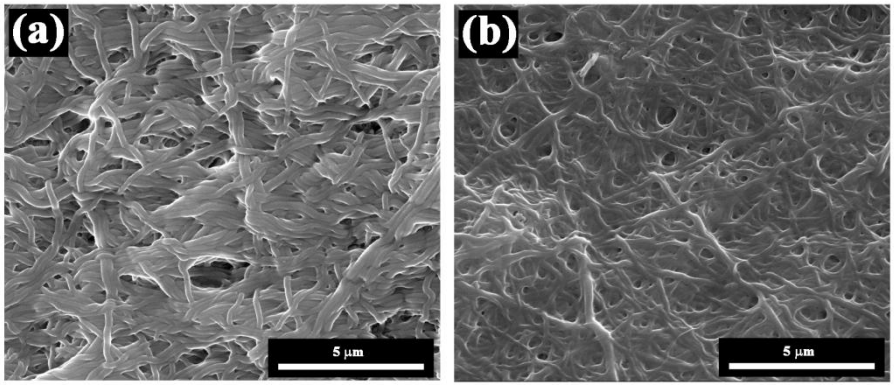

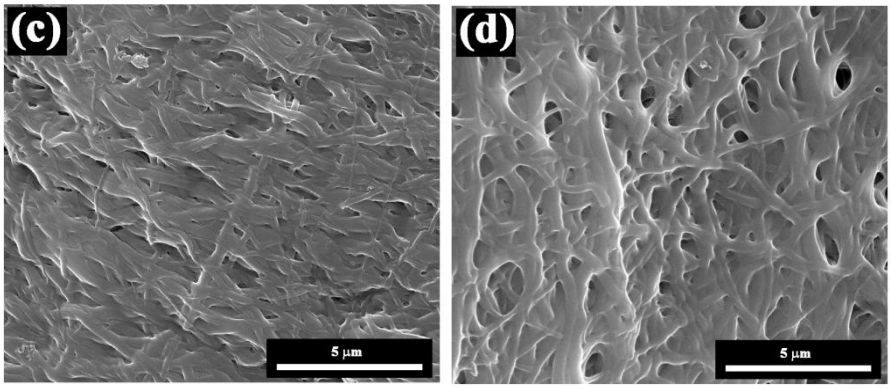

Figure 5.8: SEM images of (a) DA-CG mats, (b) DA-CG swelled mats, (c) SA-CG mats and (d) SA-CG swelled mats (swelling is done by dipping the mats in water for 24 h)

Cross-linking can be further explained from FTIR spectra and thermograms of the cross-linked mats. FTIR spectra of DA-CG and SA-CG mats show peaks at 1016 cm^{-1} due to the C-O-C stretching frequencies of dextran and sucrose moieties, which is absent in the spectra of as spun CG mat (Figure 5.9). DSC thermograms of as spun and cross-linked CG nanofibers are shown in Figure 5.10. DSC thermogram of as spun CG nanofibers shows endothermic peak at 84 ^{o}C. The cross-linked nanofiber mats show the endothermic peaks at higher temperature regions (DA-CG; 98 ^{o}C, SA-CG; 99 ^{o}C) due to the newly introduced covalent bonds as a result of cross-linking. These results reveal improved thermal stability of DA-CG and SA-CG nanofibrous mats.

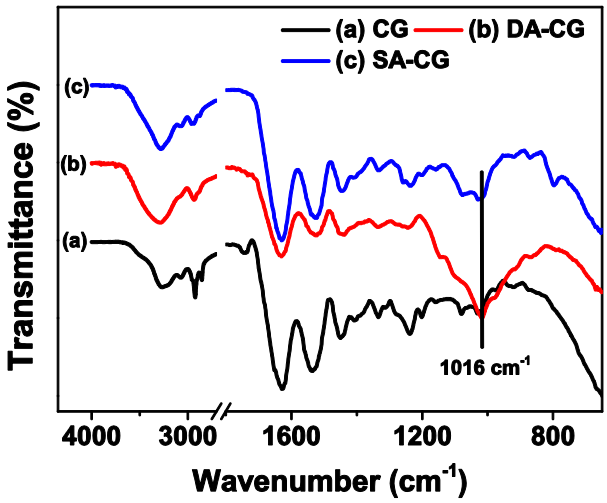

Figure 5.9: FTIR spectra of (1) CG mat, (2) DA-CG and (3) SA-CG mats

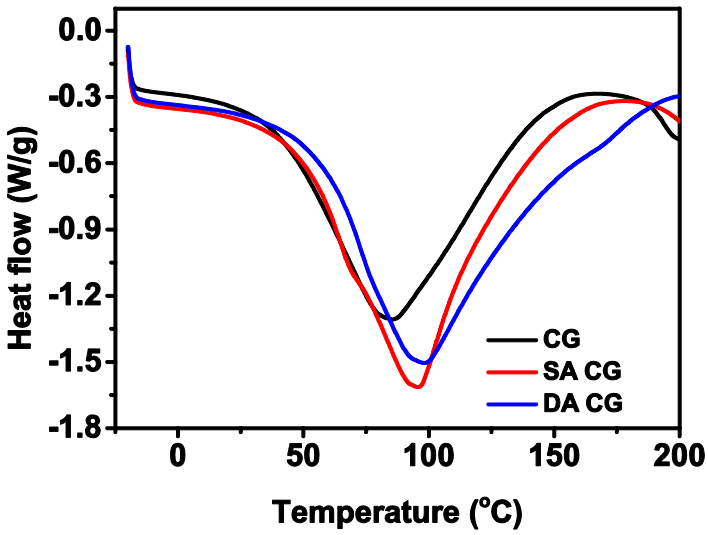

Figure 5.10: DSC thermograms of CG, DA-CG and SA-CG mats

Swelling ability of the nanofibrous scaffold helps in maintaining the shape of the scaffold and supports the growth of the cells. Here, as spun CG nanofibers dissolve in water while the cross-linked mats show a stable swelling behaviour. The results of swelling experiment (Figure 5.11) show that DA cross-linked mats exhibit a lower swelling ratio which is direct evidence of better cross-linking efficiency of DA compared to SA. Higher degree of cross-linking is due to the macromolecular chain entanglement in DA molecule which causes a better interaction among the chains of DA and gelatin. Also, the presence of small amount of borax in DA solution facilitates the cross-linking. Alkaline pH has an important role in determining the degree of cross-linking between amino groups of gelatin and aldehyde groups of the cross-linking agent. A pH higher than the isoelectric point of gelatin is found to favour the Schiff's base formation. The presence of small amount of water also favours better interaction between CG nanofibers and the cross-linking agent. Sucrose aldehyde also is reported to be an effective cross-linker for proteins, but in this case, SA is dissolved in pure ethanol and thus the interaction between the reactants is less effective. These results further validate the degree of cross-linking obtained from TNBS assay. Table 5.2 shows the degree of cross-linking of CG mats. From the table, it is clear that DA-CG exhibits higher cross-linking degree compared to SA-CG.

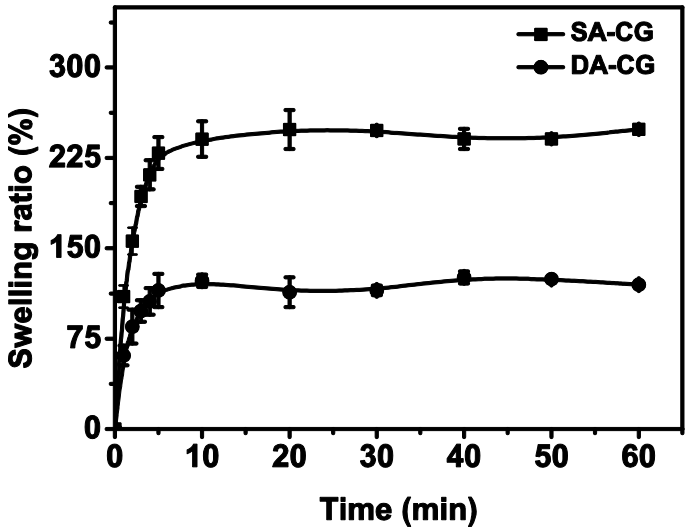

Figure 5.11: Swelling behaviour of DA-CG and SA-CG mats under physiological conditions

Table 5.2: Cross-linking degrees of cross-linked CG mats

Cross-linking agent	Degree of cross-linking (%)
Dextran aldehyde (DA)	76 ± 3
Sucrose aldehyde (SA)	60 ± 4

In vitro degradation behaviour of the cross-linked CG nanofibers as a function of degradation time is presented in Figure 5.12. The rate of weight loss is less in the case of DA-CG in comparison with SA-CG indicating that degradation pattern is affected by the cross-linking degree and the nature of the cross-linker. Cross-linked mats are stable up to one week and there after the mats undergo gradual degradation indicated by the decrease in weights with time. The higher degree of cross-linking in the case of DA-CG results in more resistance to degradation in PBS medium at 37 °C as compared to SA-CG. Similar reports are available in literature explaining the effect of cross-linking degree on the degradation behaviour of the proteins (Vaz et al., 2003). The presence of covalent bonds formed as a result of cross-linking provides strength for the sample for a longer period during degradation. In the case of cross-linked mats with higher cross-linking degree, more chains have to be cleaved in order to dissolve a fragment in the medium (Damink et al., 1996).

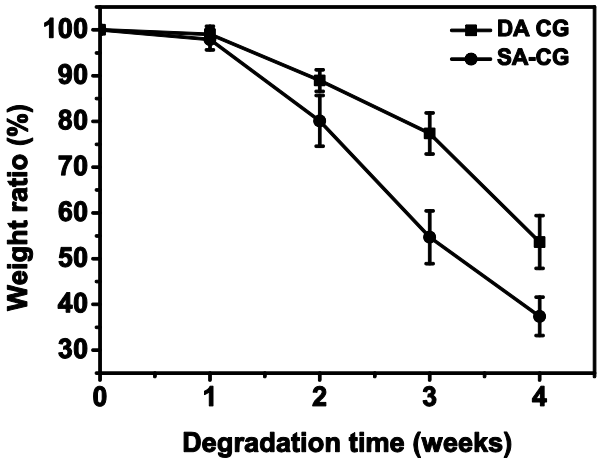

Figure 5.12: Degradation of DA-CG and SA-CG mats under physiological pH at 37 °C

5.2.4 Biological studies

5.2.4.1 Adhesion and proliferation of L-929 fibroblast cells on cross-linked mats

Cross-linked CG nanofibers are evaluated for adhesion of L-929 fibroblast cells. The morphology of fibroblast cells adhered on the DA-CG and SA-CG mats in comparison with control cover glass after 48 h of contact is shown in Figure 5.13. The results exhibit the suitability of both DA and SA as cross-linking agents for CG nanofibers. Fluorescent microscopic images of L-929 cells cultured on the cross-linked mats reveal that considerable amount of cells are grown on the DA-CG and SA-CG mats with well-distributed actin filament and nuclei. This cell attachment study clearly shows the efficiency of CG nanofibers cross-linked with the natural cross-linkers to promote cell adhesion.

L-929 cells are allowed to grow in the medium of the extract of the test materials, namely DA-CG and SA-CG. For comparison of the results, a control material, namely, glutaraldehyde cross-linked CG mats (GT-CG) is also used. GT-CG is prepared by exposing CG mats to glutaraldehyde vapours for 72 h as mentioned in the previous chapters for gelatin mats. On comparing the results, cells in DA-CG and SA-CG extracts show increase in the percentage cellular activities during 1 to 3 days which in turn relates to the cellular growth and

proliferation. On the other hand, cells in contact with the extract of GT-CG show retarded growth of L-929 cells, which can be due to the internal toxicity effects of the residual glutaraldehyde (Figure 5.14).

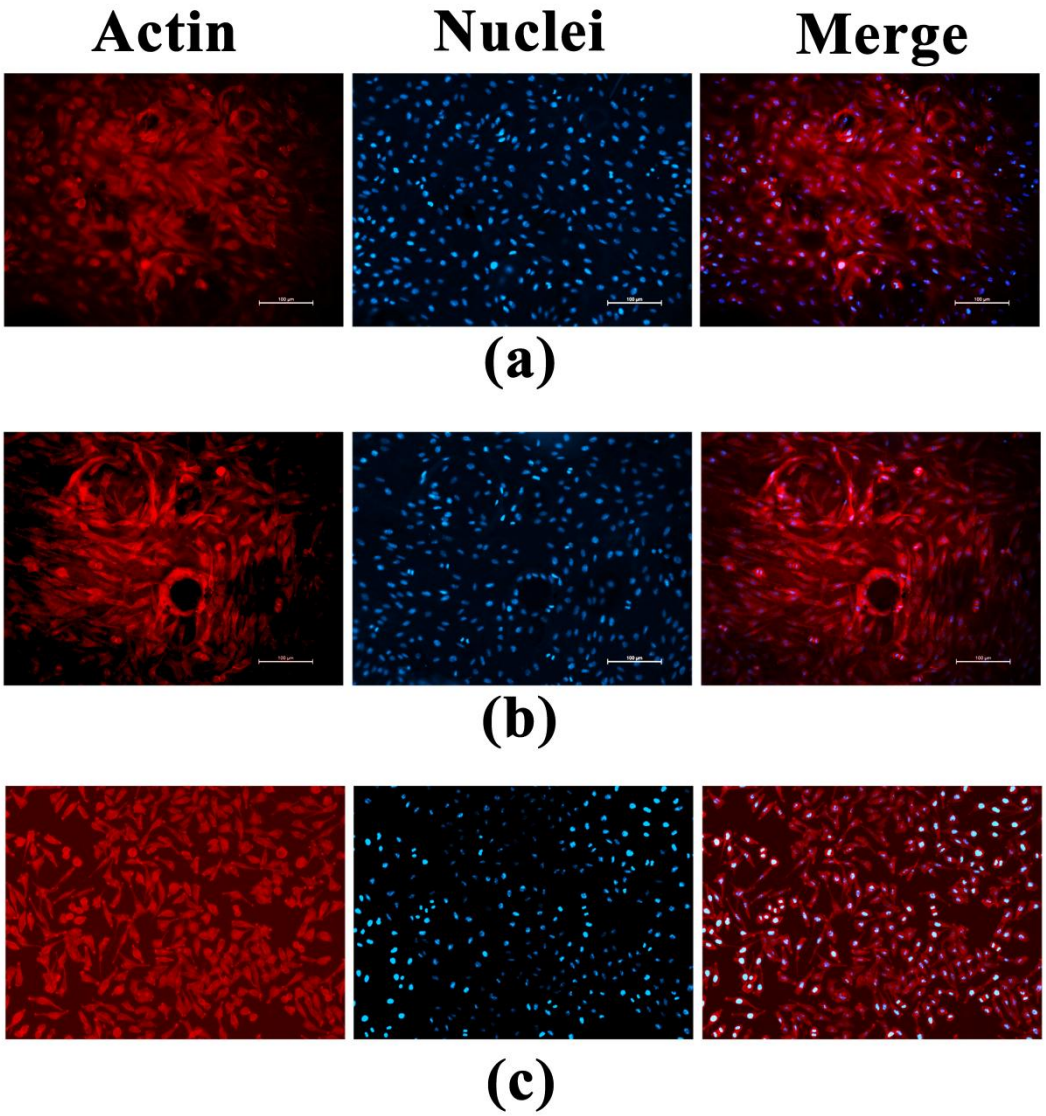

Figure 5.13: Fluorescent microscopic images of L-929 cells adhered on (a) DA-CG, (b) SA-CG mat and (c) control cover glass after 48 h culture

5.2.4.2 Adhesion and proliferation of MG-63 osteoblast cells

Cell adhesion, spreading and actin development of MG-63 cells cultured on CG nanofibrous mats are studied by confocal microscopy. The images taken on the fifth day of culture are shown in Figure 5.15. The cells grow abundantly on

DA-CG and SA-CG mats with well distributed actin filaments and prominent nuclei. The nanofibrous architecture of CG mat encourages the cell attachment due to the properties of nanofibers such as large surface area and improved surface functionality. This provides enhanced cell growth and better cell-material interactions. Moreover, the positive charges on the surface of CG nanofibers facilitate cell adhesion of different cells due to the interaction with negatively charged cell membranes.

For assessing the cell proliferation of MG-63 osteoblast cells on the cross-linked CG nanofibers, Alamar blue assay is carried out. Equal numbers of cells are seeded on the cross-linked CG mats. It is observed that cells grow normally on the mats for a period of 7 days. Till 5^{th} day, there is not much growth rate observed for the samples. This time can be considered as the adaptation period for the cells to the new environment. A good growth rate can be observed for DA-CG and SA-CG compared to GT-CG from 5 to 7 days (Figure 5.16). The data at day 3, 5 and 7 are significantly different than the first day of cell seeding, which signifies ample cell growth on the day points.

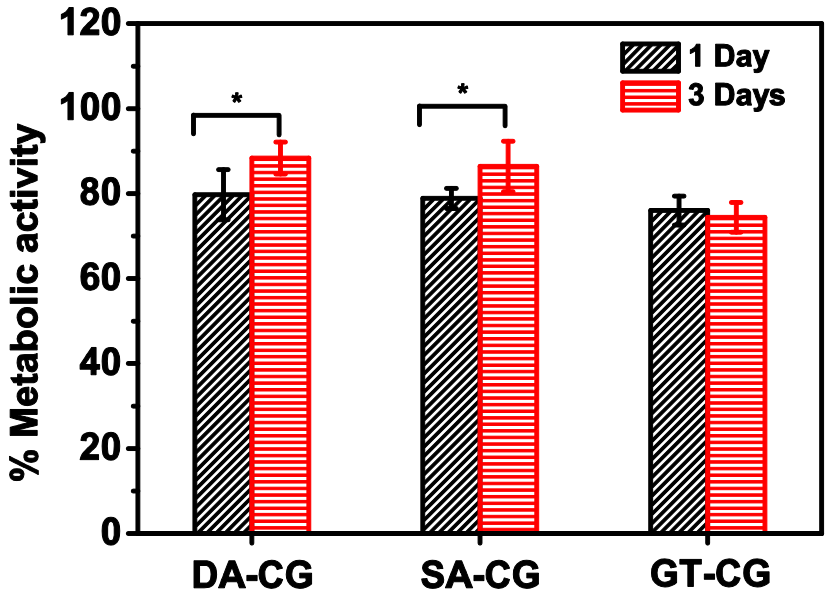

Figure 5.14: MTT assay of the L-929 cells in the extracts of DA-CG, SA-CG and GT-CG mats (* $p < 0.05$)

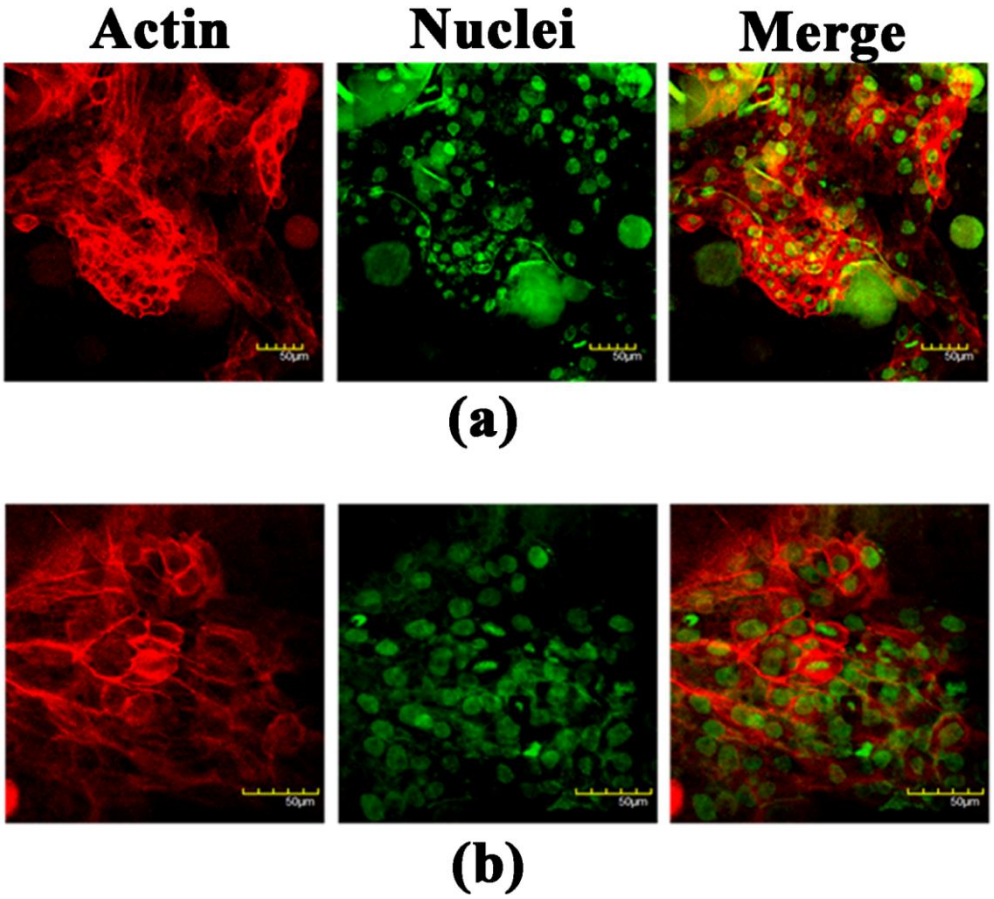

Figure 5.15: The confocal laser micrographs of human osteoblast cells (MG-63) on the cross-linked CG nanofibers stained with Rhodamine–phalloidin for actin filaments (red) and Hoechst 33342 for nuclei (green). The cells are cultured on (a) DA-CG and (b) SA-CG mats

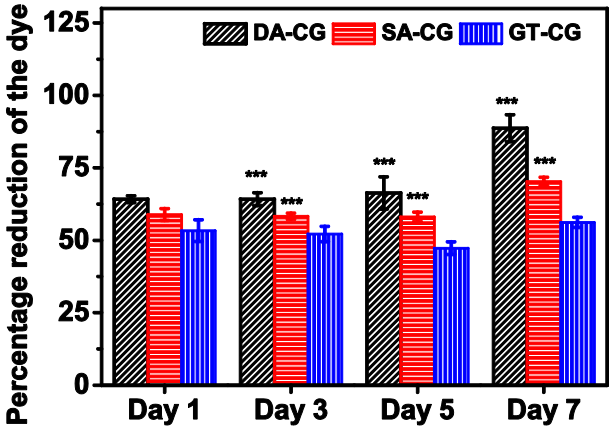

Figure 5.16: The cell proliferation (MG-63) on DA-CG and SA-CG mats. Initial cell seeding density is 2000 cells/scaffold. Data represented as the mean ± standard error (*** $p \leq 0.001$)

5.3 Conclusion

In the past, research on tissue engineering using gelatin based nanofibers focused on the production of biocompatible and *in situ* cross-linked gelatin nanofibers by minimizing the toxicity effects from solvents and cross-linking agents. The possibility to modify gelatin by altering its isoelectric point and cross-linking agents has been investigated as a tool to tune cell-material interactions. The chemical modification of gelatin *via* amination produces cationized gelatin. The modified gelatin is water soluble without forming gel at room temperature. This is the first attempt to explore a green nanofiber fabrication method using CG with pure water as the solvent. The fabricated nanofiber is cross-linked using natural and cost effective cross-linking agents. They are better alternatives for glutaraldehyde and genipin. The positive charge on the surface of CG nanofibers interacts with negatively charged cell surface, making them an exciting class of materials for tissue regeneration. The modification of gelatin and its combination with novel cross-linkers demonstrate the versatility of this biomaterial. This ensures its role as a matrix for various tissue regenerations.

CHAPTER 6

FABRICATION AND CHARACTERIZATION OF GELATIN/CHITOSAN CORE-SHELL NANOFIBERS

6.1 Introduction

Electrospinning is a simple and versatile technique which has attracted the attention of researchers in the field of nanofibers and nanotechnology (Bhardwaj and Kundu, 2010; Li and Xia, 2004b). In recent years, many modifications are attempted in the basic electrospinning process in order to enhance the quality and functionality of the resulting nanofibers. Coaxial electrospinning is an upcoming technology that has emerged from the conventional electrospinning process in order to realize the production of nanofibers of less spinnable materials with potential applications (Sun et al., 2003). A typical coaxial set-up consists of two concentric needles, through which core and shell solutions come out and meet at the tip. The droplet forms a compound Taylor cone at the tip when high electric voltage is applied at the needle. The main advantage of this method is the enhancement in the electrospinnability of a less spinnable material with the help of a highly spinnable material, used either as core or shell (Chang et al., 2003; Loscertales et al., 2002; Moghe and Gupta, 2008; Sun et al., 2003). Core-shell nanofibers of different synthetic-synthetic and natural-synthetic polymers are reported (Jiang et al., 2005; Li et al., 2004; Li et al., 2008; Liu et al., 2013; Pakravan et al., 2012; Sun et al., 2003; Wang et al., 2006; Zhang et al., 2004). They possess potential applications in the field of drug delivery, tissue engineering, and wound healing (Jin et al., 2013). However, the core-shell nanofibrous systems containing purely natural polymers are very limited in the literature. Biocompatible and natural polymers as both core and shell materials may greatly enhance its scope in biomedical arena.

Both chitosan and gelatin are natural biopolymers with extensive applications in biomedical and pharmaceutical fields. Gelatin is a highly spinnable material and numerous reports are available on the fabrication of gelatin nanofibers (Huang et al., 2004; Ki et al., 2005; Ko et al., 2010). On the other hand, chitosan is extremely difficult to be spun mainly due to its polyelectrolyte nature (Chong et al., 2007). A few reports are found on fabrication of chitosan nanofibers, where a highly corrosive and toxic solvent, namely trifluoroacetic acid (TFA) is employed for spinning (Ohkawa et al., 2004; Sangsanoh and Supaphol, 2006; Schiffman and Schauer, 2007). Geng et al. have reported fabrication of chitosan nanofibers using concentrated acetic acid (Geng et al., 2005). This method is found to be applicable to chitosan of a particular molecular weight only. Problems associated with electrospinning of chitosan are alleviated by using blends of chitosan with synthetic polymers such as polyethylene oxide (Bhattarai et al., 2005), polyvinyl alcohol (Charernsriwilaiwat et al., 2014), polylactic acid (Ignatova et al., 2009) and poly(caprolactone) (Shalumon et al., 2010). For improving the biological performance of chitosan derived nanofibers, researchers have attempted electrospinning of chitosan with natural polymers such as gelatin (Dhandayuthapani et al., 2010; Qian et al., 2011; Tsai et al., 2013), collagen (Chen and Su, 2011) and silk fibroin (Chen et al., 2012). A recent advancement in fabricating chitosan nanofiber is based on the technique of coaxial electrospinning. The core-shell nanofibers are fabricated with highly spinnable synthetic polymers as core or shell templates (Ji et al., 2013; Ojha et al., 2008; Pakravan et al., 2012). Ojha et al. have reported the fabrication of chitosan nanofibers *via* coaxial electrospinning with polyethylene oxide (PEO) as shell template. Chitosan nanofibers are obtained after removing PEO by dipping the nanofibers in distilled water (Ojha et al., 2008). Recently, core-shell nanofibers with chitosan shell and PEO core in aqueous acetic acid by coaxial electrospinning have been reported by Pakravan et al. PEO is removed by dipping the core-shell nanofibers in water for 24 h to obtain hollow chitosan nanofibers (Pakravan et al., 2012).

In the present work, novel core-shell (CS) structured nanofibers are fabricated using purely natural origin, with gelatin as the core material and chitosan as the shell. This method avoids the use of synthetic polymer as core template for chitosan nanofibers. Also, the post treatment to remove the core material is not required. Since gelatin and chitosan are hydrophilic and easily degradable materials, nanofibers from gelatin and chitosan lose the fibrous morphology when kept in contact with aqueous medium. Hence, cross-linking treatments are necessary for improving the water stability of the nanofibers prepared from gelatin and chitosan. Dextran aldehyde (DA) and sucrose aldehyde (SA) are established as effective cross-linkers for gelatin and modified gelatin nanofibers. The feasibility of utilizing DA and SA as cross-linking agents for the present core-shell nanofibers is thoroughly investigated. Chitosan as the shell can mimick the extracellular matrix because of its structural resemblance with glycosaminoglycan (GAG), a major constituent of ECM (Francis Suh and Matthew, 2000). Gelatin core can be utilized as a matrix for incorporating drugs and bioactive molecules. The present gelatin/chitosan core-shell nanofibrous structure can overcome the shortcomings due to the incorporation of synthetic polymers and may result in a novel system with improved biological properties.

6.2 Results and Discussion

6.2.1 Morphology and microstructure of core-shell nanofibers

Core-shell nanofibers are fabricated by optimizing the solution and spinning parameters. Bead free fibers are obtained when the applied voltage is 30 kV and the concentration of chitosan and gelatin in aqueous acetic acid are 5 % and 30 % (w/v) respectively. The solutions form a stable and compound Taylor cone at 25-30 kV. The flow rate of the solution is appropriately adjusted so as to obtain bead free compound core-shell fibers. The schematic representation of coaxial electrospinning set-up used in this study is shown in Figure 6.1.

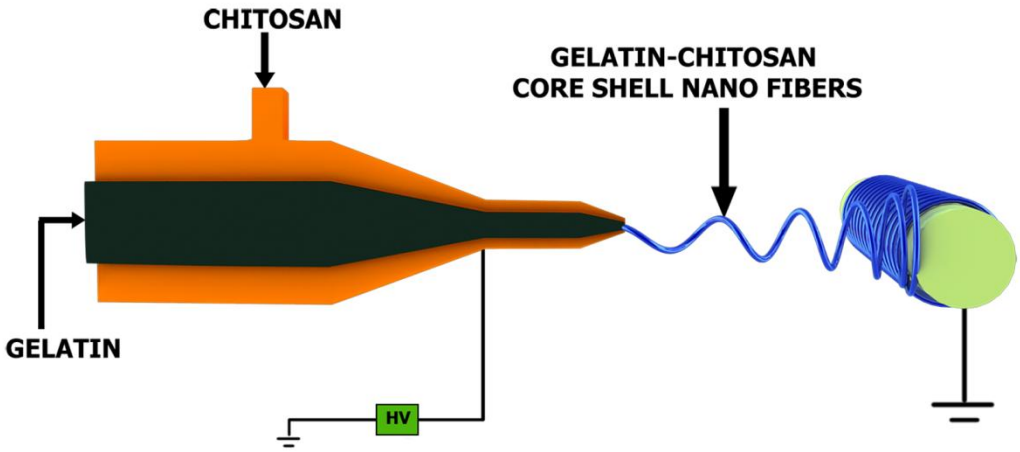

Figure 6.1: Schematic of the coaxial electrospinning set-up for gelatin/chitosan core-shell nanofibers

The morphology of the nanofibers is observed through SEM (Figure 6.2 (a)). Fibers are mostly randomly oriented with narrow fiber diameter distribution. The finer detailed single fiber core-shell structure of the prepared chitosan/gelatin nanofibers is visualized by TEM as shown in Figure 6.2 (b). A clear difference in the contrast between the core and shell region is observed in the micrograph. The contrast between the sample layers is due to the difference in the transmissibility of electron beam from chitosan and gelatin regions. This difference proves the formation of core-shell structures. The inner dark region in the TEM image corresponds to gelatin and the outer light region is identified as chitosan. The diameter of the fiber shown in the TEM image is 110 nm with a core diameter of 68 nm. The fiber diameter varies between 100-200 nm range as observed from the SEM and TEM images. The fiber diameter distribution of the nanofibers obtained by measuring the width of randomly selected 200 data points is displayed in Figure 6.2 (c). The average diameter is found to be 150 ± 60 nm.

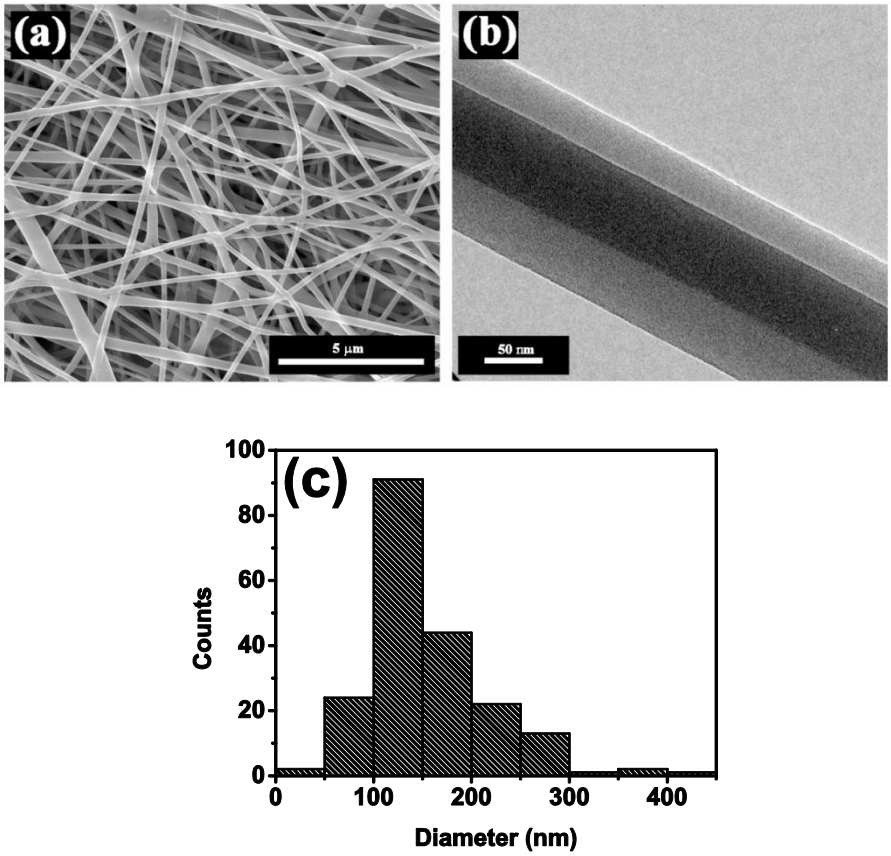

Figure 6.2: (a) SEM image and (b) TEM image and (c) diameter histogram of the gelatin/chitosan core-shell nanofibers

6.2.2 Thermal and spectroscopic analysis

The presence of chitosan and gelatin in the core–shell structure is confirmed by TGA and FTIR spectroscopy. TGA thermograms and first order derivative curves (DTG) of pure chitosan, pure gelatin and core-shell nanofibers are shown in Figure 6.3 ((a) and (b)). In the TGA thermogram, the percentage residues at 500 °C for pure chitosan, pure gelatin and core-shell nanofibers are 39, 24 and 29 %, respectively. The residue from the core-shell nanofiber is in between that of pure chitosan and gelatin. The DTG thermograms of pure chitosan and gelatin show decomposition temperatures at 288 and 291 °C respectively. The core-shell nanofiber mat exhibits two decomposition temperatures at 282 and 305 °C. Thus the decomposition pattern of the core-shell system is a combination of the patterns of pure chitosan and gelatin. These results show the presence of both chitosan and gelatin in the resulting composite nanofibers.

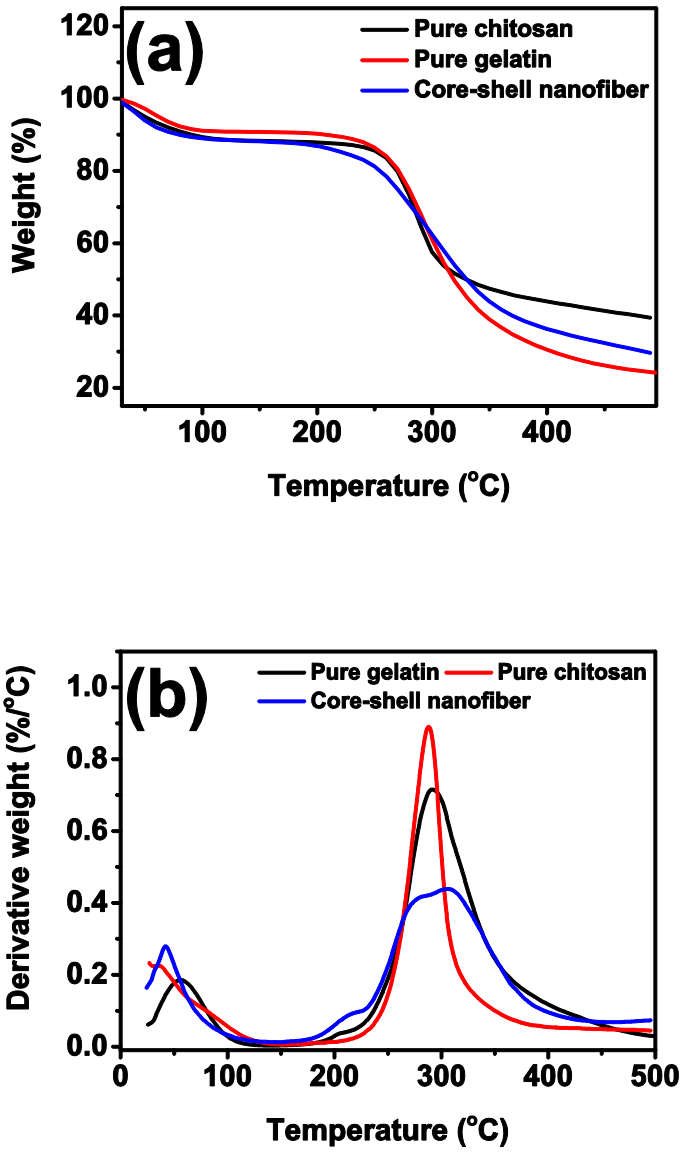

Figure 6.3: (a) TGA thermograms and (b) DTG thermograms of pure gelatin, pure chitosan and core-shell gelatin/chitosan mats

Figure 6.4 shows the FTIR spectra of pure chitosan, pure gelatin and core-shell nanofibers. All the three spectra exhibit broad bands at 3100-3500 cm^{-1} due to O-H and N-H stretchings. These spectra also demonstrate amide I (C=O stretching at 1638 cm^{-1}), amide II (N-H stretching of secondary amide at 1537 cm^{-1}) and amide III (vibrations in the plane of C-N and N-H groups in amide at 1240 cm^{-1}) bands. These are the characteristic peaks for both chitosan and gelatin. The two distinct peaks are observed in the spectra of chitosan and core-shell nanofibers at 1030 and 1149 cm^{-1} which are absent in the spectrum of gelatin.

These peaks are attributed to the C-O-C symmetric and asymmetric stretching of chitosan (Paluszkiewicz et al., 2011). Moreover, the spectrum of core-shell mat is similar to the pure chitosan spectrum indicating the presence of chitosan on the surface. This observation confirms the presence of chitosan and gelatin in the core-shell system.

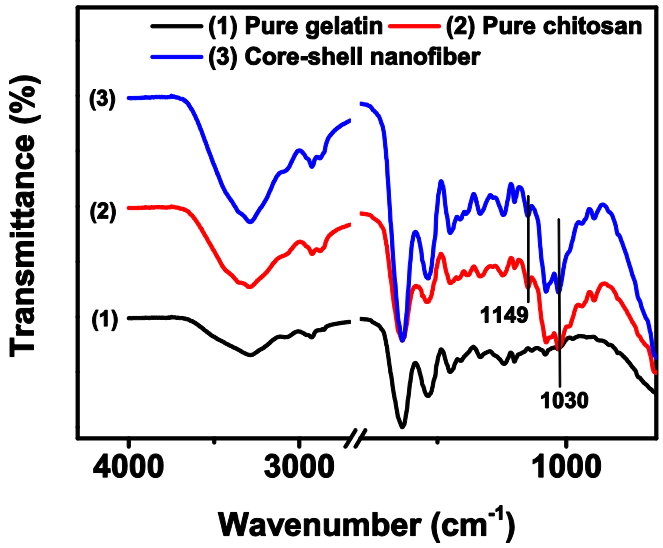

Figure 6.4: FTIR spectra of pure gelatin, pure chitosan and core-shell gelatin/chitosan mats

The chemical composition of the core-shell nanofibrous surface is investigated using X-ray photoelectron spectroscopy (XPS). This result indicates the presence of chitosan on the surface of core-shell mat. The XPS survey scan spectra of pure gelatin, pure chitosan and core-shell mats are shown in Figure 6.5. The atomic compositions of carbon, nitrogen and oxygen are calculated from high resolution XPS spectra. Gelatin and chitosan contain C, N and O in various compositions as shown in Table 6.1. In order to know the surface composition, the C/N ratios of the samples are estimated. The C/N ratio of pure gelatin and chitosan are 4.02 and 10.9 respectively, which are in agreement with the reported values (He et al., 2012). The present core-shell mat exhibits a C/N ratio of 8.6 which is nearer to that of chitosan, indicating the presence of chitosan on the surface.

Table 6.1 : Elemental atomic compositions of gelatin, chitosan and core-shell mats

Atomic composition	**Gelatin**	**Chitosan**	**Core-shell mat**
C 1s (%)	63.49	67.3	74.29
N 1s (%)	15.79	6.16	8.65
O 1s (%)	20.72	26.53	17.06

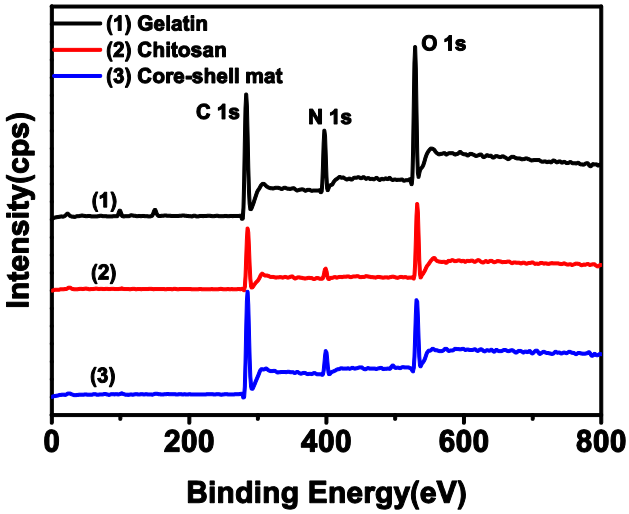

Figure 6.5: XPS survey scan spectra of gelatin, chitosan and core-shell nanofiber mat

The core-shell structure of gelatin/chitosan nanofibers are successfully demonstrated by TEM, thermal and spectroscopic analysis. The present core-shell nanofibers are different from the existing core-shell system based on the fact that core-shell nanofibers with purely natural polymers are developed in this work. Easily spinnable gelatin is used as the core template to facilitate spinning of chitosan from the aqueous solution, which is otherwise impossible. The surface properties of the core-shell nanofibers are comparable to pure chitosan which would make these nanofibers suitable in various biomedical applications where, chitosan plays the major role. Chitosan resembles the disaccharide moiety, GAG present in the ECM which assists the regeneration of cartilage, bone and skin with inherent anti bacterial properties (Di Martino et al., 2005). The core gelatin can be kept as such due to the well-known properties of gelatin such as biocompatibility, non toxicity, non antigenicity and appropriate biodegradability.

The formation of the present gelatin/chitosan core-shell composite nanofibers provides a different strategy for obtaining nanofibers with chitosan on the surface. This core-shell system can be more effective than other core-shell nanofibers based on synthetic-synthetic and natural-synthetic polymer based systems in terms of biocompatibility, biodegradability and non-toxicity. Although this work has not examined the incorporation and release of drug molecules from gelatin, it is expected that the core gelatin can be made use for loading different types of drugs and bioactive molecules.

6.2.3 Cross-linking and characterization of core-shell nanofibers

The cross-linking of gelatin and chitosan by aldehydes is predominantly due to the reaction of the primary amino groups of gelatin and chitosan with the available aldehyde groups. The amino groups present in gelatin and chitosan are likely to react with the aldehydes groups of the cross-linking agents forming the relatively stable Schiff's base or aldimine. The chitosan and gelatin based nanofibers are known to be successfully cross-linked using glutaraldehyde *via* Schiff's base formation (Schiffman and Schauer, 2007; Zhang et al., 2006). Investigations on the biological relevance of glutaraldehyde cross-linking demonstrate that the glutaraldehyde beyond a particular concentration can induce severe toxic response. Being a small molecule, it penetrates into the interiors of the nanofibrous mats leaving unreacted residues in the nano structures, which can cause toxicity (Sisson et al., 2009; Wu et al., 2011). Hence researchers explore the application of other alternative cross-linking agents. It is established that dextran aldehyde (DA) and sucrose aldehyde (SA) are suitable biocompatible cross-linking agents for gelatin based nanofibers. We make use of this approach for the cross-linking of gelatin and chitosan based core-shell nanofibers also. Cross-linking is carried out by dipping the core-shell mats in ethanol solution of DA and SA. DA and SA cross-linked core-shell gelatin chitosan mats are represented as DA-CS and SA-CS, respectively.

SEM images of the cross-linked nanofibers before and after immersing in water for 24 h are shown in Figure 6.6. The SEM images show that the cross-

linking of nanofibers preserved the fibrous structure and morphology even after keeping in contact with aqueous medium. Thus SA and DA are proved to be effective cross-linking agents for the gelatin/chitosan core-shell nanofibers.

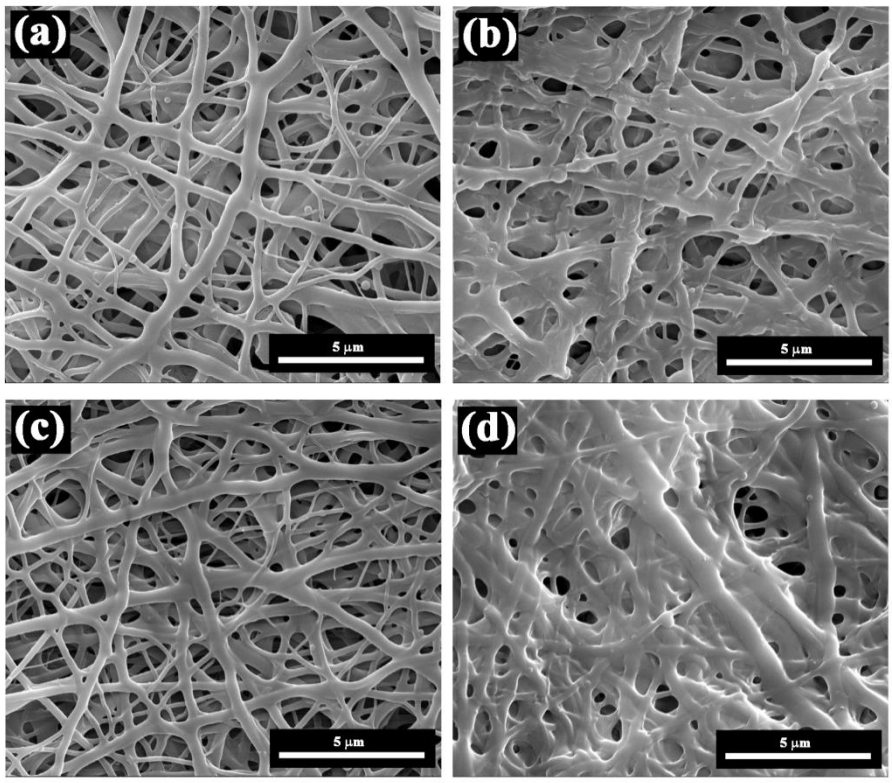

Figure 6.6: SEM images of DA-CS (a and b), SA-CS (c and d) cross-linked core shell nanofibers before and after immersing in water, respectively

Water absorption capability of the cross-linked nanofibers is evaluated by examining the swelling behaviour of the nanofibers. The swelling ratios of as spun and cross-linked mats are shown in Figure 6.7 (a). The swelling ratio of as spun mat increases initially and then decreases with time. This is due to the dissolution of gelatin core in water. DA-CS and SA-CS mats exhibit a lower and stable swelling ratio as compared to the as spun core-shell nanofibrous mats. The decrease in swelling ratio indicates reduced water absorption capacity of the cross-linked mats. This in turn is attributed to the effect of cross-linking. Nanofibrous mats cross-linked with suitable cross-linking agents exhibit lower water uptake capacity compared to the uncross-linked mats (Nguyen, 2010).

Degradation behaviour of a biomaterial is one of the key aspects in the field of tissue engineering and drug delivery. An ideal scaffold for a specific

tissue undergoes degradation with a rate similar to that of neo-tissue formation. *In vitro* degradation of the cross-linked core-shell mats are carried out under physiological conditions. The extent of degradation is estimated in terms of change in dry weight of the mats with time. DA-CS and SA-CS mats exhibit gradual degradation behaviour under physiological conditions (Figure 6.7 (b)). At the end of the fifth week, around 35-45 % of both DA-CS and SA-CS mats remain, which may be due to the inability of chitosan to degrade in the absence of enzyme. Compared to degradation of gelatin, chitosan degrades at a relatively slower rate in the absence of enzymes (Archana et al., 2013). Moreover, cross-linking imparts a decrease in the water uptake capacity that slows down the degradation of both gelatin and chitosan (Vaz et al., 2003).

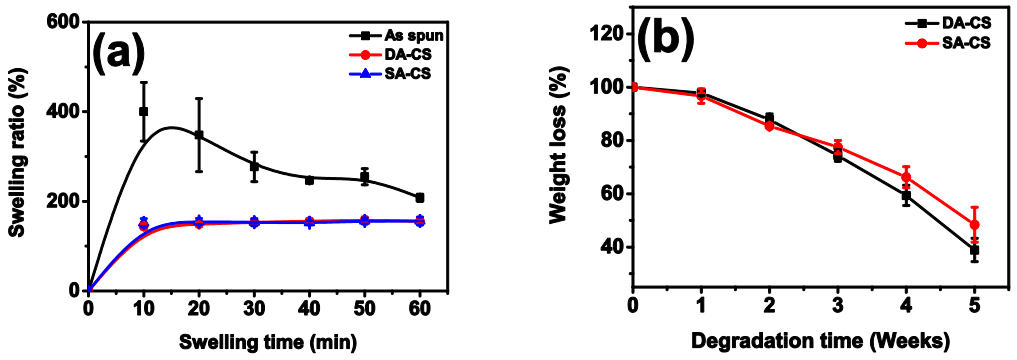

Figure 6.7: (a) The swelling ratio and (b) degradation behaviour of the cross-linked core-shell mats

The cross-linking of gelatin/chitosan core-shell nanofibers is evident from the FTIR spectra (Figure 6.8). The cross-linked mats exhibit the characteristic features of chitosan and gelatin along with certain features of the cross-linking agents too. The as spun mat shows a peak at 1640 cm^{-1} due to the amide I band. In the cross-linked mat, this peak gets shifted to lower wave number of 1629 cm^{-1} due to the cross-linking process. The peak at 1400 cm^{-1} is observed to be broadened in the spectrum of the cross-linked mat compared to that in the as spun mat. This broadening is due to the appearance of a new peak in the range of 1400-1380 cm^{-1} owing to the formation of aldimine (-C=NH-) stretching as a result of cross-linking. The intensity of peak at 1030 cm^{-1} increases (1030 cm^{-1} in as spun mat is due to the C-O-C stretching of chitosan moiety) in the case of DA-CS and

SA-CS mats due to the C-O-C peaks of dextran and sucrose (Figure 6.7).

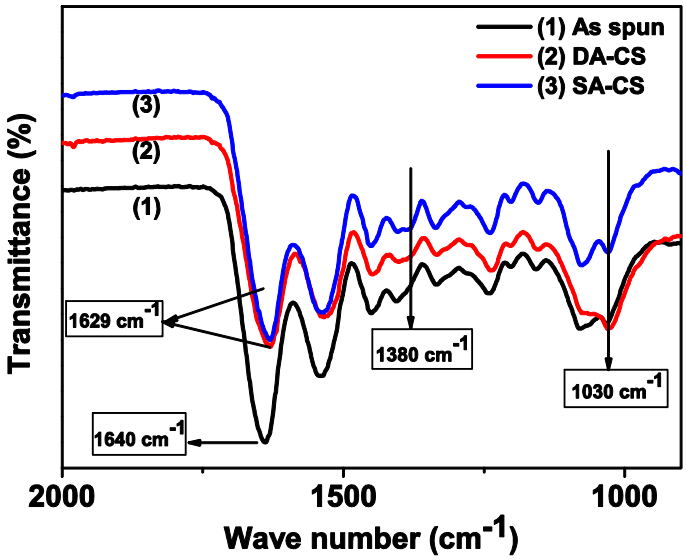

Figure 6.8: FTIR spectra of (1) as spun mat, (2) DA-CS and (3) SA-CS mats

The mechanical behaviour of as spun and the cross-linked core-shell nanofiber mats are shown in Figure 6.9. The tensile strength and Young's modulus of as spun nanofiber are 19 ± 3 MPa and 890 ± 130 MPa respectively. The failure of nanofiber mats is due to the slippage and breakage of the fibers. The tensile strength and Young's modulus of DA-CS are 65 ± 2 MPa and 1720 ± 140 MPa respectively and for SA-CS the values are 59 ± 3 MPa and 1560 ± 180 MPa respectively. Cross-linking with DA and SA introduce bonding between the fibers which reduces the slippage. As a result, the tensile strength is dramatically improved (Qian et al., 2011)

The comparison between the mechanical properties of gelatin mats and gelatin/chitosan core-shell mats are shown in Table 6.2. Core-shell gelatin-chitosan mats exhibit an improved tensile strength and modulus as compared to pure gelatin mats.

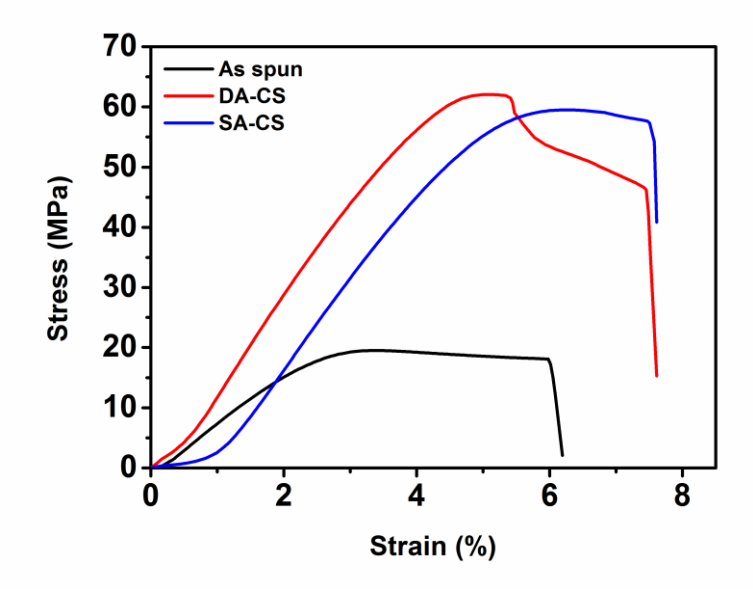

Figure 6.9: Stress-strain behaviour of as spun, DA-CS and SA-CS mats

Table 6.2: Comparison of mechanical properties of as spun and cross-linked gelatin and core-shell gelatin/chitosan nanofibers

Mechanical Properties	**As spun gelatin**	**DA-GNF**	**SA-GNF-BE**	**As spun core-shell**	**DA-CS**	**SA-CS**
Stress at break (MPa)	8.29 ± 0.53	30 ± 3.47	38 ± 5.47	19 ± 3	65 ± 2	59±3
Young's Modulus (MPa)	394 ± 96	904 ± 68	1387 ± 90	890 ± 130	1720 ± 140	1560 ± 180

6.2.4 Biological studies

6.2.4.1 Cell adhesion and proliferation of L-929 fibroblast cells on cross-linked core-shell mats

L-929 cells are allowed to adhere on DA-CS and SA-CS mats for 48 h. The cell morphology is investigated under fluorescent microscope after staining actin cytoskeleton and nuclei of the cells. Figure 6.10 shows that considerable amounts of cells are spread on the mats with flat fibroblast morphology. The result also reveals that the presence of chitosan on the surface of the core-shell

mats favours the adhesion and proliferation of L-929 cells.

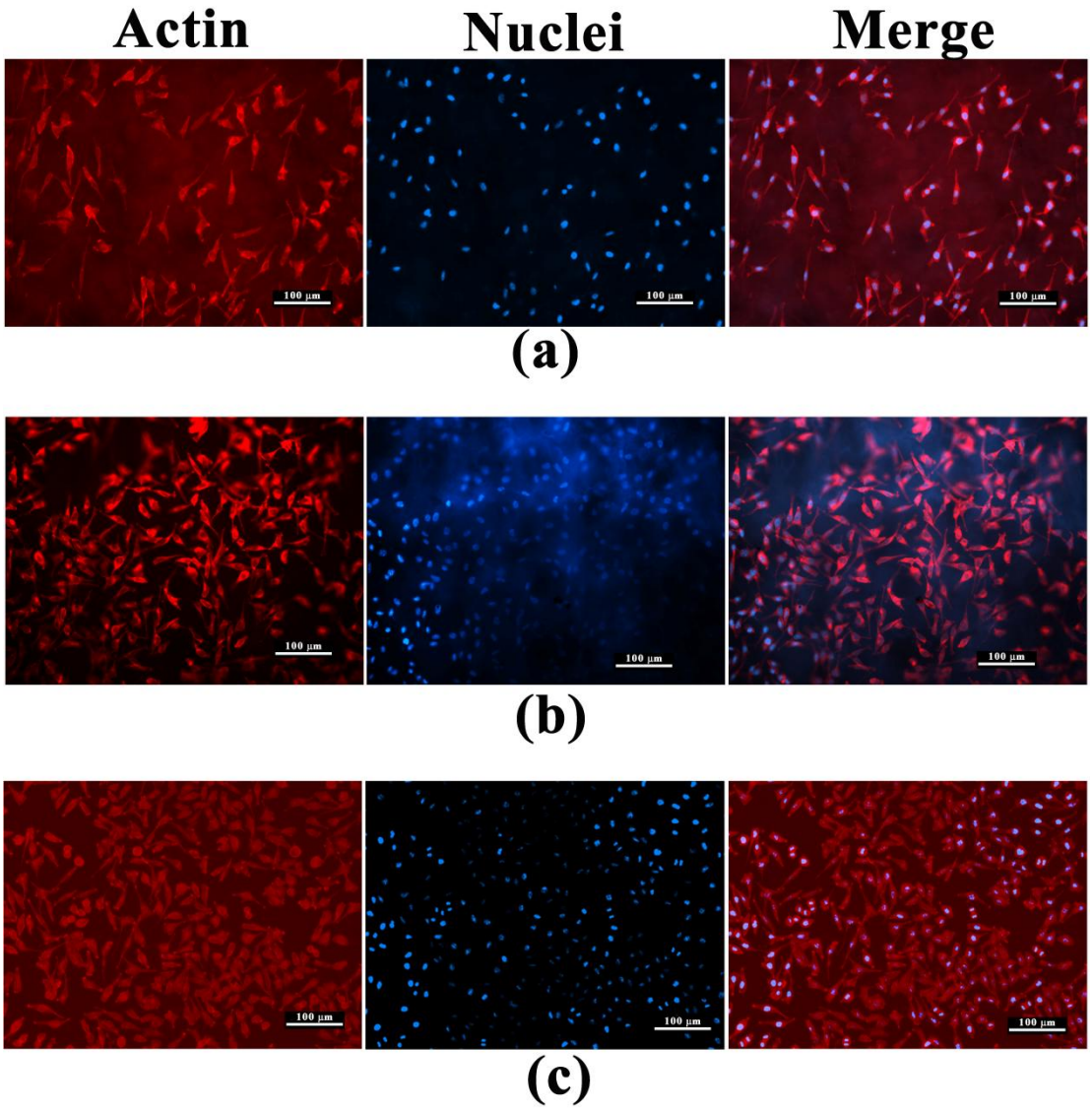

Figure 6.10: Adhesion of L-929 cells on (a) DA-CS mat, (b) SA-CS mat and (c) control cover glass

The viability of L-929 fibroblast cells in contact with DA-CS and SA-CS mats are evaluated by MTT assay using the extract of the samples. On culturing L-929 cells for 1 day and 3 days, the cell metabolic activity increased from 81 % to 104 % for DA-CS and 81 % to 94 % for SA-CS respectively (Figure 6.11). From this result it is evident that the cross-linked core-shell mats favour the proliferation of L-929 cells.

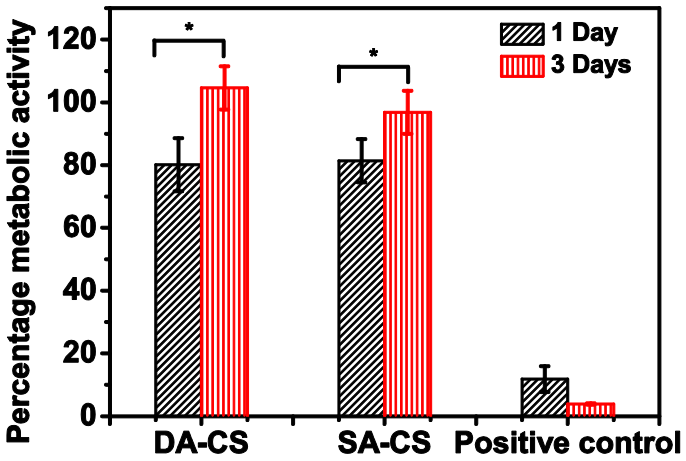

Figure 6.11: MTT assay of L-929 cells in contact with the extracts of DA-CS and SA-CS mats. Data represented as mean ± standard deviation (* $p < 0.05$)

6.2.4.2 Cell adhesion and proliferation of MG-63 cells on cross-linked core-shell mats

Human osteoblast like cells (MG-63 cells) is seeded on the mats at a density of 2000 cells/mat. The cells are allowed to proliferate for up to 5 days on DA-CS and SA-CS mats. For a comparison of the results, mats cross-linked with glutaraldehyde (GT-CS) are used as control. Over the 5 days time course, the relative cell numbers are assessed continually every other day using the Alamar blue assay, as described in Chapter 2. The results show that the cells grow normally on the mat for a period of 5 days. A considerably better growth rate can be observed in the case of DA-CS and SA-CS nanofibrous mats in comparison with glutaraldehyde cross-linked mats. Until 5^{th} day there is substantial growth rate observed for all these samples. The data on day 3 and 5 are significantly different than the first day of cell seeding which signifies good cell growth on these days. In GT cross-linked sample, the value of 3^{rd} day is not significantly different than the 5^{th} day of seeding. From the dye reduction trends, it is evident that cells on GT-CS mat are not proliferating at all and are struggling with the environment for their growth and gradually die (Figure 6.12).

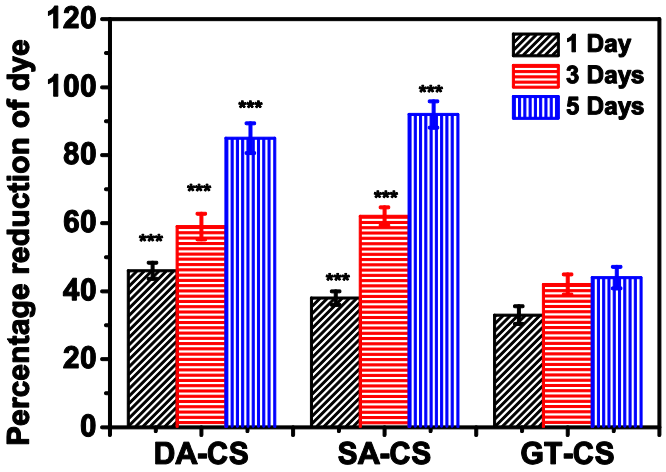

Figure 6.12: Cell proliferation (MG-63) on DA-CS, SA-CS and GT-CS mats. Initial cell seeding density was 2000 cells/scaffold. Data represented as the mean ± standard error ($p \leq 0.001$)

Confocal laser scanning microscopy of the cells adhered on the cross-linked mats after 5th day culture is shown below. Actin and nuclei are stained using different dyes. For DA-CS and SA-CS mats, cells grow abundantly with well distributed actin filaments and prominent nucleus (Figure 6.13 (a) and (b)). The auto fluoresced mat background has been minimized using the Fluoview software. In case of GT-CS mats, cells do not grow at all on the mats. Very few cells are scattered throughout the mats with deprived actin morphology (Figure 6.13 (c)). These results clearly demonstrate the advantages of the cross-linking agents, SA and DA over glutaraldehyde (GT) in the cross-linking of the present core shell mats. Besides the effects of cross-linking agents on the cytocompatibility, the presence of chitosan on the surface and gelatin in the interior also highly favours the cell attachment and proliferation. The formation of core-shell structured nanofibers integrates the properties and biological activities of gelatin and chitosan. Chitosan has been extensively studied in bone tissue engineering since it promotes growth and mineralization of osteoblast in culture. Chitosan, due to its cationic nature is capable of binding GAG, growth factors and other negatively charged cell membranes which make them promising scaffold materials for cartilage and bone repair (Di Martino et al., 2005; Zhang et al., 2003). Thus the nanofibers with chitosan shell and gelatin core cross-linked with

natural derived cross-linkers exhibit great potential to be used in tissue regeneration applications.

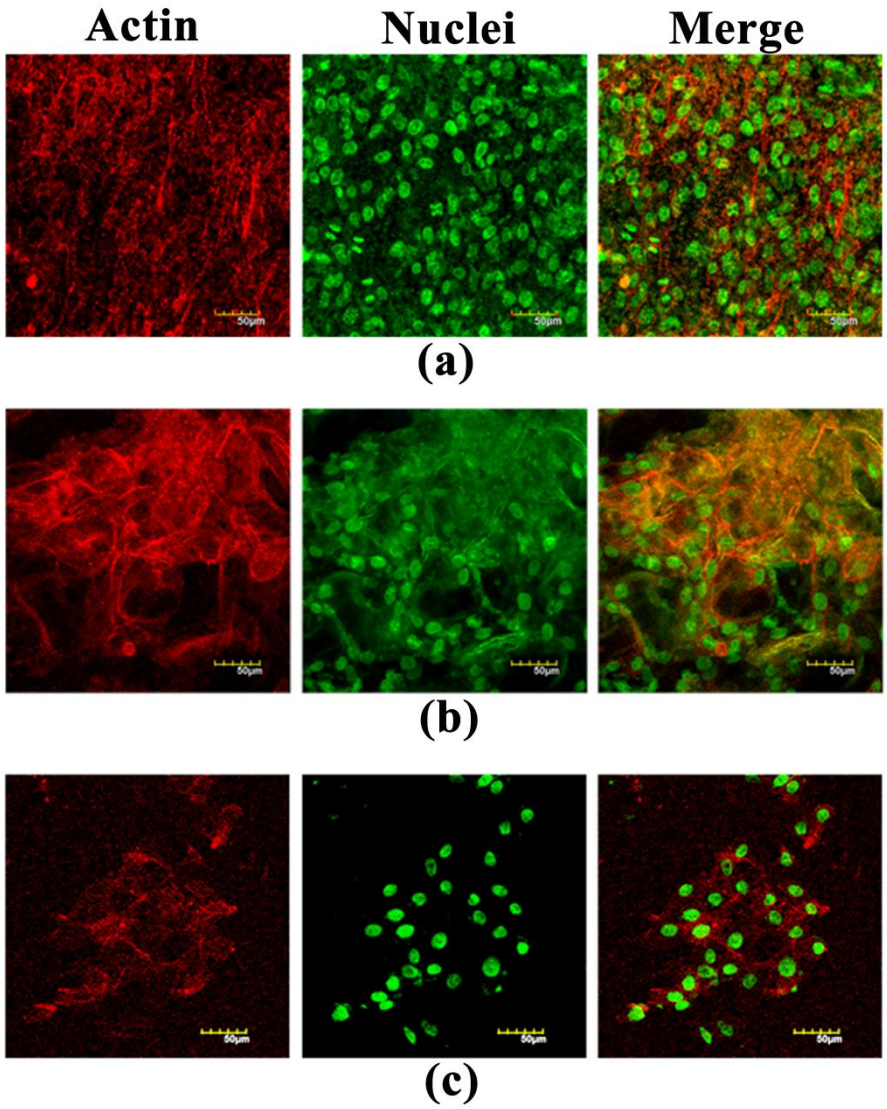

Figure 6.13: Confocal laser images of MG-63 cells on the cross-linked core-shell nanofibers stained with Rhodamine–phalloidin for actin filaments (red) and Hoechst 33342 for nuclei (green). Cells are cultured on (a) DA-CS mat; (b) SA-CS mat and (c) GT-CS mat

6.3 Conclusion

Core-shell structured gelatin/chitosan nanofibers using aqueous acetic acid as solvent are fabricated. The cross-linking is successfully achieved using natural derived cross-linkers based on oxidized dextran and sucrose. This fabrication method overcomes the problems associated with the usage of toxic solvents and synthetic polymers. Being natural polymers, chitosan and gelatin have excellent biocompatibility, and appropriate biodegradability. The cell adhesion and growth on the cross-linked gelatin/chitosan core-shell nanofibers confirm the biocompatibility of the nanofibrous mats. The gelatin/chitosan core shell nanofibers cross-linked by oxidized dextran and sucrose would be a potential candidate for different types of tissue regenerations.

CHAPTER 7

FABRICATION AND CHARACTERIZATION OF GRAPHENE OXIDE/GELATIN COMPOSITE NANOFIBERS

7.1 Introduction

Graphene, the wonder material of 21st century, has attracted enormous research interest due to their unique and extraordinary properties (Kumar, 2013). Graphene and its derivative graphene oxide (GO) are being extensively investigated as promising candidates for different types of applications (Chung et al., 2013). Graphene is a one-atom-thick layer of sp^2 bonded carbon atoms arranged in a regular hexagonal lattice similar to graphite. Since graphene is the lightest and strongest material in single-atom-thick level, it facilitates many other applications including biological properties. Owing to the poor dispersibility of graphene sheets, GO become more attractive since it is easily dispersible in aqueous medium. Single layer of GO incorporated polymer matrix provides a multifunctional feature due to the reinforcing effect of GO with a wide variety of properties. Recently, the importance of GO for cellular adhesion and proliferation of mouse fibroblast cells and human mesenchymal stem cells has been reported (Ruiz et al., 2011; Shan et al., 2009). Of late, myoblast differentiation is also evaluated on GO coated glass substrate (Ku and Park, 2013). Antibacterial activities of GO dispersion and GO coated substrates are also being studied (Hu et al., 2010; Liu et al., 2011).

Gelatin, a protein obtained by the denaturation of collagen, is one of the well-studied biocompatible, non-toxic polymers used for several biomedical applications as explained already. GO incorporated gelatin films are reported to promote bone mineralization, cell adhesion and proliferation (Wan et al., 2011).

GO is more conducting than gelatin and other polymers and its surface charge favours the adhesion of cells (Bhadra et al., 2012). Incorporating GO into the nanofibers is explored recently to improve the properties of the nanofibrous materials (Bao et al., 2010). GO incorporated nanofibers exhibit enhanced optical, electrical and biological performance based on the properties of both GO and the polymer matrix. GO loaded poly(ε-caprolactone) for muscle tissue engineering applications has been reported recently (Chaudhuri et al., 2014). Electrospinning of GO incorporated polyvinyl alcohol nanofibers is reported and enhancement in mechanical property and biological performance towards MC3T3-E1 osteoblast cells are investigated (Qi et al., 2013). These reports clearly show the role of GO in improving various properties of the nanofibers.

On this background, the present chapter explores GO incorporated electrospun gelatin nanofibers and its potential properties. GO is incorporated into gelatin nanofibers by dispersing in aqueous gelatin solution. The resulting homogeneous dispersion is electrospun to obtain GO incorporated gelatin (GO-GEL) nanofibers. Gelatin is a highly hydrophilic polymer and hence the gelatin nanofibers completely lose the fibrous morphology on exposure to the high degree of moisture. Even though GO can give structural reinforcement, it cannot provide the water resistance ability for gelatin nanofibers. Hence, an effective cross-linking treatment is required to improve the water stability (Zhang et al., 2006). Several cross-linking agents based on bifunctional molecules such as glutaraldehyde (GT) (Zhang et al., 2006), carbodiimide (Nie et al., 2010), etc., are developed for gelatin matrices. In the previous chapters, the efficiency of the dextran aldehyde and the sucrose aldehyde to cross-link gelatin nanofibers is discussed. In the current effort, the GO-GEL nanofiber is cross-linked using dextran aldehyde in a similar manner as mentioned earlier. The GO-GEL and dextran aldehyde cross-linked GO-GEL (DA-GO-GEL) mats are well-characterized in this study and their biological performances are also evaluated.

7.2 Results and Discussion

7.2.1 Preparation and characterizations of graphene oxide

GO is prepared by the treatment of expanded graphite using a strong mineral acid, H_2SO_4, and an oxidizing agent, $KMnO_4$, *via* modified Hummer's method. Highly exfoliated graphene sheets with large number of oxygen functionalities on the basal planes and edges are achieved in this process (Aboutalebi et al., 2011). In expandable graphite, inter-layer intercalating groups facilitate the exfoliation of the graphite by heat treatment. In this exfoliation process, the expandable graphite powder is exposed to a thermal shock at 1050 °C for 15 s. The resulting expanded graphite on oxidation and subsequent purification process by centrifugation gives rise to fully exfoliated GO. Single layer of GO is obtained from expanded graphite during the centrifugation process itself. Figure 7.1 shows the functional groups present in a typical GO sheet.

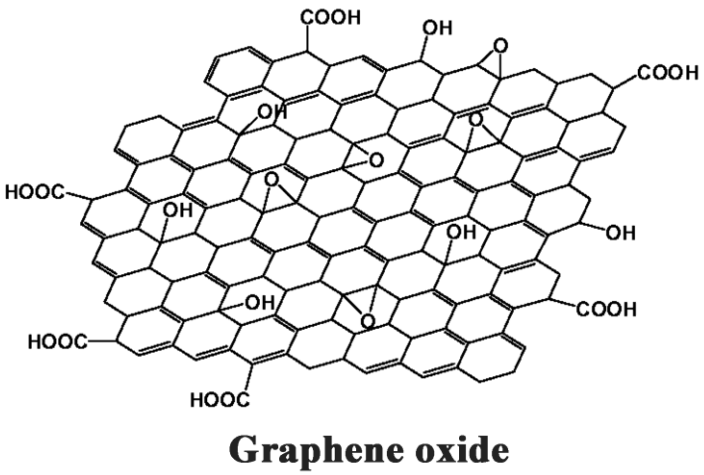

Figure 7.1: Typical chemical structure of graphene oxide

The morphology and microstructure of GO are examined using TEM analysis. Aqueous dispersion of GO is used for sample preparation for TEM. The highly wrinkled and paper-like sheet of GO is observed as shown in Figure 7.2 (a). These wrinkles and bends in the sheets are indications of various defects and functional groups carrying sp^3 carbon atoms formed as a result of oxidation

(Verma et al., 2011). The dimension and morphology of the GO are further examined using AFM image depicted in Figure 7.2 (b) where (i) and (ii) are the height profiles of the corresponding line drawn on the AFM image. It is clear from the height profiles that width of most of the graphene sheets fall around 200-400 nm with height around 1-3 nm, revealing the presence of two to four graphene layers.

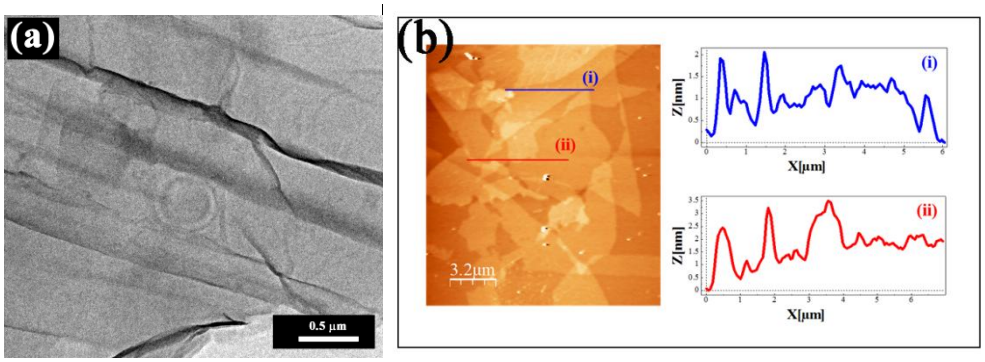

Figure 7.2: (a) TEM image and (b) AFM image with height profile of GO

TGA analysis of GO and expanded graphite is performed up to 800 °C at a heating rate of 10 °C/min. The thermograms recorded are shown in Figure 7.3 (a). It can be observed from the thermograms that GO is thermally unstable. There is a significant weight loss observed in the range of 150 to 250 °C, which is due to the decomposition of labile oxygen-containing functional groups, which yield CO and CO_2 on thermal degradation (Cui et al., 2011). At 800 °C, a char residue of around 35 wt.% is left after the decomposition steps. On the other hand, no significant weight loss is detected for the original expanded graphite. Figure 7.3 (b) represents the XRD pattern of expanded graphite and GO. The XRD pattern of expanded graphite shows a sharp peak at 26.2°, which is due to the reflection from (002) plane with a d-spacing of 3.35 Å. In the case of GO, the peak at 26.2° disappears and a broad peak appears at a 2θ value of 12° with an increase in d-spacing to 7.4 Å. This increase in d-spacing is associated with the presence of oxygen functionalities in the basal planes of GO and hence indicates the intercalation of water molecules, between the interlayer spacing of GO (Aboutalebi et al., 2011).

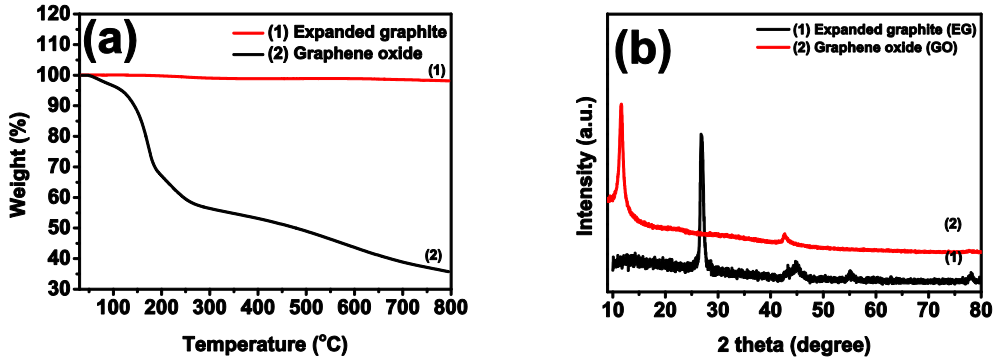

Figure 7.3: (a) TGA thermograms and (b) XRD patterns of expanded graphite and GO

7.2.2 Fabrication of GO-gelatin composite nanofibers

GO incorporated electrospun composite nanofibers are an exciting new class of materials with wide variety of properties and applications. Multifunctional property enhancement of polymer nanofibers is achieved by loading small amount of graphene-based materials. A good dispersibility of GO in the polymer solution is essential for obtaining composite nanofibers. The nature of the bonding interaction between the filler and matrix at the interface has significant impact on the properties of the composites. Most of the dispersion methods produce composites, where the polymer matrix and the filler interact through dispersive forces. GO is highly dispersible in water and fully exfoliated GO sheets are formed in water. Hence, a uniform GO suspension can be obtained. The edges and basal planes of GO are composed of oxygen functional groups that increase the hydrophilicity of GO and enhance the water dispersibility. GO incorporated polymer nanofibers are reported in the literature for various applications. Synthetic polymer nanofibers such as PAN–GO composite nanofibers are explored as effective candidates for a variety of applications such as supercapacitors and energy production and storage devices (Wang et al., 2013). GO incorporated natural polymeric bulk composites are reported for tissue engineering, wound dressing and drug delivery applications (Liu et al., 2014). GO acts as an effective reinforcing filler and biological activator in case of natural polymers matrices such as gelatin, alginate, chitosan, etc. (Wan et al., 2011). GO incorporated natural polymeric electrospun nanofibers are very rare to find in the

literature. Recently, fabrication of GO incorporated gelatin film and comparison of the properties with GO incorporated electrospun nanofibers are reported (Panzavolta et al., 2014). In the present study, GO-GEL nanofibers are prepared and the physico-chemical properties and biological performance are studied in detail.

Gelatin nanofibers with varying GO content ranging from 0.25 % to 1 % w/w are fabricated by electrospinning of GO-GEL aqueous dispersion. Nanofibers with uniform morphology are obtained by properly adjusting the solution and spinning parameters (Chapter 2). The colour of the electrospun mat changed from white to black when the concentration of GO varied from 0 to 1 % (w/w) as shown in Figure 7.4.

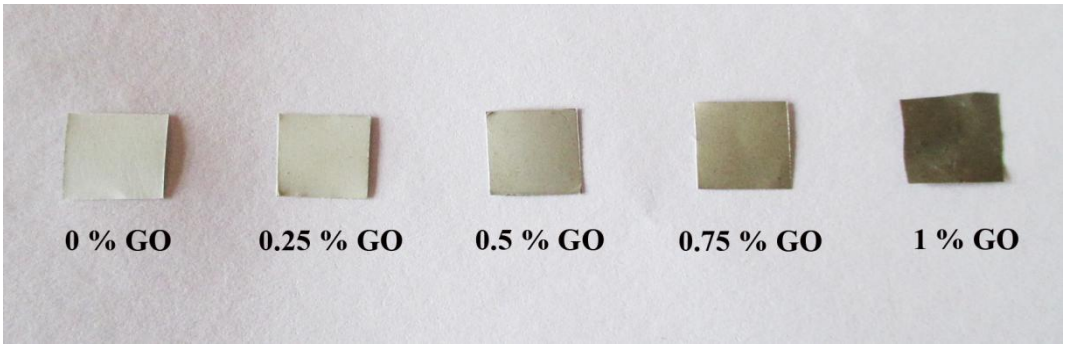

Figure 7.4: The variation in colour of electrospun GO-GEL mats with different GO loading

The interaction of GO with gelatin is evidenced from the FTIR spectra. The intensity of amide I band at 1635 cm^{-1} which is primarily attributed to the stretching vibrations of carbonyl group in the backbone of gelatin is red shifted to 1629 cm^{-1} after the introduction of GO. This observation can be explained due to the formation of strong hydrogen bonding interaction between the carbonyl group of amide and the hydroxyl or carboxylic acid functional groups of GO, which weakens C=O bond of amide and hence vibrates at lower energy. Peak at 1243 cm^{-1}, which is referred to amide III band, resulting from several complex displacements of amide group of gelatin also shifts towards 1238 cm^{-1} and is clear indication of the existence of interactive forces between gelatin and GO. The

broad band at 3288 cm^{-1}, which is due to the free N-H bond or OH group of the free -COOH vibrations of gelatin is red shifted, in turn indicating that free N-H and COOH groups of gelatin may also be involved in the hydrogen bonding interactions with carboxylic and hydroxyl groups of GO which is the reason for weakening of OH and NH bonds of gelatin (Figure 7.5).

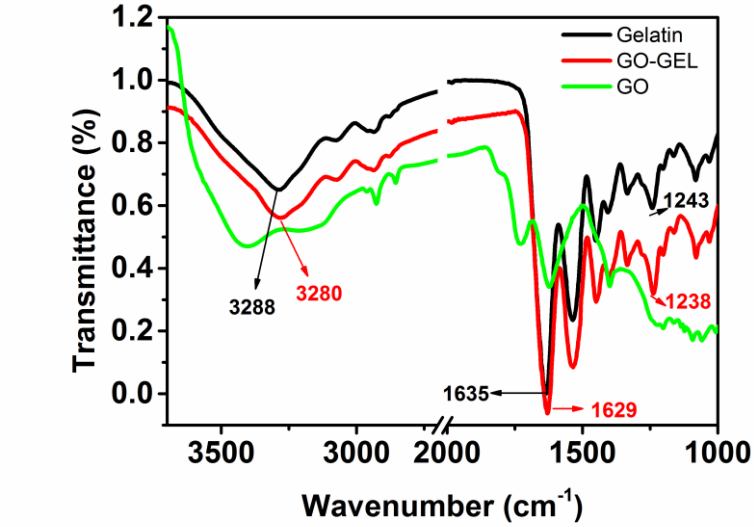

Figure 7.5: FTIR spectra of gelatin mat, GO powder and GO-GEL mats with 0.5 % (w/w) GO loading

The morphology of the GO incorporated gelatin nanofibers is shown in Figure 7.6. SEM images reveal that GO is properly dispersed in the medium and hence, the fibers are smooth with no residual agglomerates of GO outside the fibers. It is seen that, fiber diameter decreases on increasing the GO content. The decrease in diameter can be explained due to the increase in conductivity of the electrospinning solution with increase in GO content. It is well-known that GO does not exhibit conductivity. However, the conductivity increase can be attributed to the partial reduction of GO due to the presence of amino functionality in gelatin (Panzavolta et al., 2014).

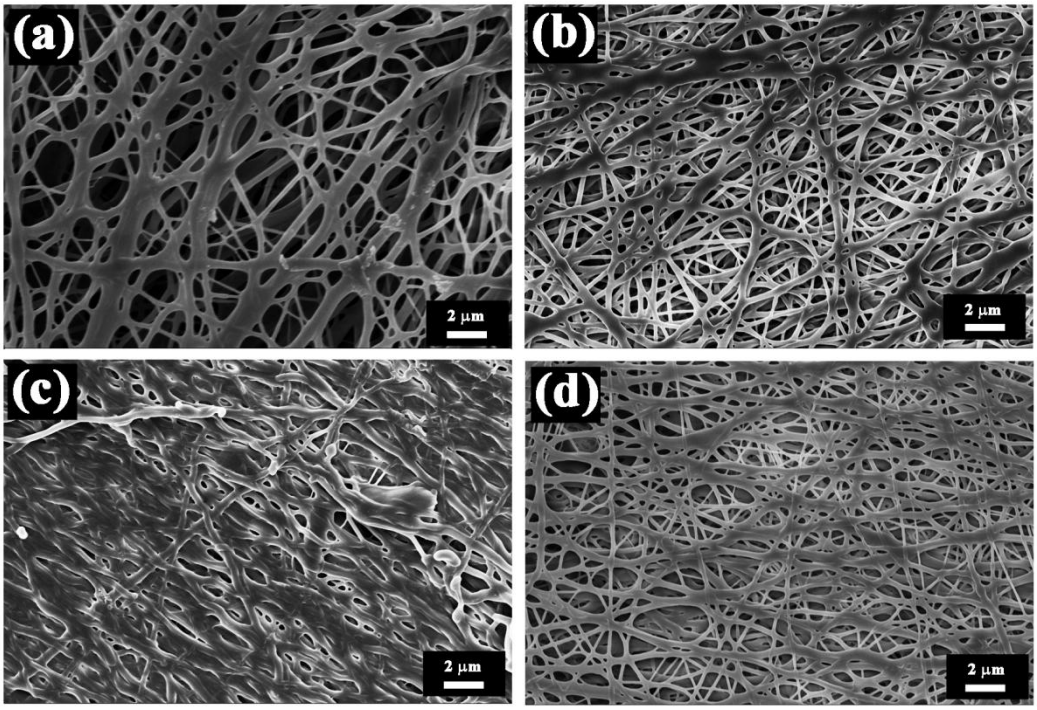

Figure 7.6: SEM images of GO-GEL mats with different GO loading (a) pure gelatin mat, (b) 0.5, (c) 0.75 and (d) 1 % (w/w) GO incorporated gelatin mats

TEM analysis is carried out in order to understand the finer details of the structure of a single fiber. TEM image shown in Figure 7.7 illustrates, the incorporation of GO into the gelatin nanofibers. In both the cases, GO is fully or partially embedded in the single nanofiber according to the size of the GO sheets. The one with size higher than the diameter of the fiber is partially embedded and the rest of them are fully embedded in the nanofiber matrix. In the fibers with higher GO content (1 % w/w), a few agglomerates are also visible on the surface of the individual fibers. The higher concentration of GO causes agglomeration, and this may affect other property enhancements of the GO-GEL composite nanofibers.

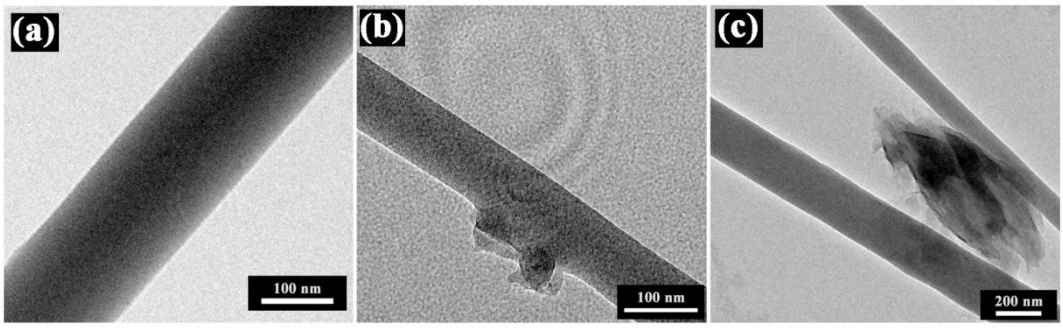

Figure 7.7: TEM images of (a) pure gelatin mat, (b) 0.5 % (w/w) GO loaded and (c) 1 % (w/w) GO loaded gelatin mats

It is interesting to note that the tensile strength of gelatin nanofibers is remarkably increased as a result of the incorporation of GO. The tensile strength of the GO-GEL nanofibers increases from 8.29 ± 0.53 to 21.6 ± 2.03 MPa when the GO loading increases from 0 to 0.5 % (w/w). Further increase in GO loading to 1 % (w/w) decreases the tensile strength of the GO-GEL nanofibers to 11.08 ± 2 MPa. The improvement in tensile strength is due to the interaction between the functional groups of GO and gelatin which increases the stress transfer (Cano et al., 2013). The decrease in tensile strength after GO loading of 0.5 % (w/w) is due to the agglomeration of GO in nanofibers matrix (Figure 7.8). The agglomerates act as the weak points of the nanofibers leading to easy breakage of the mats. The addition of GO into polymer matrix is reported to be an important method to improve their mechanical performance. Similar observation on the tensile strength and modulus of GO incorporated gelatin film is reported by Wan et al (Wan et al., 2011).

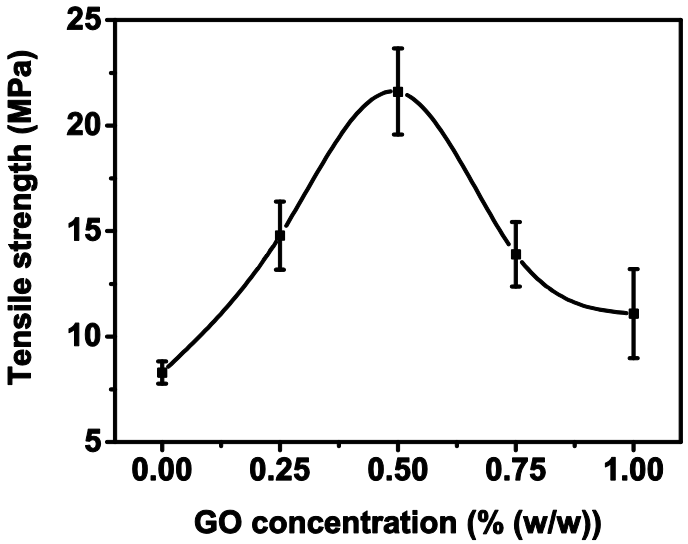

Figure 7.8: Tensile strength versus percentage GO loading of GO-GEL nanofibrous mats

X-ray diffraction patterns of gelatin mats with varying GO content (0 - 1 % (w/w)) are analysed and are depicted in Figure 7.9. The broad peak of gelatin around 2θ = 19.5° is shifted to 22.5° when the GO content increases to 1 % (w/w) and also becomes narrower. This may indicate the partial reduction of GO to form reduced GO due to the presence of amino groups on gelatin.

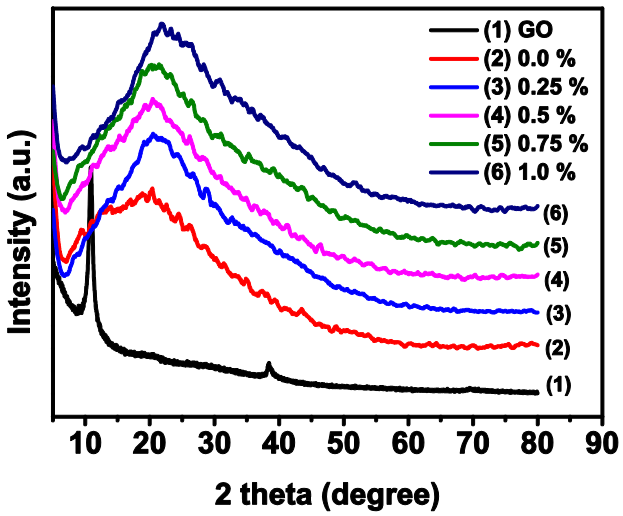

Figure 7.9: XRD patterns of pure GO and GO-GEL mats with various GO loading

This observation is further explained based on the UV characteristics. The UV-Vis spectra of aqueous solutions of GO, gelatin and GO-GEL are shown in Figure 7.10. GO shows two bands, a maximum at ~227 nm, which can be assigned to the $\pi \rightarrow \pi^*$ transition of C = C bonds; and a shoulder at ~285 nm corresponding to $n \rightarrow \pi^*$ transition of C=O bonds. In the spectrum of GO-GEL aqueous dispersion, peak corresponding to the $\pi \rightarrow \pi^*$ transition is observed at 247 nm. The red shift of the peak can be due to the partial reduction of GO and the restoration of C = C bonds in the GO-GEL mat.

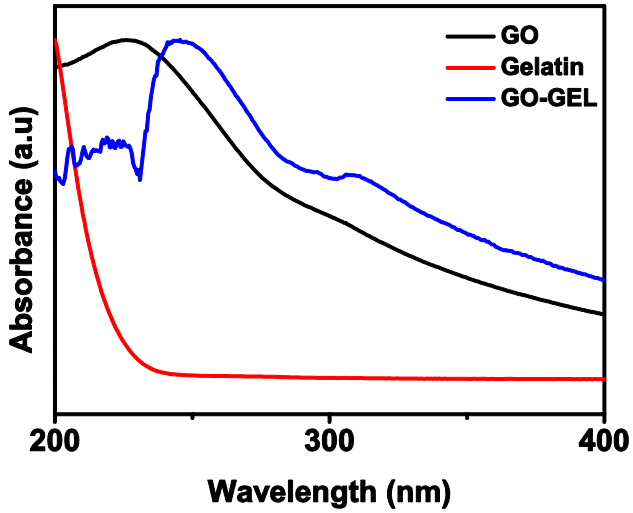

Figure 7.10: UV characteristics of aqueous dispersions of GO and GEL-GO mats with 0.5 % (w/w) GO loading

TGA thermogram shows that gelatin mat and GO-GEL mat gives char residue of 21 and 23 %, respectively, at 500 °C (Figure 7.11 (a)). The degradation onset temperature has been shifted to 217 °C in case of GO-GEL mat from 200 °C. The increase in the residue and shift in the onset temperature obviously explains the presence of GO, that increases the thermal stability of gelatin mats. DSC thermograms show that GO-GEL exhibits a shift in the denaturation temperature from 88 to 110 °C (Figure 7.11 (b)). The interaction between amino groups of gelatin and carboxyl and other functional groups of GO gives an additional stability to the composite nanofibers leading to the shift in denaturation temperature (Liu et al., 2014).

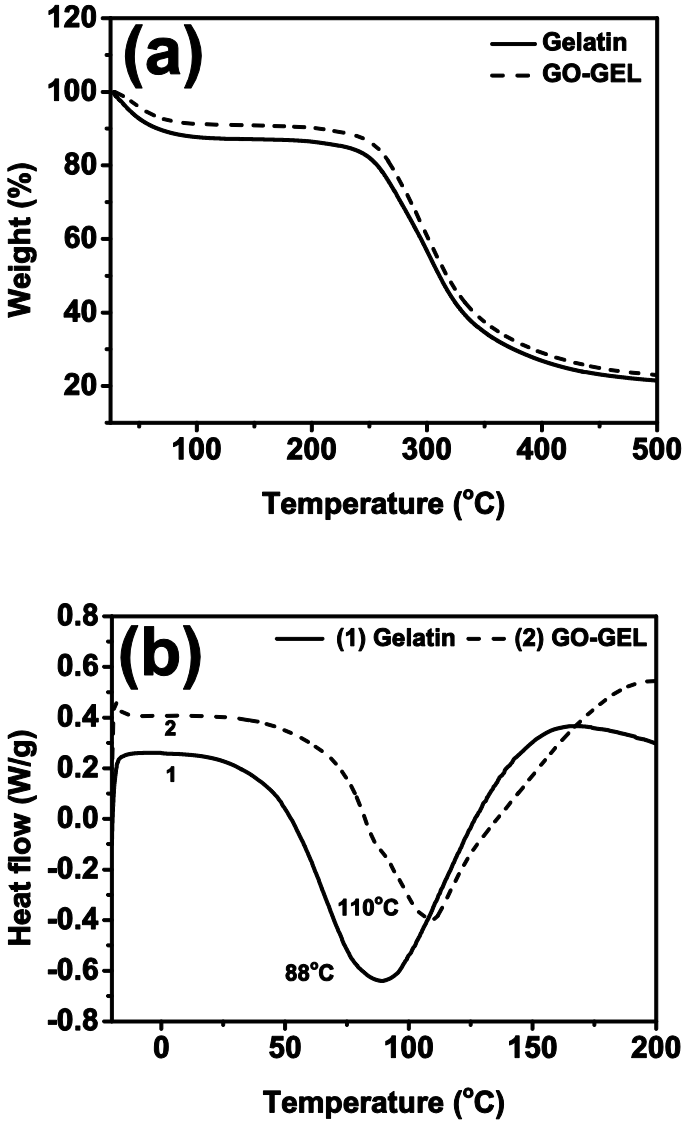

Figure 7.11: (a) TGA and (b) DSC thermograms of gelatin and GO-GEL mats

7.2.3 Water stability of GO-GEL mats: Cross-linking reaction with dextran aldehyde (DA)

Gelatin and GO are highly hydrophilic and GO-GEL mats dissolve in water. Even though the presence of GO increases the mechanical property, the water resistant ability of the nanofibers is to be enhanced using cross-linking treatment. Gelatin nanofibers can be cross-linked using various cross-linking agents. As already discussed in the previous chapters, in order to overcome issues with conventional cross-linking agents, an economically viable and non-toxic

cross-linking agent based on natural polymer namely dextran is introduced by us. For cross-linking process, dextran aldehyde (DA) is made to dissolve in ethanol in the presence of a minimum amount of aqueous borax (300 µl, 0.02 M in 10 ml of ethanol). GO-GEL mats are cross-linked by dipping in this medium for five days. The mats show improved water stability upon cross-linking with DA, which is indicated by the swelling behaviour of as spun and cross-linked GO-GEL mats (Figure 7.12). The as spun mat swells and dissolves in the medium and hence the observed reduction in the weight leading to a lower calculated value of swelling ratio. DA cross-linked GO-GEL mats (DA-GO-GEL) exhibit a lower swelling ratio compared to the as spun mat, and equilibrium swelling ratio is achieved in 10 min. These results show the improved water stability of DA-GO-GEL mats.

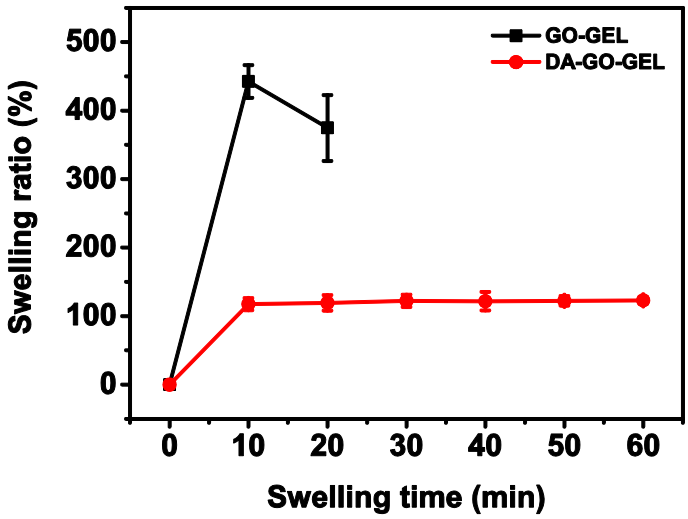

Figure 7.12: Swelling behaviour of GO-GEL and DA-GO-GEL mats

The cross-linking is further explained by SEM images of the cross-linked and swelled GO-GEL mats. SEM images show that DA-GO-GEL mat maintains the fibrous morphology and structural integrity after immersed in water whereas the fibrous morphology of the GO-GEL mats gets completely disrupted (Figure 7.13). It is observed that cross-linking for a period of 5 days is essential for obtaining the nanofibers with significant extent of cross-linking. The degree of cross-linking of GO-GEL mat is evaluated using TNBS assay. The results reveal that about 40 ± 5 % amino groups have undergone cross-linking reaction with

aldehyde groups of the dextran aldehyde. A lower cross-linking degree can be explained in terms of the secondary interactions between amino groups of gelatin with the carboxyl and hydroxyl groups of GO.

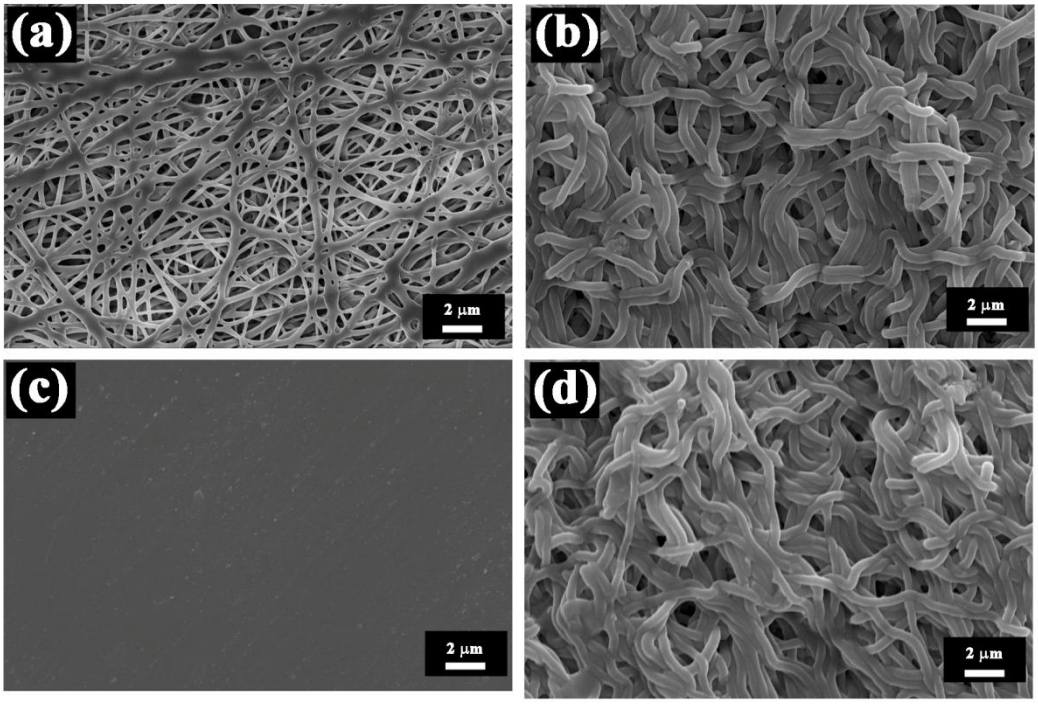

Figure 7.13: SEM images of (a) GO-GEL, (b) DA-GO-GEL (c) GO-GEL after dipped in water, (d) DA-GO-GEL after dipped in water for 24 h

The thermal behaviour of the DA-GO-GEL mats is evaluated using TGA and DSC analysis. In the TGA thermogram, DA-GO-GEL mat shows higher char residue (27 wt.%) in comparison with GO-GEL mats (23 wt.%) at 500 °C (Figure 7.14 (a)). The result indicates that the cross-linking with DA increases the thermal stability of GO-GEL mat. It is well-known that the cross-linking process increases the thermal stability and char residue (Mtshali et al., 2001). The DSC thermogram shows the endothermic peak corresponding to the denaturation temperature of gelatin. For the cross-linked mats, denaturation temperature is shifted towards higher temperature region (110 to 116 °C) and indicates the improved thermal stability of the DA cross-linked GO-GEL mats (Figure 7.14(b)).

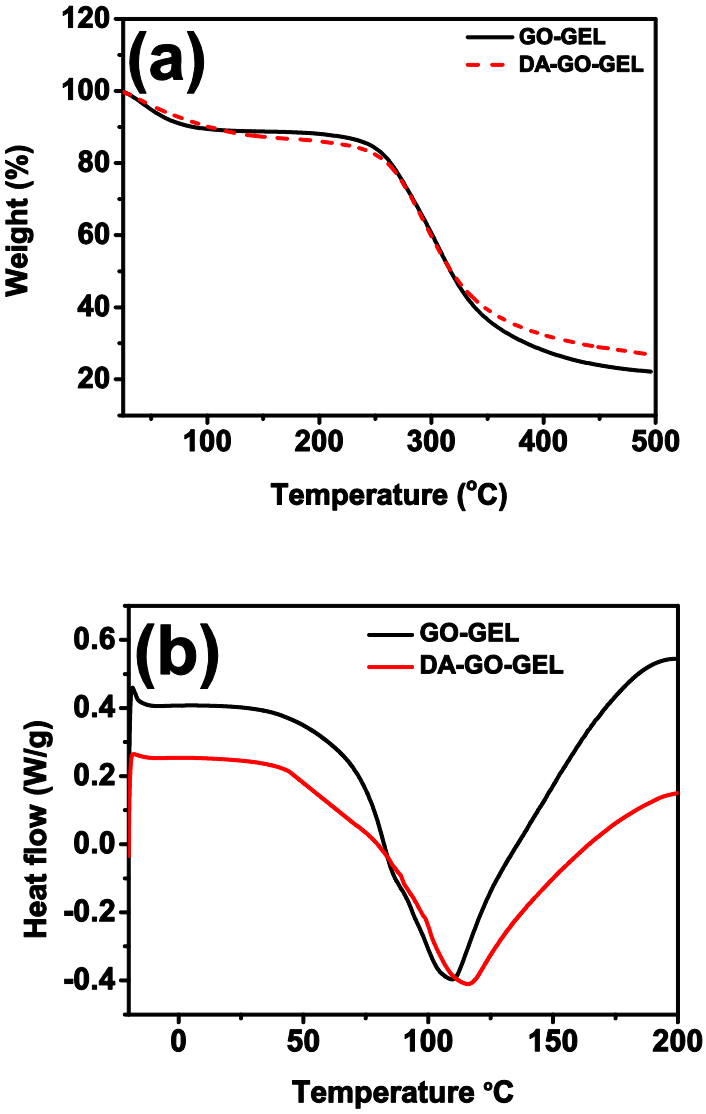

Figure 7.14: (a) The TGA thermograms and (b) DSC thermograms of GO-GEL and DA-GO-GEL mats

The mechanical properties of the DA-GO-GEL and uncross-linked GO-GEL mats are evaluated by the tensile strength measurements. The stress-strain graph of the GO-GEL and DA-GO-GEL mats is shown in Figure 7.15. The tensile strength of the DA-GO-GEL mats is remarkably increased compared to the GO-GEL mats, which in turn is higher than that of bare gelatin nanofibers. The tensile strength of DA cross-linked gelatin nanofibers (DA-GNF) is 30 ± 3.47 MPa as shown in Chapter 3. In the case of DA-GO-GEL mats, the tensile strength increases up to 56.4 ± 2.03 MPa. The covalent bonds formed among GO-GEL nanofibers as a result of Schiff's base reaction with DA significantly improve the

tensile strength. The reinforcing effect of reduced GO in the matrix due to the partial reduction of GO also might have played a role in increasing the tensile strength.

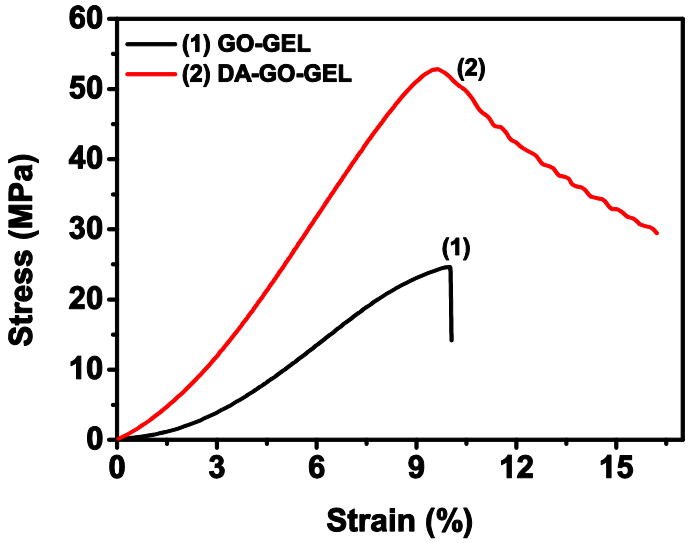

Figure 7.15: Mechanical behaviour of GO-GEL and DA-GO-GEL mats

7.2.4 Biological studies

7.2.4.1 Cell adhesion and proliferation of L-929 cells on GO-GEL mats

The viability of L-929 fibroblast cells in contact with the extract of DA-GO-GEL mats is assessed quantitatively in terms of the metabolic activity by MTT assay. Figure 7.16 represents the proliferation of L-929 fibroblast cells in the extract of DA-GO-GEL mats in comparison with the cell control for 2 and 4 days. The DA-GO-GEL mats show a very good viability as well as proliferation during this period. Analysis of this result clearly reveals a statistically significant difference in cellular activity between 2 and 4 days ($p < 0.05$). The relative increase in the metabolic activity is a measure of the increased viability due to the proliferation of the cells during the interval. Hence, it is clear that the presence of GO does not induce any toxic response to gelatin mat and instead, it favours the growth and proliferation of the L-929 cells.

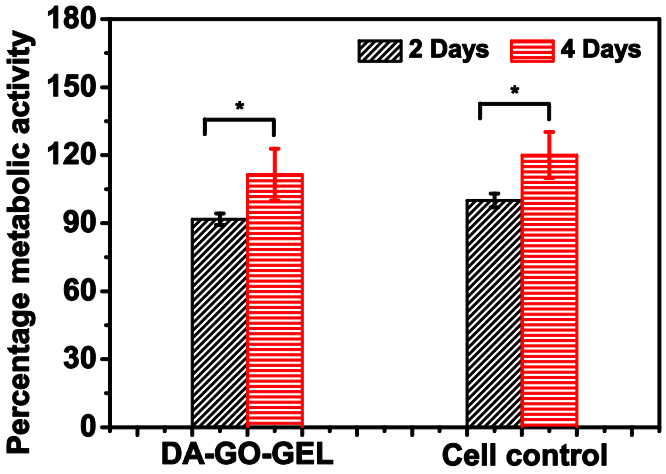

Figure 7.16: MTT assay of L-929 cells in contact with the extract of DA-GO-GEL mats (* $p < 0.05$)

The adhesion and morphology of L-929 cells on the surface of DA-GO-GEL mats are evaluated by the actin cytoskeleton staining followed by fluorescent microscopy. Figure 7.17 shows the actin cytoskeleton and nuclei structure of L-929 cells cultured on DA cross-linked GO-GEL mats. The results reveal that L-929 cells adhered well on DA-GO-GEL mats by expressing characteristic fibroblast morphology with well-distributed actin cytoskeleton. This shows the cytocompatibility of DA-GO-GEL mat.

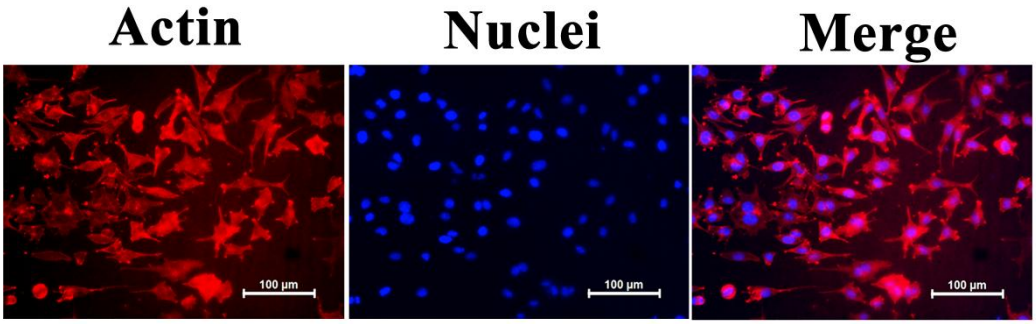

Figure 7.17: Actin cytoskeleton staining of L-929 cells adhered on DA-GO-GEL mats

7.2.4.2 Evaluation of bacterial growth on GO-GEL mats

The present study also evaluates the growth/inhibition of bacterial cells on GO loaded gelatin nanofibers. In order to investigate the effect of GO on gelatin mats for the growth of bacteria, agar diffusion test and bacterial adhesion tests are carried out. Bacterial strains gram positive *S.aureus* ATCC 25923 and gram negative *E.coli* ATCC 25922 are used for both the tests. In agar diffusion method, the antibacterial property is determined by measuring the zone of inhibition region. DA-GO-GEL mats are taken in the form of discs of 6 mm diameter each, and evaluated for agar diffusion method. Gentamicin loaded disc is used as a control material. The results reveal that there is no zone of inhibition surrounding the DA-GO-GEL mats whereas control material exhibits appreciable growth inhibition towards both *S.aureus* and *E.coli*. Table 7.1 shows the zone of inhibition for both the bacterial cells around the test samples.

The adhesion behaviour of the gram-positive bacteria *S.aureus*, and the gram-negative bacteria, *E.coli*, on the surface of DA-GO-GEL mat is also evaluated. Bacterial adhesion experiments are performed in a suspension of bacterial cells in which the samples are incubated at 37 ^{o}C for 18 h. The number of adhered bacteria is counted, and is reported in Table 7.2. The turbidity shows the presence of bacterial cells and clear solution indicates the absence of bacterial adhesion. GO suspensions are reported to induce antibacterial property (Liu et al., 2011). In the present study, GO incorporated gelatin mats are found to support the adhesion of bacteria to the surface. These two results demonstrate that the GO loaded into a polymer matrix does not show any antibacterial activity. The results can be explained based on the fact that, the functional groups on the basal planes of GO are the main source of anti bacterial property. (Hui et al., 2014) have demonstrated that the presence of functional groups in the basal planes on GO affects cytotoxicity towards HepG2 cells and bacterial cells. GO suspension kills the bacteria cells whereas non-covalently functionalized GO promotes the growth of bacteria as well as the normal cells. In this case, these functional groups in the basal planes interact with gelatin molecule, thus facilitate the growth of the cells.

7.2.4.3 Gentamicin release and antibacterial property of gentamicin loaded DA-GO-GEL mats

Electrospun gelatin nanofibers are known for its drug delivery and wound dressing applications. Since GO incorporated electrospun gelatin mats do not show any antibacterial activity, this material may not be useful for wound healing applications. The sustained delivery of antibacterial drugs into the wounded area is essential for an effective wound healing process to prevent bacterial infection and to promote the healing of wounds. Gentamicin (GEN) is selected as a model drug. GEN is active against both gram-positive and gram-negative organisms specifically *S.aureus*, which causes infection to the burn wounds. The release study and antibacterial activity of gentamicin loaded gelatin and oxidized alginate hydrogels are reported by Biji et al (Balakrishnan et al., 2012). In the present study, in order to impart antibacterial activity to the GO loaded gelatin nanofibers, gentamicin (2.5 % (by weight of gelatin)) is incorporated during the electrospinning process. The resulting composite solution containing three components (gelatin, GO and gentamicin) is electrospun under the same conditions as in the case of GO-GEL mats. The mats are cross-linked with DA to induce water resistance.

The release profile of gentamicin is studied by estimating the released gentamicin into PBS at 37 °C after regular interval of time. Aliquots of the samples were withdrawn at regular intervals and treated with o-phthalaldehyde as gentamicin does not give any UV-absorbance. The resulting solution is evaluated for UV absorbance and the cumulative release pattern of gentamicin from the electrospun mats is evaluated. The results presented in Figure 7.18 indicate that the drug loaded mat exhibits an initial brust release during the first 6 h followed by a gradual release of GEN. A drug payload of 0.25 mg/10 mg of the mat is taken in each sample. The experiment is performed in triplicate, and the average values are reported.

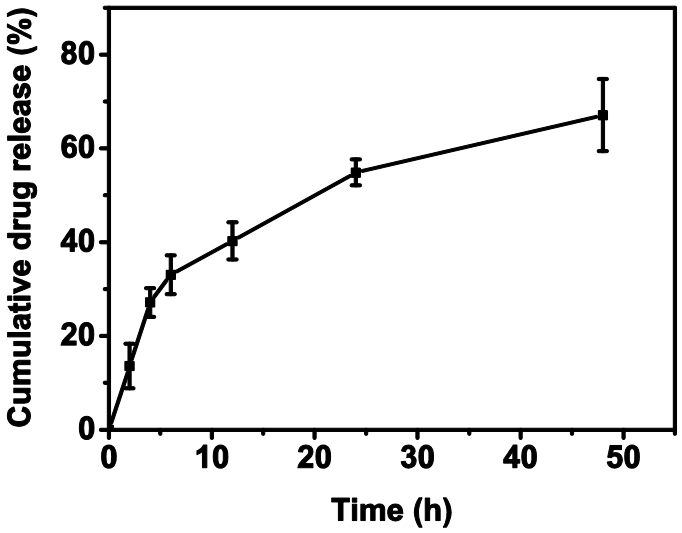

Figure 7.18: The cumulative release of gentamicin from the DA-GO-GEL-GEN mats with drug payload of 0.25 mg/10 mg of the mats

Antibacterial property of GEN impregnated GO-GEL (DA-GO-GEL-GEN) mats is examined for two bacterial strains, namely *S.aureus* and *E. coli* using agar diffusion and bacterial adhesion methods. The zone of inhibition and the results of bacterial adhesion test are presented in Table 7.1 and 7.2, respectively. The zone of inhibition regions of the samples are shown in Figure 7.19. The results reveal that GEN loaded samples are capable of preventing the growth and adhesion of both gram-positive and gram-negative bacteria. These results show the potential of electrospun GO-GEL mats loaded with antibacterial drug.

Table 7.1: Zone of inhibition of *E coli* and *S. aureus* around the test samples

Sample	**Zone of inhibition (mm)**	
	E.coli	***S.aureus***
DA-GO-GEL	0	0
DA-GO-GEL-GEN	28.33	28.66
Positive control (GEN)	25.6	25.6

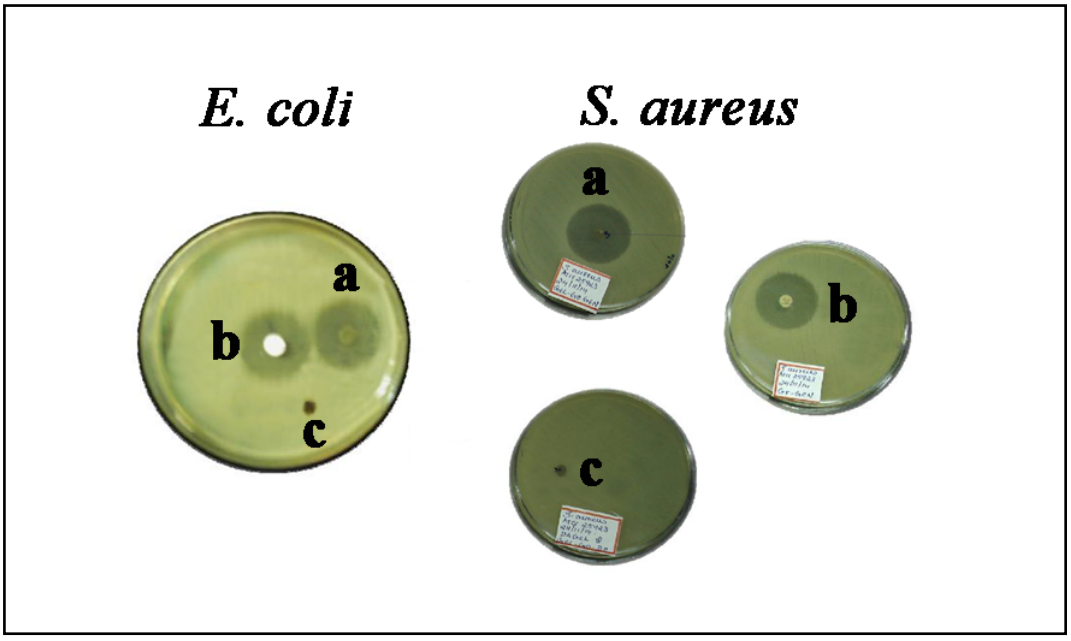

Figure 7.19: The zone of inhibition regions of *E. coli* and *S.aureus* around the test samples (a) DA-GO-GEL-GEN, (b) positive control (gentamicin), (c) DA-GO-GEL by agar diffusion method

Table 7.2: The number of viable bacteria found on the surface of the samples after bacterial adhesion test

Sample code and strain tested	Observation of test bottle after overnight incubation	Number of viable bacteria
DA-GO-GEL *E.coli*	Turbid	2.5×10^{5} cfu/test material
DA-GO-GEL *S.aureus*	Turbid	8.6×10^{4} cfu/test material
DA-GO-GEL-GEN *E.coli*	Clear	0
DA-GO-GEL-GEN *S.aureus*	Clear	0

Recent researches report that the aqueous dispersion of GO possesses an inherent antibacterial property (Hui et al., 2014). However, in the present study, it is found that the GO incorporated gelatin nanofiber mats favour the growth of bacteria as well as normal cells. The interaction of GO planes with the gelatin in the nanofibrous system is found to play a pivotal role in determining the toxicity of GO. The non-covalent interactions among GO and gelatin mask the basal planes of GO, that renders them inactive towards the bacterial cells. The

deactivation of the bacterial activity also depends on the material that is directly interacting with GO (Hui et al., 2014).

7.3 Conclusion

Graphene oxide incorporated electrospun gelatin nanofibers have been successfully developed. The mechanical behaviour of composite nanofibers shows an improved tensile strength for composite nanofibers (21.6 ± 2.03 MPa) compared to the bare gelatin mats (8.29 ± 0.53 MPa). Owing to the high hydrophilicity of GO and gelatin, the resulting nanofibers are cross-linked using dextran aldehyde. After cross-linking treatment with DA, the composite GO-GEL mats exhibit further improvement in mechanical property (56.4 ± 2.03 MPa). The cross-linked composite nanofibers are evaluated for cell compatibility and bacterial adhesion. Even though the GO dispersion is reported to be toxic towards bacterial cells, the present study demonstrates that GO loaded gelatin nanofiber mats promote the growth of the normal cells. The non-covalent interactions between gelatin and GO mask the basal planes of the GO that render them inactive against bacteria. By incorporating gentamicin, antibacterial property is imparted into GO-GEL mats through the controlled release of drugs from the mats. The present composite gelatin nanofibrous system with nano reinforcement of GO shows excellent physico-chemical and biological properties and throws light towards application of these composite nanofibers in tissue engineering and wound dressing arena.

CHAPTER 8

CONCLUSIONS AND FUTURE PERSPECTIVES

8.1 Conclusions

Gelatin based nanofibrous mats were fabricated by electrospinning avoiding toxic solvents and cross-linking agents. Novel, cost effective and natural based cross-linking agents were developed for gelatin nanofibers. The physico-chemical and biological properties of the cross-linked nanofibers demonstrated that the developed cross-linking agents are excellent substitutes for the existing toxic and expensive cross-linking agents. Nanofibers with further improved bio-physical properties were achieved using aminated gelatin, gelatin/chitosan core-shell system and graphene oxide incorporation. The key conclusions of the present work are summarized below.

Gelatin has been successfully electrospun using 8:2 (v/v) water/acetic acid solvent mixture for the first time. Acetic acid concentration of 20 % (v/v) is essential to prevent the gelation of gelatin by disrupting the hydrogen bonding interactions. Gelatin nanofibers with diameter range of 150 ± 30 nm can be produced by adjusting the electrospinning and solution parameters. The resultant smooth nanofibers can be cross-linked using a polysaccharide aldehyde or disaccharide aldehyde without disrupting the nanofiber morphology. The mechanical properties and biodegradation behaviour may be tuned based on the cross-linking agent and the medium employed for cross-linking. Being a polysaccharide, dextran aldehyde is sparingly soluble in ethanol based cross-linking medium and gives rise to lower degree of cross-linking in comparison to the disaccharide, sucrose aldehyde, which is highly soluble in the medium. Since gelatin is in the solid phase and cross-linking agents are in ethanol medium, prolonged time of at least 5 days are required to achieve effective cross-linking.

The presence of minimum quantity of aqueous borax in the cross-linking medium is found to improve the cross-linking efficiency by providing an alkaline pH favourable for Schiff's base formation responsible for the cross-linking reaction. Preliminary *in vitro* cytotoxicity study of the nanofibers reveals that the cross-linked mats are non-cytotoxic towards L-929 and MG-63 cells with good cell adhesion, viability and proliferation. Thus, oxidized dextran and sucrose can act as effective glutaraldehyde analogs for cross-linking protein based nanofibers.

Improved physico-chemical and biological properties for gelatin based nanofibers may be achieved by suitable modifications. The modifications can be based on chemical reaction, physical mixing and change in the instrumental set-up. The chemical modification of gelatin *via* amination produces cationized gelatin. The modified gelatin is water soluble without forming gel at room temperature. Through this modification, nanofibers can be fabricated using pure water as the solvent, by avoiding acetic acid in the solvent system. The water stability of the highly hydrophilic cationized gelatin nanofibers also can be improved by cross-linking with dextran aldehyde and sucrose aldehyde. These cross-linked nanofibers are biocompatible and non-cytotoxic towards L-929 and MG-63 cells with good cell adhesion and proliferation. Positive charges on the surface of the cationized gelatin nanofibers interact with negatively charged cell surface, making them an exciting class of materials for tissue regeneration.

Core-shell structured nanofibers of purely natural origin can be achieved using gelatin core and chitosan shell. Highly spinnable gelatin acts as a core template for the formation of chitosan nanofibers which is otherwise unspinnable. This fabrication method overcomes the problems associated with the usage of toxic solvents and synthetic polymers for obtaining chitosan based nanofibers. Being natural polymers, chitosan and gelatin have excellent biocompatibility, and appropriate biodegradability. The core-shell nanofibers cross-linked with dextran aldehyde and sucrose aldehyde are found to be non-cytotoxic towards L-929 and MG-63 cells with superior adhesion and proliferation due to the presence of chitosan on the surface.

Improvement in mechanical properties and biological performance can be achieved by incorporating graphene oxide into the gelatin nanofiber matrix. Graphene oxide forms a stable and homogeneous dispersion in gelatin solution which results in uniform nanofibrous structures without any beads and bundles. The composite nanofibers exhibit a significant improvement in the tensile strength. Further improvement in the mechanical properties can be achieved by cross-linking the nanofibers with dextran aldehyde. The composite nanofibers possess good adhesion and proliferation characteristics towards L-929 cells. Graphene oxide suspensions are shown to be toxic towards bacterial cells. In contrary, the present composite nanofiber mat does not prevent the growth of bacteria. The non-covalent interactions between gelatin and graphene oxide mask the basal planes of the graphene oxide that render them inactive against bacteria. By incorporating gentamicin, antibacterial property can be imparted into the composite nanofiber mat. The present composite gelatin nanofibrous system with nano reinforcement of graphene oxide having excellent physico-chemical and biological properties is a potential candidate to be investigated in detail for applications in tissue engineering and wound dressing.

In summary, two novel, naturally occurring cross-linking agents are developed for cross-linking of electrospun gelatin nanofibers obtained using benign spinning conditions. Physico-chemical and biological characteristics of the cross-linked nanofibers suggest the applicability of these nanofibers as scaffolds for tissue engineering. The cross-linking agents developed can be used for cross-linking of nanofibers from modified gelatin systems and other protein nanofibers. A green fabrication method for gelatin based nanofibers is achieved using cationized gelatin. The concept of using gelatin as a core template for fabricating chitosan nanofibers is also introduced. Composite nanofiber matrix consisting of graphene oxide and gelatin with improved mechanical performance is demonstrated.

8.2 Future Perspectives

Electrospun gelatin nanofibers with naturally derived cross-linking agents are incredibly attractive candidates to be useful for large variety of biomedical applications, where the existing cross-linking agents create unwanted side effects. Gelatin and modified gelatin based electrospun nanofibers cross-linked with dextran aldehyde and sucrose aldehyde showed excellent biocompatibility and cell adhesion properties towards various cell types. The *in vivo* studies of the established gelatin based nanofibers using specific cell types for real life tissue regeneration applications are recommended.

Nanofiber based drug delivery systems are promising materials and are more flexible and therapeutically effective with minimal side effects. The fabrication of drug loaded core-shell nanofibers based on gelatin and chitosan as a drug delivery device for certain diseases can be thought of.

Other than periodate oxidized polysaccharide and disaccharides as protein cross-linkers, we would like to explore the oligosaccharides as cross-linking agents for gelatin based nanofibers. Periodate oxidized oligosaccharides will have good solubility in ethanol as well as structural resemblance with ECM components.

REFERENCES

1. Abdel-Hady, F., Alzahrany, A., and Hamed, M. (2011). Experimental validation of upward electrospinning process. *ISRN Nanotechnology*, 2011.

2. Aboutalebi, S. H., Gudarzi, M. M., Zheng, Q. B., and Kim, J. K. (2011). Spontaneous formation of liquid crystals in ultralarge graphene oxide dispersions. *Advanced Functional Materials,* 21(15): 2978-2988.

3. Alves da Silva, M. L., Martins, A., Costa-Pinto, A. R., Costa, P., Faria, S., Gomes, M., Reis, R. L., and Neves, N. M. (2010). Cartilage Tissue Engineering Using Electrospun PCL Nanofiber Meshes and MSCs. *Biomacromolecules,* 11(12): 3228-3236.

4. An, K., Liu, H., Guo, S., Kumar, D., and Wang, Q. (2010). Preparation of fish gelatin and fish gelatin/poly (l-lactide) nanofibers by electrospinning. *International Journal of Biological Macromolecules,* 47(3): 380-388.

5. Angarano, M., Schulz, S., Fabritius, M., Vogt, R., Steinberg, T., Tomakidi, P., Friedrich, C., and Mülhaupt, R. (2013). Layered Gradient Nonwovens of In Situ Crosslinked Electrospun Collagenous Nanofibers Used as Modular Scaffold Systems for Soft Tissue Regeneration. *Advanced Functional Materials,* 23(26): 3277-3285.

6 . Anton, F. Process and apparatus for preparing artificial threads. US Patent 1975504, 1934.

7. Archana, D., Upadhyay, L., Tewari, R., Dutta, J., Huang, Y., and Dutta, P. (2013). Chitosan-pectin-alginate as a novel scaffold for tissue engineering applications. *Indian Journal of Biotechnology,* 12(4): 475-482.

8. Atchison, J. S., and Schauer, C. L. (2012). Fabrication and characterization of electrospun pristine and fluorescent composite poly (acrylic acid) ultra-fine fibers. *J. Eng. Fiber Fabr,* 7: 50-57.

9. Baiguera, S., Del Gaudio, C., Lucatelli, E., Kuevda, E., Boieri, M., Mazzanti, B., Bianco, A., and Macchiarini, P. (2014). Electrospun gelatin scaffolds incorporating rat decellularized brain extracellular matrix for neural tissue engineering. *Biomaterials,* 35(4): 1205-1214.

10. Balakrishnan, B., and Jayakrishnan, A. (2005). Self-cross-linking biopolymers as injectable in situ forming biodegradable scaffolds. *Biomaterials,* 26(18): 3941-3951.

11. Balakrishnan, B., Jayakrishnan, A., Kumar, S. P., and Nandkumar, M. A. (2012). Anti-bacterial Properties of an In Situ Forming Hydrogel Based on Oxidized Alginate and Gelatin Loaded with Gentamycin. *Trends in Biomaterials and Artificial Organs,* 26(3): 139-145.

12. Balakrishnan, B., Joshi, N., and Banerjee, R. (2013). Borate aided Schiff's base formation yields in situ gelling hydrogels for cartilage regeneration. *Journal of Materials Chemistry B,* 1(41): 5564-5577.

13. Bao, Q., Zhang, H., Yang, J. x., Wang, S., Tang, D. Y., Jose, R., Ramakrishna, S., Lim, C. T., and Loh, K. P. (2010). Graphene–polymer nanofiber membrane for ultrafast photonics. *Advanced Functional Materials,* 20(5): 782-791.

14. Barakat, N. A., Kim, B., and Kim, H. Y. (2008). Production of smooth and pure nickel metal nanofibers by the electrospinning technique: nanofibers possess splendid magnetic properties. *The Journal of Physical Chemistry C,* 113(2): 531-536.

15. Baumgarten, P. K. (1971). Electrostatic spinning of acrylic microfibers. *Journal of colloid and interface science,* 36(1): 71-79.

16. Beachley, V. (2011). "Novel nanofiber structures and advanced tissue engineering applications" Ph.D. Thesis, Clemson University.

17. Beachley, V., and Wen, X. (2009). Effect of electrospinning parameters on the nanofiber diameter and length. *Materials Science and Engineering: C,* 29(3): 663-668.

18. Beachley, V., and Wen, X. (2010). Polymer nanofibrous structures: Fabrication, biofunctionalization, and cell interactions. *Progress in polymer science,* 35(7): 868-892.

19. Bello, Y. M., Falabella, A. F., and Eaglstein, W. H. (2001). Tissue-engineered skin. *American journal of clinical dermatology,* 2(5): 305-313.

20. Bergshoef, M. M., and Vancso, G. J. (1999). Transparent nanocomposites with ultrathin, electrospun nylon-4, 6 fiber reinforcement. *Advanced Materials,* 11(16): 1362-1365.

21. Berndt, P., Fields, G. B., and Tirrell, M. (1995). Synthetic lipidation of peptides and amino acids: monolayer structure and properties. *Journal of the American Chemical Society,* 117(37): 9515-9522.

22. Bhadra, D., Sannigrahi, J., Chaudhuri, B., and Sakata, H. (2012). Enhancement of the transport and dielectric properties of graphite oxide nanoplatelets-polyvinyl alcohol composite showing low percolation threshold. *Polymer composites,* 33(3): 436-442.

23. Bhardwaj, N., and Kundu, S. C. (2010). Electrospinning: a fascinating fiber fabrication technique. *Biotechnology Advances,* 28(3): 325-347.

24. Bhattarai, N., Edmondson, D., Veiseh, O., Matsen, F. A., and Zhang, M. (2005). Electrospun chitosan-based nanofibers and their cellular compatibility. *Biomaterials,* 26(31): 6176-6184.

25. Boanini, E., Rubini, K., Panzavolta, S., and Bigi, A. (2010). Acta Biomaterialia Chemico-physical characterization of gelatin films modified with oxidized alginate. *Acta biomaterialia,* 6(2): 383-388.

26. Bohidar, H. B., and Jena, S. S. (1994). Study of sol-state properties of aqueous gelatin solutions. *The Journal of chemical physics,* 100(9): 6888-6895.

27. Cano, M., Khan, U., Sainsbury, T., O'Neill, A., Wang, Z., McGovern, I. T., Maser, W. K., Benito, A. M., and Coleman, J. N. (2013). Improving the mechanical properties of graphene oxide based materials by covalent attachment of polymer chains. *Carbon,* 52(0): 363-371.

28. Chan, B. P., and Leong, K. W. (2008a). Scaffolding in tissue engineering: general approaches and tissue-specific considerations. *European Spine Journal,* 17(Suppl 4): 467-479.

29. Chan, B. P., and Leong, K. W. (2008b). Scaffolding in tissue engineering: general approaches and tissue-specific considerations. *European Spine Journal,* 17(4): 467-479.

30. Chang, J., and Gupta, G. (2010). *Tissue Engineering for the Hand: Research Advances and Clinical Applications* World Scientific Publishing Company: Singapore.

31. Chang, W.-H., Chang, Y., Lai, P.-H., and Sung, H.-W. (2003). A genipin-crosslinked gelatin membrane as wound-dressing material: in vitro and in vivo studies. *Journal of Biomaterials Science, Polymer Edition,* 14(5): 481-495.

32. Charernsriwilaiwat, N., Rojanarata, T., Ngawhirunpat, T., and Opanasopit, P. (2014). Electrospun chitosan/polyvinyl alcohol nanofibre mats for wound healing. *International Wound Journal,* 11(2): 215-222.

33. Chaudhuri, B., Bhadra, D., Mondal, B., and Pramanik, K. (2014). Biocompatibility of electrospun graphene oxide–poly (ε-caprolactone) fibrous scaffolds with human cord blood mesenchymal stem cells derived skeletal myoblast. *Materials Letters,* 126: 109-112.

34. Chen, J.-P., Chen, S.-H., and Lai, G.-J. (2012). Preparation and characterization of biomimetic silk fibroin/chitosan composite nanofibers by electrospinning for osteoblasts culture. *Nanoscale research letters,* 7(1): 1-11.

35. Chen, J.-P., and Su, C.-H. (2011). Surface modification of electrospun PLLA nanofibers by plasma treatment and cationized gelatin immobilization for cartilage tissue engineering. *Acta biomaterialia,* 7(1): 234-243.

36. Chen, M., Przyborowski, M., and Berthiaume, F. (2009). Stem Cells for Skin Tissue Engineering and Wound Healing. *Critical reviews in biomedical engineering,* 37(4-5): 399-421.

37. Chen, Y.-S., Chang, J.-Y., Cheng, C.-Y., Tsai, F.-J., Yao, C.-H., and Liu, B.-S. (2005). An in vivo evaluation of a biodegradable genipin-cross-linked gelatin peripheral nerve guide conduit material. *Biomaterials,* 26(18): 3911-3918.

38. Chen, Z., Wang, P., Wei, B., Mo, X., and Cui, F. (2010). Electrospun collagen–chitosan nanofiber: A biomimetic extracellular matrix for endothelial cell and smooth muscle cell. *Acta biomaterialia,* 6(2): 372-382.

39. Cheung, H.-Y., Lau, K.-T., Lu, T.-P., and Hui, D. (2007). A critical review on polymer-based bio-engineered materials for scaffold development. *Composites Part B: Engineering,* 38(3): 291-300.

40. Chiono, V., Pulieri, E., Vozzi, G., Ciardelli, G., Ahluwalia, A., and Giusti, P. (2008). Genipin-crosslinked chitosan/gelatin blends for biomedical applications. *Journal of materials science. Materials in medicine,* 19(2): 889-898.

41. Choktaweesap, N., Arayanarakul, K., Aht-ong, D., Meechaisue, C., and Supaphol, P. (2007). Electrospun Gelatin Fibers: Effect of Solvent System on Morphology and Fiber Diameters. *Polym. J,* 39(6): 622-631.

42. Chong, E. J., Phan, T. T., Lim, I. J., Zhang, Y. Z., Bay, B. H., Ramakrishna, S., and Lim, C. T. (2007). Evaluation of electrospun PCL/gelatin nanofibrous scaffold for wound healing and layered dermal reconstitution. *Acta biomaterialia,* 3(3): 321-330.

43. Chronakis, I. S. (2010). Micro-/nano-fibers by electrospinning technology: processing, properties and applications. *Micromanufacturing Engineering and Technology.–Boston: Elsevier*: 264-286.

44. Chung, C., Kim, Y.-K., Shin, D., Ryoo, S.-R., Hong, B. H., and Min, D.-H. (2013). Biomedical applications of graphene and graphene oxide. *Accounts of chemical research,* 46(10): 2211-2224.

45. Chung, H. J., and Park, T. G. (2007). Surface engineered and drug releasing pre-fabricated scaffolds for tissue engineering. *Advanced drug delivery reviews,* 59(4–5): 249-262.

46. Ciapetti, G., Cenni, E., Pratelli, L., and Pizzoferrato, A. (1993). In vitro evaluation of cell/biomaterial interaction by MTT assay. *Biomaterials,* 14(5): 359-364.

47. Cooper, A., Jana, S., Bhattarai, N., and Zhang, M. (2010). Aligned chitosan-based nanofibers for enhanced myogenesis. *Journal of Materials Chemistry,* 20(40): 8904-8911.

48. Cortesi, R., Nastruzzi, C., and Davis, S. S. (1998). Sugar cross-linked gelatin for controlled release: microspheres and disks. *Biomaterials,* 19(18): 1641-1649.

49. Cui, P., Lee, J., Hwang, E., and Lee, H. (2011). One-pot reduction of graphene oxide at subzero temperatures. *Chemical Communications,* 47(45): 12370-12372.

50. Damink, L., Dijkstra, P., Van Luyn, M., Van Wachem, P., Nieuwenhuis, P., and Feijen, J. (1996). *In vitro* degradation of dermal sheep collagen cross-linked using a water-soluble carbodiimide. *Biomaterials,* 17(7): 679-684.

51. Dash, R., Foston, M., and Ragauskas, A. J. (2013). Improving the mechanical and thermal properties of gelatin hydrogels cross-linked by cellulose nanowhiskers. *Carbohydrate Polymers,* 91(2): 638-645.

52. Dawlee, S., Sugandhi, A., Balakrishnan, B., Labarre, D., and Jayakrishnan, A. (2005). Oxidized chondroitin sulfate-cross-linked gelatin matrixes: a new class of hydrogels. *Biomacromolecules,* 6(4): 2040-2048.

53. Desai, K., Kit, K., Li, J., and Zivanovic, S. (2008). Morphological and surface properties of electrospun chitosan nanofibers. *Biomacromolecules,* 9(3): 1000-1006.

54. Dhandayuthapani, B., Krishnan, U. M., and Sethuraman, S. (2010). Fabrication and characterization of chitosan-gelatin blend nanofibers for skin tissue engineering. *Journal of Biomedical Materials Research Part B: Applied Biomaterials,* 94(1): 264-272.

55. Dhandayuthapani, B., Yoshida, Y., Maekawa, T., and Kumar, D. S. (2011). Polymeric scaffolds in tissue engineering application: a review. *International Journal of Polymer Science,* 2011.

56. Di Martino, A., Sittinger, M., and Risbud, M. V. (2005). Chitosan: A versatile biopolymer for orthopaedic tissue-engineering. *Biomaterials,* 26(30): 5983-5990.

57. Dong, B., Arnoult, O., Smith, M. E., and Wnek, G. E. Electrospinning of Collagen Nanofiber Scaffolds from Benign Solvents. 539-542.

58. Doshi, J., and Reneker, D. H. (1993). Electrospinning process and applications of electrospun fibers. *Industry Applications Society Annual Meeting, 1993., Conference Record of the 1993 IEEE* (pp. 1698-1703): IEEE.

59. Draye, J. P., Delaey, B., Van de Voorde, a., Van Den Bulcke, a., Bogdanov, B., and Schacht, E. (1998). In vitro release characteristics of bioactive molecules from dextran dialdehyde cross-linked gelatin hydrogel films. *Biomaterials,* 19(1-3): 99-107.

60. Draye, J.-P., Delaey, B., Van de Voorde, A., Van Den Bulcke, A., De Reu, B., and Schacht, E. (1998). In vitro and in vivo biocompatibility of dextran dialdehyde cross-linked gelatin hydrogel films. *Biomaterials,* 19(18): 1677-1687.

61. Dror, Y., Ziv, T., Makarov, V., Wolf, H., Admon, A., and Zussman, E. (2008). Nanofibers made of globular proteins. *Biomacromolecules,* 9(10): 2749-2754.

62. Du, J., and Hsieh, Y.-L. (2007). PEGylation of chitosan for improved solubility and fiber formation via electrospinning. *Cellulose,* 14(6): 543-552.

63. Dutta, P. K., Dutta, J., and Tripathi, V. (2004). Chitin and chitosan: Chemistry, properties and applications. *Journal of Scientific and Industrial Research,* 63(1): 20-31.

64. El-Hady, M. A. (2013). Electrospun gelatin nanofibers: effect of gelatin concentration on morphology and fiber diameters. *Journal of Applied Sciences Research,* 9(1): 534-540.

65. Elahi, M. F., Lu, W., Guoping, G., and Khan, F. (2013). Core-shell Fibers for Biomedical Applications-A Review. *J Bioengineer & Biomedical Sci 3: 121. doi*.

66. Farris, S., Song, J., and Huang, Q. (2009). Alternative Reaction Mechanism for the Cross-Linking of Gelatin with Glutaraldehyde. *Journal of Agricultural and Food Chemistry*, 58(2): 998-1003.

67. Feng, L., Li, S., Li, H., Zhai, J., Song, Y., Jiang, L., and Zhu, D. (2002). Super-Hydrophobic Surface of Aligned Polyacrylonitrile Nanofibers. *Angewandte Chemie International Edition*, 41(7): 1221-1223.

68. Francis Suh, J. K., and Matthew, H. W. T. (2000). Application of chitosan-based polysaccharide biomaterials in cartilage tissue engineering: a review. *Biomaterials*, 21(24): 2589-2598.

69. Freyman, T. M., Yannas, I. V., and Gibson, L. J. (2001). Cellular materials as porous scaffolds for tissue engineering. *Progress in Materials Science*, 46(3–4): 273-282.

70. Fujii, H., Matsuyama, A., Komoda, H., Sasai, M., Suzuki, M., Asano, T., Doki, Y., Kirihata, M., Ono, K., Tabata, Y., Kaneda, Y., Sawa, Y., and Lee, C. M. (2011). Cationized gelatin-HVJ envelope with sodium borocaptate improved the BNCT efficacy for liver tumors in vivo. *Radiation oncology (London, England)*, 6: 8-8.

71. Garg, K., and Bowlin, G. L. (2011). Electrospinning jets and nanofibrous structures. *Biomicrofluidics*, 5(1): 013403.

72. Geng, X., Kwon, O.-h., and Ã, J. J. (2005). Electrospinning of chitosan dissolved in concentrated acetic acid solution. 26: 5427-5432.

73. Gómez-Guillén, M., Giménez, B., López-Caballero, M. a., and Montero, M. (2011). Functional and bioactive properties of collagen and gelatin from alternative sources: A review. *Food Hydrocolloids*, 25(8): 1813-1827.

74. Gorgieva, S., and Kokol, V. (2011). Collagen-vs. gelatine-based biomaterials and their biocompatibility: review and perspectives. *Biomaterials Applications for Nanomedicine*: 17-58.

75. Graham, K., Ouyang, M., Raether, T., Grafe, T., McDonald, B., and Knauf, P. (2002). Fifteenth Annual Technical Conference & Expo of the American Filtration & Separations Society. *Galveston, TX*, 4: 9-12.

76. Greiner, A., and Wendorff, J. H. (2007). Electrospinning: a fascinating method for the preparation of ultrathin fibers. *Angewandte Chemie International Edition*, 46(30): 5670-5703.

77. Gupta, B., Tummalapalli, M., Deopura, B., and Alam, M. (2014a). Preparation and characterization of< i> in-situ</i> crosslinked pectin–gelatin hydrogels. *Carbohydrate Polymers*, 106: 312-318.

78. Gupta, K. C., Haider, A., Choi, Y.-r., and Kang, I.-k. (2014b). Nanofibrous scaffolds in biomedical applications. *Biomaterials Research*, 18(1): 5.

79. Hao, Y., Xu, P., He, C., Yang, X., Huang, M., Xing, J., and Chen, J. (2011). Impact of carbondiimide crosslinker used for magnetic carbon nanotube mediated GFP plasmid delivery. *Nanotechnology,* 22(28): 285103.

80. Hartgerink, J. D., Beniash, E., and Stupp, S. I. (2002). Peptide-amphiphile nanofibers: a versatile scaffold for the preparation of self-assembling materials. *Proceedings of the National Academy of Sciences,* 99(8): 5133-5138.

81. He, J.-H., Wu, Y., and Zuo, W.-W. (2005). Critical length of straight jet in electrospinning. *Polymer,* 46(26): 12637-12640.

82. He, L., Shi, Y., Han, Q., Zuo, Q., Ramakrishna, S., Xue, W., and Zhou, L. (2012). Surface modification of electrospun nanofibrous scaffolds via polysaccharide–protein assembly multilayer for neurite outgrowth. *Journal of Materials Chemistry,* 22(26): 13187-13196.

83. Helan, X., and Yiqi, Y. (2014). 3D Electrospun Fibrous Structures from Biopolymers. *Lightweight Materials from Biopolymers and Biofibers* (pp. 103-126): American Chemical Society.

84. Hou, H., and Reneker, D. H. (2004). Carbon nanotubes on carbon nanofibers: a novel structure based on electrospun polymer nanofibers. *Advanced Materials,* 16(1): 69-73.

85. Hu, W.-W., and Yu, H.-N. (2013). Coelectrospinning of chitosan/alginate fibers by dual-jet system for modulating material surfaces. *Carbohydrate Polymers,* 95(2): 716-727.

86. Hu, W., Peng, C., Luo, W., Lv, M., Li, X., Li, D., Huang, Q., and Fan, C. (2010). Graphene-Based Antibacterial Paper. *ACS nano,* 4(7): 4317-4323.

87. Hu, X., Liu, S., Zhou, G., Huang, Y., Xie, Z., and Jing, X. (2014a). Electrospinning of polymeric nanofibers for drug delivery applications. *Journal of Controlled Release,* 185(0): 12-21.

88. Hu, Y., Liu, L., Gu, Z., Dan, W., Dan, N., and Yu, X. (2014b). Modification of collagen with a natural derived cross-linker, alginate dialdehyde. *Carbohydrate Polymers,* 102(0): 324-332.

89. Huang, Q. (2012). *Nanotechnology in the food, beverage and nutraceutical industries* Woodhead Publishing: UK.

90. Huang, Z.-M., Zhang, Y.-Z., Kotaki, M., and Ramakrishna, S. (2003). A review on polymer nanofibers by electrospinning and their applications in nanocomposites. *Composites science and technology,* 63(15): 2223-2253.

91. Huang, Z.-M., Zhang, Y. Z., Ramakrishna, S., and Lim, C. T. (2004). Electrospinning and mechanical characterization of gelatin nanofibers. *Polymer,* 45(15): 5361-5368.

92. Hui, L., Piao, J.-G., Auletta, J., Hu, K., Zhu, Y., Meyer, T., Liu, H., and Yang, L. (2014). Availability of the basal planes of graphene oxide determines whether it is antibacterial. *ACS applied materials & interfaces,*

6(15): 13183-13190.

93. Hutmacher, D., Goh, J., and Teoh, S. (2001). An introduction to biodegradable materials for tissue engineering applications. *Annals of the Academy of Medicine, Singapore,* 30(2): 183-191.

94. Ignatova, M., Manolova, N., Markova, N., and Rashkov, I. (2009). Electrospun Non-Woven Nanofibrous Hybrid Mats Based on Chitosan and PLA for Wound-Dressing Applications. *Macromolecular Bioscience,* 9(1): 102-111.

95. Ji, X., Yang, W., Wang, T., Mao, C., Guo, L., Xiao, J., and He, N. (2013). Coaxially electrospun core/shell structured poly (L-lactide) acid/chitosan nanofibers for potential drug carrier in tissue engineering. *Journal of biomedical nanotechnology,* 9(10): 1672-1678.

96. Jiang, H., Hu, Y., Li, Y., Zhao, P., Zhu, K., and Chen, W. (2005). A facile technique to prepare biodegradable coaxial electrospun nanofibers for controlled release of bioactive agents. *Journal of Controlled Release,* 108(2): 237-243.

97. Jin, G., Li, Y., Prabhakaran, M. P., Tian, W., and Ramakrishna, S. (2014). In vitro and in vivo evaluation of the wound healing capability of electrospun gelatin/PLLCL nanofibers. *Journal of Bioactive and Compatible Polymers: Biomedical Applications*.

98. Jin, G., Prabhakaran, M. P., Kai, D., and Ramakrishna, S. (2013). Controlled release of multiple epidermal induction factors through core–shell nanofibers for skin regeneration. *European Journal of Pharmaceutics and Biopharmaceutics,* 85(3): 689-698.

99. Kanani, A. G., and Bahrami, S. H. (2010). Review on electrospun nanofibers scaffold and biomedical applications. *Trends Biomater Artif Organs,* 24(2): 93-115.

100. Kelleher, C. M., and Vacanti, J. P. (2010). Engineering extracellular matrix through nanotechnology. *Journal of the Royal Society Interface,* 7(Suppl 6): S717-S729.

101. Khadka, D. B., and Haynie, D. T. (2012). Protein- and peptide-based electrospun nanofibers in medical biomaterials. *Nanomedicine: Nanotechnology, Biology and Medicine,* 8(8): 1242-1262.

102. Ki, C. S., Baek, D. H., Gang, K. D., Lee, K. H., Um, I. C., and Park, Y. H. (2005). Characterization of gelatin nanofiber prepared from gelatin–formic acid solution. *Polymer,* 46(14): 5094-5102.

103. Kiernan, J. A. (2000). Formaldehyde, formalin, paraformaldehyde and glutaraldehyde: what they are and what they do. *Microscopy Today,* 1(5).

104. Kim, H.-J., Choi, E.-Y., Oh, J.-S., Lee, H.-C., Park, S.-S., and Cho, C.-S. (2000). Possibility of wound dressing using poly (L-leucine)/poly (ethylene glycol)/poly (L-leucine) triblock copolymer. *Biomaterials,* 21(2): 131-141.

105. Kim, H. W., Song, J. H., and Kim, H. E. (2005). Nanofiber Generation of Gelatin–Hydroxyapatite Biomimetics for Guided Tissue Regeneration. *Advanced Functional Materials,* 15(12): 1988-1994.

106. Kim, J. s., and Reneker, D. H. (1999). Mechanical properties of composites using ultrafine electrospun fibers. *Polymer composites,* 20(1): 124-131.

107. Ko, J., Yin, H., An, J., Chung, D., Kim, J.-H., Lee, S., and Pyun, D. (2010). Characterization of cross-linked gelatin nanofibers through electrospinning. *Macromolecular Research,* 18(2): 137-143.

108. Ku, S. H., and Park, C. B. (2013). Myoblast differentiation on graphene oxide. *Biomaterials,* 34(8): 2017-2023.

109. Kuijpers, A. J., Engbers, G. H., Krijgsveld, J., Zaat, S. A., Dankert, J., and Feijen, J. (2000). Cross-linking and characterisation of gelatin matrices for biomedical applications. *Journal of Biomaterials Science, Polymer Edition,* 11(3): 225-243.

110. Kumar, P. (2013). Laser flash synthesis of graphene and its inorganic analogues: An innovative breakthrough with immense promise. *RSC Advances,* 3(30): 11987-12002.

111. Kumbar, S. G., Nukavarapu, S. P., James, R., Nair, L. S., and Laurencin, C. T. (2008). Electrospun poly (lactic acid-co-glycolic acid) scaffolds for skin tissue engineering. *Biomaterials,* 29(30): 4100-4107.

112. Kundu, S., Gill, R. S., and Saraf, R. F. (2011). Electrospinning of PAH Nanofiber and Deposition of Au NPs for Nanodevice Fabrication. *The Journal of Physical Chemistry C,* 115(32): 15845-15852.

113. Laurencin, C. T., Kumbar, S. G., Nukavarapu, S. P., James, R., and Hogan, M. V. (2008). Recent patents on electrospun biomedical nanostructures: an overview. *Recent patents on biomedical engineering,* 1(1): 68-78.

114. Lee, K. Y., Jeong, L., Kang, Y. O., Lee, S. J., and Park, W. H. (2009). Electrospinning of polysaccharides for regenerative medicine. *Advanced drug delivery reviews,* 61(12): 1020-1032.

115. Leung, V., and Ko, F. (2011). Biomedical applications of nanofibers. *Polymers for Advanced Technologies,* 22(3): 350-365.

116. Li, D., Babel, A., Jenekhe, S. A., and Xia, Y. (2004). Nanofibers of conjugated polymers prepared by electrospinning with a two-capillary spinneret. *Advanced Materials,* 16(22): 2062-2066.

117. Li, D., McCann, J. T., Xia, Y., and Marquez, M. (2006a). Electrospinning: a simple and versatile technique for producing ceramic nanofibers and nanotubes. *Journal of the American Ceramic Society,* 89(6): 1861-1869.

118. Li, D., and Xia, Y. (2004a). Direct fabrication of composite and ceramic hollow nanofibers by electrospinning. *Nano Letters,* 4(5): 933-938.

119. Li, D., and Xia, Y. (2004b). Electrospinning of Nanofibers: Reinventing the Wheel? *Advanced Materials,* 16(14): 1151-1170.

120. Li, M., Guo, Y., Wei, Y., MacDiarmid, A. G., and Lelkes, P. I. (2006b). Electrospinning polyaniline-contained gelatin nanofibers for tissue engineering applications. *Biomaterials,* 27(13): 2705-2715.

121. Li, M., Mondrinos, M. J., Gandhi, M. R., Ko, F. K., Weiss, A. S., and Lelkes, P. I. (2005). Electrospun protein fibers as matrices for tissue engineering. *Biomaterials,* 26(30): 5999-6008.

122. Li, S., Sun, B., Li, X., and Yuan, X. (2008). Characterization of electrospun core/shell poly (vinyl pyrrolidone)/poly (L-lactide-co-ε-caprolactone) fibrous membranes and their cytocompatibility in vitro. *Journal of Biomaterials Science, Polymer Edition,* 19(2): 245-258.

123. Li, Y. (2013). "Electrospinning of Core-shell Collagen Nanofibers" M.S. Thesis, University of Western Ontario.

124. Liu, H., Cheng, J., Chen, F., Bai, D., Shao, C., Wang, J., Xi, P., and Zeng, Z. (2014). Gelatin functionalized graphene oxide for mineralization of hydroxyapatite: biomimetic and in vitro evaluation. *Nanoscale,* 6(10): 5315-5322.

125. Liu, S., Zeng, T. H., Hofmann, M., Burcombe, E., Wei, J., Jiang, R., Kong, J., and Chen, Y. (2011). Antibacterial activity of graphite, graphite oxide, graphene oxide, and reduced graphene oxide: membrane and oxidative stress. *ACS nano,* 5(9): 6971-6980.

126. Liu, W., Ni, C., Chase, D. B., and Rabolt, J. F. (2013). Preparation of multilayer biodegradable nanofibers by triaxial electrospinning. *ACS Macro Letters,* 2(6): 466-468.

127. Liu, W., Thomopoulos, S., and Xia, Y. (2012). Electrospun nanofibers for regenerative medicine. *Advanced healthcare materials,* 1(1): 10-25.

128. Long, Y.-Z., Li, M.-M., Gu, C., Wan, M., Duvail, J.-L., Liu, Z., and Fan, Z. (2011). Recent advances in synthesis, physical properties and applications of conducting polymer nanotubes and nanofibers. *Progress in polymer science,* 36(10): 1415-1442.

129. Loscertales, I. G., Barrero, A., Guerrero, I., Cortijo, R., Marquez, M., and Ganan-Calvo, A. (2002). Micro/nano encapsulation via electrified coaxial liquid jets. *Science,* 295(5560): 1695-1698.

130. Lu, A., Zhu, J., Zhang, G., and Sun, G. (2011). Gelatin nanofibers fabricated by extruding immiscible polymer solution blend and their application in tissue engineering. *Journal of Materials Chemistry,* 21(46): 18674-18680.

131. Lu, H., Chen, W.-J., Xing, Y., Ying, D.-J., and Jiang, B. (2009a). Design and preparation of an electrospun biomaterial surgical patch. *Journal of Bioactive and Compatible Polymers,* 24(1 suppl): 158-168.

132. Lu, X., Wang, C., and Wei, Y. (2009b). One-Dimensional Composite

Nanomaterials : Synthesis by Electrospinning and Their Applications. (21): 2349-2370.

133. Lu, X., Wang, C., and Wei, Y. (2009c). One-Dimensional Composite Nanomaterials: Synthesis by Electrospinning and Their Applications. *Small,* 5(21): 2349-2370.

134. Lu, Y., Jiang, H., Tu, K., and Wang, L. (2009d). Mild immobilization of diverse macromolecular bioactive agents onto multifunctional fibrous membranes prepared by coaxial electrospinning. *Acta biomaterialia,* 5(5): 1562-1574.

135. Ma, P. X., and Elisseeff, J. (2010). *Scaffolding in tissue engineering* CRC press:

136. Maeda, N., Miao, J., Simmons, T. J., Dordick, J. S., and Linhardt, R. J. (2014). Composite polysaccharide fibers prepared by electrospinning and coating. *Carbohydrate Polymers,* 102: 950-955.

137. Malafaya, P. B., Silva, G. A., and Reis, R. L. (2007). Natural–origin polymers as carriers and scaffolds for biomolecules and cell delivery in tissue engineering applications. *Advanced drug delivery reviews,* 59(4–5): 207-233.

138. Manju, S., Muraleedharan, C. V., Rajeev, A., Jayakrishnan, A., and Joseph, R. (2011). Evaluation of alginate dialdehyde cross-linked gelatin hydrogel as a biodegradable sealant for polyester vascular graft. *Journal of Biomedical Materials Research Part B: Applied Biomaterials,* 98B(1): 139-149.

139. Martin, C. R. (1994). Nanomaterials: A Membrane-Based Synthetic Approach. *Science,* 266(5193): 1961-1966.

140. Martín, J., Maiz, J., Sacristan, J., and Mijangos, C. (2012). Tailored polymer-based nanorods and nanotubes by "template synthesis": From preparation to applications. *Polymer,* 53(6): 1149-1166.

141. Matthews, J. A., Wnek, G. E., Simpson, D. G., and Bowlin, G. L. (2002). Electrospinning of Collagen Nanofibers. *Biomacromolecules,* 3(2): 232-238.

142. McKinley, G. H., and Sridhar, T. (2002). Filament-stretching rheometry of complex fluids. *Annual Review of Fluid Mechanics,* 34(1): 375-415.

143. Metcalfe, A. D., and Ferguson, M. W. (2007). Tissue engineering of replacement skin: the crossroads of biomaterials, wound healing, embryonic development, stem cells and regeneration. *Journal of the Royal Society Interface,* 4(14): 413-437.

144. Migneault, I., Dartiguenave, C., Bertrand, M. J., and Waldron, K. C. (2004). Glutaraldehyde: behavior in aqueous solution, reaction with proteins, and application to enzyme crosslinking. *Biotechniques,* 37(5): 790-806.

145. Moghe, A., and Gupta, B. (2008). Co-axial Electrospinning for Nanofiber

Structures: Preparation and Applications. *Polymer Reviews,* 48(2): 353-377.

146. Morimoto, K., Chono, S., Kosai, T., Seki, T., and Tabata, Y. (2008). Design of cationic microspheres based on aminated gelatin for controlled release of peptide and protein drugs. *Drug delivery,* 15(2): 113-117.

147. Mtshali, T., Krupa, I., and Luyt, A. (2001). The effect of cross-linking on the thermal properties of LDPE/wax blends. *Thermochimica acta,* 380(1): 47-54.

148. Nair, L. S., and Laurencin, C. T. (2007). Biodegradable polymers as biomaterials. *Progress in polymer science,* 32(8): 762-798.

149. Nair, S., Remya, N. S., Remya, S., and Nair, P. D. (2011). A biodegradable in situ injectable hydrogel based on chitosan and oxidized hyaluronic acid for tissue engineering applications. *Carbohydrate Polymers,* 85(4): 838-844.

150. Neves, N. M., Campos, R., Pedro, A., Cunha, J., Macedo, F., and Reis, R. L. (2007). Patterning of polymer nanofiber meshes by electrospinning for biomedical applications. *International Journal of Nanomedicine,* 2(3): 433-438.

151. Nguyen, T.-H. (2010). Fabrication and characterization of cross-linked gelatin electro-spun nano-fibers. *Journal of Biomedical Science and Engineering,* 03(12): 1117-1124.

152. Nguyen, T.-H., and Lee, B.-T. (2010). Fabrication and characterization of cross-linked gelatin electro-spun nano-fibers. *Journal of Biomedical Science and Engineering,* 3(12): 1117.

153. Nie, H., He, A., Wu, W., Zheng, J., Xu, S., Li, J., and Han, C. C. (2009). Effect of poly (ethylene oxide) with different molecular weights on the electrospinnability of sodium alginate. *Polymer,* 50(20): 4926-4934.

154. Nie, H., Li, J., He, A., Xu, S., Jiang, Q., and Han, C. C. (2010). Carrier System of Chemical Drugs and Isotope from Gelatin Electrospun Nanofibrous Membranes. *Biomacromolecules,* 11(8): 2190-2194.

155. Ohkawa, K., Cha, D., Kim, H., Nishida, A., and Yamamoto, H. (2004). Electrospinning of chitosan. *Macromolecular Rapid Communications,* 25(18): 1600-1605.

156. Ojha, S. S., Stevens, D. R., Hoffman, T. J., Stano, K., Klossner, R., Scott, M. C., Krause, W., Clarke, L. I., and Gorga, R. E. (2008). Fabrication and Characterization of Electrospun Chitosan Nanofibers Formed via Templating with Polyethylene Oxide. *Biomacromolecules,* 9(9): 2523-2529.

157. Pakravan, M., Heuzey, M.-C., and Ajji, A. (2012). Core–shell structured PEO-chitosan nanofibers by coaxial electrospinning. *Biomacromolecules,* 13(2): 412-421.

158. Palangetic, L., Reddy, N. K., Srinivasan, S., Cohen, R. E., McKinley, G.

H., and Clasen, C. (2014). Dispersity and spinnability: Why highly polydisperse polymer solutions are desirable for electrospinning. *Polymer*, 55(19): 4920-4931.

159. Paluszkiewicz, C., Stodolak, E., Hasik, M., and Blazewicz, M. (2011). FT-IR study of montmorillonite–chitosan nanocomposite materials. *Spectrochimica Acta Part A: Molecular and Biomolecular Spectroscopy*, 79(4): 784-788.

160. Pandya, D. S., Arinzeh, T., and Collins, G. (2010). Elevated temperature electrospinning of aqueous gelatin solution and crosslinking for tissue engineering applications. *Bioengineering Conference, Proceedings of the 2010 IEEE 36th Annual Northeast* (pp. 1-2).

161. Pant, H. R., and Kim, C. S. (2013). Electrospun gelatin/nylon-6 composite nanofibers for biomedical applications. *Polymer International*, 62(7): 1008-1013.

162. Panzavolta, S., Bracci, B., Gualandi, C., Focarete, M. L., Treossi, E., Kouroupis-Agalou, K., Rubini, K., Bosia, F., Brely, L., and Pugno, N. M. (2014). Structural reinforcement and failure analysis in composite nanofibers of graphene oxide and gelatin. *Carbon*, 78: 566-577.

163. Panzavolta, S., Gioffrè, M., Focarete, M. L., Gualandi, C., Foroni, L., and Bigi, A. (2011). Electrospun gelatin nanofibers: optimization of genipin cross-linking to preserve fiber morphology after exposure to water. *Acta biomaterialia*, 7(4): 1702-1709.

164. Papenburg, B. J. (2009). *Design strategies for tissue engineering scaffolds* University of Twente:

165. Pham, Q. P., Sharma, U., and Mikos, A. G. (2006). Electrospinning of polymeric nanofibers for tissue engineering applications: a review. *Tissue engineering*, 12(5): 1197-1211.

166. Picciani, P. H., Medeiros, E. S., Orts, W. J., and Mattoso, L. H. (2011). Advances in Electroactive Electrospun Nanofibers. *Nanofibers-Production, Properties and Functional Applications*: 116.

167. Pourjavadi, A., Aghajani, V., and Ghasemzadeh, H. (2008). Synthesis, characterization and swelling behavior of chitosan-sucrose as a novel full-polysaccharide superabsorbent hydrogel. *Journal of Applied Polymer Science*, 109(4): 2648-2655.

168. Puppi, D., Chiellini, F., Piras, A., and Chiellini, E. (2010). Polymeric materials for bone and cartilage repair. *Progress in polymer science*, 35(4): 403-440.

169. Qi, Y. Y., Tai, Z. X., Sun, D. F., Chen, J. T., Ma, H. B., Yan, X. B., Liu, B., and Xue, Q. J. (2013). Fabrication and characterization of poly(vinyl alcohol)/graphene oxide nanofibrous biocomposite scaffolds. *Journal of Applied Polymer Science*, 127(3): 1885-1894.

170. Qian, Y.-F., Zhang, K.-H., Chen, F., Ke, Q.-F., and Mo, X.-M. (2011). Cross-linking of gelatin and chitosan complex nanofibers for tissue-

engineering scaffolds. *Journal of Biomaterials Science, Polymer Edition,* 22(8): 1099-1113.

171. Rajzer, I., Menaszek, E., Kwiatkowski, R., Planell, J. A., and Castano, O. (2014). Electrospun gelatin/poly(ε-caprolactone) fibrous scaffold modified with calcium phosphate for bone tissue engineering. *Materials Science and Engineering: C,* 44(0): 183-190.

172. Ramakrishna, S., Fujihara, K., Teo, W.-E., Lim, T.-C., and Ma, Z. (2005). *An introduction to electrospinning and nanofibers* World Scientific:

173. Ratanavaraporn, J., Damrongsakkul, S., Sanchavanakit, N., Banaprasert, T., and Kanokpanont, S. (2006). Comparison of gelatin and collagen scaffolds for fibroblast cell culture. *Journal of Metals, Materials and Minerals,* 16(1): 31-36.

174. Ratanavaraporn, J., Rangkupan, R., Jeeratawatchai, H., Kanokpanont, S., and Damrongsakkul, S. (2010). Influences of physical and chemical crosslinking techniques on electrospun type A and B gelatin fiber mats. *International Journal of Biological Macromolecules,* 47(4): 431-438.

175. Ratner, B. D. (2004). *Biomaterials science: an introduction to materials in medicine* Academic press:

176. Rayleigh, L. (1882). XX. On the equilibrium of liquid conducting masses charged with electricity. *The London, Edinburgh, and Dublin Philosophical Magazine and Journal of Science,* 14(87): 184-186.

177. Reddy, C., Arinstein, A., Avrahami, R., and Zussman, E. (2009). Fabrication of thermoset polymer nanofibers by co-electrospinning of uniform core-shell structures. *Journal of Materials Chemistry,* 19(39): 7198-7201.

178. Riboux, G., Marin, A. G., Loscertales, I. G., and Barrero, A. (2011). Whipping instability characterization of an electrified visco-capillary jet. *Journal of Fluid Mechanics,* 671: 226-253.

179. Ruiz, O. N., Fernando, K. S., Wang, B., Brown, N. A., Luo, P. G., McNamara, N. D., Vangsness, M., Sun, Y.-P., and Bunker, C. E. (2011). Graphene oxide: a nonspecific enhancer of cellular growth. *ACS nano,* 5(10): 8100-8107.

180. Rujitanaroj, P.-o., Pimpha, N., and Supaphol, P. (2008). Wound-dressing materials with antibacterial activity from electrospun gelatin fiber mats containing silver nanoparticles. *Polymer,* 49(21): 4723-4732.

181. Rutledge, G., Yu, J., and Fridrikh, S. Production of submicron diameter fibers by two-fluid electrospinning process. US Patent 20060213829, 2005.

182. Sahay, R., Kumar, P. S., Sridhar, R., Sundaramurthy, J., Venugopal, J., Mhaisalkar, S. G., and Ramakrishna, S. (2012). Electrospun composite nanofibers and their multifaceted applications. *Journal of Materials Chemistry,* 22(26): 12953-12971.

183. Salehahmadi, Z., and Hajiliasgari, F. (2013). Nanotechnology Tolls the Bell for Plastic Surgeons. *World Journal of Plastic Surgery,* 2(2): 71-80.

184. Samal, S. K., Dash, M., Van Vlierberghe, S., Kaplan, D. L., Chiellini, E., van Blitterswijk, C., Moroni, L., and Dubruel, P. (2012). Cationic polymers and their therapeutic potential. *Chemical Society reviews,* 41(21): 7147-7194.

185. Sangsanoh, P., and Supaphol, P. (2006). Stability improvement of electrospun chitosan nanofibrous membranes in neutral or weak basic aqueous solutions. *Biomacromolecules,* 7(10): 2710-2714.

186. Santoro, M., Tatara, A. M., and Mikos, A. G. (2014). Gelatin carriers for drug and cell delivery in tissue engineering. *Journal of controlled release : official journal of the Controlled Release Society*.

187. Schacht, E., Bogdanov, B., Bulcke, A. V. D., and De Rooze, N. (1997). Hydrogels prepared by crosslinking of gelatin with dextran dialdehyde. *Reactive and Functional Polymers,* 33(2): 109-116.

188. Schiffman, J. D., and Schauer, C. L. (2007). Cross-linking chitosan nanofibers. *Biomacromolecules,* 8(2): 594-601.

189. Schiffman, J. D., and Schauer, C. L. (2008). A review: electrospinning of biopolymer nanofibers and their applications. *Polymer Reviews,* 48(2): 317-352.

190. Schoevaart, R., Siebum, A., van Rantwijk, F., Sheldon, R., and Kieboom, T. (2005). Glutaraldehyde Cross-link Analogues from Carbohydrates. *Starch - Stärke,* 57(3-4): 161-165.

191. Sell, S. A., Wolfe, P. S., Garg, K., McCool, J. M., Rodriguez, I. A., and Bowlin, G. L. (2010). The Use of Natural Polymers in Tissue Engineering: A Focus on Electrospun Extracellular Matrix Analogues. *Polymers,* 2(4): 522-553.

192. Shalumon, K., Anulekha, K., Girish, C., Prasanth, R., Nair, S., and Jayakumar, R. (2010). Single step electrospinning of chitosan/poly (caprolactone) nanofibers using formic acid/acetone solvent mixture. *Carbohydrate Polymers,* 80(2): 413-419.

193. Shan, C., Yang, H., Han, D., Zhang, Q., Ivaska, A., and Niu, L. (2009). Water-soluble graphene covalently functionalized by biocompatible poly-L-lysine. *Langmuir,* 25(20): 12030-12033.

194. Shan, Y.-H., Peng, L.-H., Liu, X., Chen, X., Xiong, J., and Gao, J.-Q. (2015). Silk fibroin/gelatin electrospun nanofibrous dressing functionalized with astragaloside IV induces healing and anti-scar effects on burn wound. *International Journal of Pharmaceutics,* 479(2): 291-301.

195. Shen, H., Hu, X., Yang, F., Bei, J., and Wang, S. (2007). Combining oxygen plasma treatment with anchorage of cationized gelatin for enhancing cell affinity of poly(lactide-co-glycolide). *Biomaterials,* 28(29): 4219-4230.

196. Sheu, M.-T., Huang, J.-C., Yeh, G.-C., and Ho, H.-O. (2001). Characterization of collagen gel solutions and collagen matrices for cell culture. *Biomaterials,* 22(13): 1713-1719.

197. Sikareepaisan, P., Suksamrarn, A., and Supaphol, P. (2008). Electrospun gelatin fiber mats containing a herbal—Centella asiatica—extract and release characteristic of asiaticoside. *Nanotechnology,* 19(1): 015102.

198. Simons, H. L. Process and apparatus for producing patterned non-woven fabrics. US Patent 3280229, 1966.

199. Sisson, K., Zhang, C., Farach-Carson, M. C., Chase, D. B., and Rabolt, J. F. (2009). Evaluation of Cross-Linking Methods for Electrospun Gelatin on Cell Growth and Viability. *Biomacromolecules,* 10(7): 1675-1680.

200. Sokolsky-Papkov, M., Domb, A. J., and Golenser, J. (2006). Impact of aldehyde content on amphotericin B-dextran imine conjugate toxicity. *Biomacromolecules,* 7(5): 1529-1535.

201. Sridhar, R., Lakshminarayanan, R., Madhaiyan, K., Barathi, V. A., Lim, K. H. C., and Ramakrishna, S. (2015). Electrosprayed nanoparticles and electrospun nanofibers based on natural materials: applications in tissue regeneration, drug delivery and pharmaceuticals. *Chemical Society reviews*.

202. Stiefel, D., Schiestl, C., and Meuli, M. (2010). Integra Artificial Skin® for burn scar revision in adolescents and children. *Burns,* 36(1): 114-120.

203. Su, Y., and Mo, X. (2011). Genipin crosslinked gelatin nanofibers for tissue engineering. *Journal of Controlled Release,* 152, Supplement 1(0): e230-e232.

204. Sun, Z., Zussman, E., Yarin, a. L., Wendorff, J. H., and Greiner, a. (2003). Compound Core–Shell Polymer Nanofibers by Co-Electrospinning. *Advanced Materials,* 15(22): 1929-1932.

205. Sung, H.-W., Huang, R.-N., Huang, L. L., and Tsai, C.-C. (1999). In vitro evaluation of cytotoxicity of a naturally occurring cross-linking reagent for biological tissue fixation. *Journal of Biomaterials Science, Polymer Edition,* 10(1): 63-78.

206. Tan, S., Inai, R., Kotaki, M., and Ramakrishna, S. (2005). Systematic parameter study for ultra-fine fiber fabrication via electrospinning process. *Polymer,* 46(16): 6128-6134.

207. Taravel, M. N., and Domard, a. (1996). Collagen and its interactions with chitosan, III some biological and mechanical properties. *Biomaterials,* 17(4): 451-455.

208. Taylor, G. (1969). Electrically driven jets. *Proceedings of the Royal Society of London. A. Mathematical and Physical Sciences,* 313(1515): 453-475.

209. Tomihata, K., and Ikada, Y. (1996). Cross-linking of gelatin with

carbodiimides. *Tissue engineering,* 2(4): 307-313.

210. Tonda-Turo, C., Cipriani, E., Gnavi, S., Chiono, V., Mattu, C., Gentile, P., Perroteau, I., Zanetti, M., and Ciardelli, G. (2013a). Crosslinked gelatin nanofibres: preparation, characterisation and in vitro studies using glial-like cells. *Materials science & engineering. C, Materials for biological applications,* 33(5): 2723-2735.

211. Tonda-Turo, C., Cipriani, E., Gnavi, S., Chiono, V., Mattu, C., Gentile, P., Perroteau, I., Zanetti, M., and Ciardelli, G. (2013b). Crosslinked gelatin nanofibres: Preparation, characterisation and in vitro studies using glial-like cells. *Materials Science and Engineering: C,* 33(5): 2723-2735.

212. Touyama, R., Inoue, K., Takeda, Y., Yatsuzuka, M., Ikumoto, T., Moritome, N., Shingu, T., Yokoi, T., and Inouye, H. (1994). Studies on the blue pigments produced from genipin and methylamine. II: On the formation mechanisms of brownish-red intermediates leading to the blue pigment formation. *Chemical and pharmaceutical bulletin,* 42(8): 1571-1578.

213. Tsai, C.-C., Huang, R.-N., Sung, H.-W., and Liang, H. C. (2000). In vitro evaluation of the genotoxicity of a naturally occurring crosslinking agent (genipin) for biologic tissue fixation. *Journal of biomedical materials research,* 52(1): 58-65.

214. Tsai, R.-Y., Hung, S.-C., Lai, J.-Y., Wang, D.-M., and Hsieh, H.-J. (2013). Electrospun chitosan–gelatin–polyvinyl alcohol hybrid nanofibrous mats: Production and characterization. *Journal of the Taiwan Institute of Chemical Engineers*.

215. Valizadeh, A., and Farkhani, S. M. (2014). Electrospinning and electrospun nanofibres. *Nanobiotechnology, IET,* 8(2): 83-92.

216. Vasita, R., and Katti, D. S. (2006). Nanofibers and their applications in tissue engineering. *International Journal of Nanomedicine,* 1(1): 15-30.

217. Vatankhah, E., Prabhakaran, M. P., Jin, G., Mobarakeh, L. G., and Ramakrishna, S. (2014a). Development of nanofibrous cellulose acetate/gelatin skin substitutes for variety wound treatment applications. *Journal of biomaterials applications,* 28(6): 909-921.

218. Vatankhah, E., Prabhakaran, M. P., Semnani, D., Razavi, S., Morshed, M., and Ramakrishna, S. (2014b). Electrospun tecophilic/gelatin nanofibers with potential for small diameter blood vessel tissue engineering. *Biopolymers,* 101(12): 1165-1180.

219. Vaz, C. M., de Graaf, L. A., Reis, R. L., and Cunha, A. M. (2003). In vitro degradation behaviour of biodegradable soy plastics: effects of crosslinking with glyoxal and thermal treatment. *Polymer Degradation and Stability,* 81(1): 65-74.

220. Verma, S., Mungse, H. P., Kumar, N., Choudhary, S., Jain, S. L., Sain, B., and Khatri, O. P. (2011). Graphene oxide: an efficient and reusable carbocatalyst for aza-Michael addition of amines to activated alkenes. *Chemical Communications,* 47(47): 12673-12675.

221. Wan, C., Frydrych, M., and Chen, B. (2011). Strong and bioactive gelatin–graphene oxide nanocomposites. *Soft Matter,* 7(13): 6159-6166.

222. Wang, H.-S., Fu, G.-D., and Li, X.-S. (2009a). Functional polymeric nanofibers from electrospinning. *Recent patents on nanotechnology,* 3(1): 21-31.

223. Wang, J., Tabata, Y., Bi, D., and Morimoto, K. (2001). Evaluation of gastric mucoadhesive properties of aminated gelatin microspheres. *Journal of controlled release : official journal of the Controlled Release Society,* 73(2-3): 223-231.

224. Wang, M., Yu, J. H., Kaplan, D. L., and Rutledge, G. C. (2006). Production of submicron diameter silk fibers under benign processing conditions by two-fluid electrospinning. *Macromolecules,* 39(3): 1102-1107.

225. Wang, Q., Du, Y., Feng, Q., Huang, F., Lu, K., Liu, J., and Wei, Q. (2013). Nanostructures and surface nanomechanical properties of polyacrylonitrile/graphene oxide composite nanofibers by electrospinning. *Journal of Applied Polymer Science,* 128(2): 1152-1157.

226. Wang, W., Itoh, S., Konno, K., Kikkawa, T., Ichinose, S., Sakai, K., Ohkuma, T., and Watabe, K. (2009b). Effects of Schwann cell alignment along the oriented electrospun chitosan nanofibers on nerve regeneration. *Journal of Biomedical Materials Research Part A,* 91A(4): 994-1005.

227. Wu, S.-C., Chang, W.-H., Dong, G.-C., Chen, K.-Y., Chen, Y.-S., and Yao, C.-H. (2011). Cell adhesion and proliferation enhancement by gelatin nanofiber scaffolds. *Journal of Bioactive and Compatible Polymers*: 0883911511423563.

228. Wu, S.-c., Chang, W.-h., Dong, G.-c., Chen, Y.-s., and Yao, C.-h. Cell adhesion and proliferation enhancement by gelatin nanofiber scaffolds.

229. Xu, C., Inai, R., Kotaki, M., and Ramakrishna, S. (2004). Aligned biodegradable nanofibrous structure: a potential scaffold for blood vessel engineering. *Biomaterials,* 25(5): 877-886.

230. Xu, F., Weng, B., Gilkerson, R., Materon, L. A., and Lozano, K. (2015). Development of tannic acid/chitosan/pullulan composite nanofibers from aqueous solution for potential applications as wound dressing. *Carbohydrate Polymers,* 115(0): 16-24.

231. Xu, L., Wang, X., Lei, T., Sun, D., and Lin, L. (2011). Electrohydrodynamic deposition of polymeric droplets under low-frequency pulsation. *Langmuir,* 27(10): 6541-6548.

232. Xu, Y., Li, L., Yu, X., Gu, Z., and Zhang, X. (2012). Feasibility study of a novel crosslinking reagent (alginate dialdehyde) for biological tissue fixation. *Carbohydrate Polymers,* 87(2): 1589-1595.

233. Yanzhong, Z. (2006). Electrospinning of Biomimetic and Bioactive Composite Nanofibers.

234. Yoo, H. S., Kim, T. G., and Park, T. G. (2009). Surface-functionalized electrospun nanofibers for tissue engineering and drug delivery. *Advanced drug delivery reviews,* 61(12): 1033-1042.

235. Yu, J., Lee, A.-R., Lin, W.-H., Lin, C.-W., Wu, Y.-K., and Tsai, W.-B. (2014). Electrospun PLGA fibers incorporated with functionalized biomolecules for cardiac tissue engineering. *Tissue Engineering Part A,* 20(13-14): 1896-1907.

236. Zandi, M. (2008). "Studies on the gelation of gelatin solutions and on the use of resulting gels for medical scaffolds" Ph.D. Thesis, Universität Duisburg-Essen.

237. Zeeman, R. (1998). *Cross-linking of collagen-based materials* Universiteit Twente:

238. Zeleny, J. (1917). Instability of electrified liquid surfaces. *Physical Review,* 10(1): 1.

239. Zha, Z., Teng, W., Markle, V., Dai, Z., and Wu, X. (2012). Fabrication of gelatin nanofibrous scaffolds using ethanol/phosphate buffer saline as a benign solvent. *Biopolymers,* 97(12): 1026-1036.

240. Zhan, J., and Lan, P. (2013). The review on electrospun gelatin fiber scaffold. *Journal of Research Updates in Polymer Science,* 1(2): 59-71.

241. Zhang, R., and Ma, P. (2001). Processing of polymer scaffolds: phase separation. *Methods of tissue engineering*: 715-724.

242. Zhang, X. (2014). *Fundamentals of Fiber Science* DEStech Publications, Inc:

243. Zhang, Y., Huang, Z.-M., Xu, X., Lim, C. T., and Ramakrishna, S. (2004). Preparation of core-shell structured PCL-r-gelatin bi-component nanofibers by coaxial electrospinning. *Chemistry of Materials,* 16(18): 3406-3409.

244. Zhang, Y., Ni, M., Zhang, M., and Ratner, B. (2003). Calcium phosphate-chitosan composite scaffolds for bone tissue engineering. *Tissue engineering,* 9(2): 337-345.

245. Zhang, Y., Ouyang, H., Lim, C. T., Ramakrishna, S., and Huang, Z.-M. (2005a). Electrospinning of gelatin fibers and gelatin/PCL composite fibrous scaffolds. *Journal of Biomedical Materials Research Part B: Applied Biomaterials,* 72B(1): 156-165.

246. Zhang, Y., Ouyang, H., Lim, C. T., Ramakrishna, S., and Huang, Z. M. (2005b). Electrospinning of gelatin fibers and gelatin/PCL composite fibrous scaffolds. *Journal of Biomedical Materials Research Part B: Applied Biomaterials,* 72(1): 156-165.

247. Zhang, Y., Venugopal, J. R., El-Turki, A., Ramakrishna, S., Su, B., and Lim, C. T. (2008). Electrospun biomimetic nanocomposite nanofibers of hydroxyapatite/chitosan for bone tissue engineering. *Biomaterials,* 29(32): 4314-4322.

248. Zhang, Y. Z., Su, B., Venugopal, J., Ramakrishna, S., and Lim, C. T. (2007). Biomimetic and bioactive nanofibrous scaffolds from electrospun composite nanofibers. *International Journal of Nanomedicine,* 2(4): 623-638.

249. Zhang, Y. Z., Venugopal, J., Huang, Z., Lim, C. T., and Ramakrishna, S. (2006). Crosslinking of the electrospun gelatin nanofibers. *Polymer,* 47: 2911-2917.

250. Zhao, H., and Heindel, N. (1991). Determination of Degree of Substitution of Formyl Groups in Polyaldehyde Dextran by the Hydroxylamine Hydrochloride Method. *Pharmaceutical Research,* 8(3): 400-402.

251. Zhao, W., Liu, W., Li, J., Lin, X., and Wang, Y. (2015). Preparation of animal polysaccharides nanofibers by electrospinning and their potential biomedical applications. *Journal of Biomedical Materials Research Part A,* 103(2): 807-818.

252. Zhou, J., Liu, J., Cheng, C. J., Patel, T. R., Weller, C. E., Piepmeier, J. M., Jiang, Z., and Saltzman, W. M. (2012). Biodegradable poly (amine-co-ester) terpolymers for targeted gene delivery. *Nature materials,* 11(1): 82-90.

253. Zong, X., Kim, K., Fang, D., Ran, S., Hsiao, B. S., and Chu, B. (2002). Structure and process relationship of electrospun bioabsorbable nanofiber membranes. *Polymer,* 43(16): 4403-4412.

LIST OF PUBLICATIONS BASED ON THE THESIS

1. Jalaja, K., & James, N. R. (2015). Electrospun gelatin nanofibers: A facile cross-linking approach using oxidized sucrose. *International Journal of Biological Macromolecules*, 73: 270-278.

2. Jalaja, K., Kumar, P. R. A., Dey, T., Kundu, S. C., & James, N. R. (2014). Modified dextran cross-linked electrospun gelatin nanofibres for biomedical applications. *Carbohydrate Polymers*, 114: 467-475.

3. Jalaja, K., & James, N. R. (2015) Potential of Electrospun Graphene Oxide-Gelatin Composite Nanofibers for Biomedical Applications. *Materials Science Forum*, Vols. 830-831 (2015) pp 581-584.

4. Jalaja, K., Naskar,D., Kundu,S.C., & James, N. R (2015). Electrospun Cationized Gelatin Nanofibers: A green Fabrication Approach for Tissue Regeneration. Submitted after revision in *Carbohydrate polymers*.

5. Jalaja, K., Naskar,D., Kundu,S.C., & James, N. R (2015). Potential of Coaxially Electrospun Core-Shell Structured Gelatin-Chitosan Nanofibers Cross-linked by Natural Molecules for Biomedical Applications. Submitted after revision in *RSC Advances*

6. Jalaja, K.,Sreehari, V.S., & James, N. R (2015). Fabrication and biological evaluation of Graphene oxide/Gelatin composite nanofibers by electrospinning (Submitted)

7. Jalaja, K., & James, N. R (2015). Evaluation of antibacterial activity and drug release studies of electrospun gentamicin loaded graphene oxide/gelatin composite nanofibers (Submitted)

PRESENTATIONS IN CONFERENCES/SEMINARS

Oral Presenatations

1. Jalaja, K.; Nirmala, R. J.; Electrospun Gelatin Nanofibers : Fabrication and Crosslinking. *Research scholars day, IIST, (2012).*

2. Jalaja, K.; Nirmala, R. J.; A novel Cross-linking approach to electrospun gelatin nanofibers. *25th Kerala Science congress, Thiruvananthapuram, India (2013).*

3. Jalaja, K., Nirmala, R. J. Biocompatible elctrospun gelatin nanofiber scaffold for tissue engineering applications; *ICAPM-2013, MG University, Kottayam (2013).*

4. Jalaja, K., Nirmala, R. J. A Facile crosslinking approach for electrospun gelatin nanofibers for biomedical applications. *MRSI, VSSC, Trivandrum (2014).*

Poster presentations

1. Jalaja, K.; Nirmala, R. J.; Nanofibrous scaffolds based on natural polymers for tissue engineering applications. *2nd International conference on nanotechnology at biomedical interface, Amritha centre for nano science and molecular medicine, Kochi, India (2012).*

2. Jalaja, K.; Nirmala, R. J Fabrication of chitosan nanofibers using gelatin as a core template for coaxial electrospinning, *IUMRS-ICA 2013, IISc Bangalore (2013).*

3. Jalaja, K.; Nirmala, R. J; A Facile Cross-Linking Approach Using Sucrose Based Material for Gelatin Nanofibers. *NCMST, 2013, IIST (2013).*

4. Jalaja, K.; Nirmala, R. J; Nanofibers using cationised gelatin. *Nano India-2013, NIIST, Trivandrum (2013).*

5. Jalaja, K.; Nirmala, R. J; Electrospun nanofibers based on cationized gelatin:A green nanofabrication method for biomedical applications; *ICAFM-2014, NIIST (2014).*

6. Jalaja, K.; Nirmala, R. J; Electrospun nanofibers based on cationized gelatin:A green nanofabrication method for biomedical applications; *WRASM, Payyanur college, Kannur University (2014).*